Bioprocess Intensification: Production of Bioethanol from *Saccharomyces cerevisiae* W303 in Monolithic Microreactor

A thesis submitted to the Newcastle University
for the Degree of Doctor of Philosophy in Chemical Engineering

By

WAN SALWANIS WAN MD ZAIN

School Of Chemical Engineering & Advanced Materials
Newcastle University
August 2013

CONFIDENTIAL

AUTHOR'S DECLARATION

This thesis is submitted in fulfilment of the requirements for the degree of Doctor of Philosophy at University of Newcastle, United Kingdom. All the studies described within are solely my work unless expressly stated otherwise, and were undertaken at the School of Chemical Engineering and Advanced Materials under the guidance and supervision of Professor Galip Akay and Dr Janet Quinn between August 2008 and August 2012.

I certify that none of the material offered in this thesis has been previously submitted for a degree or any other qualification at the above or any other university or institute. Neither the author nor the University of Newcastle upon Tyne accepts any liability for the contents of this document.

ABSTRACT

This study reveals the development of new 3-D support for ethanol production by *Saccharomyces cerevisiae* W303. The production of bioethanol by immobilising this organism had been demonstrated to have greater advantages over a suspended culture of free cells of *S.cerevisiae* W303. The production of ethanol is proportional to the growth of yeast, so preparing suitable supports with unlimited spaces that permit the cell proliferation are crucial for a long term continuous operation. The 3-D scaffold prepared from high internal phase emulsion (HIPE) offers good mechanical strength, and has a high surface area for allowing monolayer cell proliferation which was necessary in order to avoid additional stresses for the nutrient and oxygen transfer in the micro-environment. The enhanced porosity of this 3-D scaffold that was characterised by highly interconnected pores, not only promoted the dynamic condition in the monolith, but also facilitated easy flushing of dead cells and metabolic product. This study reveals that sulphonated polyHIPEs, a highly hydrophilic polymer which had pore and interconnect sizes of 45 μm and 16 μm respectively, had shown good bio-compatibility with the model organism, subsequently allowing its growth and glucose conversion. The ethanol productivity in the microreactor was greatly enhanced to 4.72 $gL^{-1}h^{-1}$, being over 12 times higher than that observed in the suspended shake flask culture (0.41 $gL^{-1}h^{-1}$) by free cell *S.cerevisiae* W303, despite only 60.1% of glucose being consumed. Since the remaining sugar must be kept low, the glucose utilization was further enhanced by introducing the two-stage reactor in series. The consumption of glucose was enhanced by 20.1% (compared to single stage reactor), where nearly 72.2 % of the supplied glucose was converted per pass during the pseudo steady state condition. This, on the other hand, increased the ethanol productivity to 5.84 $gL^{-1}h^{-1}$, which was 14 fold higher than the productivity obtained in the shake flask culture. The increment might be associated with the altered metabolical functions in the immobilised cells. This alteration is attributed to the reduction of the diffusion path of the growth nutrient (e.g: carbon, nitrogen and oxygen) that enhanced the availability and promoted the growth of yeast in the microreactor, thus enhancing the catalytic conversion of glucose to ethanol.

ACKNOWLEDGEMENT

I would like to express my sincere appreciation especially to Professor Galip Akay for his supervision, support, advice and patience during my study. His encouragement and kind words helped me facing the hard times throughout my study. I am also thankful to Dr Janet Quinn from the Medical School, Newcastle University for the useful advices and providing training in the microbiology work on the yeast handling.

My gratitude goes to my colleagues, Hasni, Rozita, Wail, Aziz, Teresa, Ahmed and Malek for the words of encouragement, experience and knowledge sharing. Dzun and Steve deserve special mention for their help and support which have been very valuable and appreciated. Credits are also extended to the academic and support staff at the department, especially all the technicians (Paul Sterling, Simon Daley and Rob Dixon), Dr Ronan O'Kennedy and Pauline from SEM for their help. Not to forget, many thanks to the members of C500 (Joseph, Elizabeth, Afolabi, Naimah, Paul, Luke, Arul, Ahmad, Rafa, James and Thea) and my friends (Azlina, Nasratun and Dilla) who have made life in Newcastle joyful and meaningful.

Heartiest gratitude must go to my mum and my family, for their endless prayers and support. To my dear husband, Ahmad Johari Mohamad and son Ayyash Mukhlis, thank you very much for the wonderful and undivided support.

A token of appreciation is extended to my sponsors, Ministry of Higher Education Malaysia (MOHE) and Universiti Malaysia Pahang (UMP) for the chance and financial support. Last but not least, foremost gratitude for the Almighty who has made all this possible.

TABLE OF CONTENTS

LIST OF FIGURES

LIST OF TABLES

NOMENCLATURE

d - interconnect diameter (μm)

D - pore diameter (μm)

DCW - dry cell weight (g)

D_o - diameter of reactor

D_l - diameter of impeller

H - height (cm)

PHP - polyHIPE polymer

R - radius of PHP (cm)

R_D - dosing rate (ml/s)

R_M - mixing rate (ml/s)

T - total mixing time (min)

T_D - dosing time (min)

T_H - homogenization/mixing time (min)

V - volume (cm^3/ml)

V_A - volume of aqueous phase (ml)

V_0 - volume of oil phase (ml)

W - weight of biomass (g)

WUC - water uptake capacity (g)

W_1 - weight of polymer after immersion

W_0 - weight of polymer before immersion

σ^B - sigma factor

Φ - internal phase volume ratio

Ω - rotational speed of the impeller (rev/min)

τ_d - doubling time (hr)

μ_{max} - specific maximum growth (hr^{-1})

% w/v - percentage of weight per volume

%v/v - percentage of volume per volume

ABBREVIATIONS

CFU	- colony forming unit (cells/ml)
ATP	- adenosine triphosphate
BA	- 2-butyl acrylate
BR	- bioreactor
CMC	- carboxymethyl cellulose
CO_2	- carbon dioxide
DCW	- dry cell weight
DVB	- divinylbenzene
ED	- Entner Doudoroff
EMP	- Embden Meyer Pathway
EHA	- ethylhexyl acrylate
G	- glucose
HA	- hydroxyapatite
HCl	- hydrochloric acid
HIPE	- high internal phase emulsion
HLB	- hydrophilic-lipophilic balance
H_3PO_4	- phosphoric acid
MATS	- microbial adhesion towards solvents
MTBE	- methyl tert-butyl ether
O/W	- oil in water emulsion
O_2	- oxygen
P	- peptone
PBS	- phosphate buffered saline
PEG	- polyethylene glycol
PEO	- polyethylene oxide
PHP	- polyHIPE polymer
PS-DVB PHP	- polystyrene-divinylbenzene polyHIPE
SEM	- scanning electron microscopy
SF	- shake flask
Span 80	- sorbitan monooleate
TVP PHP	- 2- vinylpyridine polyHIPE

TCA	- tricarboxylic acid
YE	- yeast extract
YPG	- media containing yeast extract, peptone and glucose.
W/O	- water in oil emulsion

CHAPTER 1: INTRODUCTION AND OBJECTIVES

1.1 Background of the Study

Despite the potential benefit of bioethanol, the first generation of this product has been debated due to its dependency on food crops, and also the local environmental damage it causes. While in European countries (e.g. UK), an insufficient supply of raw material (food based crops e.g. wheat and sugar beet) with regards to the forecasted demands resulted in its skyrocketing price, which caused a significant increase in the ethanol production cost (Gnansounou, 2010). A marginal and continuous increase is expected in the near future. Nevertheless, the introduction of the lignocellulosic compound as a feedstock created a profitable option in bringing ethanol to the next promising level. Current research is not only focused on the search for cheap biomass feedstock, but is also interested in maximising the profit by reducing the steps in the production line. Extensive study was focused on recycling the unreacted feedstock/cells as well as increasing the microorganism tolerance to high sugar and ethanol concentration to enhance the conversion of sugar to ethanol. The aim was to increase the productivity while avoiding any escalation in the production cost.

Since the ethanol market has developed fantastically, the diversification of processes in terms of operating mode, feedstock, and searching for an effective and efficient microorganism has been extensively studied. The major R&D challenges for bioethanol production from biomass basically involve several factors, as follows (Gnansounou, 2010):

- the improvement of quality and feedstock for the bioethanol production.
- the logistics relating to harvesting, storage, pre-processing, handling and transportation.
- maximising the yield of the second generation bioethanol.
- techno-economic and environmental assessment by minimising the negative impact on the environment relating to agricultural issues on land and wastes.

In the early days, commercial ethanol was derived from fossil fuel via ethylene hydration using phosphoric acid as a catalyst. Nowadays, 90% of the total ethanol is derived from sugar through microbial action (fermentation process). It involves three major steps which are: i) the production of simple sugar from the main feedstock via enzyme or chemical hydrolysis, ii) conversion of sugar to ethanol by microorganisms, and iii) a treatment process to separate ethanol from the fermentation broth (Balat *et al*., 2008). Current fermentation operation is achieved through conventional batch or fed-batch modes utilising various feedstocks such as sugarcane, corn, wheat, beet root and tapioca.

Although the utilisation of batch fermentation is simple and straightforward, the high cost associated with the continuous start up and shut down nature of such processes make it less feasible. This system involves the routine batch process of "fill and shut", involving preparation of an inoculum that requires multiple stages of cell development which are time consuming and can lead to contamination. Besides requiring long fermentation time, inhibition by high sugar and ethanol concentration limits the productivity. As an alternative, continuous culture offers lower operating costs and energy requirements as it reduces the construction cost for bioreactors. It also cuts the non-productive time for cleaning and filling besides keeping the inhibition effects to maximum level (Sanchez and Cardona, 2008). Unfortunately, difficulties in maintaining high cell concentrations in the continuous cultures requires longer fermentation times in order to achieve complete conversion, thus reducing the volumetric productivities. Furthermore, long fermentation times can also lead to genetic instabilities among the strains used, as well as the contamination issues caused by *Lactobacillus*. Brethauer (2009) reported that in an investigation of 62 Brazilian distilleries, batch production with cell recycling was the best in reducing the effect of contamination, while continuous culture is more susceptible to contamination. Contamination lowers the yield and the productivity, while the production cost was increased significantly because of the additional requirement for the antibiotics and sulphuric acid. Apart from this, the stability of the continuous culture is also questionable, since the productivity can be negatively affected if changes or oscillation occurred during operation. Nonetheless, some successful operations showed that this issue can be dealt with accordingly, and one of the major factors that determine its success is high cell concentration (Monte Alegre *et al*., 2003).

In order to make continuous process economically feasible, optimisation of fermentation conditions, improvements in microorganism tolerance towards toxic metabolites (e.g. producing robust strains), efficient transport system and optimising the carbon flux to yield high ethanol concentration are some of the important strategies that must be carried out in detail (Fortman *et al*., 2008). There is also a need to explore novel processes that could improve the current production systems in order to meet the anticipated demand for the bioethanol by optimising the yield to the maximum, but at much lower cost.

Ethanol production was mainly established through conventional batch or fed-batch fermentation, while only a few plants operated in continuous mode despite having all the desirable attributes. Even in Brazil, which was widely known for its mature technology, only 30% of the existing distilleries employed such a mode, corresponding to only 10% of total national production. 70-80% of total ethanol production was produced via batch/fed batch processes (Brethauer and Wyman, 2009). Although continuous process helps to reduce the cost and operation time by terminating some of the production steps in the batch operation, the washout effect and contamination resulting from the long operation time reduces its effectiveness. The limit on continuous process with regard to the washout effect can be improved by introducing the immobilisation technique. It is a technique where the microorganisms were grown in/insoluble matrix (support) which permits the flow of liquid in and out but retains the cells within its capsules. Cells were either entrapped or bound themselves to this special support, but still allowed metabolic processes to occur without interruptions. This procedure helps to maintain high cell concentration within the reactor, thus, continuous operation with stable high conversion can be achieved in an extended run. Besides this, immobilisation also increases the cell's ability to tolerate high ethanol concentration in the fermentation medium, allowing higher conversion yield and increased volumetric productivities. Apart from this, the effect of catabolic repression (e.g. high gravity fermentation) can be reduced significantly with immobilisation where the support protects and shields the cells from nutrient-product/pH and also from the shear stress caused by dynamic fluid and stirring (Qi *et al*., 2006). Furthermore, the confined area in the support increased cell-cell contact resulting in higher yields. Most important of all, the immobilisation technique allows the reuse of cells/enzymes, thereby reducing the operating cost.

Cell immobilisation can be carried out using various techniques such as gel entrapment, surface attachment, natural adhesion and co-culture. Most of the available data has reported considerable success within the laboratory scale, but some have reported a decrease or similar productivity in both the immobilised and suspended culture (Jamai *et al*., 2001). The earlier matrices for cell immobilisation were derived from natural sources such as calcium-alginate beads (Birol *et al*., 1998a), carrageenan (Wada *et al*., 1980), gelatine and chitosan, have incurred additional production cost. Therefore, cheaper and readily available natural supports were investigated such as sugar cane baggase, fibrous material and sweet sorghum stalk but with less success (Chandel *et al*., 2009; Kilonzo *et al*., 2009 and Yu *et al*., 2010). Nonetheless, most of the existing techniques have been proven to enhance the tolerance of cells towards ethanol and high substrate concentration, which further boosted the growth and ethanol yield. However, the above technique has shown several disadvantages in terms of the stability and fermentation performance. Many problems have been identified, which are mainly due to the lower conversion per g feedstock, the longer operating time and cell losses. The poor mechanical strength of the support enhances cell leakage during prolonged operation, making the immobilisation technique less accurate. Besides this, overpopulated growth, especially in the bead-type support, induced the formation of biofilm. Biofilm results in increased mass transfer resistance and prohibits the supply of nutrients or oxygen to the cells. This leads to a continuous reduction of viable cells and finally impairs the reactor performance, thus resulting in low productivity and negating the previously mentioned advantages. In addition, low mechanical strength supports may rupture in prolonged runs due to overgrowth and the evolution of carbon dioxide (CO_2), thus causing cell leakage into the medium. Although diffusion hindrance is unavoidable at high cell concentration, we still require a high cell density to boost the reaction rates. At this stage, it is crucial to produce a stable support with appropriate mechanical strength that will not break or deteriorate. But, most important of all, it must allow the penetration and homogenous distribution of cells to prevent cell localisation, thus reducing the restriction in mass transfer for an established, efficient and successful immobilized fermentation.

Although there were many claims by researchers that immobilised systems improve the yield and productivity of ethanol compared to free cell fermentation, applying the laboratory works into the real industrial process is almost impossible if the

problems relating to mass transfer resistance and the robustness of the carrier matrix (e.g. calcium alginate beads, k-carrageenan) have not been resolved. Introduction of the 3-D supports derived by polymerisation of monomeric continuous high internal phase emulsion (HIPE) created a new dimension for cell support. This new 3-D support, known as polyHIPE can be produced in the form of beads or moulded shapes. It has a foam-like morphology, generally with highly connected pores; therefore it is very porous (Hentze and Antoniette, 2002). PolyHIPEs have good mechanical strength and large surface areas to promote a monolayer growth for the immobilised system, hence reducing localisation of cell growth (Akay *et al*., 2005a). The importance of this type of growth is to avoid additional stresses in the confined micro-environment by reducing the path for mass transport for the nutrient supply as well as providing easy removal of product from the system. Besides this, the high porosity of polyHIPE encourages the smooth flow of the medium, thus avoiding the scarcity of nutrients and oxygen in the deeper area of the support. In addition, it also promotes the unrestricted flushing of toxic metabolites, hence prolonging the cell viability and the continuity of ethanol production.

Recent studies of polyHIPE as a scaffold for the new dimension of immobilised systems offer a solution, and it has superior advantages over both conventional immobilised and suspended cultures (Bokhari *et al*., 2006 and Jimat, 2011). Significant differences were observed in terms of cell growth, cell differentiation and yield. An increase in productivity was also observed in several bioprocess routes such as in the in-vitro osteoblast production, the phenol degradation process and α-amylase production (Akay *et al*., 2002; Bokhari *et al*., 2005; Akay *et al*., 2005b; Bokhari *et al*., 2007). Up to 20 fold increases in productivity were achieved in these processes compared to the control experiments.

Therefore, the aim of this study is to investigate polyHIPE for the immobilisation of yeast (*Saccharomyces cerevisiae* W303), which thus behaves as a microreactor that will be used for the continuous bioethanol production. In this project, the microenvironment of 3-D cell culture will be controlled as a means of controlling physiological stress through the size and connectivity of the pores as well as its surface properties. The production of ethanol is proportional to the growth of yeast, so

preparing suitable conditions and unlimited spaces that permit the proliferation of yeast is crucial for a long term continuous operation. Several types of polyHIPEs and methods of immobilisation will be thoroughly studied. Besides this, optimisation of dilution rates and nutrient requirements will be carried out to maximise the ethanol production in this microreactor. Most importantly, this work focused on the interaction mechanism between the support and the metabolic function of microorganisms, thereby providing integrated knowledge that will further provide a promising alternative to the existing process, especially in the production of bioethanol.

1.2 Objectives

The objective of the research is to establish an intensified bioprocessing method for the production of bioethanol in 3-D monolithic microreactors with aimed to reduce the processing volume or the production time with increased or at least comparable yield to the existing fermentation scheme. This microreactor is made frompolyHIPE in a disc form, placed in a polytetraflouroethylene (PTFE) chamber where it performed as housing for the polyHIPE. Such a system, but with different rig arrangements, had been demonstrated for the production of α-amylase from immobilised *Bacillus subtilis* sp., antibiotic production and in-vitro growth of osteoblast cells. It was proven in these studies and via several other projects in the Process Intensification and Miniaturisation (PIM) group at the Newcastle University, that the metabolic behaviour of the bacterial system was changed slightly when grown in the polyHIPE compared to the suspended system. The change is an attribute of reduced mass transfer resistance which resulted in an intensified process, where the yield increased significantly.

1.3 Scopes of study

The study has been divided into several scopes in order to achieve the objectives, which are:

i) **Control of the chemical properties of the microenvironment**: Preparation of various kinds of polyHIPE and selection for the best polymer which can provide better attachment of cells to the polyHIPE wall and enhance the migration of cell throughout the support.

ii) **Control of the physical properties of the microenvironment**: The effect of the physical parameters of the microenvironment (porosity, surface area, pores and interconnects sizes) that supported the growth of yeast by having a high surface area for cell proliferation, enough porosity for transfer of the nutrients, pore sizes that reduced the mass transfer resistance between the medium and yeast cells, and sufficient interconnects size that not only allow migration of cells to the other areas of polyHIPEs but also manage to retain the cells in the matrix.

iii) **Optimization of process conditions**: The conditions and medium requirements that provide the optimum yield of bioethanol were thoroughly studied in the continuous mode by varying the dilution rate and carbon-nitrogen concentration in the feed medium. The growth of *S.cerevisiae* W303 and its effect on the ethanol production were analysed intensively.

iv) **Biological aspects**: Understanding and applying the proper techniques of handling, culturing and analysis of yeast cells and products.

1.4 Thesis Layout

This chapter briefly introduces the motivation for the study by addressing the problems with the world energy crisis and the weaknesses of the current process in dealing with this subject matter. It also includes the desirable features of the proposed systems compared to the existing ones, as well as outlining the related works to achieve the objectives. The remainder of this thesis is organised into eight chapters as follows:

- **Chapter 2** details the literature review on two major topics: i) polyHIPEs and ii) bioethanol production.

- **Chapter 3** details all the general and repetitive materials and methods that were carried out throughout the study, including the polyHIPEs preparation, SEM analysis, and the fermentation procedure.

- **Chapter 4** discusses the preliminary study on the characteristics, physical and chemical properties of the polyHIPEs.

- **Chapter 5** reports the preliminary studies of ethanol production *Saccharomyces cerevisiae* W303 in batch systems by free and immobilised cells. It also discusses briefly the partial characterisation of the yeast and also the effect of different types of polyHIPEs on the growth, cells-surface interaction and the efficiency of ethanol productivity.

- **Chapter 6** presents the continuous ethanol production and the effects of different polyHIPEs properties (surface chemistry and pore sizes) on the growth and productivity.

- **Chapter 7** discusses the effects of the operating conditions that affected the metabolic behaviour of the immobilised cells by varying the nutrients compositions such as glucose and nitrogen concentrations, flow-rates and oxygen requirements.

- **Chapter 8** discusses the implementation of two- stage reactors in aerobic and microaerobic conditions.

- **Chapter 9** summarized the results, problems and contributions of this study. The conclusions were derived and some recommendations had been highlighted for future improvement.

CHAPTER 2: LITERATURE REVIEW

2.1 Global Energy Reviews

The consumption and continuous demand for energy from fossil fuel has created debates among the experts due to its impact on the environment and the emerging doubts concerning its sustainability for the future. Despite the debates, the dependency on oil and gas as the primary energy sources, has continued to increase tremendously over the years since the beginning of the industrial revolution in Europe almost 200 years ago, and shows no sign of slowing down. However, in 2009, however, the world energy demand dropped suddenly by 4.4% compared to the previous year due to the economic crisis faced by many countries. This resulted from the economic knockdown that caused industrial inactivity in industrial regions such as USA and Europe, while in developing countries like India and China, the demand for the domestic energy usage within that year remained high. However, in 2010, the demand was back on track and soared by 5.5% which was 4.5% higher than in 2008, as the economic downturn began to resolve itself slowly (EIA, 2011). The consumption grew by 6.7%, 4%, and 3.7% in Japan, Europe and United States, respectively (Enerdata, 2010).

The largest energy consumers in the world come from the OECD (Organisation for Economic Co-operation and Development) countries, where industrial activities were very active. For over several decades, USA, a member of this huge economic organisation, remained the highest energy consumer in the world, until recently overtaken by China in the year 2010 due to its spectacular economic growth. During this year, the energy consumption in China was 20.3% of the global consumption, surpassing USA at 11%, while India was third in the list. These two highly populated countries showed a very high demand for domestic purposes as energy consumption per capita increased proportionally to the improvement of living standard (Fronk *et al*., 2010). Although the total energy demand from industrial countries (USA, Europe, etc.) was behind that of China and India, the energy usage per capita remained the highest. Figure 2.1 shows the intensity of energy consumption by region in 2010.

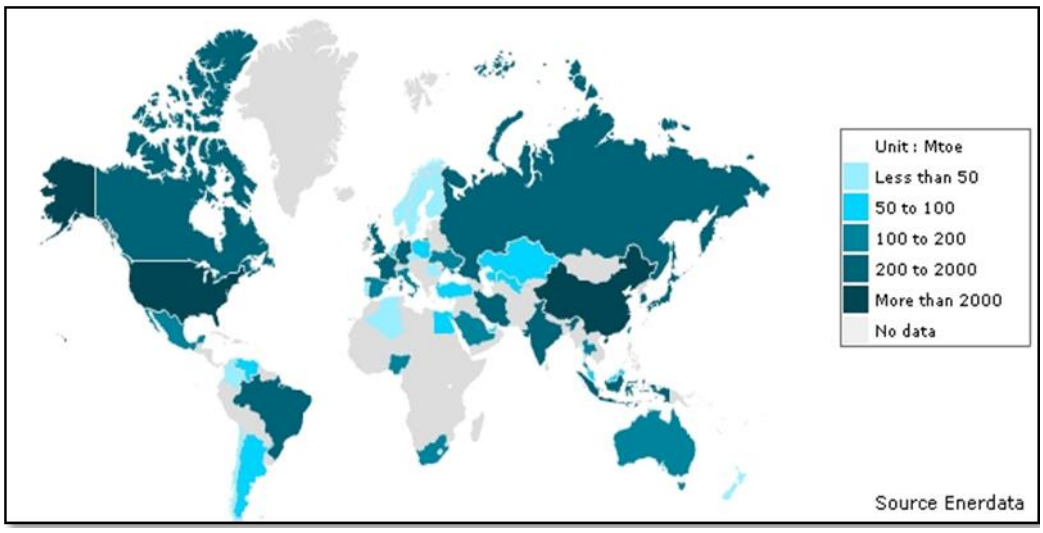

Figure 2.1 Energy consumptions in 2010 (Enerdata, 2011)

The global oil consumption in 2010 grew by 2.7 million barrels per day, with demand increasing by 3.5% and 7.5% for the OECD and Non-OECD countries respectively, after the recession in 2008-2009 (BP, 2011). The accelerated consumption that soars above average for almost all regions was enhanced by the economic recovery and accommodated by the strong growth of the oil production in countries like Nigeria and Qatar. Besides this, the oil prices remained stable over the year before increasing sharply in the final quarter of 2009. Referring to Figure 2.2, the OECD countries were the major energy consumers from 1990-2008, consuming more than 50% of the world's total energy. However, after 2008, the Non-OECD countries showed strong growth in energy use compared to the OECD countries due to its stable economic and rapid population growth in China and India. The overall energy consumption is forecasted to increase by 53%, from 505 quadrillion Btu in 2008 to 770 quadrillion Btu in 2035 (EIA, 2011).

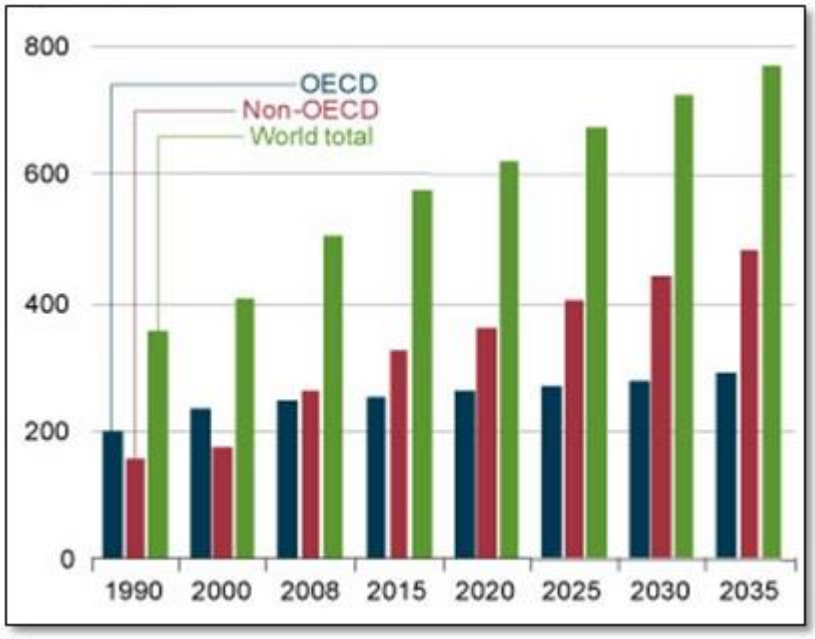

Figure 2.2: Energy consumption (in quadrillion Btu) from OECD and non-OECD countries (EIA, 2011).

According to Balat and Aray (2005), energy was split into three categories; fossil fuel, nuclear and renewable energy. Fossils fuel was further categorised into natural gases, oil and coal. According to Figure 2.3, the demand for all the energies increased gradually with time. It was projected that after 2008, the demand for energy increased significantly not only for the fossil fuels but also for the renewable energy, which was one of the fastest growing categories with an estimated increase of 2.8% per year (EIA, 2011). Although oil has been the primary fossil energy with a substantially cheaper price, the production failed to accommodate the continuously growing demand. Therefore in 2030, the energy source was estimated to switch to coal that will cover up to 45% of the overall demand (Balat, 2005). This switching, however, contributes to increasing emissions of carbon dioxide (CO_2), yielding more harmful products such as sulphur dioxide (SO_2), nitrogen oxide (NO_x) particulates, and mercury (Hg) compared to natural gases and oil. A concern over the looming changes in the global climate and the declining number of reserves due to excessive usage of this energy has boosted the search for a sustainable and cleaner energy. With current consumption rates, it is expected that the reported reserves will only last for less than 50 years, although the actual figures are not known (Balat, 2007). The fact that this form of energy is finite, means establishment of an alternative energy source is crucial. Figure 2.4(a) shows the usage percentage of energy by types in 2001, with the largest proportion contributed by

oil (39%), and followed closely by coal and natural gas at 23% and 21%, respectively (Muller-Steinhagen and Nitsch, 2005). On a worldwide basis, liquid consumption will increase continuously, but the demand for this energy is mainly limited to the industrial and transportation sectors. A significantly declining and plateau demand from commercial, residential and electric power sectors for this energy was evident in Figure 2.5, resulting from the steadily rising world oil prices, which led to switching to alternative fuels where possible (EIA, 2011).

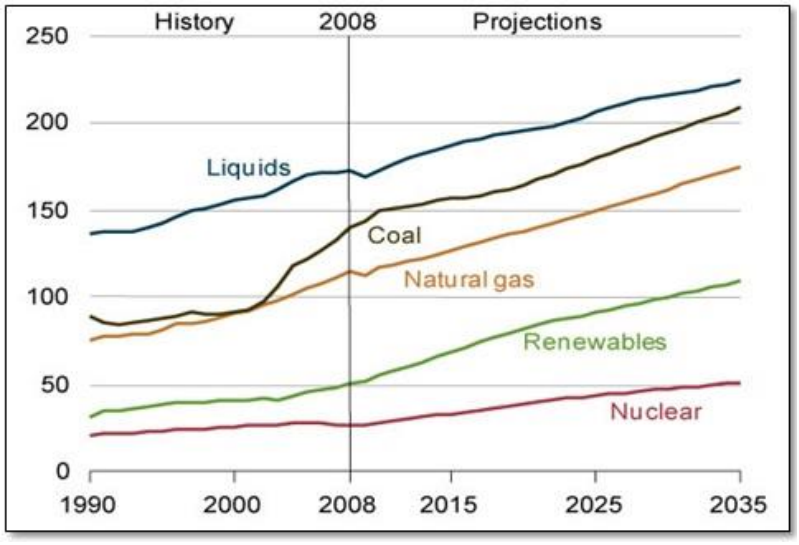

Figure 2.3: World energy consumption by fuel (in quadrillion btu) (EIA, 2011)

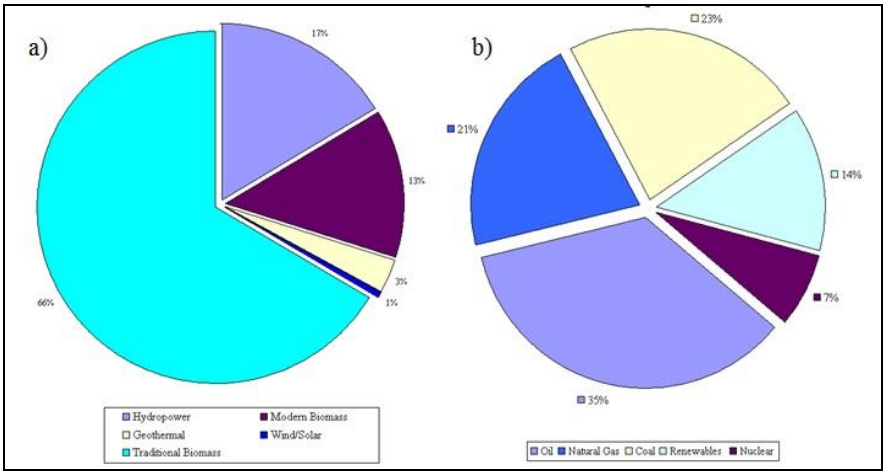

Figure 2.4: a) Structure of global primary energy consumptions by types in 2001. b) The percentage of consumptions of the renewable energy by types in 2001 (Muller-Steinhagen and Nitsch, 2005).

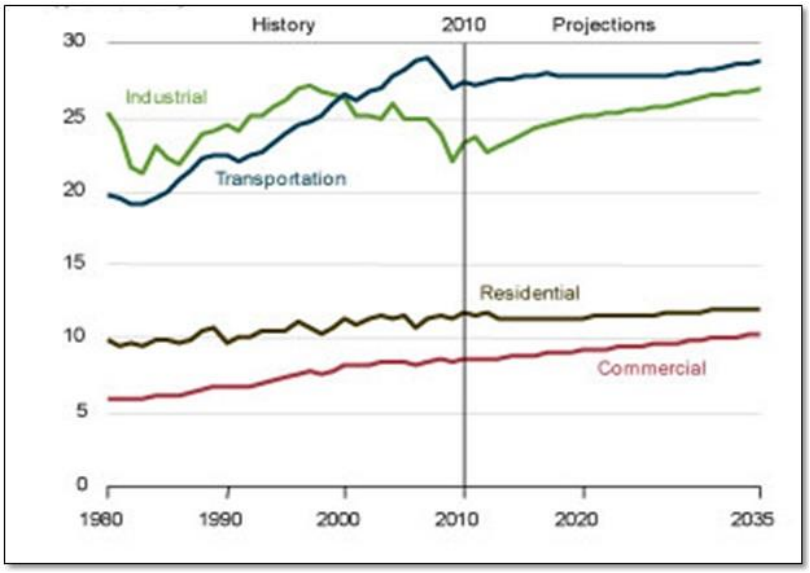

Figure 2.5: Profile of energy consumptions (in quadrillion btu), from 1980-2035 in various sectors in the US 1980-2035 (EIA, 2011).

According to the Energy Information Administration (EIA, 2007), world consumption of fossil fuel is expected to grow tremendously from 83 million barrels/day in 2004 to 118 million barrels/day in 2030. The pressure on fossil fuel supplies was caused not only by the increasing global demand but was also imposed by the political crisis in the oil producing countries especially in the Middle East, requiring a diversified energy portfolio for maintaining and sustaining the continuous economic growth across the nation. As a result, in 2001, the use of alternative energy became significant. 14% of the total energy consumption in 2001 was contributed by renewable energy, and within this, hydropower yielded the largest percentage at approximately 66%, while biomass energy showed a remarkable contribution of 17%, (Figure 2.4b). While the market for fossil energy declined slightly in the past decade, the consumption of renewable energy continued to grow strongly even during the 2009 recession. The reason behind this was that renewable energy, especially from biomass, was heavily subsidised by the government such that many incentives were introduced including tax credits, state renewable portfolio standards, and a federal renewable fuels standard (Kondili and Kaldellis, 2007). Apart from this, other renewable energy sources, including geothermal, wind and solar, are also extensively exploited, with solar growing at the fastest rate but starting from a rather small base.

The use of biomass energy was widely accepted not only because of its widespread availability, but most importantly, the net carbon emission from its combustible material can be reduced significantly. In the early stages of its introduction, it was estimated that no net CO_2 accumulates simply by assuming that all the CO_2 released from combustion will be re-used by the plant material during the photosynthesis process (Wyman, 1994). A decade later, a more realistic study revealed that the actual emission can be reduced by only 90% since CO_2 released from the fermentation process and from transporting the materials, starting from planting the energy crops to the logistics is also significant (Akay, 2006). However, a recent study revealed that the aim of reducing CO_2 emission was accompanied by more nitrous oxide being released to the atmosphere, resulting from the preparation of the fertilizer used for growing the crops. NO_x was reported to pose a 200 times more severe effect as a greenhouse gas compared to CO_2. Despites all these debates, biomass energy also offer a strategy to deal with the waste product, especially from agriculture/forestry/agriculture and municipal waste, as these materials can be used as the starting material for generating energy. Due to its various significant contributions, research on biomass energy has greatly developed over the years and the worldwide interest has bloomed fantastically since the mid 90's, focusing on alternative transport fuels (Calle and Walter, 2006).

Biomass energy refers to energy that comes from land, ocean or seawater habitats, either through combustion, or microbial fermentation. This biomass energy is considered advantageous for numerous reasons such as (Balat and Ayar, 2005):

- zero emission in carbon dioxide cycle.
- Low emission of sulphur and hazardous materials gives increased air quality.
- Feedstock widely available in both developed and developing countries
- Potential utilisation of ash produced from the combustion of biomass as fertilizer.
- Potential to prolong the availability of fossil fuel
- Possibility to overcome or treat waste from various sectors
- Reduce oil imports and boost rural economy activity

Although biomass energy is showing great potential economically, the production of biomass energy is still not feasible enough due to its high production cost linked with the low energy density of the raw materials. In fact, the production cost for the biomass energy is currently 2.3 times higher than that of fossil fuel (Kondili and Kaldellis, 2007). The use of food crops as the feedstock (for the synthesis of ethanol) is not only very costly, but imposes serious competition with food commodities like corn (USA) and wheat (UK). Worst of all, the use of these energy crops was held responsible for the increased rate of hunger in 2008 due to increased food prices. For instance, the land used for growing food crops has been replanted with energy plants, thus reduced the food production significantly. The growers preference for the energy plant was induced by various incentives offered by the local government in addition to its high market price, but was denied by Brazil, one of the biggest manufacturers and consumers of bioethanol. As continuous competition arise between the importance of sustainable energy and food for human consumption, alternative feedstocks were sought out to overcome this issue. Waste from forestry and agriculture was continuously exploited to replace the food crop. Although the use of lignocellulosic materials is cheaper compared to food crops, additional production costs for enzymatic hydrolysis prior to fermentation are quite significant, and imposed over 20% of the overall production cost (Sanchez and Cordona, 2008). However, continuous study had been carried out to optimise the enzymatic process by introducing a simultaneous saccharification and fermentation (SSF) that promotes efficient hydrolysis and making low cost ethanol feasible (Balat *et al*., 2008). Figure 2.6 depicts some of the alternative energy plants that are available all over the world, including solar, hydro, geothermal and wind plant.

Figure 2.6: a) and b) Solar plant in Seville and Ukraine, respectively. c) Hydropower energy generating in the Efestiniog power plant in Wales, UK, d) Oohaki geothermal power station in New Zealand, e) Bioethanol AE plant in USA and f) Fenton wind farm in Minnesota US (*www.wikipedia.org* retrieved on February 2012).

2.2 Introduction to Bioethanol

In 2008, the transportation sector accounted for 27% of the total world energy consumption, which came solely from natural gas. EIA in its annual report (2011) projected that from 2008–2035, the energy demand will increase almost proportionally for all sectors, while the estimated 1.4% yearly increase for the transportation was the highest, above other sectors. This is due to increase living standards correspond to the soaring demand for personal travel and freight transport for goods delivery (EIA, 2011). In the past eight years, the energy consumption for transportation in the OECD countries was 34% higher compared to the non-OECD countries, but, it was predicted that in the next 25 years, the demand from the non-OECD countries will plummeted by 19% compared to the OECD countries due to increasing population and social status. Since the transportation sector is estimated to develop substantially over the next few years (Figure 2.7), the natural gas faces substitution with cheaper, safer, cleaner energy with a hope of continued sustainability and enables it to cope with the emerging demand from this sector. Recently, the contribution of biomass energy for the transportation sector is quite significant, and varies by country. Brazil was reported to allocate 30% of

the national biomass energy, produced solely from sugarcane, for transport purposes. Similarly, the EU estimates that 18.46 million tonnes, corresponding to less than 10% of the total energy for transportation (321 million tonnes), will be contributed by biomass energy (Kondili and Kaldellis, 2007; Gnansounou, 2010).

Figure 2.7: World liquids energy consumption by sector, 2004-2030. (EIA, 2004)

Referring to Figure 2.7 above, two-thirds of the growth for the liquid energy consumption is in the transportation and industrial sectors. From year 2004 to 2030, the transportation shows a greater increase in fuel consumption which is mainly due to the expansion of the automobile industries and competition in both local and international market. Due to high demand on the fuel, the volume of world oil reserves declined dramatically during 2000-2007, with the largest declines reported in Mexico, China, Norway and Australia (EIA, 2007). As a result, alternative energy such as ethanol, methane and hydrogen are being considered as potential substitutes for fossil fuel. The flexibility of choosing various starting materials has made ethanol a promising alternative for liquid fuel. Since it can provide a cleaner and safer sustainable energy, the availability of abundant biomass, estimated at approximately 170 billion tons, has created great interest in exploring this new area of renewable energy (Kunz, 2008).

Due to its escalating demand, ethanol has been proposed as an alternative fuel to substitute gasoline from natural gases. Biomass ethanol is not only feasibly cheap, but also a sustainable energy source as it can be produced from various feedstocks, ranging from food crops to waste. Apart from this, bioethanol can be easily integrated into the existing road transport fuel system in quantities up to 5%, without the need for engine modifications. In countries like US and Brazil, the blending of ethanol in unleaded petrol achieved as high as 10 and 30%, respectively. Brazil was the first country to launch the use of ethanol in an automobile, dated almost a century ago in 1927 (Musatto *et. al*., 2010). The blending of bioethanol with gasoline was introduced to reduce the heavy reliance on fossil fuel, starting at 1%, and increased to 30% recently. This great achievement was obtained with the introduction of flex-fuel vehicles in 2003, which allowed the use of both gasoline and ethanol (Rosillo-Calle, 2006). In the 1970s, this project was followed by the USA and European countries by introducing gasohol, a blending of gasoline with alcohol at 2.5%, a percentage which has increased slowly, with the highest composition achieved today of approximately 10% (Gnansounou, 2010). In the meantime, all the cars in Brazil are using a blend of gasoline with at least 25% (E20) of anhydrous ethanol, although a successful run with 95% of ethanol (E95) had been achieved in the 1980s (Solomon *et al*., 2007). Although ethanol blending is successful and does not have a negative impact on the engine performance, its percentage was limited to 10% because of its corrosive nature. A higher blending percentage to gasoline requires modification of conventional engines, and this high maintenance cost had become less attractive to the end-user.

Another factor that contributed to the increasing demand for bioethanol after the slow growth was due to the banning of methyl tert-butyl ether (MTBE) by 25 states in the US (e.g. California, New York and Connecticut). The banning was caused by an MTBE leakage that contaminated the underground water supply, causing not only bad taste and smells, but was also carcinogenic (Ademe, 1999). This incident had created a new market for ethanol, although its price at that time was relatively higher compared to MTBE (Solomon *et al*., 2007). The total usage of MTBE that accounted for 42% of its national consumption, had switched to ethanol and soaring demand for this new fuel additives improves drastically after a slow growth in 2005. Unlike MTBE, ethanol has been proven to be a better additive for petrol (Wyman, 1994). Moreover, ethanol was preferable due to its high octane number, while the availability of oxygen in its main

chain provides more oxygen during combustion. The high oxygen to fuel ratio leads to complete combustion, therefore reducing the emission of carbon monoxide (CO), particulates and hydrocarbons that are generally produced in the absence of oxygen (Balat *et al*., 2008).

2.2.1 *Ethanol Production*

In the meantime, bioethanol was mostly produced by batch production utilising various feedstocks, mainly derived from food crops. In the US, the capacity of the various batch plants produced between 400,000 to 270 Mgal annually (Solomon *et al*., 2007). To date, the largest bioethanol producer in the world has been Brazil, utilising sugarcane as the feedstock and producing about 27.5 billion litres in 2009, accounting for approximately 35.6% of the total world production. This was followed closely by corn ethanol from USA, and both Brazil and USA contributed nearly 70% of the total world production (Figure 2.8). The reason Brazil is the largest producer of bioethanol is because the use of sugarcane as the feedstock is more competitive in terms of the cost compared to other feedstocks. Besides, the operating cost remains the lowest, in the range of US$0.68-0.95/per gallon, which is contributed by a cheap labour and a mature infrastructure.

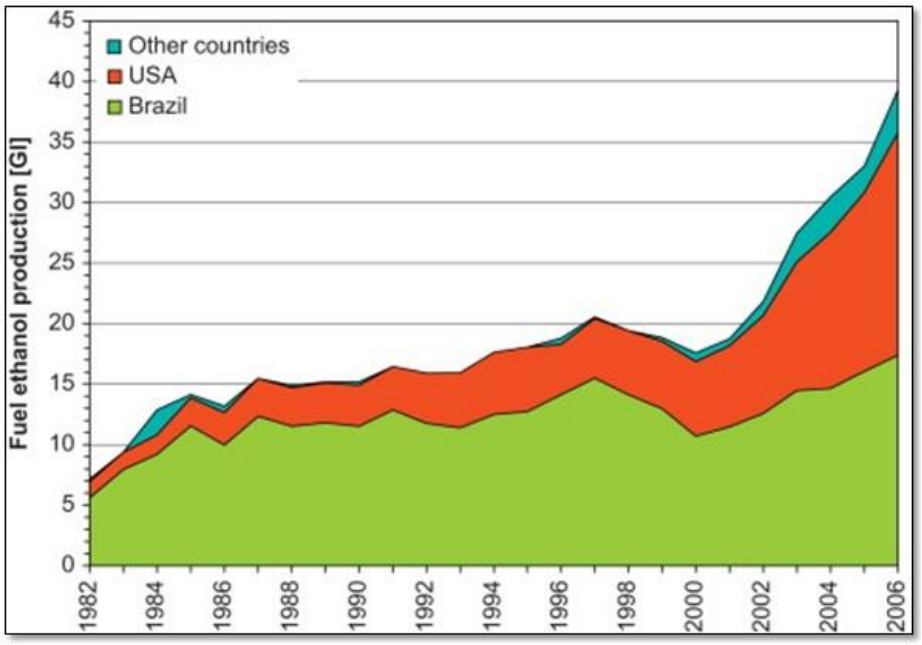

Figure 2.8: World production of fuel ethanol (Walter *et al*., 2008)

Ethanol production in 2006 was reported at 13.5 billion gallons and rising to 17.2 billion gallons in 2008 (Alonso *et al*., 2010). This growth is expected to increase annually, and its estimated supply is expected to replace 353 billion litres of gasoline, corresponding to 32% of the global gasoline consumption (Gnansounou, 2008). There were a number of factors which contributed to this growth, including (Solomon *et al*., 2007):

- Reduced oil imports and continued replacement of MTBE by ethanol as a gasoline additive.
- Competitive demand for fossil fuel from various sectors resulting in higher crude oil prices, which also raised the price of gasoline and thus increased the demand for, and price of, ethanol as a substitute.
- Various incentives for ethanol by local government, for example PROALCOOL in Brazil and ETA in the US, which reduced the excise tax by more than 15% in 2005.
- The Kyoto Protocol enforcement to reduce CO_2 emission.
- Improvement of production and treatment processes to increase the yield
- Availability of a cheaper feedstock from e.g. cellulosic materials as an alternative to food crops.

Bioethanol production has increased rapidly in many countries, especially in the USA where production increased almost 4 fold in 2000-2004, but still, the production only managed to supply approximately 2% of the total fuel in the US market (Rosillo-Calle, 2006). Although Brazil was the main bioethanol producer, producing more than half of the total world production in 2005, its use was mostly for local markets and only a small amount was exported to the US and China (Solomon *et al*., 2007). However, in 2006, US production had surpassed Brazil by nearly 10%, but the experts predicted that to a certain extent, the expensive labour cost, and limited land will put US back behind Brazil. Moreover, sugarcane ethanol was more competitive and cheaper compared to US corn ethanol due to elimination of liquefaction and saccharification steps. In addition, the sugarcane harvest in Brazil also grows rapidly, tripling in 2007, which was able to accommodate both food and energy sectors, satisfying the claim that no competition arises between food and energy commodities (Mitchell, 2008). While, in the US, the corn supply does not comply with the increasing demand from the energy sectors which causes the price to increase. While in the EU, after 10 countries (Czech Republic, Cyprus, Estonia, Hungary, Latvia, Lithuania, Malta, Poland, Slovakia and Slovenia) joined the union on 1 May 2004, vast tracts of land are now available for agricultural purposes. It creates an opportunity for a cheaper feedstock within the EU, as these countries can be a supplier for other EU countries that are facing problems with land shortage (e.g. the UK). To date, the overall EU ethanol feedstock (e.g. wheat) is cultivated on 54.9 Mha, but the actual land needed for the purposes was only 4.7 Mha, hence feedstock availability should not be a problem (Kondili and Kaldellis, 2007).

Different countries have utilised different feedstocks as the starting materials and their production in 2006 is listed in Table 2.1. Currently, the best feedstock for ethanol is the sugarcane although there was a slight competition with the sugar industry in the late 1980s, causing a shooting high price (Solomon *et al*., 2007). In the UK, bioethanol is produced by the fermentation of sugar beet or wheat supplied under contract by the existing growers, and the most recent plant producing ethanol from wheat started its first operation in late 2009, with an estimated production of 420 million litres/year (*Pump Industry Analyst, 2007*). China was the third largest producer in the world, and its ethanol program has expanded due to the many incentives and support given by its government. While in Europe, Romania has been seen as a net exporter within the EU in the near future, due to the vast availability of sweet sorghum

(Kondili and Kaldellis, 2007). Figure 2.9 shows a picture of a bioethanol plant which is currently active, located in West Burlington, USA.

Table 2.1: List of feedstock for bioethanol production (Sanchez and Cardona, 2008)

Countries	Feedstock	Blending	Production
Brazil	Sugar cane	24	16,998
USA	Corn	10	18,376
China	Corn, wheat	-	3,849
India	Sugar cane	5	1,900
UK	Wheat	-	280
Canada	Wheat, barley and corn	7.5-10	579
Thailand	Cassava, sugar cane	10	352
France	Sugar beet, wheat, corn	-	950
Colombia	Sugarcane	10	269
Spain	Wheat, barley	-	462

Figure 2.9: Ethanol plant in West Burlington, Iowa USA. (*www.wikipedia.org* retrieved on the 14 February 2012).

2.3 Overview of PolyHIPE

PolyHIPE was initially developed by the Unilever research group in Cheshire, UK, using high internal phase emulsions (HIPE), and it possesses a skeleton like structure with high porosity (Delueze *et al*., 2002). In general, this material is often regarded as a porous, low density material, typically less than 0.1 gcm^{-3} (Cameroon and Sherington, 1997). It can be produced with either an open or closed structure, which is simply achievable by varying its chemical composition. The open cellular structures are built with pores/voids that are fully connected to each other by small windows called interconnects (Figure 2.10). To date, polyHIPE has found applications in separation technology (Akay *et al*., 1995, Calkan *et al*., 2006), agriculture (Burke *et al*., 2007, Fleming, 2012), gas clean-up (Akay *et al*., 2005a) and wastewater treatment (Erhan, 2002). A recent application of polyHIPEs as hydrogen storage materials was studied by McKeown *et al*. (2007). While in the bioprocess intensification study, the polyHIPE has been successfully demonstrated for production of biodiesel (Dizge *et al*., 2009; Dizge *et al*., 2009a), tissue engineering (Akay *et al*., 2003; Akay *et al*., 2004; Akay *et al*., 2005; Christenson *et al*., 2007), alcohol (Griffith and Bosley, 1993; Karagoz *et al*., 2008), antibiotic (Ndlovu, 2009), α-amylase production (Jimat, 2011) and agriculture (Burke, 2007; Fleming, 2011).

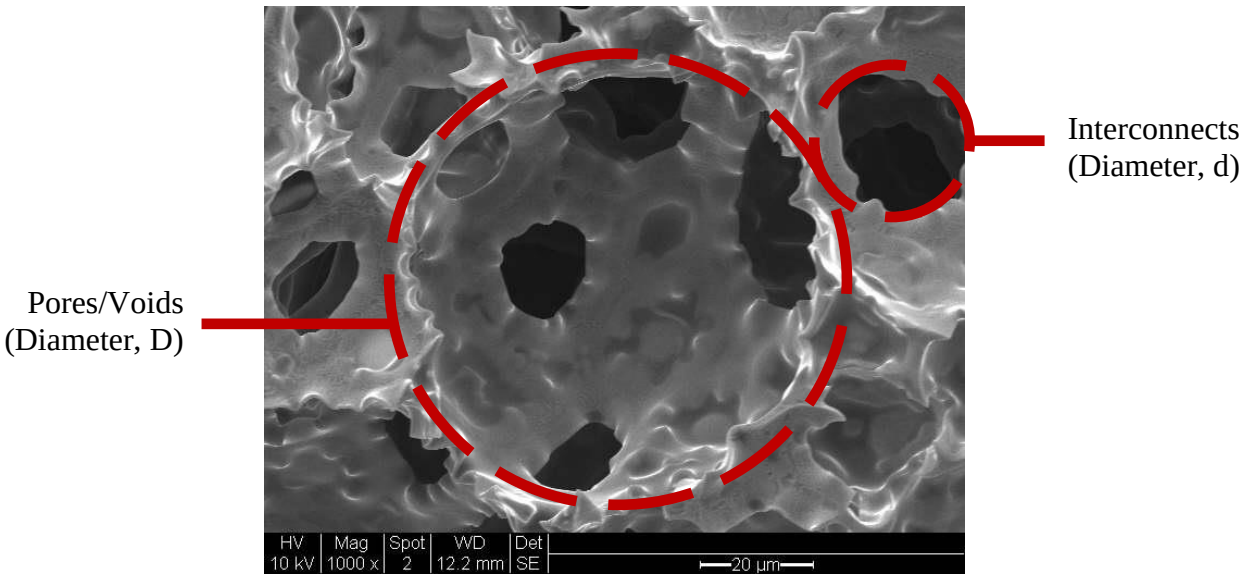

Figure 2.10: SEM images taken at 1000x magnification showing a highly porous polyHIPE, with large interconnect size prepared from the polymerisation of styrene/divinylbenzene to be use as a fertilizer (Fleming, 2012).

PolyHIPEs are highly flexible, and can be moulded into blocks or prepared in particulate forms for use in different types of reactors/applications. The ease of its preparation offers numerous selections of surface chemistry as well as a wide range of pores diameter (D) and interconnects (d). The D and <d/D> can be tailored independently, within the range of 0.5 μm-5000 μm, and 0 to 0.5 μm, respectively (simply by altering the composition, processing and polymerisation conditions) (Akay *et al*., 2005a). These materials have a hierarchical pore size and connectivity in the range of 100 μm – 10 nm. PolyHIPE is also generalised by its high pore volume (porosity) that can reach up to 99% with large surface area (3-550 m^2g^{-1}).

2.3.1 *Preparation of High Internal Phase Emulsion (HIPE)*

High internal phase emulsion (HIPE) is defined as an emulsion that has a high percentage of internal phase volume, also known as the dispersed phase (Ø). In contrast to regular emulsions, where the dispersed phase is the minimum, its volume in HIPE usually varies from 74%-99% (Cameron, 2005). The dispersed phase forms uniform sized spheres in the emulsion at volumes less than 74%, but as the percentage increases, the droplets deform into non-uniform droplets or polyhedra (Figure 2.11). The addition of the dispersed phase into the continuous phase during the preparation of HIPE was controlled by varying the flowrate, and often coupled with constant mixing at various speeds and mixing times which later on contributes to the size distribution of pore (D) and interconnect (d) of the polyHIPEs.

The emulsion is prepared by mixing the aqueous and oil phases, in which both can be either the dispersed phase or the continuous phase (Menner and Bismarck, 2006). The aqueous phase, in general, is composed of distilled water and the initiator (salt), while the oil phase is a mixture of monomer, surfactant and the cross-linking agent. For the initiator, this substance can be added to either the aqueous or the oil phase depending on the desired emulsion type. If the aqueous phase is chosen to be the dispersed phase, the emulsion is termed as water-in-oil (W/O) emulsion; therefore the initiator (salt) will be added to the aqueous phase. And if otherwise, where the oil phase is the dispersed phase, the emulsion is termed as oil-in-water (O/W) emulsion, and the

initiator is added to the oil phase. Alternatively, the aqueous phase can be replaced with the non-aqueous phase during the HIPE's formation, achievable by selecting two immiscible organic solvents (Cameron, 2005; Cameron and Sherrington, 1997; Cameron and Sherrington, 1996). This formulation has been demonstrated to give considerable stability with the right choice of high polarity solvent (Cameron and Sherrington, 1996).

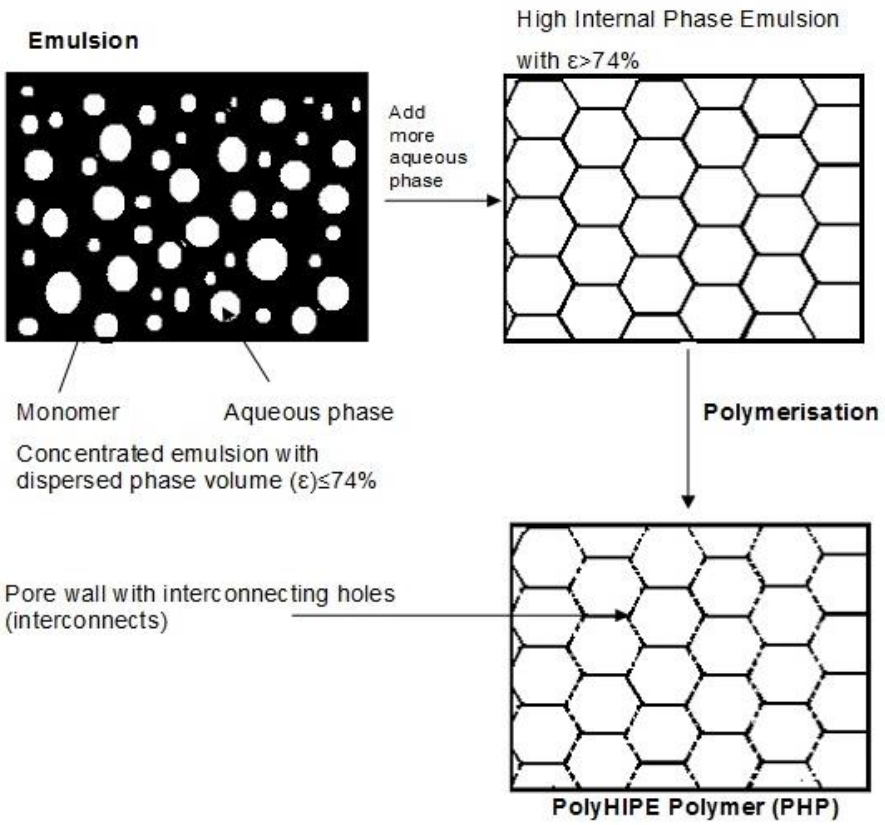

Figure 2.11: Schematic diagram of polyHIPE formation (Byron, 2000).

The experimental rig for emulsion preparation is set up in the fume hood as shown in Figure 2.12. Both liquids were mixed into the reactor using a peristaltic pump, followed by continuous stirring. The mixing can be achieved in two ways: either by 1) bringing both phases together during dosing or 2) single dosing of one particular phase or 3) alternate addition. In most preparations, the dispersed phase was added to the continuous phase, prior added into the mixing vessel and were mixed together by intense mixing (300 rpm), until it formed a milky white emulsion. However, the emulsions are often unstable and can easily demulsify or separate. Therefore, surfactant

was used to stabilise the emulsion, where it adsorbs onto the surface of the liquids and facilitates the positioning of the droplets within the bulk phases (Figure 2.13). The surfactant, which has both hydrophobic and hydrophilic properties, produces steric attraction and agglomerates in separate phases, holding the components together and preventing them from separating during preparation and polymerisation processes. Although the surfactant plays an important role in emulsion preparation, this substance is not involved in the polymerisation. It acts like a glue that holds the phases together, and if there is any residual surfactant that does not attach to the liquid interface, it will form an individual phase in the oil phase. This agglomerated surfactant, once removed from the polymeric material, will create an additional window on the polyHIPEs walls that connects the adjacent pores, (Figure 2.14).

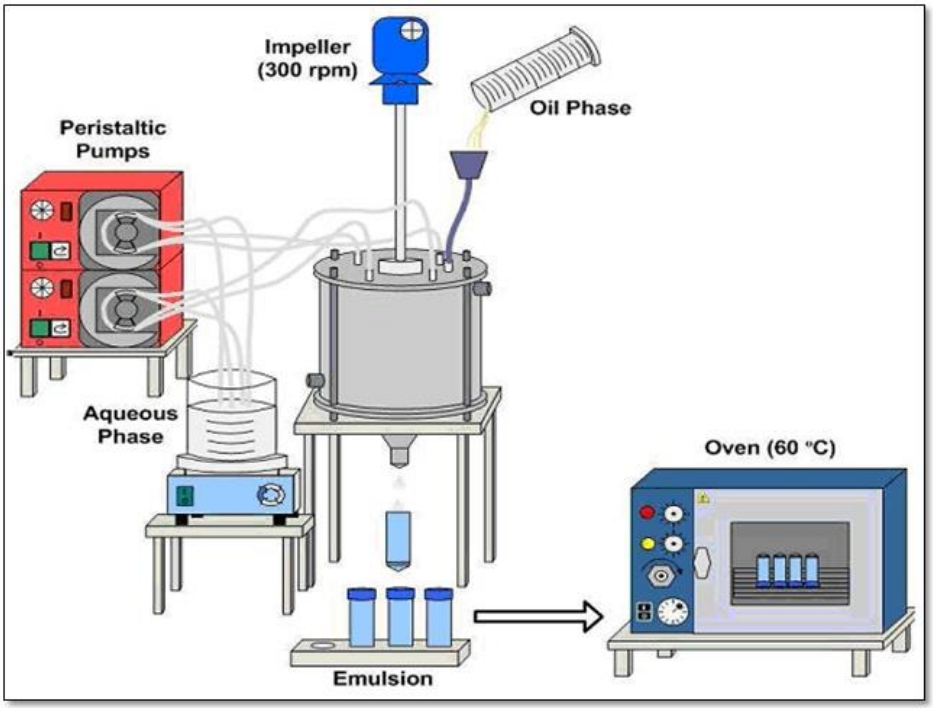

Figure 2.12: Experimental rig for HIPE preparation. Emulsion from the reactor vessel was transferred to the PTFE tube and set to polymerise in oven for at least 8 hours at 60^{o}C (Calkan, 2007).

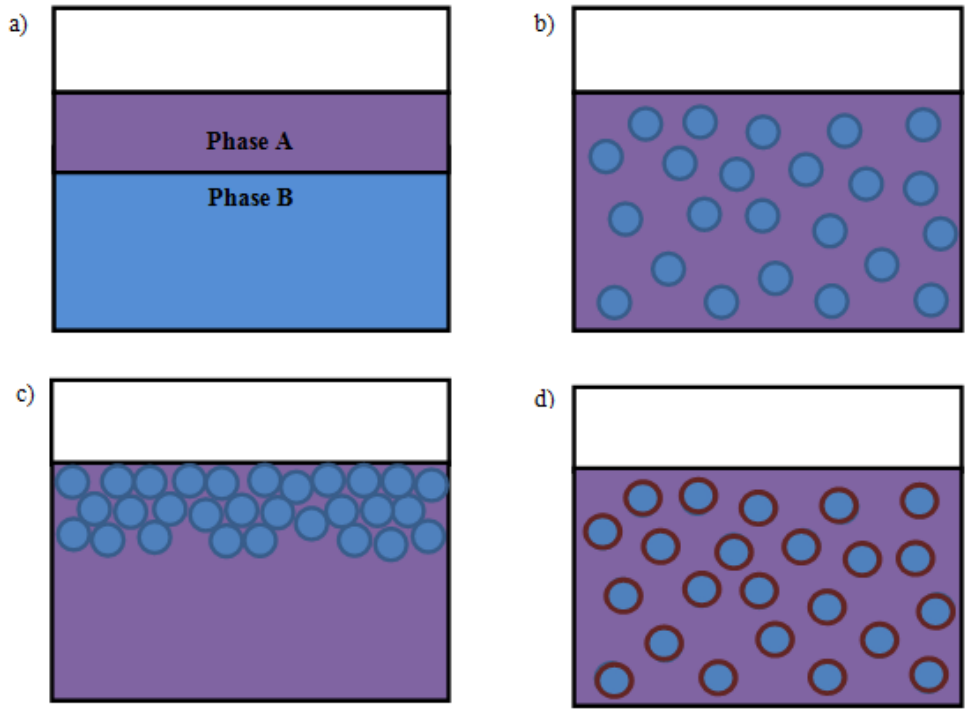

Figure 2.13: Formation of emulsion. a) Two separated immiscible phases; b) Droplets of phase B dispersed in phase A. c) Separation of unstable emulsion d) The dark colour represents the surfactant surrounding the droplets of phase B helping to position the liquid interphase in the bulk solution, thus stabilising the emulsions.

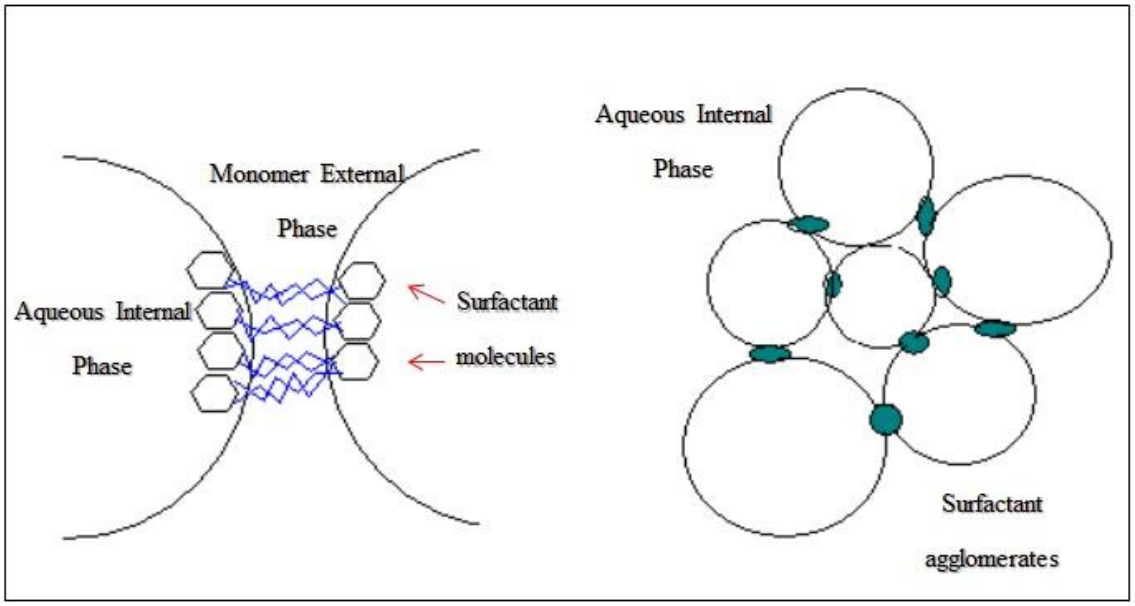

Figure 2.14: The formation of pores in PHP by surfactant molecules (Bhumgara, 1995).

2.3.2 *HIPE Composition*

Two immiscible liquids are needed for preparing the HIPE emulsion, where the aqueous phase is normally used for the dispersed phase, and organic liquids (oil phase) as the continuous phases. Styrene, a water-immiscible monomer is widely used in most W/O emulsions and comprises around 70-78% of the total volume of the oil phase (Akay *et al*., 2005a). A combination of styrene and divinylbenzene (cross-linking agent) produces a brittle polyHIPE with strong hydrophobic properties, but easily fragments to particles under mechanical stress (Cameron and Sherrington, 1997). However these properties can be altered and a rigid or elastomeric polymer is achievable by varying the ratio of styrene to cross-linking agents. Attempts have been made to use other hydrophobic monomers such as 2-ethylhexyl acrylate (2-EHA) and butyl acrylate (BA) to modify the physical and chemical properties of the polymer. Nevertheless, the selection of the monomer for HIPE preparation is based on a few criteria such as:

- the rigidity of the polymers will depend on the type of monomer. A straight chain, cross-linked polymer possess a rigid characteristic, while elastomeric properties can be achieved using monomers that can create a highly branched polymer.
- the monomer must be immiscible with the dispersed phase.
- the temperature required for the polymerisation process must be less than the boiling temperature of the internal phase.
- the polymerisation should start immediately after the emulsion is formed and must not produce any unnecessary by-products than may cause breakage of the emulsions.

Divinylbenzene (DVB) is the most used cross-linker, and its role is for enhancing the stability of the polymer structure. Cross linking prevents the polymer from swelling when in contact with the solvent, or from collapsing after polymerisation. DVB is normally used in smaller portions, but can range between 8%-100%. Any type of cross-linker can be used, provided that it is not highly hydrophilic, otherwise it will dissolve when in contact with water, therefore distorting the stability of the HIPE (Cameron *et al*., 1996). Increasing the ratio of DVB enhances the polyHIPEstability

with smaller pores and increases the surface area, but, on the other hand, reduces its mechanical properties (Hentze and Antoinietti, 2002; William *et al*., 1990; Barbetta *et al*., 2000). Another cross-linking agent, 4-vinylbenzyl chloride (VBC) was reported to produce a stable emulsion that is better than DVB, because it reduced the interfacial tension between the phases (Barbetta *et al*., 2000; Cameron and Barbetta, 2000). Figure 2.15 illustrates the reaction between DVB and styrene to yield a polyHIPE block.

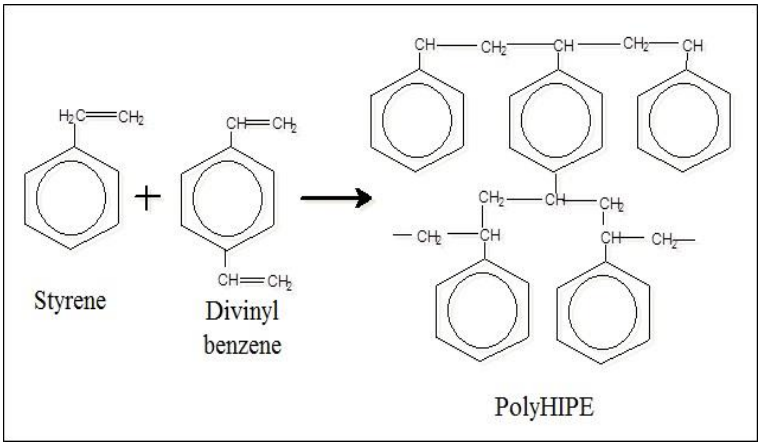

Figure 2.15: Polymerisation reaction between styrene and DVB.

Other important chemical in HIPE preparation is initiator. It can either be oil or salt based, and can be added either to the oil or the aqueous phase, respectively. Williams *et al*. (1990) suggested that oil initiators (lauryl peroxide) can be used to obtain a polymer with large pore size. The use of salt, e.g. potassium persulphate and calcium chloride dehydrate, produces a polyHIPE with a smaller pore size compared to PHP using the oil initiator. The salt helps to stabilise the emulsions by suppressing the effect of Ostwald ripening, thus, produced smaller pores and interconnects (Menner *et al*., 2008; Cameron and Sherrington, 1997). Increasing the salt concentration produces a polyHIPE with a smaller pore size.

The surfactant is grouped under hydrophile-lipophile balance (HLB) numbers, which indicates the ratio of its hydrophile-lipophile content. Ranging from 0-20, the number is an indicator showing the level of the most hydrophobic to the most hydrophilic surfactant. The types of surfactants will determine the types of emulsion

produced, either W/O or O/W emulsions. In general, a surfactant with HLB numbers ranging from 3-6 is recommended for W/O, and 8-18 are best for the O/W emulsion because it has more active hydrophilic groups. An example of a highly hydrophilic surfactant is the sodium dodecyl sulphate (SDS) used for the preparation of O/W emulsions, while Span 80, or sorbitan monooleate as depicted in Figure 2.16, is the common surfactant used in most W/O emulsions (Akay *et al*., 2005c; Cameron *et al*., 2005).

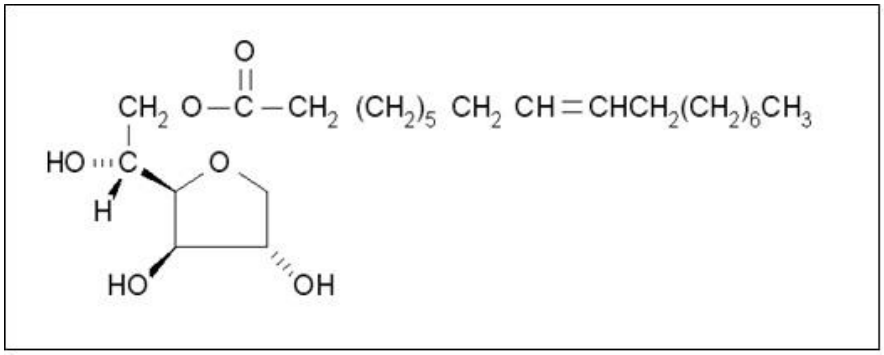

Figure 2.16: Chemical structure of Span 80.

Since the polymerisation process is time-consuming, and normally takes 3 to 8 hours, a proper selection of the surfactant is often critical to ensuring the stability of the emulsion as well as to be able to withstand the polymerisation temperature (60^{o}C), ultimately producing a well formed polymer. Selection of the surfactant in HIPE preparation is very important in determining the emulsifying power. It also differs according to the type of emulsion that is required from the process. There are some criteria for choosing a surfactant such as:

- It must have a suitable migration rate to the interface to overcome the interfacial tension during HIPE preparation.
- It must be able to form a condensed film between itself and water/oil (monomer/cross-linking agent) molecules.
- It must have a good surface activity and produce low interfacial tension within the emulsion

2.3.3 *Operating Variables for HIPE Preparation*

The preparation of high internal phase emulsion (HIPE) was divided into two stages. The first stage involved the dosing of the dispersed phase into the continuous phase, followed by the second stage, where further mixing is carried out upon completion of the dosing. The mixing time was varied accordingly in order to achieve the desired size of the aqueous phase droplets in the emulsion. The relative dosing rate which has the dimension of deformation rate is used to characterise the dosing rate of the aqueous phase:

$$R_D = \frac{V_A}{T_D V_O} \qquad \text{Equation 2.1}$$

where:

R_D = dosing rate, (min^{-1})

V_A = volume of aqueous phase (ml)

V_0 = volume of oil phase (ml)

T_D = dosing time (min)

The total mixing time is defined as:

$$T = T_D + T_H \qquad \text{Equation 2.2}$$

where:

T = total mixing time (min)

T_D = period of dosing process (min)

T_H = mixing time (min), the prolonged mixing time

The mixing rate is defined as:

$$R_M = \frac{D_i}{D_O}\Omega \qquad \text{Equation 2.3}$$

where:

R_M = mixing rate (rev/min)

D_i = diameter of the impellers (cm)

D_0 = diameter of the batch vessel (cm)

Ω = rotational speed of the impellers (rev/min)

HIPE cannot be formed at a relatively large dosing rate and small mixing rate. Under this condition, dilute internal oil in water (O/W) is formed instead of a stable viscous HIPE emulsion. The stability of the HIPE formed is crucial to avoid phase separation during the polymerisation process. In some cases, where the dosing rate is very small, further mixing is not required to stabilise the emulsions.

2.3.4 *Morphology and Physical Characteristics of PolyHIPE*

In a stable emulsion, the aqueous droplets are separated from each other by the continuous phase, and each droplet creates a pore after being polymerised. In some cases, where the oil phase that surrounds the aqueous droplets becomes very thin or else ruptured, it will cause the coalescence of two or more adjacent droplets, thus producing larger pores, called coalescence pores. Its size is dependent upon the size of the primary pores. Besides this, the unreacted chemical that was leached out during washing generates much smaller interconnects on the polyHIPE wall, often known as nano-pores. Therefore, the morphology of PHP is often very complex, and consists of numbers of large and small pores which are connected by varying sizes interconnects (Figure 2.17).

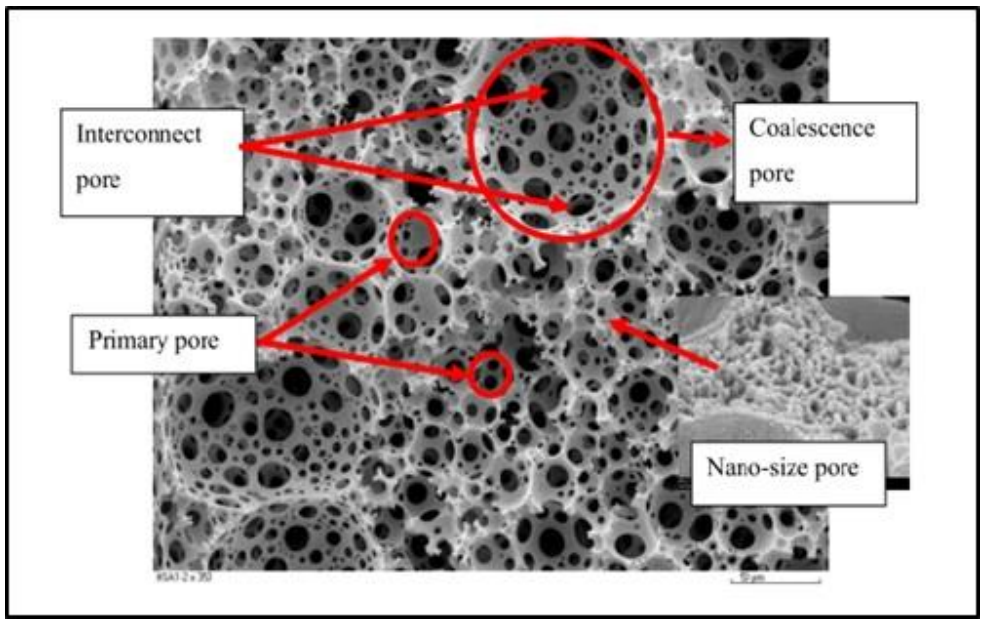

Figure 2.17: Structure of polyHIPE displaying a variety of pores and interconnects (Mohamed, 2011).

PolyHIPEs can be used in many different applications which require them to have different morphology and properties. Two important properties: i) surface chemistry and ii) pore/interconnect size can be altered by adjusting the chemical and physical parameters. Chemical control can be done by either: i) adjusting the proportions of the two phases; ii) adjusting the individual components in the oil and the aqueous phase or iii) using different ingredients, while physical control can be carried out by adjusting: i) the time of dosing the aqueous phase into the oil phase; ii) the mixing period; iii) the emulsification temperature and iv) the mixer speed. Variation of pore sizes can be achieved in a range of 1- 200 μm, and can reach up to 500 μm (Akay *et al*., 2005). PolyHIPEs with extremely large pores can be achieved by promoting coalescence, i.e. the swelling and collapsing of two primary pores. This can be achieved by adding fillers into the continuous phase. Filler is not involved in the polymerisation and can be leached out during polymerisation and washing, which will provide additional nano-porosity to the wall as mentioned previously. At much higher concentrations, fillers will alter the stability of the emulsion, which promotes the coalescence of primary pores, creating larger pores. Therefore, the resulting polyHIPEs can have very large pores, which can approach several millimetres, and are usually dispersed within the primary pores (Akay *et al*., 2005a). Some examples of fillers/oil additives are sodium carboxymethyl cellulose (CMC) and polyethylene oxide (PEO) which produce a wide range of pore size, ranging from 12 – 4300 μm (Akay *et al*., 2005a). An illustration of the coalescence pores formed within the primary pores is shown in Figure 2.18 (c) and (d).

The amount of aqueous phase used determines the porosity of the polyHIPE. However, an accurate calculation of the porosity percentage must include the amount of surfactant or fillers, as all these substances will be washed away during washing and leave voids in the polyHIPE wall. Due to this, the actual porosity of the polyHIPE can reach as high as 99%. Apart from the open structured polyHIPE, this material can be produced with a closed cell structure, as shown in Figure 2.18 (b).The closed structured polyHIPE has higher densities than the open cells, and can be prepared by lowering the surfactant composition to less than 5% of the oil phase volume (Cameron, 2005).

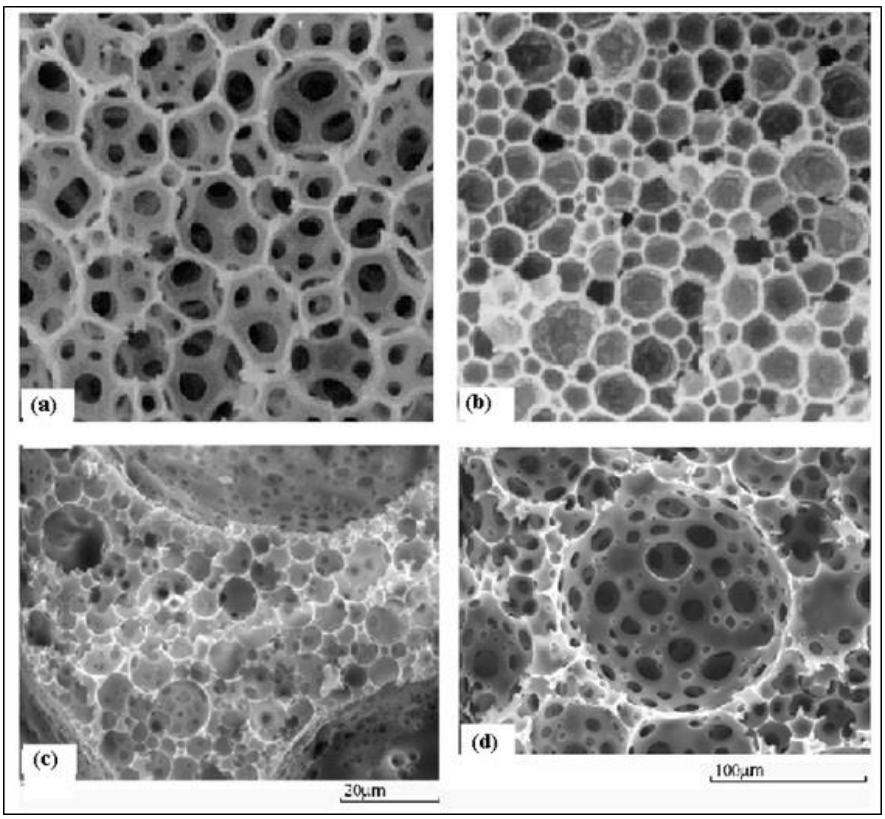

Figure 2.18: Basic polyHIPE structures: (a) Primary pores with large interconnecting holes; (b) primary pores with nano-sized interconnecting holes; (c) large coalescence pores (three such pores are partially shown) dispersed into the primary pores in the process of coalescence ; and (d) detail of the coalescence pores (Akay *et al*., 2005a).

The time of mixing and the emulsification temperature can be adjusted to achieve variety of pore sizes. Figure 2.19 shows the effect of the mixing time and the emulsification temperature on the average pore size of the polyHIPE (Akay *et al*., 2005a). Prolonged mixing produces smaller pores, while increasing the emulsification temperature produces the opposite effect. Reffering to Figure 2.19, increasing the mixing time beyond 60 minutes imposes a negligible effect on the pore sizes, but produces a thicker emulsion. On the other hand, an increased intensity of mixing by increasing the impeller speed has been reported to give high quality emulsions, with a homogenous pore size (Sherma, 1968). A later study carried out by Lepine *et al*. (2008) revealed that the effect of the mixing intensity on the reduction of pore and interconnect sizes was more pronounced compared to the mixing time. As an example, a polyHIPE with average pore size of 1.3 μm was achievable within 35 min using a mixing rate at 22 min^{-1}. However, when the mixing intensity was reduced to 14 min^{-1}, 300 min was needed to obtain a polyHIPE with similar pore size. The average pore size was also

affected by the fraction of the aqueous phase in the HIPE, which shows a reduction in size at high water content, while other parameters were held constant (the time and degree of mixing) (Figure 2.19). On the other hand, the pore sizes increased steadily when the temperature was increased from 30 – 80^{o}C (Figure 2.20). The increase of the pore size at high temperature was correlated to the increasing solubility of the surfactant in the organic phase and enhancement of droplet coalescence. However, the temperature has to be controlled below the boiling point to avoid evaporation of the phases during emulsification.

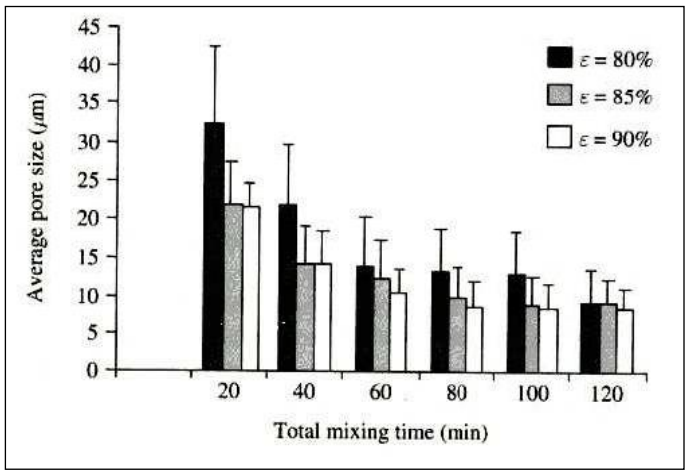

Figure 2.19: The effect of mixing time (t) versus pore size (D) as a function of dispersed phase volume fraction (ε). Dosing time = 10 min, impeller speed Ω = 300 rpm, emulsification temperature T = 25ºC (Akay *et al*., 2005a).

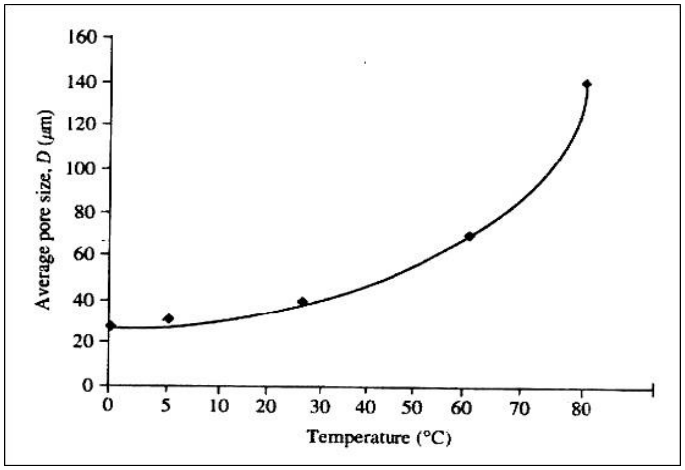

Figure 2.20: Variation of average pore size at varying emulsification temperatures at fixed dosing time = 40 s, mixing time = 100 s, mixing speed = 300 rpm, phase volume = 90 %. (Akay *et al*., 2005a).

Apart from all the physical parameters mentioned above, the type of moulding case was also reported to influence not only the surface morphology of the polyHIPEs but also the HIPEs stability (Cameroon, 2005). The moulding case which is usually made either from glass, PTFE or polyvinyl chloride (PVC) plastic; exhibited different interactions with the polyHIPEs.

2.3.5 *Post Modification of PolyHIPE Surfaces*

Post-modification of the surface chemistry of the polyHIPE can be carried out, provided that the interconnects are large enough to ensure the smooth penetration of the coating material within the interior cavities of the polyHIPE. The coating materials were introduced for various purposes such as to improve the surface characteristics (e.g. hydrophobic/hydrophilic), increase the biocompatibility or its mechanical strength. For example, hydroxyapatite was coated to the polymer surface to increase the osteoconductivity of the osteoblast tissue into the matrix (Bokhari, 2003). Bhumgara (1995) introduced a method to produce hydrophilic sulphonated polyHIPEs with high water absorption capacity from the styrene-based hydrophobic polymer. It was achieved by the soaking the polymers with sulphuric acid, following incubation in a preheated oven at various temperatures and periods. The sulphuric acid migrated and attached to the benzene rings and produced $-SO_3$ groups. The reaction of clean dried PS-DVB HIPE with sulphuric acid is shown in Figure 2.21 below:

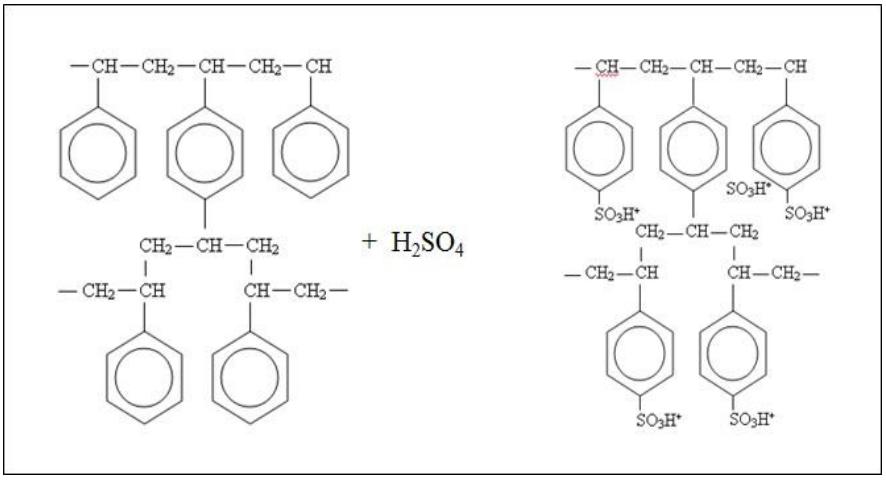

Figure 2.21: Reaction of PS-DVB polyHIPE with concentrated sulphuric acid.

Post treatment with the sulphuric acid produced a polymer with different surface characteristics. Its hard surfaced structure became soft and spongy, and the pores size enlarged compared to its original diameter. It also changed its properties, from highly hydrophobic to highly hydrophilic. Its wetting ability was also very high and could absorb water at approximately 10-20 folds more than its own weight. The hydrophilic and wetting ability properties were due to the addition of charged sites (SO_3^+) that attached to the polymer surface and which can be easily hydrolysed by aqueous solution (Bhumgara, 1995). The degree of sulphonation, however, is highly associated with the degree of exposure (microwave irradiation), the concentration of sulphuric acid and the rate of sulphuric acid migration. Therefore, there were some locations in the polyHIPE (interior parts) that were not sulphonated and remained hydrophobic.

Improving on the above process, Akay *et al*. (2005) and Ndlovu (2009)/Burke (2007) employed a much simpler and faster method to produce a spongy, hydrophilic polyHIPEs. Sulphuric acid was introduced into the aqueous phase, thus producing a readily hydrophilic polyHIPE. However, in order to increase its wetting capability, these polymers need to undergo a similar treatment as mentioned previously, but instead of going into the oven, these polyHIPEs were irradiated intermittently using a microwave. This process not only produced a superior hydrophilic polyHIPE by uniform sulphonation, but also cut the lengthy operation proposed by Bhumgara (1995). Apart from sulphonation, the polyHIPE has also been functionalised through nitration and bromination (Cameroon *et al*., 1996). Although post modification is possible, homogenous post modification is hard to achieve for a bulky and thick sample (Akay *et al*., 2005a).

2.3.6 *Application of PolyHIPEs*

PolyHIPEs have found wide uses in diverse areas. Table 2.2 lists some of the applications in the various fields of biotechnology and bioprocessing.

Table 2.2 Application of PHP

Area	Types of PHP	Remarks	References
Tissue Engineering	PS-DVB PHP coated with HA/incorporation RAD16-I peptide hydrogel	-Increased biocompatibility of cell-PHP, cells differentiation and cell penetration	Akay *et al*., (2005c); Bokhari *et al*., 2005; Akay *et al*., (2004)
Waste water treatment	PS-DVB PHP in packed bed bioreactor	- Removal of phenol by immobilized *S.cerevisiae* -Operated up to 120 days -cell colonised the top surface - Gas build up reduces column efficiency	Erhan *et al*., (2004)
Phenol degradation	PS-DVB microreactor in monolithic form	-Monolayer growth was obtained with D = 25 μm -Stable up to 30 days -Efficiency increased by 20 fold compared to packed bed	Akay (2006)
Agriculture	Sulphonated PHP	-Impregnation of bacterial suspension increased crops yield - Acted as a slow release fertilizer and water storage	Burke *et al*., (2006), Fleming 2012.
Biodiesel	PS-DVB PHP in packed bed reactor	-Simple configuration and stable -Reusable enzyme with stable production was achievable up to 10 repeated batch reaction.	Dizge *et al*., (2009); Dizge *et al*., (2009a)
Ethanol production	PS-DVB PHP in packed bed bioreactor	-Less diffusional limitation -Stable ethanol production -Reduces cell wash out during continuous operation -Efficient toxic waste and dead cell removal	Karagoz *et al*., (2008)

2.4 Introduction to Ethanol Production

2.4.1 *Ethanol Producers*

Journals and patents have reported many ethanol producing strains of bacteria, and fungi that are capable of producing ethanol. *Saccharomyces cerevisiae*, the most widely utilised in industry, is considered the best organism because of its high yield and robustness. However, its application was found to be limited because of its inability to utilise C5 sugars. This is necessary since feedstock for the ethanol production is undergoing a shift from using food crops (corn and sugar cane) to cheaper lignocellulosic materials, therefore a more robust strain is required to ferment the C5 and C6 sugars that are produced from cellulose and hemicellulose hydrolysis. Apart from this, the new strain must be able to withstand the toxicity effect arising from lignin degradation (Jamai *et al*., 2001). *Zymomonas mobilis* has been reported as the strain with the most potential to replace *S.cerevisiae* because it produces a higher ethanol yield, but its application is still limited because of its narrow sugar selection. Table 2.3 lists some of the reported ethanol producers.

There are some basic requirements that must be fulfilled for selecting a microorganism as an ethanol producer, such as (Dien *et al*., 2003):

- Ethanol yield must be more than 90% of theoretical
- Ethanol tolerance must exceed >40 gL^{-1}
- Ethanol Productivity > 1 $gL^{-1}h^{-1}$
- Robust, require inexpensive medium formulation with various substrate.
- High resistance to inhibitors and osmotic stress (high sugar concentration)
- Able to grow in acidic environment and higher temperatures
- Elimination of by-product formation (Kunz, 2008)

Table 2.3 Lists of the ethanol producer and its advantages and disadvantages.

Microorganism	Advantages	Disadvantages	References
Saccharomyces cerevisiae	▪ Considerable high ethanol yield ▪ Fast growth ▪ Robust ▪ Stable ▪ High tolerance to inhibitor	▪ Growth related production ▪ Susceptible to high ethanol concentration ▪ Limited substrate ▪ Contamination	Karagoz *et al*., (2008); Kunz (2008); Balat *et al*., (2008)
Zymomonas mobilis	▪ Produce less biomass ▪ Higher yield (5-10% more ethanol per g glucose) ▪ High tolerance towards ethanol (up to 120 gL^{-1}). ▪ High productivity ▪ Safe	▪ Ferments only glucose, sucrose and fructose ▪ Low tolerance to acetic acid ▪ Unstable	Amin and Verachtert, (1982); Delgenes *et al*., (1996); Kesava *et al*., (1996); Dien *et al*., (2003).
Klebsiella oxytoca	▪ Able to grow in acidic pH and higher temperature. ▪ Utilises wide range of sugars (C5-C6)	▪ Yields many by-products ▪ Low ethanol yield	Dien *et al*., (2003)
Recombinant *Escherichia coli*	▪ Able to ferment various sugars ▪ Produce less biomass compare to *S.cerevisiae*	▪ Low tolerance to pH (6.0-8.0) ▪ Less hardy cultures ▪ Problems with biomass and public perceptions	Dien *et al*., (2003).
Candida tropicalis	▪ Thermotolerant ▪ Able to ferment various carbon sources (alcohols and sugar) ▪ Ability to tolerate lignin like-polyphenols	▪ Lower productivity compared to *S.cerevisiae.* ▪ Lower tolerance towards ethanol ▪ Slow adaptation to anaerobic condition	Jamai *et al*., (2001); De Deken (1966).
Pichia Stipitis	▪ Able to ferment C5-carbon source	▪ Low yield	Balat *et al*., (2008);

2.4.2 *Yeast~ Saccharomyces cerevisiae*

Yeast, *Saccharomyces cerevisiae* as depicted in Figure 2.22, has been the major microorganism used in ethanol production. Yeast is a unicellular microorganism which belongs to the fungi group. Typical yeast shapes are either spherical or oval, with clear internal cell structures. Most yeasts are unicellular and their size can vary from 3-5 μm in diameter, although some can reach 7 μm. Yeast grows normally by budding (the common *S.cerevisiae*), but very rarely can multiply by binary fission as in *Saccharomyces pombe*. The yeast surface is normally negatively charged and it can be easily immobilised on solid surfaces. Yeast in general is hydrophobic therefore it prefers hydrophobic surfaces, and attaches weakly to hydrophilic surfaces (e.g. glass). However, stronger adhesion of the yeast to surfaces can be achieved by introducing electrostatic interaction between the yeast and the solid surfaces (Norton and D'Amore, 1994).

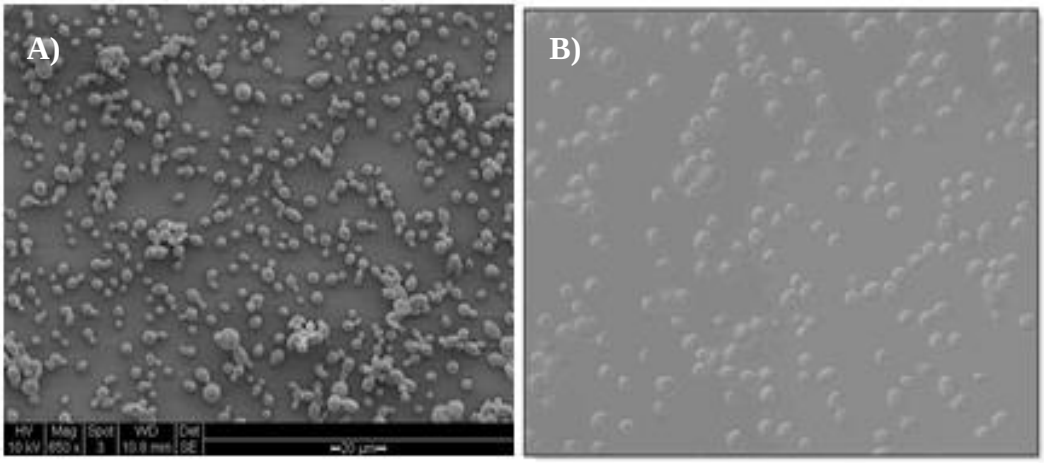

Figure 2.22: The shape of *S. cerevisiae* W303 examined under a) SEM using 650x magnification (Scale bar – 20 μm) and b) fluorescent microscope.

S.cerevisiae consists of vacuole, mytochondria, cytoplasm and nucleus, as depicted in Figure 2.23 (Werner-Washburne *et al*., 1993). The outer membrane is made of glucan, β-1,4 and β-1,3 linked polysaccharides. Its surface is covered with protein and peptidoglycan, which results in its hydrophobic properties. The surface protein also results in a negatively charged surface in *S.cerevisiae*, but can vary significantly

depending on the environment (medium types), pH and ionic strength. The surface charge of the yeast is also dependant on the age, and normally loses its negativity as it enters the stationary phases. The dead cells of yeast are generally neutral in charge.

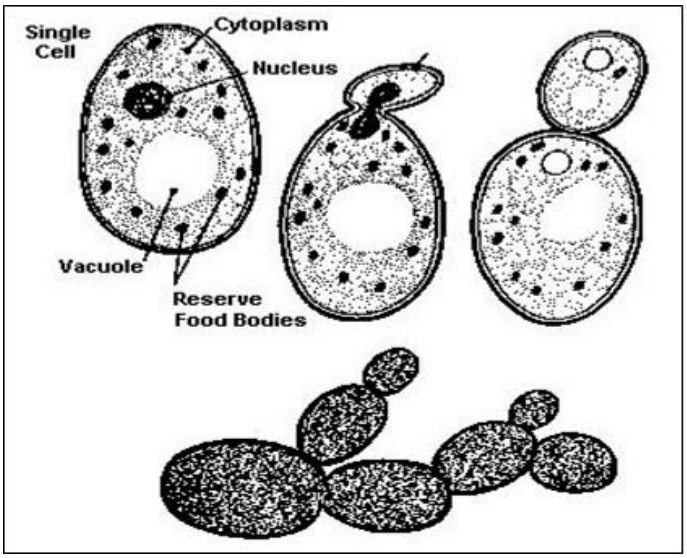

Figure 2.23: Schematic diagram of *S.cerevisiae*

Yeast converts glucose to ethanol in the glycolysis cycle (Figure 2.23) in the absence of oxygen and yields two moles of adenosine triphosphate (ATP) and CO_2 as by-products as shown in Equation 2.4;

$$C_6H_{12}O_6 \rightarrow 2C_2H_5OH + 2CO_2 + 2ATP \qquad \text{Equation 2.4}$$

The best feature of wild *S.cerevisiae* is that it can produce ethanol in both aerobic and anaerobic conditions, although the preference is with the availability of oxygen (van Maris *et al*., 2006). *S.cerevisiae* produces ethanol through the Embden-Meyer pathway (EMP). The ATP produced from the reaction above will enter the tricarboxylic acid (TCA) cycle and electron exchange route, and yield new cells in the presence of oxygen (Figure 2.24).

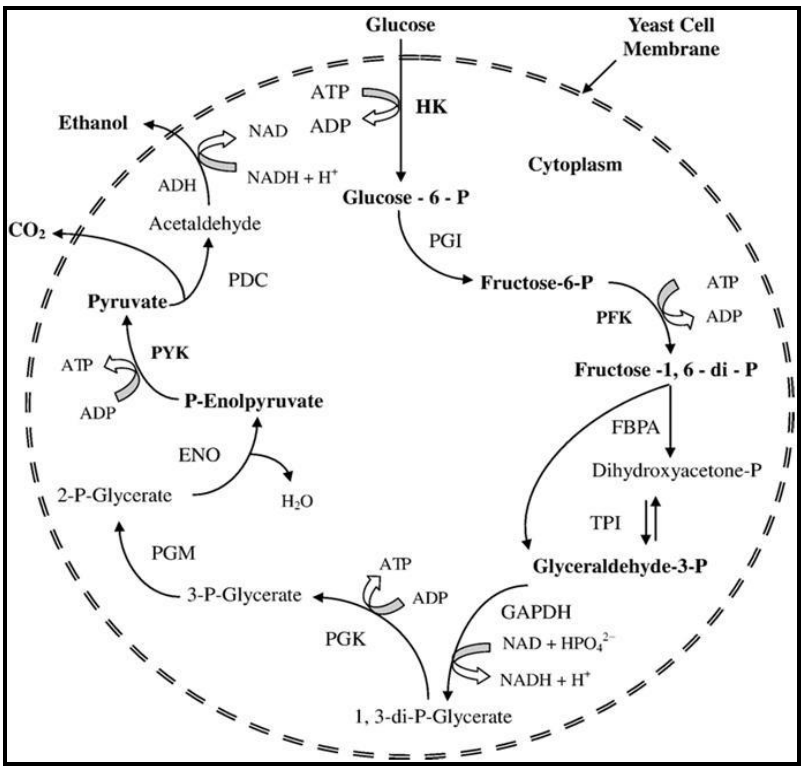

Figure 2.24: Metabolic pathway of ethanol fermentation in *S. cerevisiae* utilising the EMP route (Bai *et al*., 2008).

Although the ethanol production can also occur in anaerobic conditions, a small amount of oxygen is necessary for the maintenance of cellular processes, lipid biosynthesis and the growth of new cells. A complete absence of oxygen for a long period will retard the cells' viability. Depletion of oxygen results in an accumulation of unused ATP which inhibit the production of phosphofructokinase, thus impeding the overall glycolysis process. The growth is gradually reduced and therefore this to some extent reduces the ethanol production. The theoretical yield for the ethanol based on the glucose consumption is 0.51 gg^{-1} and for synthesis and evolution of CO_2 is 0.48 gg^{-1}. The optimal temperature for the yeast activities was observed at 30^{o}C-35^{o}C. However, some thermophilic yeast requires a higher temperature which may range from 50-60^{o}C to maintain its metabolic activity. Optimal growth is achieved in a slightly acidic environment, with pH ranging from 4-5.5, which helps to prevent contamination by other organisms (Yang and Khan, 1994). However, yeast can tolerate pH below 4, and therefore this presents a method of minimising the loss due to bacterial contaminants, because bacteria grow best at pH range 6.5 to 7.5. If the yeast growth can be optimised at this lower pH, it would be possible to eliminate the need for sterilisation (Balat *et al*., 2008). Furthermore, *S.cerevisiae* is able to survive in a nutrient-deprived environment

for up to 3 months, and can easily regain the characteristics when re-cultured in a nutrient-rich medium (Werner-Washburne *et al*., 1993).

Apart from its two major by-products (biomass and CO_2), glycerol, acetaldehyde, succinic acid and acetic acid are often produced simultaneously. The production of these metabolic acids will reduce the pH of the medium, and thus will retard the growth of yeast. The production of these metabolites is lower in the immobilised cells compared to the free cells, which corresponds to the varying changes observed within the cytoplasmic pH of the immobilised cell (Norton and D'Amore, 1994).

S.cerevisiae has been successfully employed in industry, but further improvement is still desirable with respect to increased productivity, stability and tolerance towards stressors. Improvements are still evolving and relying on the random mutagenesis, classical breeding and genetic crossing of two strains and a successful strain with the previously mentioned qualities will be selected for the optimisation Kunz, 2008). Much work has been carried out to introduce the pathways for xylose and arabinose utilisation in *S.cerevisiae* in order to increase its substrates range (Fortman *et al*., 2008). Recent studies were also directed to the thermotolerant strains, because high temperature is needed to withstand the requirement of high temperature (45-50^{o}C) for the saccharification process in the simultaneous saccharification and fermentation (SSF) process (Edgardo *et al*., 2008; Ylitervo *et al*., 2011).

2.4.3 *Factors Affecting Ethanol Production*

Apart from severe inhibition caused by ethanol accumulation, CO_2 production has been reported to repress the growth of yeast, which later reduces the ethanol production. Figure 2.25 summarises some of the possible stresses that have negative impacts on the growth of *S.cerevisiae* and ethanol production.

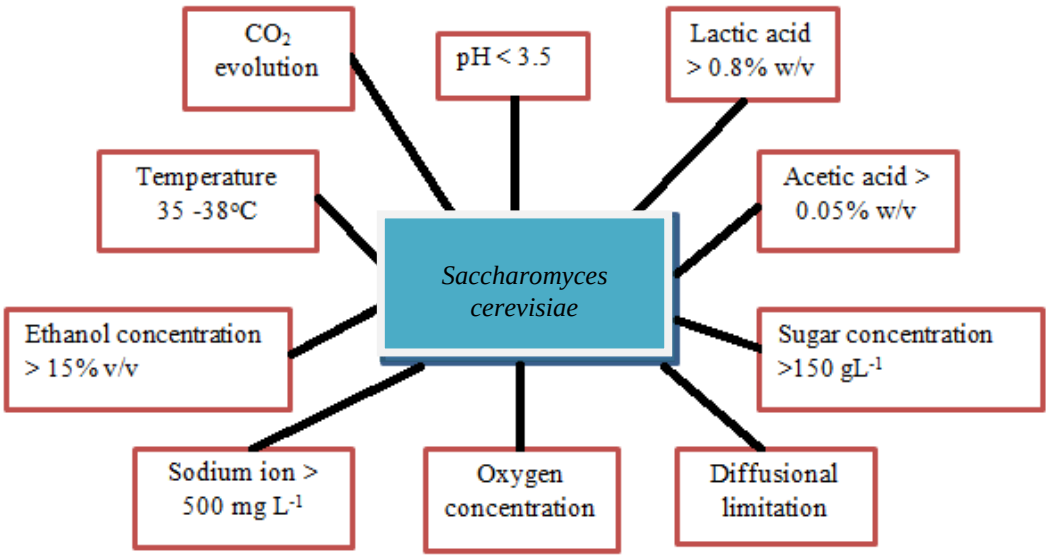

Figure 2.25: Potential environmental stresses on *S.cerevisiae* during ethanol fermentation in both free and immobilised cells (Bai *et al*., 2008).

Ethanol is produced using various operating modes, with typical processing modes of batch, fed-batch and continuous processes. Switching from batch processes to continuous processes needs further study in order to avoid losses and the instability of production. Currently, there are less than 30% of bioethanol plants operating using continuous modes, while the rest still employ either batch or fed batch modes (Brethauer and Wyman, 2009). Table 2.4 below listed some of the advantages and disadvantages of three different types of fermentation modes.

Table 2.4: Advantages and disadvantages of fermentation modes.

Modes	Advantages	Disadvantages
Batch	▪ High yield ▪ Lower risk of infections and microbial mutations ▪ Low risk of by-product formation	▪ High capital cost and controlling expenditure ▪ Extra cost for the non-productive time (loss 20%), which include cleaning, inoculum preparation, heating, sterilising
Fed-batch	▪ High flexibility with reduced non-productive time ▪ Considerable high yield with well-defined fermentation time. ▪ Easier control for optimisation of the process conditions	▪ Labour intensive ▪ High instrumentation and controlling expenditure ▪ Lower risk of infections and microbial mutations
Continuous	▪ Lower capital cost with reduced non-productive time ▪ Steadier process with constant product quality ▪ Biomass concentration can be control by supply of growth component or the dilution rates ▪ Substrate limited growth can be maintained and changes in cell composition and metabolic activity can be studied by changing the growth limiting nutrient ▪ By the pulse and shift technique, medium composition can be optimised for biomass and product formation. This technique uses injection (pulsing) of nutrient directly into the chemostat and observing changes in biomass and substrates. ▪ Higher productivity with per unit volume or per unit time.	▪ Need for stable raw material quality ▪ High fermentation/growth rate –difficulties in controlling and maintaining the yield ▪ Susceptible to microbial fermentation ▪ Higher risk of microbial mutation due to prolonged operation and can result in loss of the original strain owing to take over by fast growing strain (contamination). ▪ Wall growth and cell aggregation can prevent true steady state ▪ Wash out problems lead to low reactor productivity

2.5 Immobilisation

2.5.1 *Importance of Immobilisation*

Immobilisation techniques have been widely utilised for various biotechnology purposes including enzyme production, chemical production, and tissue engineering. Various methods have been utilised including adsorption, entrapment, containment behind a barrier or cell aggregation (Verbelen, 2006). The importance of the immobilisation system is to increase the concentration of cells within the reactor volume, hence increasing the product formation. Whole cell immobilisation is defined as the localisation of intact cells in the physical containment in a certain defined region and the sustaining of the cell catalytic activity after the immobilisation process (Karel *et al*., 1985). The immobilisation process creates a microenvironment that refers to the entrapped fluid within its porous structure which might be different from the original bulk solution (Figure 2.26). There are three important aspects involved in immobilisation systems: i.e. the cells, supports and the microenvironment or the liquid within the matrix.

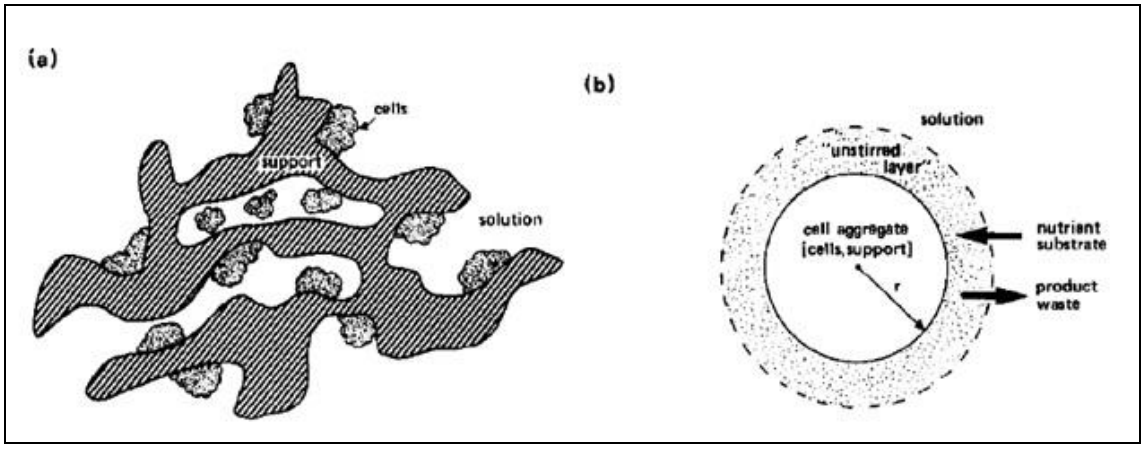

Figure 2.26: a) The three phases that comprise the immobilisation cell, which are the cell, matrix, and interstitial fluid. b) Schematic representation of the immobilisation cell system. (Karel *et al*., 1985).

The benefits of the immobilisation process in microbial fermentations are as follows (Kargi, 2001; Karagoz *et al*., 2008):

- ❖ Produces high cell concentrations that maintain high productivity throughout the operation period, and avoid wash out during high dilution rate.
- ❖ Provides protection for the cells from the harsh environment and is highly beneficial to shear sensitive organisms when operating at high dilution rates.
- ❖ The supports are stable and resistant to extreme environments such as pH, temperature, and toxic metabolites.
- ❖ Attachment of the cells to the polymer matrix changes the physiological properties of the biocatalyst, which normally are more stable compared with free cells, to overcome the inhibition during fermentation.
- ❖ Facilitates the development of a microenvironment which reduces the barrier in mass transfer, increases cell-cell interaction, and also improves the biocatalyst performance.
- ❖ The immobilized cells are stable and can be re-used, thus reducing the cost and time for preparation.

A major disadvantage of the immobilisation process is the additional resistance of flow created by the matrix (Erhan *et al*., 2004). Aerobic processes will suffer from oxygen limitation due to low solubility which might be the rate limiting factor in such processes. However, the use of highly porous structures may improve the mass transfer of substrates and the products from the matrix cavity (Margaritis and Kilonzo, 2005).

2.5.2 *Existing Immobilisation Techniques in Yeast Fermentation and the Production of Ethanol*

Yeast can be immobilised by various techniques such as entrapment within the porous structure (Tyagi *et al*., 1992; Birol *et al*, 1998a; Koyama and Seki, 2003), encapsulation (Peinado *et al*., 2006), adhesion of cells onto a solid surface (Tyagi *et al*., 1992) and self-flocculation. The stability of microbial cells and enzymes is often challenged in the solvent solution, so the immobilisation technique offers protection

against the denaturation of the microbial cells/enzymes, thus prolonging their life-span (Fukui and Tanaka, 1982).

Polyacrylamide gel has been reported to be a potential support for yeast encapsulation because of its considerable mechanical strength, but the remaining reactive monomers in the beads cause deactivation of the enzymes and cells thus limiting its uses (Fukui and Tanaka, 1982).The alginate beads are preferred compared to other gel entrapment techniques due to the milder processing conditions, and the cells retain their cellular viability after the immobilisation procedure, therefore permitting multiple uses of this system (Birol *et al*., 1998). This system reduced the effect of the high substrate concentration, subsequently encouraging growth. The beads allow product diffusivity due to its high porosity and wide distribution of pore sizes. Nonetheless the poor mechanical strength of the alginate beads was considered as the main drawback of this approach. The lack of spaces for cell proliferation and osmotic action after the long operation hours caused the bursting of beads and cell leakage (Koyama and Seki, 2003). The evolution of CO_2 contributed to the thinning of the gel wall and caused a severe bursting effect. A study performed by Tyagi *et al*. (1992), reported that the entrapped *S.cerevisiae* cells suffered from the limitation of mass transfer, thus resulting in a lower sugar uptake and a reduced ethanol formation rate.

A study of the effect of immobilisation by the yeast flocculation technique has been performed by Baptista *et al*. (2005). A comparison study was carried out to test the effect of immobilisation in a packed bed reactor. It was found that highly flocculated cells produced a higher ethanol concentration (40 gL^{-1}) than less flocculated cells (28 gL^{-1}). However, the highly flocculated cells tended to block the column and could only achieve 192 hours of steady production, whereas the latter could prolong its steady production for up to 576 hours. It would be necessary to provide a packed column with high porosity so that some of the flocculated cells could be flushed off, while retaining some of the viable cells in order to maintain a high productivity of ethanol for a longer operating period.

Apart from the study using whole yeast cell immobilisation, Murata (1993) performed a comparison study on the effectiveness of immobilisation using either intact yeast cells or yeast spores. During ten consecutive runs, the immobilised spores had shown a stable pattern of fermentative activity, reflected by a stable ethanol production during the fermentation. On the other hand, fermentative activity by intact cells showed a gradual increase of ethanol production initially, but at the end of fermentation they lost 40% of the initial activity resulting in a lower ethanol production.

A newly introduced 3-D hydrophobic polyHIPE has been successfully utilised for ethanol production by Karagoz *et al*. (2008). The hydrophobic nature of the polyHIPE created a strong bonding with the *S.cerevisiae* (Karagoz *et al*., 2008). Although successful immobilisation was achieved, little growth was observed within the interior region. This might be due to small interconnect sizes, which inhibit the mobility of cells towards the central part of the polyHIPEs. Messing *et al*. (1979) stated that the interconnect size must be large enough to allow the penetration of cells within the polymer matrix, but at the same time must hinder the leakage of the viable cell. Earlier studies suggested that an appropriate pore size for yeast immobilization was 1 - 4 times bigger than the size of the mature cells, but Hough *et al*. (1991) suggested that the optimal values should be in the range of 6 - 12 times. High porosity materials can maintain the dynamic flow inside the polyHIPE which can prevent the formation of biofilm, besides ensuring efficient removal of toxic metabolites and dead cells. Norton and D'Amore (1994) emphasised that it is necessary to ensure a monolayer growth on the carrier matrix to remove the effects of mass transfer resistance, and this can be achieved by preparing a large surface area for cell proliferation.

The use of a microporous polymer made from HIPE emulsion as a solid support for yeast has been used in a packed bed reactor system (Hough *et al*., 1991; Karagoz *et al*., 2008) for the production of ethanol. The usage of a microporous polyHIPE has been claimed to have advantages over previously mentioned methods such as:

- The size of voids and interconnects can be tailored individually to suit various processes (Akay *et al*., 2005b; Hough *et al*., 1991)

- The porosity can be achieved at very high range, between 74-99%, with preferred porosity between 90-98%.
- The big void and interconnect sizes prevent blockage on the top surface by allowing easy penetration and migration of cells into the support matrix. It also circumvents the mass transfer limitations which generally occur in most support matrices with smaller pores.
- Combination of voids and porosity provides a large surface area for cell attachment between 2 to 200 m^2g^{-1}.
- Fully interconnected pores with appropriate sizes allow easy transport of the gaseous product from the fermentation, and allow easy removal from the system, to ensure large spaces are always available for the reactions. It is also easier to achieve a high loading rate of cell into the support.
- The materials are robust, stable, able to withstand high temperature during sterilisation, mechanically strong, and easily moulded into a variety of shapes and sizes to fit the reactors.
- The surface chemistry encourages the interaction of cells with the matrix surfaces. A strong attachment of the cell reduces cell wash out during continuous operation.

While most studies reported improvements in ethanol productivity and an enhancement of growth by the immobilised technique, a contrasting finding was observed by Jamai *et al*. (2001). No improvement of ethanol productivity was observed using immobilised C*andida tropicalis* and *S.cerevisiae* in calcium-alginate beads compared to the free cells system. Besides this, these immobilised yeasts required a longer time to complete the fermentation compared to free cells.

2.5.3 *Effect of Immobilisations on Yeast Morphology*

Numerous authors have reported that the immobilisation technique has significantly or slightly altered the physiology and the metabolic capacity of yeast compared to free cells. The shape of the cells was also altered due to cytomechanical effects that change the physical appearance from an ellipsoid shape to a rod-shape

(Jirku, 1994). Apart from this, the content of the cell walls, such as surface proteins, lipids and amino acid sugars, is different than that with the free cells. The mechanism of these changes was still unclear and was attributed to either the difference between the microenvironment and the bulk environment, or was caused by a modification of cellular physiology induced by the immobilisation (Norton and D'Amore, 1994). A study performed by Parascandola (1997) revealed the immobilisation and ethanol stress affected the production of glucans and mannoproteins within the cell wall. These substances are known to alter the rigidity and porosity of the membrane cell respectively. Different types of mannoproteins were produced in the immobilised and ethanol stressed cells, but none was found in the free cell suspension with similar stresses. The production of this mannoprotein within the cell wall was associated with the protective response of the immobilised cells to the adverse environment caused by the high ethanol content. A higher content of glycogen and trehalose was also observed in the immobilised cells compared to the free cells (Talebnia and Taherzadeh, 2007). These carbohydrates served as reserve carbon sources and provided protection to the cytosol component against osmotic shock, due to the limitation of nutrients.

2.5.4 *Effect of Surface Chemistry*

Selection of a suitable support depends on two characteristics, which are: i) the adsorption capacity for cells adhesion and ii) the strength of binding (Kilonzo *et al*., 2011). These are the important criteria because they can prevent cell wash out/or dislodgement during the long run of continuous operation. The strong binding of cells can be achieved by ionic binding, which can be carried out by treating the support with an ionic solution. In the case of immobilised *S.cerevisiae* on bagasse, the system using surfaces treated with the aminohexyl group managed to reduce 68% of the cell losses that occurred in the untreated bagasse (Tyagi *et al*., 1992). Furthermore, the treatment also showed a 66% increase in terms of the critical sloughing off velocity due to an improvement of the binding strength. This could be explained by saying that the physical binding has switched to ionic binding, which provides a stronger bond between the cell and the surface matrix. The treatment of bagasse with the aminohexyl group, provides a positive surface charge, which can attract negatively charged *S.cerevisiae*, which then bind strongly to the surface. In contrast to the binding properties, the surface

chemistry using three different support matrixes does not significantly affect the production rate of ethanol (Fujii *et al*., 1999). In addition, the growth of cells in the beads utilising different types of matrix only showed a minor variation. The use of binding agents was just to ensure the availability of the viable yeast within the reactor system, and does not influence the rate of growth or the ethanol productivity.

2.5.5 *Effect of Dilution Rate on Growth and Ethanol Production*

The continuous operation was carried out to reduce the inhibitory effect of ethanol in batch processes, and to offer stability during a longer operating time. Besides this, the reactor performance can easily achieve steady state even after changes in the feed were made in terms of substrate concentration and dilution rates (Melin and Shieh, 1990). Continuous mode is normally operated at the dilution rate, which is slightly lower than the maximum specific growth rate (μ_{max}). However, operating at the dilution rate above the μ_{max} modifies the microbial physiology due to changes in the physico-chemical microenvironment surrounding the cells (Tyagi *et al*., 1992). The highest ethanol production was obtained at the highest dilution rate, but the efficiency of substrate assimilation was significantly reduced. A low dilution rate achieved better substrate consumption and a higher product yield, but took longer time to achieve steady state (Zhao and Lin, 2003). Although operating at high dilution rates shifted the yeast metabolism towards ethanol production, the retention times of the medium in the reactor were greatly impaired, which subsequently reduced the time for the conversion of ethanol. This caused a reduction of ethanol production by half (~34.5 gL^{-1}), as the dilution rate of the feed medium containing 125gL^{-1} glucose was increased from 0.2 h^{-1} to 0.6 h^{-1}(Zhao and Lin, 2003).

The time taken to reach steady state was longer in the immobilised cells compared to the suspended cells because of the additional diffusional resistance in the supports. However, the time can be reduced significantly by intermittent supply of oxygen, which helps to maintain and increase cell growth and viability, subsequently speeding up the ethanol production (Lee and Chang, 1985). Though losses in ethanol productivity were also reported due to the reduction of cell viability, the intermittent

supply of oxygen to the culture helped to prevent this problem. Besides this, employing cell recycling results in an increased ethanol productivity of up to 4.5 times compared to normal continuous production using immobilised yeast (Ghose and Tyagi, 1982).

2.5.5 *Effect of Substrate Concentration on the Growth and Ethanol Production*

A higher ethanol concentration can be achieved by supplying the culture with more glucose. However, to a certain extent, the glucose concentration inhibited both growth and ethanol production. Ethanol production by Very High Gravity (VHG) fermentation using a three serial stage tubular reactor showed significant results concerning the effects of substrates on the cell viability (Bai *et al*., 2004). The viability of *S.cereviase* was lower in the first reactor compared to the second reactor, attributable to the high glucose concentration (280 gL^{-1}) which exerted a high osmotic pressure on the cells and subsequently induced lysis. However, the lowest cell viability was observed in the third reactor due to the accumulation of a high ethanol concentration (nearly 94.7% of the theoretical value), and thus it was concluded that the ethanol toxicity imposed a more severe impact on the cell viability compared to the osmotic effect cause by a high glucose concentration. However, the increased osmolality in the medium was not only caused by a high sugar concentration but also by other minerals which generated the same effect of reducing either the cell viability or the fermentation capability of the cells (Takeshige and Ouchi, 1995).

This finding was also supported by Zhao and Lin (2003) where a reduction of biomass was detected when the sugar concentration in the feed medium was increased from 100 gL^{-1} to 300 gL^{-1}, contributing to the high osmotic effect. However they also found that the viability of cells was not affected, which was in contrast with the study by Thomas and Ingledew (1992), where the number of viable cells decreased with increased sugar concentration. The use of different media accounted for the disparity between these two studies, where the viscosity of the defined medium used by Zhao and Lin was lower which allowed the release of CO_2 from the media broth compared to the media used by Thomas and Ingledew. The ethanol production was also improved from 3.67 gL^{-1} to 40.03 gL^{-1} by increasing the sugar concentration from 10 gL^{-1} - 300 gL^{-1}. In

contrast, the yield coefficient ($Y_{x/s}$) decreased significantly from 0.40 (10 gL^{-1}) to 0.24 (100 gL^{-1}), and the values were not affected after increasing the glucose concentration from 100 gL^{-1} up to 300 gL^{-1} (Zhao and Lin, 2003). This was expected as more substrate was channelled to produce osmoprotectant substances, indicated by the increases in the alanine, proline, glycerol and trehalose concentration. The production of these substances was induced to overcome the high osmotic environments caused by the high sugar concentration. However, the specific functions of these substances were not discussed thoroughly and are still under investigation.

Signs of inhibition were also detected by Karagoz *et al*. (2008) at much lower sugar concentrations. The reactor efficiency decreased at higher glucose concentrations (>150 gL^{-1}), subsequently reducing the ethanol production by the immobilised *S.cerevisiae* in the microporous divinylbenzene (DVB). At this concentration, the substrates' utilisation was reduced due to high osmolality effects. Liu *et al*. (2009) also reported a decrease in ethanol yield when the glucose concentration was increased above 150 gL^{-1}.

2.5.6 *Effect of Ethanol Accumulation on the Growth of Yeast*

The production of ethanol was generally limited to 12-13% (v/v) because of it strong inhibition on growth and ethanol production. The toxicity of ethanol on growth has been reported in many studies, both in batch and continuous processes (Medawar *et al*., 2003). Ethanol affects the solubility of the cell membrane, in which the membrane's permeability is increased by the presence of ethanol. This causes excessive transport of inert and cell components in and out of cell, subsequently altering the cell constituents that are often fatal to the cell. The rapid accumulation of ethanol due to high cell loading can increase cell death.

In a study on the effect of inhibition by ethanol (by increasing the initial ethanol concentration in the medium from 0 gL^{-1} to 85.9 gL^{-1}), not only it prolonged the lag phase but also reduced the final cell concentration (Medewar *et al.*, 2003). No sign of

growth was detected at 91 gL^{-1} of ethanol, suggesting that it was the critical ethanol concentration that inhibits the growth of *Brettanomyces intermedius* in the shake flask culture. Hilge-Rotmann and Rehm (1991) reported that no sign of ethanol inhibition was observed below an ethanol concentration of 100 gL^{-1} for *S.cerevisiae* immobilised either on calcium alginate beads or on a Raschig ring.

2.5.7 *Effect of Carbon Dioxide on Growth and Ethanol Production*

The carbon dioxide produced as a co-by product in the synthesis of bioethanol was assumed in earlier studies to be an inert end product, however later studies have shown that it has a significant influence on cell growth (Norton and Krauss, 1972). A study on the effects of CO_2 discovered that the production of new cells was reduced significantly either by the production of endogenous carbon dioxide during fermentation or by the addition of the gas to the reactor chamber. The multiplication of cells, both by budding and cell division, was completely hindered with the addition of CO_2 up to 40 psi. On the other hand, the DNA content in the cell was increased to double that of the control which resulted in an increase of the biomass, but not of the cell size. However, there are no clear explanations about the inhibition mechanism of CO_2 on the cessation of cell replication, but it showed negligible effects on the replication of DNA.

This finding was supported by a study performed 10 years later by Jones and Greenfield (1982). The same inhibition pattern was observed, in which the cessation of cell replication was observed when the CO_2 concentration was increased in the reactor system; on the other hand there was a marked increase in cell growth. A stronger inhibition towards cell replication compared to ethanol production was observed after introducing carbon dioxide to the reactor. The inhibitory effects of CO_2 at a pressure of more than 0.2 atm were said to affect either or both of: i) the fluidity of the membrane system, and ii) the metabolic activity in the cell. However, the aggravated combined effects of the accumulation of metabolic products, ethanol and carbon dioxide within the reactor system are more severe on cell replication (Jones and Greenfield, 1982). Though inhibition by CO_2 is pronounced, a minimum level of CO_2 was still needed to maintain the cellular activity of *S.cerevisiae* and its viability. Even though the carbon

dioxide inhibition is not regarded as an inhibitory factor, Jones and Greenfield emphasised that neglecting this factor for modelling the growth and ethanol production would be erroneous.

The CO_2 effect has been more profound in the immobilisation system, where its accumulation reduced the reactor performances. The CO_2 which has been produced extensively creates dead zones which restrict the transfer of the medium to the cells. In the biocapsules immobilisation technique, the accumulation of CO_2 resulted in a swelling of the containment, but managed to retain its original size, which demonstrates its elasticity (Peinado *et al*, 2006). The opposite result was obtained when using calcium alginate gel; here the accumulation of the CO_2 caused a bursting of the beads and cells were released to the medium. The weak mechanical strength of the gel prepared from pectin, k-carrageenan and calcium alginate failed to support the expanding of sizes which occurred as a result of: i) a proliferation of cells and ii) an accumulation of CO_2 within the gel matrix. In the bioreactor system using immobilised *Z.mobilis* in pectin beads, the bursting effect was observed as early as 7 hours after the fermentation started (Kesava *et al*., 1995).

As the entrapment of CO_2 within the reactor system may result in dead areas, hence reducing the overall reactor productivity, the dimensions of the reactor used must be of a sufficient size. The use of an appropriate H/D ratio for the reactor design is necessary to minimise the length (distance) for the gas passage throughout the column or reactor. In the case of the monolithic microreactor, the selected size of pore and interconnect must ensure that the collapsing of the nutrient flow and the bubbles will not create much in the way of a dead zone. This can be achieved by increasing the size of the pores and interconnects, but the possibility of cell wash out might happen if the interconnect is too large. However, cell dislodgement can be avoided if a material with good surface chemistry is available. Tyagi *et al*. (1992) observed that the (H/D) ratio of 2.5 was the optimum value for the ethanol production from immobilised yeast, as it promotes better gas migration throughout the column.

2.6 Comparison of Ethanol Production in Various Reactor Designs by Immobilised Yeast

The designs for immobilised bioreactors are complex and the design criteria must suit three distinguishable phases: the solid (carrier/support), liquid (the medium) and gas (air, oxygen, CO_2 and other gases) phases (Verbelen *et al*., 2006). It was almost impossible to design a reactor able to accommodate all the needs and positive improvements for greater ethanol production. Generally, a reactor is only able to tackle one or two issues, for example substrates inhibition favours the fluidised bed reactor, while the packed bed reactor offers less product inhibition (Vega *et al*., 1988). In ethanol production by immobilised cells, the criteria that is neccesary for a good and efficient reactor must allow efficient mass transfer: i) the external and internal mass transfer of the bulk medium to cell and ii) the removal of the respiration and fermentation product (e.g: cells, ethanol, CO_2 etc.). Besides this, the choice of reactor configuration is highly dependent on the type of support. Reactors with a low shear rate are preferable for the mechanically weak support to avoid disruption and instability. Ethanol production using immobilised cells was tested in various reactor designs, and the packed bed bioreactor was the most frequently used type. On the other hand, the packed bed bioreactor is less stable, especially for long-term operation which is highly associated with the mass transfer limitation and CO_2 build up (Amin dan Doelle, 1992). The usage of CSTR, although enhancing mass transfer rates by introducing forced agitation, imposes a very high shear rate that contributes to the disruption of the support especially for those with low mechanical strength like pectin and alginate beads. Five common types of immobilised reactor with different configurations are shown in Figure 2.27. Table 2.6 lists some of the kinetic data for ethanol production, which has been reported in the literature using various reactors.

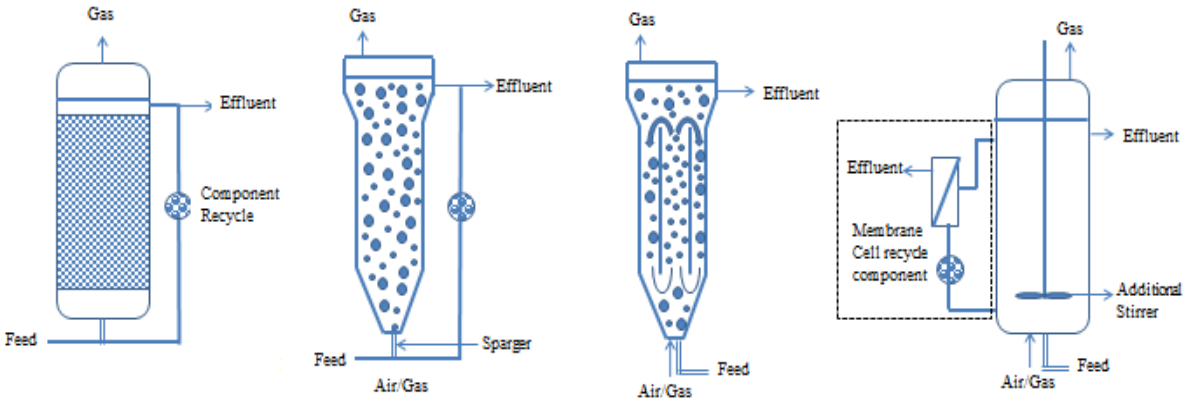

Figure 2.27: a) Packed bed bioreactor; b) Fluidised bed reactor; c) Gas lift reactor; d) Stirred tank reactor and membrane cell-recycle reactor.

2.7 Conclusions

This chapter has reviewed the current energy scenario that creates a new dimension for alternative energies. Ethanol, one of the proposed alternative energies has been thoroughly evaluated in terms of its production techniques and performances. This chapter also covers the aspects of production (yields and productivity), and has evaluated the existing problems with the current technology, especially in the immobilisation system. The problems associated with cell metabolism and low ethanol yield in this system have been explicitly addressed with detailed explanations. Integrating the knowledge of polymer processing and ethanol technology, will provide further understanding on how a new system should be established, as well as providing solutions for some of the existing problems. A wholly new system must be able to tackle certain productivity issues, thus serving as a better system compared to those currently existing. The current system and its productivity will be used later as the benchmark for the system proposed in this study.

Table 2.5: Fermentation data of ethanol production by immobilised *S. cerevisiae* W303 in various continuous reactors

Reactor	Dilution (h^{-1})	Support	Sugar Content (gL^{-1})	Ethanol (gL^{-1})	g cell/g support	Glucose consume (%)	$Y_{P/S}$	P ($gL^{-1}h^{-1}$)	Stability	Reference
CSTR	0.05-3.0	Treated Sugar cane stalk	Molasses-111.67	40	0.45	74.6	85.6	29.64	60 days	Vasconcelos *et al.*, (2004)
Packed Bed	1 ml/min	PS-DVB PHP	Glucose-50	Na	2	Na	83.7	12.5	Na	Karagoz *et al*., (2008)
Packed bed	-	PS PHP (45µm)	Sucrose- 150	6-10.5	-	-	-	-	Na	Hough *et al*., (1991)
Fixed bed	-	Pectin gel D=3-4 mm D=1-1.5 mm	Starch	Na	Na	94.0 97.0	83.0 92.0	5.8 11.7	275 hours	Trovati *et al*., (2009)
Fluidized bed	0.4	Calcium alginate-3.2 mm	Glucose-150	66	Nd	93.0	95.3	26.7	Na	Liu *et al*., (2009)
Packed bed	0.53	Sugar cane bagasse	Molasses - 200	31.8	-	-	-	-	76 days	Tyiagi *et al*., (1991)
Packed bed	1.5	k-carrageenan	Glucose -82.3	28	-	78.3	86.3	42.8	87 days	Nigam, (2000)
Expanded Bed (Batch)	-	Pectin gel	Glucose-100	39	0.47	91.4	84.5	2.44	16 hours	Kesava *et al*., (1995)
Vertical Rotating Reactor	0.7	Polyurethane foam	Glucose-100	80	-	-	-	63	72 days	Amin and Doelle (1992)

Na – Data not available

CHAPTER 3: MATERIALS & METHODOLOGY

3.1 Materials

Unless stated otherwise, all the chemicals were of analytical grade. Styrene (99%), sorbitan monoleate (Span 80), divinylbenzene (DVB), potassium persulphate ($K_2S_2O_8$), vinylpyridine, hydroxyapatite, phosphoric acid (H_3PO_3), sodium hydroxide (NaOH), dinitrosalicylic acid, sodium sulphite, ethanol of GC standard and the NADH-ADH kit (N7160) for alcohol determination were purchased from Sigma Aldrich Chemicals, UK. The biological materials glucose, peptone and glycine were of biological grade and were purchased from Sigma Aldrich Chemicals, UK. The yeast extract was purchased from Merck, while the peptone and nutrient agar were from Fluka.

3.2 Methods: PolyHIPE Preparation

3.2.1 *HIPE Preparation*

The HIPE was prepared according to the method of Akay *et al*. (2005c). The composition and the volume of oil and the aqueous phase were determined according to the desired type of the polyHIPE, as mentioned in Table 3.1. The experimental rig was set up in a fume hood as depicted in Figure 3.1 and Figure 3.2, where all the emulsification process was carried out at room temperature. In all preparations, the total volume for both phases was fixed at 250 ml, and the volume of each individual phase varied depending on the desired porosity. The oil phase was placed in a stirred stainless steel vessel (ID =12 cm) with a heating jacket (however in this study, the temperature of the vessel was not controlled since emulsification was carried out in room tempeperature). The aqueous phase, which contained 1% (w/v) initiator, was pumped into the vessel using a peristaltic pump at a specified flow rate, which varied for each type of polyHIPE. The composition of oil and aqueous phase were listed in

Table 3.1. The mixing was carried out using two flat blade impellers (d = 8 cm, width = 1.4 cm) at 90^{o} and was kept as close as possible to the base of vessel. The operating condition (mixing time) is unique depending on the types of polyHIPEs and is stated in Table 3.2.

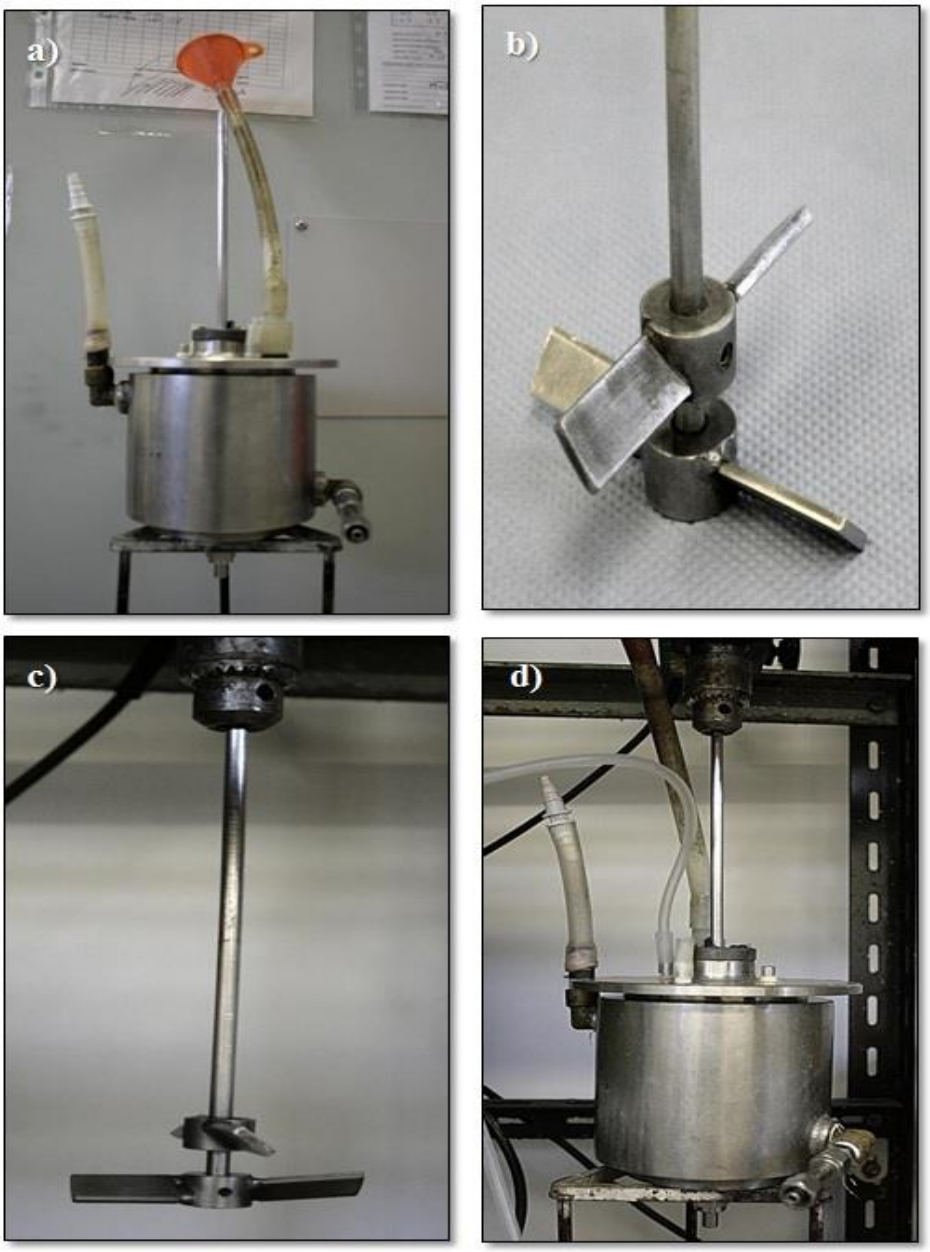

Figure 3.1: a) Stainless steel vessel used for HIPE preparation. An impeller, (b) & (c) have two flat blade paddles connected to the motor. d) Figure of the vessel and impeller connected to the motor.

Figure 3.2: Experimental set up for HIPE preparation.

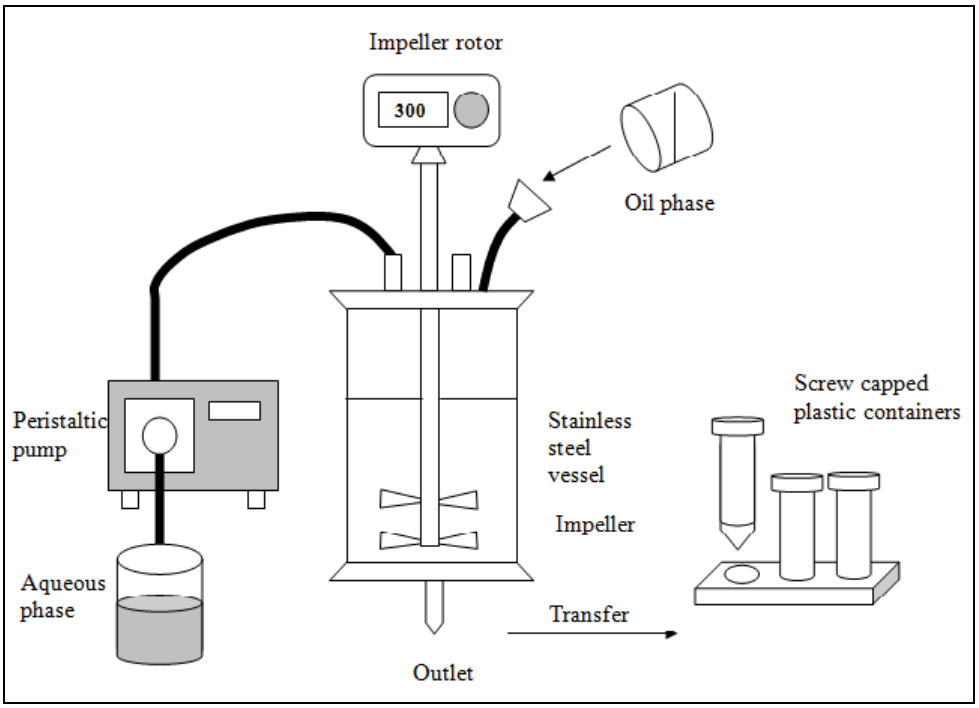

Figure 3.3: Schematic diagram of polyHIPEpreparation

The impeller speed was controlled at 300 rpm throughout the mixing process. The emulsion was then transferred to cylindrical plastic containers (ID = 28 mm) and left to polymerise at 60^{o}C in an oven for at least 8 hours. After polymerisation, the

hardened polyHIPE were cut into discs of approximately 5 mm in thickness using a bandsaw and leave in 60^{o}C to dry. Finally, the polyHIPE discs washed with a mixture of water and isopropanol in a Soxhlet system to remove all the toxic chemicals and the residual cross-linker/monomer prior to use in all fermentation work.

Table 3.1: Individual composition of oil and aqueous phase in the polyHIPE

PHP	Oil Phase		Aqueous Phase		Reference(s)
	Content	%(v/v)	Content	%(w/v)	
Polystyrene-divinylbenzene (PS-DVB)	Styrene	78	Potassium persulphate	1	Akay *et al*., (2005c)
	DVB	8			
	Span 80	14			
2-vinylpyridine (TVP)	Styrene	73	Potassium persulphate	1	Noor, (2006)
	DVB	8			
	Span 80	14			
	TVP	5			
Sulphonated	Styrene	76	Potassium persulphate H_2SO_4	1 5	Ndlovu, (2009)
	DVB	10			
	Span 80	14			
Hydroxyapatite (HA)	Styrene	76	Potassium persulphate H_3PO_4 Hydroxyapatite	1 30 0.5	Bokhari, (2003)
	DVB	8			
	Span 80	14			

Table 3.2 Summary of the operationg conditions for the preparation of PHPs

PHP	Dosing time, T_D (min)	Mixing time, T_H (min)*	Temperature (^{o}C)	Polymerization time
PS-DVB	2	3-30 min	Room temperature	8 hours
TVP	2	3-30 min	Room temperature	8 hours
HA	2	3-30 min	Room temperature	8 hours
Sulphonated	5-10	1-30 min	Room temperature	8 hours

*Mixing time was varied in each preparation to produce polyHIPEs with different pore size. Results was discussed in Chapter 4 (Section 4.1)

3.2.2 *Preparation of Sulphonated PHP*

The sulphonated PHP was prepared according to the method described in Section 3.2.1. After drying in an oven at 60^{o}C overnight, the polymer discs were soaked in concentrated sulphuric acid for 2 hours, and then microwaved for 6 x 30 sec until the polymers turned black. This was followed by soaking and washing with distilled water for 6 x 30 minutes. The last two steps were done by soaking the polymers with 5N NH_4OH solution to neutralise the acid. It was then washed in a soxhlet prior to use.

3.2.3 *Improvement of Surface Chemistry*

3.2.3.1 *Coating of Sulphonated PHP with Hydroxyapatite (HA)*

The prepared, sulphonated PHP discs (Section 3.2.1) were dried at 60^{o}C overnight before soaking in a solution containing 0.5% w/v HA dissolved in 30% H_3PO_4 for 4 hours followed by drying in an oven at 60^{o}C overnight. The discs were then soaked in 1M KOH/NaOH solution to neutralise excess acid. They were dried again and finally washed with a mixture of isopropanol-water to remove the excess base and cross-linker/monomer.

3.2.3.2 *Coating of Sulphonated PHP with Silica (Bindzil 10)*

The sulphonated PHP discs were dried at 60^{o}C overnight before being soaked in Bindzil 10 solution (silica dispersion solution) for 4 hours, followed by drying in an oven at 60^{o}C overnight. The discs were then soaked in 1M KOH/NaOH solution to neutralise the excess acid. The discs were dried again and finally washed with a mixture of isopropanol-water to remove the excess base and cross-linkers/monomers.

3.2.4 *Washing of PolyHIPEs*

The polyHIPE discs were stacked in a column of a soxhlet system (Figure 3.4) and 50% (w/v) fresh isopropanol was run continuously to wash the polymer to remove any residual surfactants, monomers and electrolytes. The discs were initially washed with a running mixture of isopropanol-water for 4 hours, followed by pure distilled water overnight. The washed discs were finally left to dry in an oven at 60^{o}C and stored in a sealed plastic bag until further use. All the polyHIPE discs were autoclaved prior to use in all the microbiological works.

Figure 3.4: Diagram of Soxhlet system for washing polyHIPE

3.3 Methods: Biological Works

3.3.1 *Preservation of Stock Culture*

S.cerevisiae W303 was obtained from the Laboratory of the Cell and Molecular Biosciences Department, School of Medical Science, Newcastle University. For long term preservation, the culture was kept in 20% (v/v) glycerol, in a freezer at -80^{o}C. For use in subsequent microbial work, the yeast stock was stored at -20^{o}C, transferred to an agar plate and incubated for 24 hours at 30^{o}C.

3.3.2 *Media preparation*

3.3.2.1 *Agar Medium for S.cerevisiae W303*

1.5% (w/v) agar powder was added to the growth medium which contained 20 gL^{-1} glucose, 20 gL^{-1} bactopeptone and 10 gL^{-1} yeast extract, and adjusted to pH 5.5 using 0.1 M sulphuric acid and 0.1 M NaOH solution. The mixture was stirred vigorously on a heating mantle to dissolve all the components. The glucose was autoclaved separately from the other components and added to the medium after the temperature had reduced to 50-60^{o}C. The solution was inverted several times to mix it and were left to solidify at room temperature and stored at 4^{o}C until further use.

3.3.2.2 *Growth Medium for S.cerevisiae W303*

The medium for growth was prepared according to the procedure described in Section 3.3.2.1without the addition of agar.

3.3.2.3 *YPG Media*

YPG media is consisting of 2.5% (w/v) glucose, 10% (w/v) peptone, and 5% (w/v) yeast extract. The pH was adjusted to 5.5 using 0.1 M H_2SO_4 and 0.1 M NaOH prior to sterilisation. The glucose and nitrogen sources were autoclaved separately at 121^oC for 20 minutes. The medium was allowed to cool to 50-60^oC before adding the glucose, and stirred rigorously.

3.3.2.4 *Production Media of S.cerevisiae W303 (Continuous Fermentation)*

4.5 L of production medium for the continuous operation of ethanol production was prepared in 5 L fermenter vessel (Bioflo 1000), equipped with a heating and cooling system. The medium consisted of 2-25% (w/v) glucose, 1-10% (w/v) peptone, and 1-5% (w/v) yeast extract. The pH was adjusted to 5.5 using 0.1 M H_2SO_4 and 0.1 M NaOH prior to sterilisation. The glucose and nitrogen sources were autoclaved separately at 121^oC for 20 minutes. The medium was allowed to cool to 50-60^oC before adding the glucose, and stirred rigorously.

3.3.2.4 *Phosphate Buffer Saline (PBS) Solution*

PBS solution was prepared according to the composition listed in Table 3.3. The solution was autoclaved at 121^oC for 20 minutes prior to use.

Table 3.3: Composition of PBS solution

1M K_2HPO_4	0.802 ml
1M KH_2PO_4	0.198 ml
5M KCl	1.0 ml
0.1M $MgSO_4$	1.0 ml
Distilled water	97.0 ml
NaCl	0.85 g

3.3.3 *Culture Preparation*

3.3.3.1 *Germination of Stock Culture and Inoculum*

A loopful of refrigerated stock culture was transferred onto a petri dish containing medium agar and incubated at 30^{o}C. A colony of germinated yeast cells was transferred to a 250 ml shake flask containing 30 ml of growth medium (without agar), then placed in an orbital shaker, set at 30^{o}C and 200 rpm, for 16 hours. The cells were then centrifuged at 5000 rpm for 5 minutes, washed once with 0.85% (w/v) NaCl, and re-centrifuged for 3 minutes (Jamai *et al*., 2001). The supernatant was discarded and the pellet was suspended in saline solution by vortexing. The total cell concentration was adjusted to an absorbance of approximately ~0.8 at 600 nm using a spectrophotometer (Jenway, model 6100). This would give approximately ~2 x 10^{7}/ml of viable cells.

3.3.4 *Immobilisation Procedure*

3.3.4.1 *Shake Flask Seeding Technique*

5% (v/v) of the yeast inoculum was inoculated into the growth medium, giving a final volume of 25 ml. A sterilised PolyHIPE disc was immersed in the medium, and incubated at 30^{o}C for 30 hours in an orbital shaker at 200 rpm. After 24 hours of incubation, the disc was taken out, and washed once with distilled water to remove unbounded cells and cell debris. It was then transferred to the 250 ml flask containing 50 ml of production medium for the production of ethanol.

3.3.4.2 *Force Seeding Technique*

Yeast inoculum was force seeded into the polyHIPE disc using a syringe pump as shown in Figure 3.5. This technique ensures a uniform distribution of cells across

the matrix supports compared to the natural seeding technique (Akay *et al*., 2005). The PolyHIPE disc was placed in the cell loading chamber and autoclaved prior to the seeding process. Sterilised distilled water was run continuously at 1 ml/min for 30 minutes to pre-wet the disc. A total of 2.6 ml of yeast inoculum (OD fixed at 0.8), was force seeded using a syringe pump. Inoculum was pumped at a constant flowrate of 0.5 ml/min and left for 10 minutes to give time for cell attachment (Bokhari, 2003). PBS buffer was pumped into the microreactor at 1 ml/min to wash the unbound cells before starting the fermentation. The seeded disc was then transferred to the reactor well in a sterile environment.

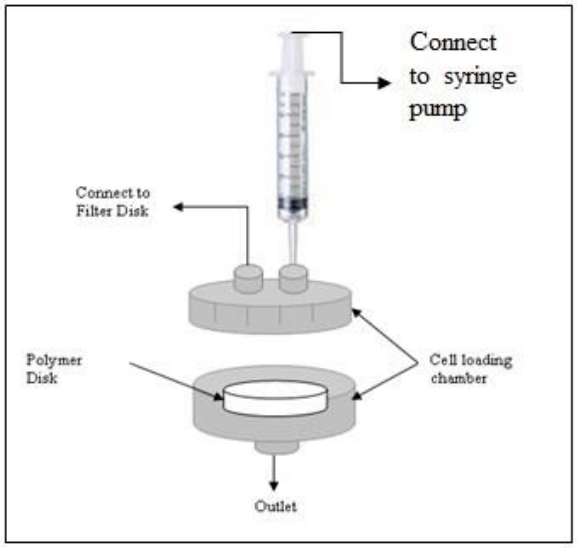

Figure 3.5: Diagram of force seeding technique

3.4 Analysis

3.4.1 *Determination of PolyHIPE Properties*

3.4.1.1 *Determination of Pore and Interconnect Sizes using the Scanning Electron Microscope (SEM)*

Since the pore and interconnect sizes might vary with different locations of the polyHIPE disc, the measuring was done by taking an average from three main locations: the top surface, the bottom surface and the centre pores (Figure 3.6). The

fragments of PHP were glued individually on aluminium stubs using a glued-sticker and Acheson's silver alectroDag, and were left overnight to dry. Finally the samples were coated with gold dust (20 nm) using a Polaron e5100 sputter coater and stored in a dessicator until processing (Shim and Yang, 1999). The imaging process was carried out using a SEM, Cambridge s40. All images were characterised at magnifications of 100x, 250x, 350x, 500x, and 1000x. A total of 50-100 different pores and interconnects were measured for their diameter using the ImageJ (Bokhari, 2003).

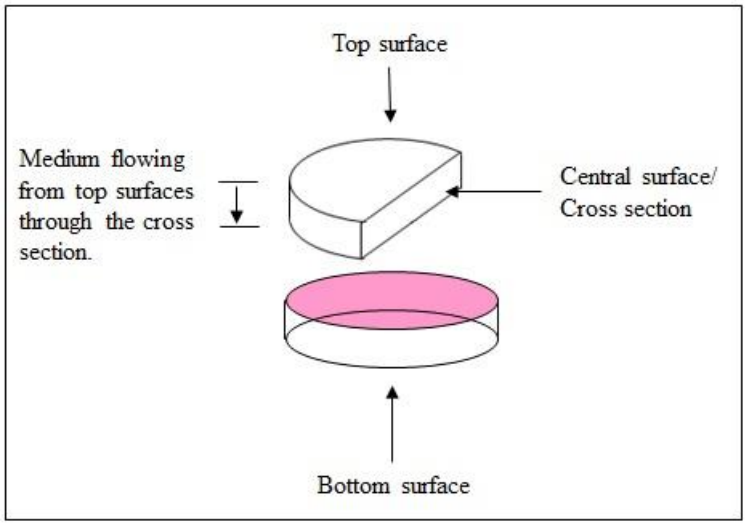

Figure 3.6: Location of surfaces taken for viewing with the SEM

3.4.1.2 *Surface Area Analysis*

The surface area of the polymer was determined using a Brunauer-Emmet-Teller (BET) analyser. A polyHIPE disc was dried overnight in an oven at 60^{o}C prior to crushing and grinding. Initially, 1 g of finely ground polymer was transferred into a sampling tube followed by the degassing of samples for 300 minutes at 50^{o}C using nitrogen and helium to remove any impurities. The sample was then analysed in the evacuated sample chamber where the tube was immersed in liquid nitrogen to provide a constant temperature. This analysis was carried out using the Beckman Coulter (Palo Alto, CA) SA3100 BET Gas Adsorption Surface Area Analyser, and a typical analysis usually took approximately 3 hours to complete.

3.4.1.3 *Viewing Cells with the SEM*

1.5 ml of the sample was centrifuged at 6000 rpm for 5 minutes, and the supernatant was discarded. Cells were then washed with a 1.5 ml phosphate buffer saline and spun for 3 minutes. This process was repeated 3 times. A 2% glutaraldehyde solution was then added to the sample, vortexed and left for an hour at room temperature. The cell solution was then spun and the glutaraldehyde was discarded. Finally, fresh glutaraldehyde was added to the sample following vortexing and stored at 4^{o}C prior to mounting and gold coating.

3.4.1.4 *Determination of Water Uptake by PolyHIPE*

The determination of the water uptake by the polyHIPE was carried out by immersing the polyHIPE disc in a beaker of distilled water for 1 hour. The weight of the polyHIPE before and after immersion was recorded and the calculation was as follows:

$$\text{Water Uptake} = \frac{W_1 - W_0}{W_0} \qquad \text{Equation 3.1}$$

W_1 = The weight of the disc after immersion in water

W_0 = The actual dry weight of the disc

The water uptake capacity was measured as a ratio of the weight of water held in the polyHIPE to the dry weight of the disc alone. The data was taken as an average of three readings using three different discs of the same type.

3.4.2 *Determination of Biological Properties*

3.4.2.1 *Washing and Prefixing of Immobilised S.cerevisiae W303*

The immobilised yeast in the polyHIPE disc was prefixed prior to SEM imaging. The immobilised yeast+polyHIPE was soaked in 0.1M glutaraldehyde/phosphate buffered saline (pH 7) which served as a fixing agent, and the discs were then stored at 4^{o}C until processing. Prior to SEM analysis, the disc was subjected to dehydration in ethanol series as shown in Table 3.4. At the end of the dehydration process, the samples were left in 100% ethanol before further drying with liquid CO_2 Samdri 780 or Baltec Critical Point Dryer and left in a dessicator. Finally, the sample was mounted on an aluminium stub with Acheson's silver alectroDag and dried overnight, prior to coating with gold dust using a Polaron e1500 Sputter Coater. The sample was then placed in a desiccator to dry before viewing with the SEM (Cambridge s240).

Table 3.4: Dehydration steps prior to SEM analysis (Fratesi *et al*., 2004)

Ethanol concentration (%v/v)	Time (mins)
35	10
50	10
75	10
95	10
100 x 2	30

3.4.2.2 *Fixing of Free S.cerevisiae W303 for SEM Viewing*

The cells were harvested from a liquid sample by spinning for 5 minutes at 6000 rpm. The liquid was then discarded and replaced with the same amount of 0.1 M PBS pH 7 and spun again for 3 minutes. The liquid was then discarded. This step was

repeated twice. Finally, the glutaraldehyde solution was added to the cells and vortexed for one minute. The solution was then removed and the cells were re-suspended with fresh glutaraldehyde. Cells were dried before viewing using the procedure described in Section 3.4.2.1. A drop of the cells mixture in 100% ethanol was spread on a glass slide, air dried for 30 minutes prior to drying using critical point drying.

3.4.2.3 *Cell Surface Hydrophobicity/Microbial Adhesion to Solvents (CSH/MATS)*

The characteristics of the cells have been reported to be influenced by the cells' age and density/concentration. Cell suspensions were prepared from the 16 hours and 66 hours cultures to study the cells' surface characteristics during the exponential and stationary phase. Four types of solvents (hexadecane, chloroform, ethyl acetate and decane) were used to determine the electron donor/acceptor properties of the cells. 0.4 ml solvent was added to the 2.6 ml of cell suspension with the optical density fixed at 0.700, read at 600 nm with a UV spectrophotometer (Jenway 600). The mixture was then mixed and vortexed for 60 seconds and allowed to separate at room temperature for 15 minutes. Finally the optical density of the cell suspension (aqueous phase) was measured against a blank PBS buffer. The affinity of cells at each stage was calculated using the following equation 3.2 (Vergnault *et al*., 2004):

$$\text{Affinity} = 1 - \frac{A_{600}}{A_{600,i}} \qquad \text{Equation 3.2}$$

A_{600} = The absorbance before reaction set at 0.700.

$A_{600,i}$ = The absorbance after reaction.

All measurements were carried out in triplicate and the results presented were the average values.

3.4.2.4 *Determination of S.cerevisiae* W303 *Size*

Determination of the yeast size was carried out using: i) the SEM and ii) the Particle Size Analyser (PSA). Cells at the exponential and stationary state were collected by growing the yeast in a shake flask for 16 h and 66 hours, respectively. Cells were then centrifuged, washed and re-suspended in saline solution (8.5 gL^{-1} NaCl). For PSA analysis, the yeast-saline solution was prepared at four different concentrations with absorbance fixed at 0.6, 0.8, 1.0 and 1.2 (read at 600 nm), which represented cells at 10^7-10^9 cells/ml. Samples were injected into a Particle Size Analyser (Coulter LS230) and the saline solution was used for the background calibration.

3.4.3 *Determination of Ethanol Concentration Using Gas Chromatography*

An ethanol assay was conducted by injecting 0.5 μL of the supernatant into a gas chromatograph (Varians 450). The sample was filtered through a 0.20 μm filter disc prior to injection. The filtrate was injected into a Wax 52CB GC column (Cp7763) coupled with a flame ionisation detector (FID). The column oven was operated isothermally at 180°C while the FID and injection port temperatures were both kept at 200°C. Nitrogen was used as the carrier gas and the combustion gas was a mixture of hydrogen and air. The concentrations of ethanol in the samples were determined based on a standard calibration curve. Ethanol concentrations ranging from 1 to 10 gL^{-1} were used to obtain the standard curve. Isopropyl alcohol was used as the internal standard at 1 gL^{-1}.

3.4.4 *Determination of Ethanol Concentration Using a Alcohol Dehydrogenase (ADH) Assay*

The reaction of alcohol dehydrogenase with ethanol produces one mole of acetaldehyde which can be detected by changes in the absorbance value. The increase in the absorbance value read at 340 nm is proportional to the amount of ethanol converted to acetaldehyde. However, there might be a slight variation in the accuracy of the measurement because the yeast ADH can also react with the other alcohols.

$$\text{Ethanol} + \text{NAD} \xrightarrow[\text{ADH}]{} \text{Acetaldehyde} + \text{NADH} \qquad \text{Equation 3.3}$$

16 ml of the 0.5 M glycine buffer, pH 9.0, were added to NAD-ADH Reagent Multiple Test Vial and inverted several times to dissolve the contents. 3 ml of prepared solution was then transferred to a labelled test tube. 10 µL of the samples was added to the reagent and the test tube was covered immediately and mixed by gentle inversion. The reaction mixture was then incubated at 25^{o}C for 10 minutes, and the absorbance was measured immediately at 340 nm. The samples were tested against distilled water as a blank. One unit of alcohol dehydrogenase converts 1.0 µmole of ethanol to acetaldehyde per minute at pH 8.8 at 25 °C. The value is linear up to absorbance 1.5.

3.4.5 *Analysis of Growth*

3.4.5.1 *Determination of Growth in polyHIPE*

i) ***Protein Quantification***

Determination of growth in the polyHIPE was quantified by measuring the amount of protein available in the support matrix (Ndlovu, 2009). The polyHIPE disc was sliced into small pieces using sterile apparatus, and then soaked in 1 ml of 1M

NaOH for 1 hour at room temperature. All dissolved proteins were separated from the polyHIPE slice by centrifugation. The supernatant was collected and neutralised with 1 ml of 1M HCl, and finally assayed for the protein content following the Lowry method (Section 3.4.7).

ii) ***Biomass in the PolyHIPE***

After termination of the fermentation process, the PBS buffer was run through the polyHIPE disc for about an hour at a 1ml/min. The micro reactor was taken out of the PTFE block and dried at 105^{o}C for 24 hours and transferred to the desiccator to absorb excess moisture. The disc then weighed with a microbalance.

$$\text{Dry Cell Weight (DCW)} = \frac{M_1 - M_0}{M_0} \qquad \text{Equation 3.4}$$

M_1 = Weight of polyHIPE disc after fermentation (g)

M_0 = Weight of polyHIPE disc before fermentation (g)

DCW = g biomass / g polyHIPE

3.4.5.2 ***Quantification of the Released Cell***

Biomass concentration was determined by centrifuging 1 ml of cell suspension at 6000 rpm for 5 minutes. The supernatant was decanted off, washed once using 1 ml of 0.85% (w/v) NaCl and re-centrifuged for 3 minutes. The supernatant fluid was discarded and the pellet was suspended in 1 ml of distilled water, then transferred into aluminium dishes and dried for 24 hours in a 105 °C oven. The samples were placed in a desiccator to absorb moisture before weighing. The calculation was as follows:

$$\text{Dry Cell Weight (DCW)} = \frac{W_1 - W_0}{W_0} \qquad \text{Equation 3.5}$$

W_1 = Weight of aluminium dish + cells (g)

W_0 = Initial weight of aluminium dish (g)

DCW = g biomass / g polyHIPE

3.4.5.3 *Colony Forming Unit (CFU)*

The detached yeast cells from the microreactor were collected from the outlet stream and were quantified using a plating method. The sample was diluted up to 10^{-2}-10^{-6} dilution using sterilised distilled water. 10 µL of aliquots were transferred to an agar plate and incubated at 30^{o}C for 24 hours. The number of colonies formed on the agar surface were counted and measured as CFU/ml.

3.4.6 *Glucose Analysis – Dinitrosalicylic Acid (DNS) Method*

The quantification of residual sugar was conducted using the DNS method (Miller, 1959), and using glucose as a standard. The DNS method works based on the principle that 3,5–dinitrosalicylic acid is reduced to 3-amino-5-nitrosalicyclic acid and an equivalence is established between the amino-nitrosalicylic acid produced and the sugar present. The DNS solution was prepared by dissolving 10 g of 3,5-dinitrosalicylic acid, 2 g phenol, and 0.5 g sodium sulphite in 1 L distilled water (Wang, 2007). 3 ml of DNS solution was pipetted into a test-tube containing 1 ml of sample, and then heated for 15 minutes in boiling water. The test tubes were then cooled under running tap water and brought to ambient temperature. The optical density was measured at 540 nm using a spectrophotometer (Jenway 6100) against a reagent blank. The concentration of reducing sugars was determined by using a calibration curve obtained for glucose concentrations at range 1-4 mg/ml.

3.4.7 *Protein Content*

Prior to analysis, the Modified Lowry and Folin-Ciocalteu reagents must be freshly prepared. The reagent was prepared by adding the Reagent A (20 g Na_2C0_3 + 4 g NaOH dissolved in 1L distilled water) and Reagent B (2.5 g $CuSO_4.5H_2O$ + 5 g sodium citrate dissolved in 1 L distilled water) in the proportion of 50:1. While the Folin-Ciocalteu reagent was freshly prepared by diluting with 1:1 distilled water.

Each standard or crude enzyme (supernatant) of 0.2 ml was pipetted into appropriately labelled test tubes. 0.2 ml of the distilled water was used for the blank. 1.0 ml of the Modified Lowry reagent was added to each tube, mixed and incubated for 10 minutes at room temperature. 0.1 ml of the diluted 1 N Folin-Ciocalteu reagent was then added to the reaction mixture and mixed immediately. The tubes were allowed to stand at room temperature for 30 minutes. The absorbance of each tube was measured at 750 nm and the protein content was determined using the standard curve. A fresh set of protein standards was prepared by diluting the 2.0 mg/ml BSA (bovine serum albumin) stock standard.

3.5 Fermentation Set up

3.5.1 Shake Flask Fermentation by Free Cell *Saccharomyces cerevisiae* W303 (Suspended Culture).

Fermentation by free cell *S.cerevisiae* W303 was carried out in 250 ml volumetric flask employing 45 ml YPG media (Section 3.3.2.2). 5 ml of yeast suspension, prepared from seed culture grown for 16 hours (Section 3.3.3) was added to the YPG media (Section 3.3.2.3). Fermentation was carried out for 48 hours at 30^{o}C with shaking at 200 rpm and samples were taken at two-hourly intervals. The biomass, number of colony forming unit and ethanol concentration was determined for each sample and the results are discussed in Section 5.1

3.5.2 Shake Flask Fermentation by Immobilised *Saccharomyces cerevisiae* W303

Preliminary fermentation of immobilised *S.cerevisiae* W303 was carried out in 250 ml volumetric flask employing 50 ml YPG media (Section 3.3.2.3). The yeast suspension were inoculated into the polyHIPE (Section 3.3.4) and transferred to the YPG media. Fermentation was carried out for 24 hours at 30^{o}C with shaking at 100 rpm. Samples were taken at the end of fermentation for the determination of protein

content (growth of yeast), number of cell released and ethanol concentration. The results are discussed in Section 5.4.

3.5.3 Microreactor Set Up and Continuous Operation

The microreactor was made from polyHIPE in a disc form. The thickness of the disc was 5 mm with diameter of 28 mm. For the ethanol production, the polyHIPE disc was placed in a well of housing that was made from polytetrafluoroethylene (PTFE). The well size was tailored to fit the diameter of a polyHIPE disc. This PTFE block was then placed in an incubator where the temperature was set at 30^{o}C.

The microreactor connected to a 5L flat bottom borosilicate glass fermenter (with working volume of 4.5L, Bioflo 1000 NewBrunswick, Switzerland), with a height:diameter (D) ratio of 3:1. This vessel was used as a medium reservoir into which air was pumped continuously to enrich the medium. The glass reservoir was equipped with a peristaltic pump, temperature and dissolved oxygen (DO) controllers. It was also fitted with two six bladed turbine impellers (diameter, d = 40 mm) mounted on an agitator shaft and the rotation speed was fixed at 200 rpm.

The production media (Section 3.3.2.4) contained glucose, yeast extract and bactopeptone at various concentrations. Glucose was autoclaved separately from the other nutrients to avoid caramelising. The reactor parts and mediums were sterilised at 121^{o}C by autoclaving for 20 minutes in the 5L Bioflo 1000 vessel. Continuous conversion of glucose to ethanol was carried out in the microreactor (polyHIPE), and the YPG media was pumped into the microreactor using a peristaltic pump at the desired flowrates. All experiments were replicated and the temperature of the media (in the vessel) and the microreactor was maintained at 30^{o}C.

All the outlet/opening was secured with a 0.2 µm filter disc to reduce the risk of contamination. The actual experimental set up is depicted in Figure 3.7 and schematic diagram (Figure 3.8) shows the overall fermentation system, assembled in a

strictly sterile environment to ensure zero contaminations. All the joints and openings were secured using o-rings and plastic seals. Sampling was carried out using flames, and alcohol was sprayed on the area and the joints/openings involved during the sampling, and before and after the sampling.

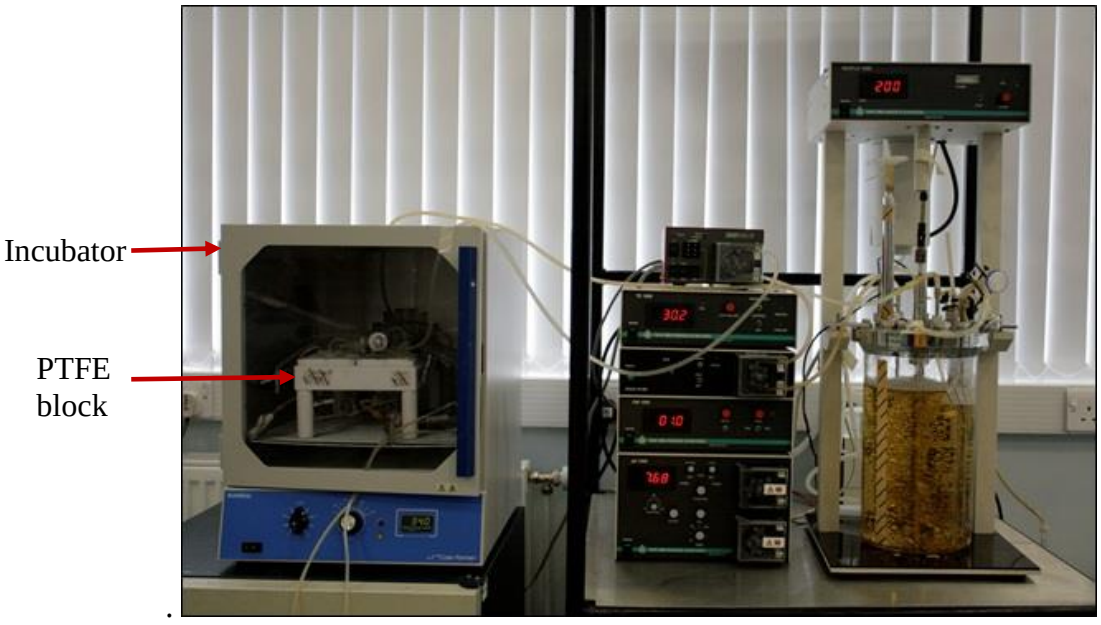

Figure 3.7: Experimental set up for the microreactor. The microreactor (polyHIPE) was placed in the PTFE block, which then incubated in the incubator to maintain the temperature at 30^{o}C.

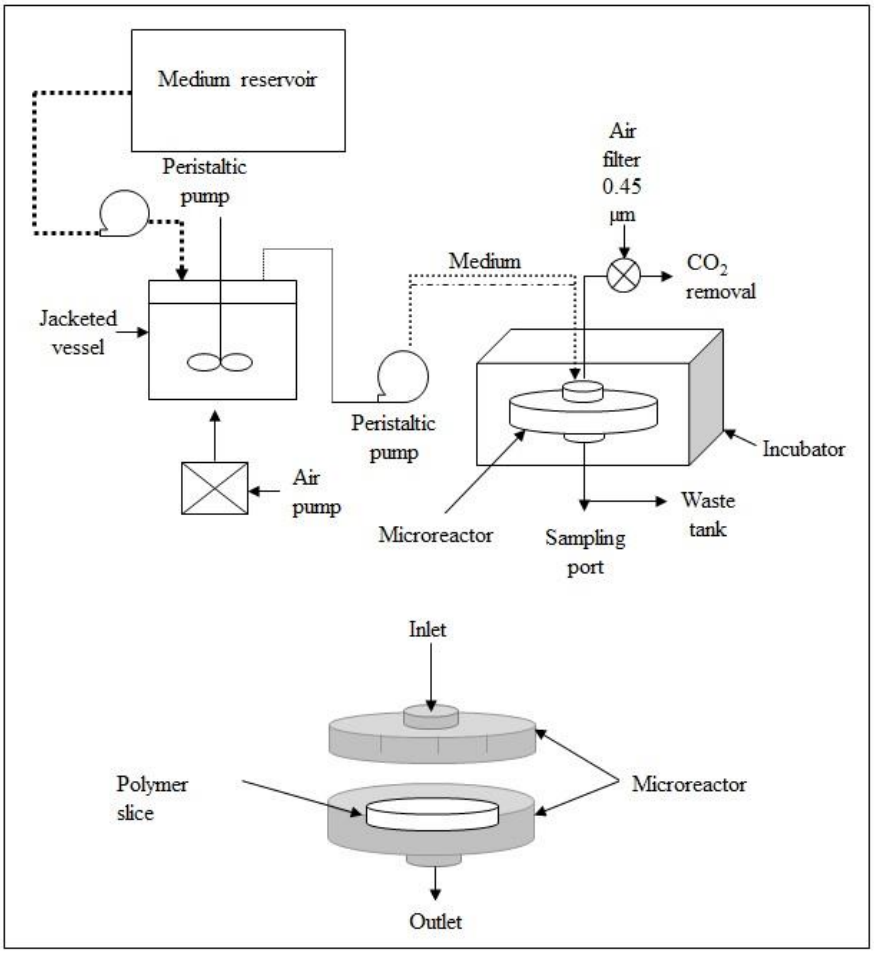

Figure 3.8: Schematic diagram of the experimental rig for the continuous operation of ethanol production by immobilized *S.cerevisiae* W303.

CHAPTER 4: PRODUCTION OF THE POLYHIPE POLYMER

4.1 Effect of Mixing Time on Pore and Interconnect Sizes.

Significant contributions of the polyHIPE can be found in various areas in the literature, with uses in a wide variety of applications. It has been applied with success, although not at a commercial level, in biomass gasification, gas technology, bioprocessing, tissue engineering, waste water treatment and agriculture. The ability to chemically/biologically synthesise and functionalise the polyHIPE for applications must be supported with the knowledge of the microorganisms and their specific behaviour when they interact with solid surfaces. For the purpose of immobilisation, it was crucial to have a good pore distribution with an open structure to avoid blockage during fermentation since yeast cells have a tendency to form clusters especially in an oxygen deprived and poor nutrient environment. Therefore, this chapter aimed to produce a polyHIPE that is compatible for the adhesion, mobility and growth of *S.cerevisiae* W303.

As has been discussed thoroughly in the literature review, the properties of the polyHIPE were divided into three groups: i) architectural, ii) chemical and iii) mechanical. These properties were generally considered when selecting a polyHIPE for any purpose. However, in this study, our major concerns only revolved around the architectural (pore/interconnect size) and chemical properties that best suited the yeast adhesion and proliferation. These architectural properties are not only affected by the chemical composition (types and composition of chemicals) but also controlled by manipulating the mixing intensity (Lepine *et al*., 2008), the mixing time and the dosing time (Akay *et al*., 2005b). In this chapter, preparations of four types of polyHIPEs were carried out extensively in order to obtain a suitable surface chemistry and architectural properties that would support and promote the yeast adhesion and proliferation. These polyHIPEs were: i) polystyrene-divinylbenze polyHIPE (PS-DVB PHP); ii) hydroxyapatite polyHIPE (HA PHP); iii) 2-vinylpyridine polyHIPE (TVP PHP) and iv) sulphonated polyHIPE (sulphonated PHP). The controls of these

parameters were achieved by varying the mixing times (Table 3.2), while the chemical compositions were fixed depending on the polyHIPE's type (Table 3.1).

Since the yeast exhibits different sizes depending on the stages of growth, which varies appreciably between 3-5 µm, we aimed to produce a polyHIPE with pore and interconnect sizes of more than 40 µm and 10 µm, respectively. In the production of the osteoblast tissue using the HA PHP cultured in a spinner flask (Figure 4.1 a), large interconnect sizes (30 µm) were beneficial for the cell penetrations and the speed of migration into the polyHIPE cavity, but with smaller interconnects, a dense layer of cells was observed on the top surface, which can be a sign of poor accessibility (Bokhari, 2003). But in this study, as yeast migration will be enforced by the hydrodynamic flows exerted by the flowing medium (Figure 4.1b), a minimal interconnect size of 8 µm *(*double the size of mature yeast) was considered appropriate. A very large interconnect size will allow efficient exchange of nutrients, but there will be a risk of cell washout, especially in the long term continuous reaction. The summary of the evaluation of pore and interconnect sizes for PS-DVB PHP and TVP PHP with respect to the mixing time are shown in Table 4.1.

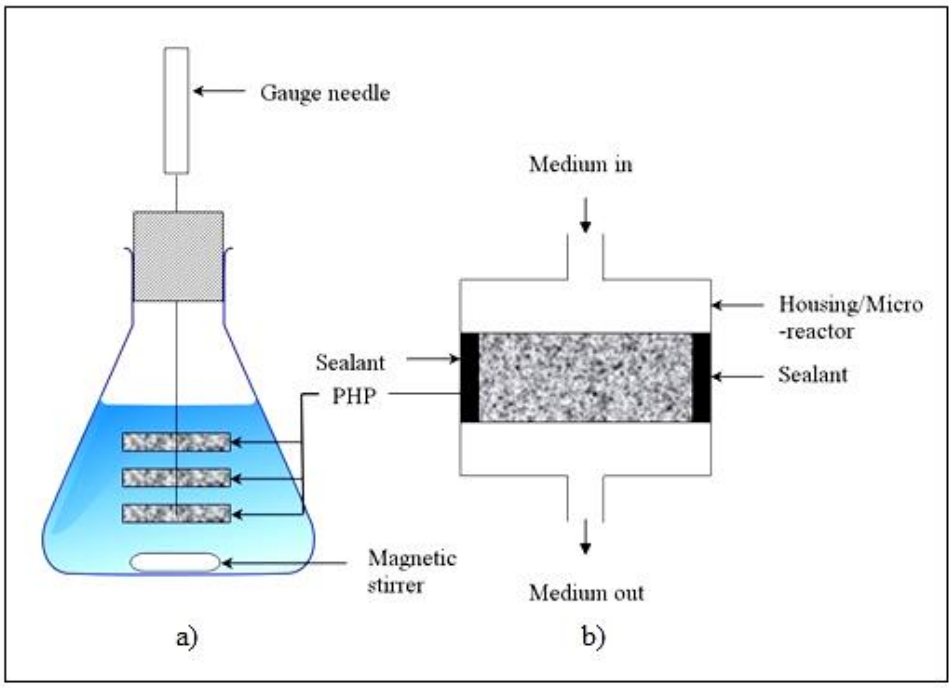

Figure 4.1: Different rig arrangements a) Spinner flask with polyHIPE (Bokhari, 2003) and b) this study.

Table 4.1: Effect of mixing time on the pore and interconnect sizes of PS-DVB and TVP PHP

Dosing time, T_D (min)	**Mixing time, T_H (min)**	**PS-DVB PHP**		**TVP PHP**	
		Pores Size (µm)	**Interconnect Size (µm)**	**Pores Size (µm)**	**Interconnect Size (µm)**
2	3	57.0 ± 7.6	14.7 ± 2.8	38.2 ± 4.1	9.3. ± 1.9
2	5	48.2 ± 6.8	12.1 ± 1.2	35.7 ± 4.2	8.2 ± 1.4
2	15	40.1 ± 4.1	10.2 ± 1.5	30.2 ± 4.1	6.7 ± 1.2
2	30	32.5 ± 3.2	8.3 ± 0.9	28.4 ± 3.8	5.6 ± 0.7

- Refer to Section 3.1

The data shown in Table 4.1 has proved that the mixing time has a profound effect in determining the pore and interconnects sizes of the polyHIPE. Besides this, two different chemical compositions would also contribute to the dissimilarities in pore distribution. Referring to Table 4.1 above, the distribution of pores and interconnects for TVP PHP was relatively smaller than PS-DVB PHP at all mixing and dosing times, by approximately 30%. The underlying reason for this phenomenon was not quite understood, but was expected to be due to the higher degree of cross-linking in the TVP PHP compared to the PS-DVB PHP. However, the results obtained in this study differed from Jimat (2011) who reported that no apparent changes were observed for the pore and interconnect sizes of the PS-DVB PHP and the TVP PHP prepared in a similar manner.

Notably, the size of the pores and interconnects for both polyHIPEs were reduced with increased mixing time. Increasing the mixing time from 3 to 30 minutes, reduced the pore size of the PS-DVB PHP (57.7 ± 7.6 µm to 32.5 ± 3.2 µm) by 43.6% and the TVP PHP (38.2 ± 4.1 µm to 28.4 ± 3.8 µm) by 25.7%. The interconnect size for both polyHIPEs was also reduced significantly by 43.5% and 39.0%, respectively. Extended mixing allowed enough time for the aqueous droplets to be broken up into more uniform sizes, subsequently producing polyHIPEs with a more defined and uniform structure. Besides this, longer mixing resulted in a more uniform size of interconnects, distributed evenly within the polyHIPE. According to Bokhari (2003), a very short mixing time produces a PHP with larger pores, due to the formation of

thicker interfacial films (unstable emulsion). In some cases, mixing for a very short time produced low viscosity HIPEs which often unstable, while prolonging the mixing increased the viscosity. A viscous emulsion is often more stable because it provides a kinetic barrier to prevent droplet coalescence (Cameron and Sherington, 1997). In this study, extending the mixing time resulted in a more viscous emulsion due to the higher interaction of high energy droplets, as mixing provides enough energy for the droplets to exist at higher energy states, which also corresponded to its smaller pore sizes (PS-DVB PHP = 32.5 $\pm$ 3.2 µm, TVP PHP = 28.4 $\pm$ 3.8 µm) (Bokhari, 2003).

The smallest standard deviation for both pore and interconnect was observed for the polyHIPE prepared at 30 minutes of mixing time, suggested that the pore and interconnect distribution was more homogenised. Further mixing beyond 30 minutes is expected to have less, or a negligible effect on the pore and interconnect sizes. Though the pore size reduces significantly with increased mixing times, it will reach a plateau when increasing the mixing time and no longer affect the structure. Images can be observed in Figure 4.2(a-c) comparing the TVP PHP produced at 3, 5, and 30 minutes of mixing time.

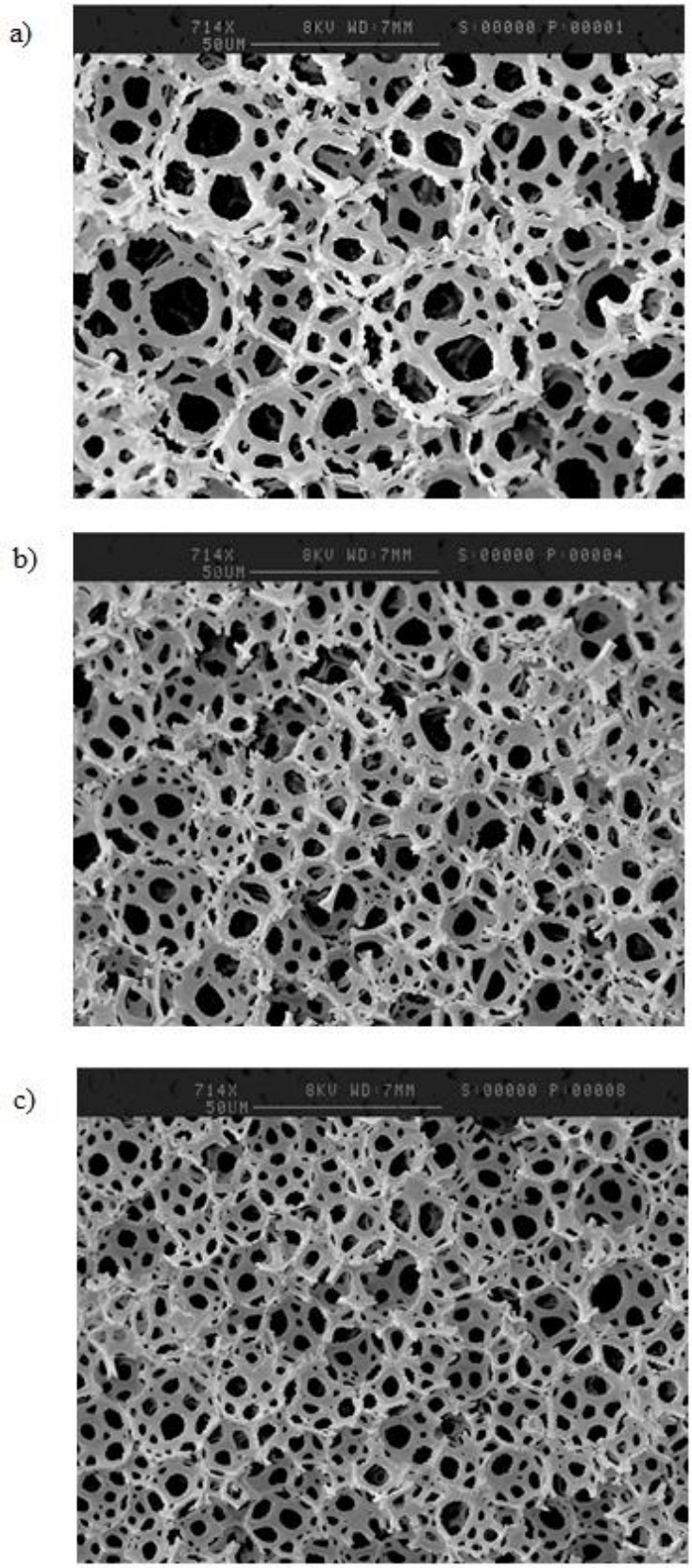

Figure 4.2: TVP PHP at 90% porosity prepared with the addition of 2-vinyl pyridine produced highly interconnected pores with hydrophilic properties. The SEM images at 700x magnification show TVP PHPs with a dosing time fixed at T_D = 2 minutes, while the mixing time, $T_{H,}$ varies at: a) 3 minutes; b) 15 minutes; and c) 30 minutes.

The largest interconnects size for the TVP PHP was obtained at 9.3 µm (T_H= 3 min), which was two times larger than the size of the matured yeast cells. An attempt had been made to increase the pore size by reducing the mixing time, but this resulted in the production of an unstable emulsion. This finding was in agreement with Bokhari (2003) who observed the same phenomenon for the production of the HA PHP. Figure 4.3 shows an example of a sulphonated polyHIPE with a short mixing time, T_H = 60s, which produced an unstable polyHIPE structure with non-uniform pores and fewer openings (closed pores). Apart from reducing both the mixing time and the dosing time, there are other parameters that can be manipulated for producing polyHIPEs with large pore sizes such as the temperature (Bokhari, 2003), the dosing rate (Akay *et al*., 2005a), the impeller types (Akay *et al*., 2000), the phase volume (Akay *et al*., 2005a), surfactant composition and fillers. In this process, single feed is used, but it was proven in previous studies that multiple feed points can be used to produce polyHIPEs with larger pores (Akay *et al*., 2005a).

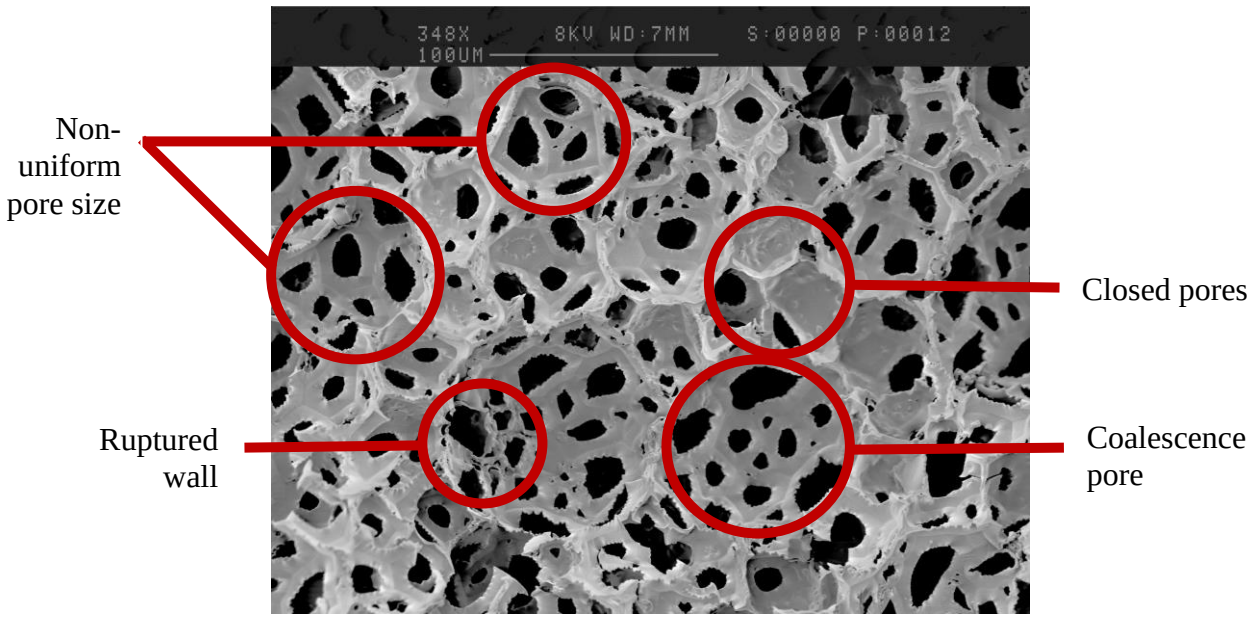

Figure 4.3: Example of sulphonated polyHIPE prepared with a very short mixing time, T_H = 60s, which produced some closed cells, ruptured walls, and irregular pore shapes and sizes.

Apart from size difference, no other distinguishable changes in the polyHIPE's cellular structure were observed when the mixing time was varied and this observation was similar in all types of polyHIPEs. An example of an unaltered cellular structure of TVP PHP against mixing time was shown in close up images taken with the SEM

in Figure 4.4. A close up view from SEM images in Figure 4.5 shows the surface textures of PS-DVB, TVP, HA, and sulphonated PHPs at various magnifications (1500-6000x). The TVP (Figure 4.5a), PS-DVB (Figure 4.5b) and HA PHPs (Figure 4.5c) have a visibly smooth structure. Addition of 2% of vinyl pyridine to the TVP PHP (Figure 4.5b) and hydroxyapatite to the HA PHP (Figure 4.5c) in the aqueous phase during preparation did not produce any effect on the structure's surfaces or the shape of the microstructure. In contrast, Lepine *et al*. (2008) had reported that a change of cellular structure was observed for a polyHIPE derived from PS-DVB/ethylstyrene when mixing was increased from 2 minutes to 15 minutes. At 2 minutes of mixing, the polyHIPE presented a phenomenon called liquid drainage, where the polyHIPE had very large connections with limited walls (skeleton) and then shifted to a 'classical' polyHIPE structure when mixing was increased beyond 15 minutes. Whereas for the sulphonated PHP (Figure 4.5d), small lumps or blisters were observed on its surfaces resulted in increased surface roughness, thus expected to increase the cells' adherence. These blisters were created during microwaving, where the entrapped sulphuric acid in the polyHIPE escaped due to heating, thus increasing the surface roughness. Surface roughness is often reported as a regulator for biological processes such as cell-surface adherence, proliferation, growth and migration.

In general, all the polyHIPEs obtained in this study had a very porous structure with highly interconnected pores. The pores and interconnects had a ragged edge, probably caused by drying. The PS-DVB PHP was brittle, while the TVP and HA PHPs were more rigid. On the other hand, the sulphonated PHP was spongy and softer than the others.

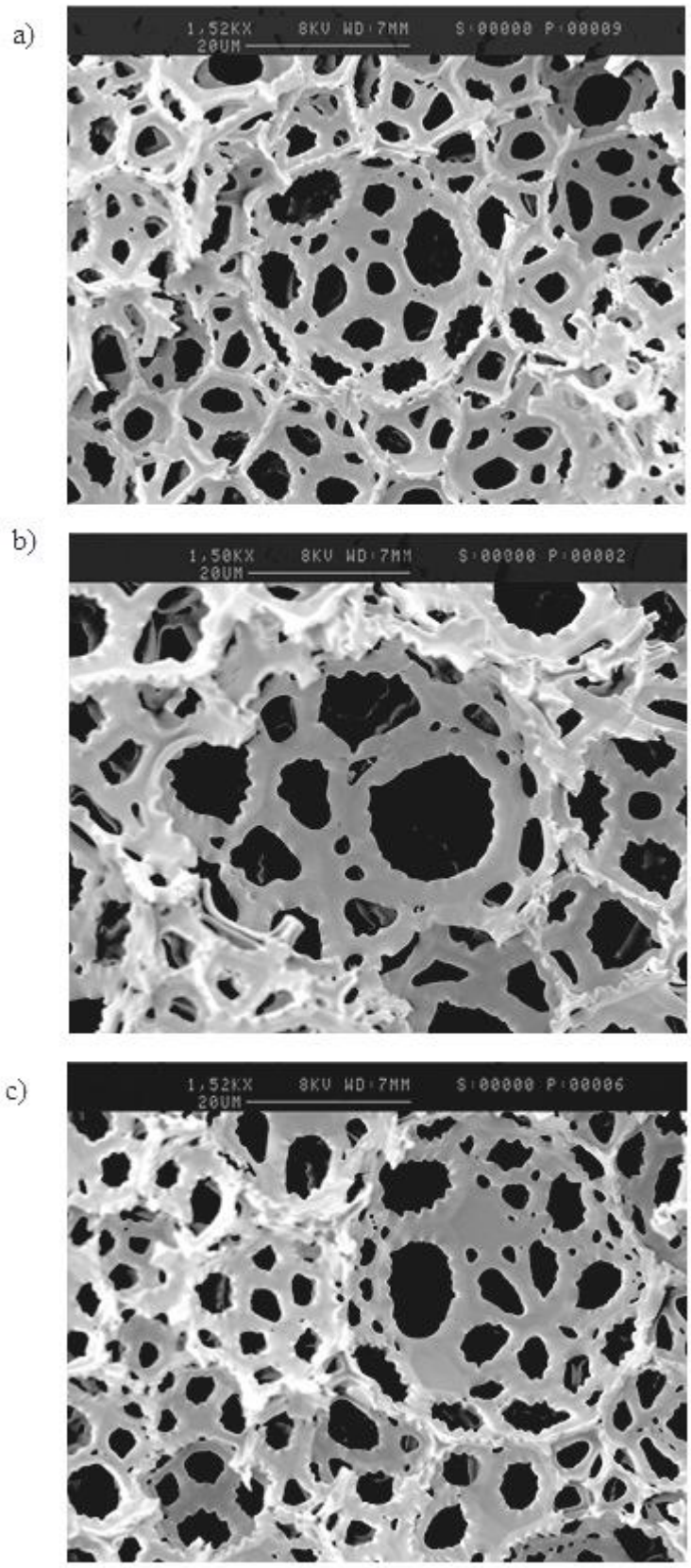

Figure 4.4: Close up images at 1500x magnification for TVP PHP prepared using two minutes dosing time and a) 3, b) 15 and c) 30 minutes of mixing time, which produces polyHIPEs with different pores and interconnects sizes.

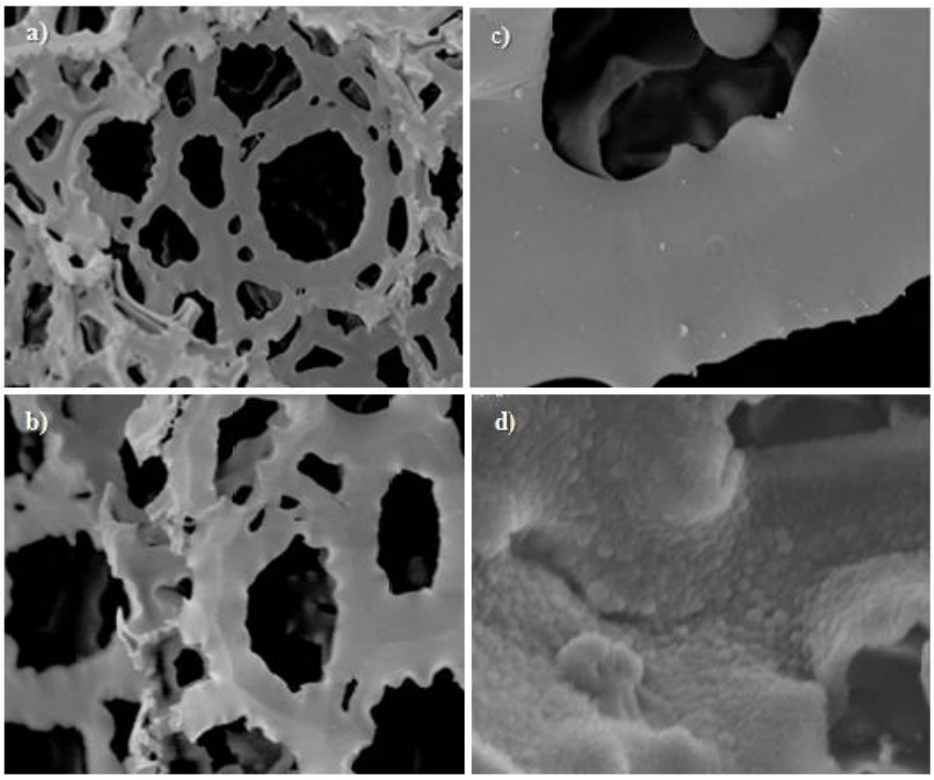

Figure 4.5: Images of a) TVP PHP, b) PS-DVB PHP, c) HA PHP and d) sulphonated PHP captured with the SEM at various magnifications (1500x-6000x).

4.2 Surface Area and Water Uptake Capacity

Apart from producing a polyHIPE with suitable architectural properties, another key parameter to establish is a surface element that not only favours/attracts yeast cells but also permits liquid flow. The importance for having a polyHIPE that is highly hydrophilic was considered as crucial as having a suitable size of pores and interconnects. In a previous study, the migration of primary rat osteoblasts in the HA PHP was terminated and a plateau was reached after 35 days of incubation with respect to all pore sizes tested. The migration of cells was hindered below 1.4 mm from the surface due to the scarcity of the medium (Bokhari, 2003). A water uptake test was carried out for all the polyHIPEs that have the same architectural structure (pore and interconnect size between 45-55 µm and 10-15 µm, respectively). This test was carried out by completely immersing the whole polyHIPE disc in distilled water for 24 hours. Before weighing, the polyHIPEs were dabbed with tissue to wipe off excess water on the surfaces, and the results are as follows (Table 4.2):

Table 4.2: Effect of chemical constituents on the properties of polyHIPEs.

PolyHIPE Type	Surface Area (m^2g^{-1})	% increased	Water uptake (g H_2O/g PHP)	Fold Increased
PS-DVB	1.23 ± 0.24	-	0.42 ± 0.13	-
TVP	1.69 ± 0.25	37.4	1.61 ± 0.15	3
HA	1.75 + 0.19	42.2	3.41 ± 0.94	7
Sulphonated	1.90 ± 0.48	54.4	11.09 ± 1.25	24

- Fold increase over PS-DVB PHP. PS-DVB – polystyrene-divinylbenzene, TVP – 2-vinylpyridine, HA – hydroxyapatite.

The ability for soaking or retaining water was the poorest for the PS-DVB PHP. This type of PHP had been reported to exhibit a very strong hydrophobic property (Cameron and Sherrington, 1997). Addition of 2-vinylpyridine increased the hydrophilicity of the polymers, and the water uptake capacity increased up to 3 fold compared to the PS-DVB PHP. The presence of a branching system and the polarity of 2-vinyl pyridine attract water more than the hydrophobic nature of the polystyrene-DVB. The HA PHP on the other hand, shows a significantly greater improvement, which suggests that HA contributed to the enhancement of water affinity. However, the most significant increase in water uptake properties was observed with the sulphonated PHP, where water uptake was 11.09 ± 1.25g H_20/g of PHP, which is equivalent to a 24 times increase compared to the PS-DVB PHP. In addition, this polyHIPE managed to soak up water rapidly, and when it was broken into pieces it showed that the polyHIPE was fully wetted. Unlike the sulphonated PHP, some dried areas were observed in some of the tests carried out with the PS-DVB, TVP and HA PHPs.

All the polyHIPEs generated in this study exhibited a different surface area although it was not statistically different. They possessed a low surface area (< $5m^2g^{-1}$) compared to the established well-known polymers that can achieve up to 500 m^2g^{-1}. The TVP PHP (1.69 gcm^{-3}) had a considerably larger surface area, at 37.4% compared to the PS-DVB PHP because of its relatively smaller pore size. The surface area for the HA PHP (1.75 gcm^{-3}) was increased by 40% compared to the PS-DVB PHP (1.23 gcm^{-3}) due to HA incorporation and the addition of acids that might provide

nanoporosity to its skeleton. The highest surface area was observed with the sulphonated PHP (1.90 $\pm$ 0.48 m^2g^{-1}), and this was expected to be contributed by the nano pores as well as the blisters that appeared to be all over the surface. However, the previous study by Burke *et al*. (2009) showed that this sulphonated PHP would give a surface area of 5.2 m^2g^{-1} for both rigid and spongy polyHIPEs. Statistical analysis shows that the differences were not significant for all the polyHIPEs tested. This could be accounted by errors during the preparation. Before BET analysis, the polyHIPE samples were crushed and ground into small particles before being placed in the sampling chamber. The size of the particles was expected to contribute significantly to the measurement and we found difficulty preparing a sample with an even particle size. Although the pore size for the polyHIPEs tested varies considerably, Burke *et al*. (2010) had proved that differences in the pore size of the same type did not impose any effect on the surface area measurement. Therefore, it might be appropriate to suggest that the differences observed in this study were due to the different chemical composition of each polyHIPE. The sulphonated PHP exhibited the highest surface area, which was accounted for by the nano-structure and the higher DVB content. The DVB composition used in the sulphonated PHP was 10%, while the other PHPs were fixed at 8%.

Hydrophobic surfaces have been proven in many studies to provide good communication/adherence between the cells and the surfaces, while hydrophilic surfaces have been shown to be less effective, but its high affinity towards water is beneficial for increasing the flow of media into the polyHIPE matrix (Jimat, 2011). Unlike hydrophobic surfaces, the availability of N chains in the TVP PHP, means that it can easily absorb moisture from its surroundings for the use of bacteria, besides making the scaffold a suitable 'housing' for their growth. In this case, the TVP PHP acted like an absorbent that absorbs moisture to retain the humidity and make it a suitable environment for the microorganisms. In contrast, for the submerged fermentation, liquid media can be easily distributed throughout the scaffold by molecular diffusion, absorption and through capillary action, thus reducing the risk of medium scarcity during fermentation. For the HA PHP, the availability of Ca^{2+} in its structure provides protonated surfaces which can increase the strength of binding with yeast which can be highly beneficial for use at high dilution rates. It has been proved by Bokhari (2003) that the modified HA PHP induces cells to penetrate deeper into the

polyHIPE matrix. All these polyHIPEs were used as a microreactor for yeast growth and ethanol production in the continuous operation

4.3 Sulphonated PolyHIPE Polymers (Sulphonated PHP)

An advantageous aspect of the highly hydrophilic sulphonated PHP is that it was derived from W/O emulsion, and has supreme stability as opposed to other hydrophilic polyHIPEs mostly derived from O/W emulsions, such as acrylamide (Zhang and Cooper, 2002), polysaccharide based-polyHIPE (Barbetta *et al*., 2005), 2-hydroxyethyl acrylate (Cohen and Silverstein, 2012; Butler *et al*., 2003) and 2-hydroxyethyl methaclarylate (Kulygin and Silverstein, 2007). The sulphonated PHP has been successfully developed and tested in agriculture as an alternative to commercial fertilizer (Burke *et al*., 2010; Fleming, 2012), in α-amylase production from *Bacillus subtilis* (Jimat, 2011) and also in the antibiotic production from *Streptomyces coelicolor* (Ndlovu, 2009) etc. Bacteria used in the mentioned applications show good adherence to this polyHIPE surface. In addition, due to their ion exchange properties, these sulphonated polyHIPEs are also suitable to be used as an electrode in fuel cell systems.

4.3.1 *Preparation and Characteristics of Sulphonated PHPs*

All polyHIPEs prepared in the previous section were generally hydrophobic or slightly hydrophilic. The sulphonated PHP is highly hydrophilic polymer acting like a superabsorbent, and is prepared by incorporating 5% v/v of concentrated sulphuric acid into the aqueous phase. The polyHIPE discs (5mm thickness) was soaked in concentrated sulphuric acid and was microwave-irradiated for 30 second intervals, repeated six times, equivalent to 180 seconds. The polyHIPE was then neutralised with either ammonium hydroxide or potassium hydroxide until the final pH was between 6.5 and 7.5. Finally, the impurities in the polyHIPE discs were removed by extraction using the soxhlet apparatus, mentioned previously in Section 3.2.4.

Microwaving is well known for creating hot spots in materials. In order to minimise this effect, the polyHIPE was cut into discs (thickness of 5 mm) and microwaved for 30 sec per cycle for six times. Microwaving was carried out using the domestic microwave oven, with a maximum power consumption of 1400 watt. Upon microwaving, the polyHIPE became black (a sign of carbonisation), thus making the polyHIPE electrically conductive (Calkan, 2007). Besides this, formations of blisters on the skeleton of the polyHIPE were clearly noticeable, as seen in Figure 4.5(d). Blisters, as mentioned previously, occurred when the sulphuric acid that was added to the aqueous phase during HIPE preparation tried to escape after being heated up during the microwaving. This hypothesis was confirmed in additional studies carried out by Calkan (2007) through: i) soaking a polystyrene polymer in concentrated sulphuric acid before going through the microwave, and ii) carrying out a sulphonation process for the sulphonated PHP using a thermal method (oven) instead of microwave irradiation. SEM analysis confirmed that no blisters had been formed on both surfaces, but signs of carbonisation were visible.

In Figure 4.6, the formation of coalescence pores was also evident, suggesting that it was a less stable polyHIPE compared to the polyHIPEs discussed previously (Section 4.1). The coalescence pore was a result of the instability of the emulsion, caused by the addition of sulphuric acid into the aqueous phase during HIPE preparation.

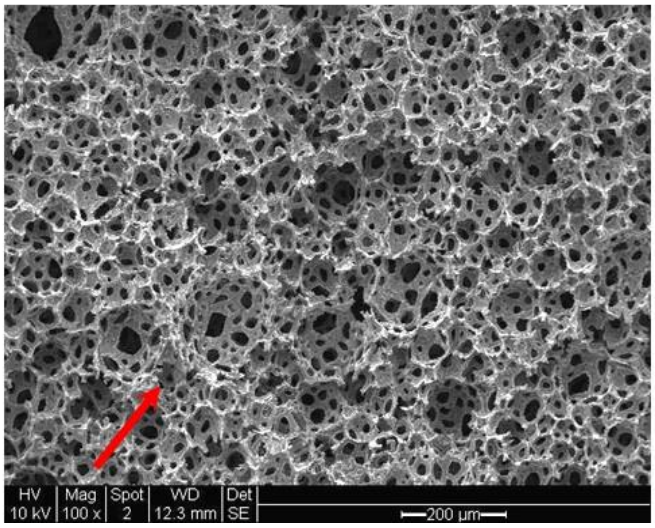

Figure 4.6: Image of the coalescence pores in the sulphonated PHP scaffold before the post modification treatment (sulphonation).

.

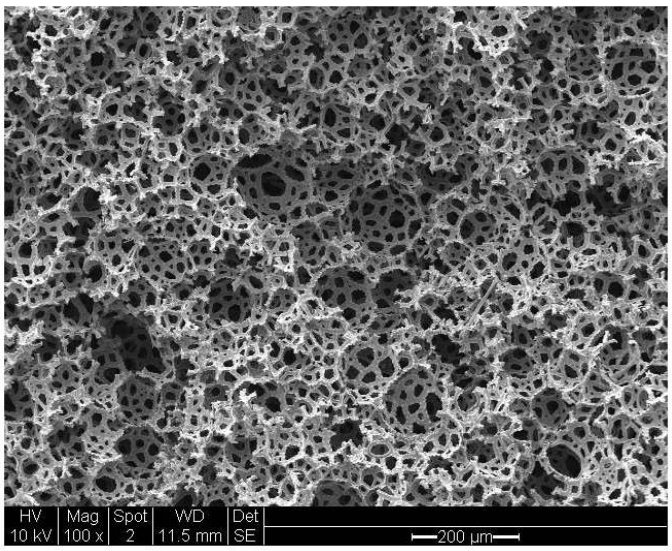

Figure 4.7: Sulphonated polyHIPE after the neutralisation process

The unreacted aqueous sulphuric acid that was mixed in the aqueous phase acted as filler, and was not involved in the polymerisation. Upon microwaving, the sulphuric acid that was entrapped in the polyHIPE skeleton was heated up, and some of it escaped to form nano-pores. The nano-pores and the small cracks (size < 1 µm) in the polyHIPE skeleton can be clearly seen in Figure 4.8. These small cracks essentially induced the water absorption, and the high degree of cross-linking increases its ability to soak up or retain water/liquid more than the other polyHIPEs tested earlier. The additional $SO_3^-H^+$ functional group on the benzene rings increases its hydrophilicity compared to the PS-DVB PHP, where it can hold water at almost 12 times of its own weight. Unlike the TVP PHP, although both were hydrophilic, the sulphonated PHP tends to swell when too much water is absorbed within its skeleton. The size of the sulphonated PHP was enlarged by 5-25% from its original dimensions (diameter), and in some extreme examples, breakage or visibly large cracks occurred as shown in Figure 4.9 (a), especially in cases where the polyHIPE was highly sulphonated which can be easily recognised by its texture and colour. A highly sulphonated PHP is normally soft (spongy) and black, indicating a high degree of burn resulting from microwave irradiation. Figure 4.9(b) shows images of a highly sulphonated PHP, while Figure 4.9(c) shows a normal/moderately sulphonised PHP. Swelling is common for polyHIPEs that exhibit strong hydrophilic properties, and it is also an indicator of a reduced degree of cross-linking, determined by the molar ratio of

polystyrene to DVB (Calkan, 2007). In the present study, the swelling might be attributed to the low DVB content, where only 10% was used during the HIPE preparation. 14-18% of DVB was required to obtain a higher degree of cross-linking, which can therefore eliminate the swelling effect following microwave treatment and the water absorption test. However, the swelling observed in this study was lower compared to the sulphonated PHP and the ethylhexyl acrylate, derived from O/W emulsions, with a swelling ratio reported at 42-44% (Cohen and Silverstein, 2012).

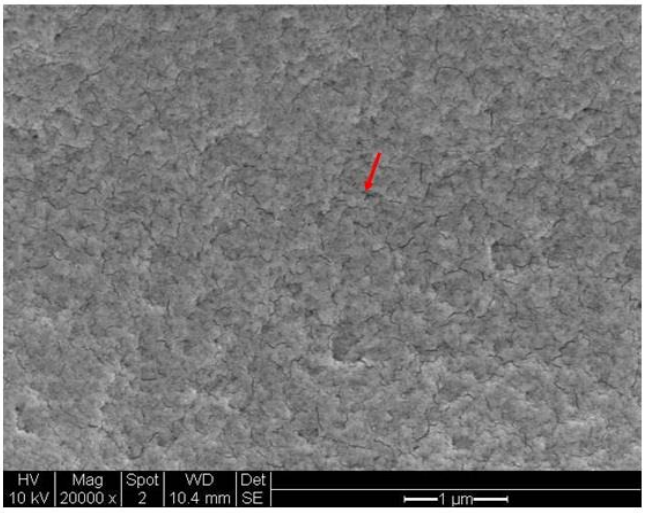

Figure 4.8: Arrow showing micro-scale cracks (<1 µm) on the polyHIPE surface.

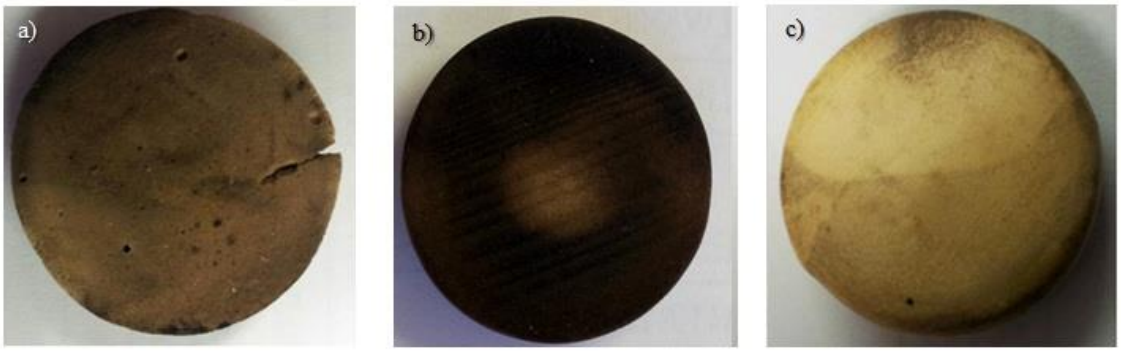

Figure 4.9: a) A large crack occurred in the highly sulphonated PHP after undergoing a water uptake test; b) A highly sulphonated PHP and c) A moderately sulphonated PHP.

The sulphonation mechanism was initiated by temperature and had been discussed in detail by Calkan (2007). When a low temperature (<140 ^{o}C) was used, sulphonation only occurred in the surfactant, and the polyHIPE restored its original

hydrophobic nature after washing, provided all the surfactant was removed. In this study, we observed that water uptake was reduced with reduced pore sizes (Table 4.3). Since the migration of the sulphuric acid during soaking is a function of time, the polyHIPE with small interconnects requires more time for the sulphuric acid to migrate to the entire matrix. Since the soaking time was fixed at 2 hours, there was a chance that some areas in the polyHIPE were not soaked with the sulphuric acid, thus reducing the degree of sulphonation. This was indicated by the reduced water uptake capacity as shown in Table 4.3 below.

Table 4.3: Effects of pore sizes on the water uptake capacity of the sulphonated PHP

Mixing time (min)	**Dosing time (min)**	**Pore (µm)**	**Interconnect (µm)**	**Water Uptake (g H_2O/g polyHIPE)**	**Improvements Over PS-DVB PHP**
5	1	58 $\pm$ 9	20 $\pm$ 3	10.4 $\pm$ 1.1	24
5	5	56 $\pm$ 11	15 $\pm$ 2	9.8 $\pm$ 1.0	22
10	10	46 $\pm$ 5	10 $\pm$ 1	8.9 $\pm$ 0.7	19
10	30	25 $\pm$ 8	5 $\pm$ 0.5	0.5 $\pm$ 0.1	1.2

*Fold increase compared to PS-DVB PHP

Although the yeast adhesion occurred mainly by hydrophobic interactions, this sulphonated PHP was expected to give a good degree of cell interaction due to its increased surface roughness. Moreover, as sulphonated PHP (Figure 4.10) possesses very strong hydrophilic properties, with ability to contain water within its structure through molecular diffusion and convective mechanisms, the scarcity of medium/nutrient in the innermost part can be dealt with easily.

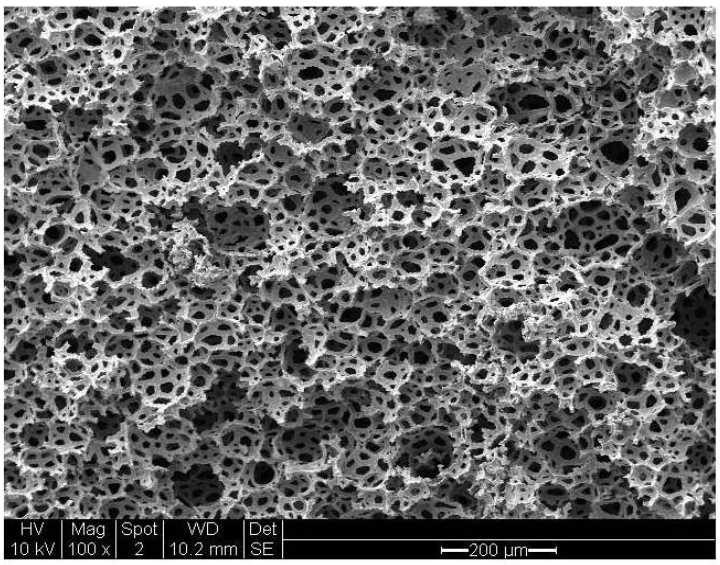

Figure 4.10: Sulphonated PHP after washing.

4.3.2 *Modification of Sulphonated PHP's Surface Chemistry*

The use of the sulphonated PHP was expected to provide a favourable environment for the cell growth. This type of polymer is spongy, and swelled when it absorbed water. The confined well in the PTFE block, which is built just to fit the size of a normal polymer disc without allowing room for polymer expansion, will damage the structure of polymers where tendency to crack is particularly high. If cracking occurs, the nutrient will flow through the crack and neglected most parts of the polyHIPEs. Therefore, in an attempt to increase its strength and rigidity, sulphonated PHP undergone a post-treatment with silica (Bindzil 10).

Another option to alter the surface properties of the sulphonated PHP is by coating it with hydroxypatite (HA). The reinforcement of Ca^{2+} ions from the HA within the polymer matrix, produces a polyHIPEs with a positive surface charge. The increased surface positivity is expected to provide electrostatic attraction of the negatively charge yeast and strengthen the binding. Besides this, Ca^{2+} was reported to induce flocculation of *Citrobacter freundii* in the polyHIPE, which inhibits cell wash out during fermentation and also increases the alcohol production (Griffiths and Bosley, 1993).

Table 4.4: Effect of post modification treatment (Coating with Bindzil 10/HA solution) on the characteristics and architectural properties.

PolyHIPE Type	Pore Size (µm)	Interconnect Size (µm)	Surface Area (m^2g^{-1})	Water uptake capacity[1]	Characteristic
Sulphonated	60 ± 7	20 ± 3	1.90 ± 0.48	12 Folds	Spongy Soft
Bindzil 10 coating (B10-S)	94 ± 10	25 ± 4	58.18 ± 8.16	7 Folds	Hard/Rigid Brittle
HA coating (HA-S)	66 ± 13	20 ± 3	13.88 ± 3.74	8 Folds	Spongy Slightly hard

From the BET analysis, the surface areas of the polyHIPE were further increased up to 6 and 30 fold for HA-S and B10-S, respectively compared to the sulphonated PHP. The incorporation of Bindzil 10 and HA increased the surface roughness and thus increased the surface area. This finding was in agreement with Menner *et al*. (2008), who found that an increased surface roughness contributed to a large surface area, which was obtained by incorporating the nanoparticles (silica) in the aqueous phase. A high surface area is necessary for cell proliferation in order to ensure a monolayer growth, thus reducing the effect of additional resistance for nutrient and oxygen transfer (Akay *et al*., 2005).

Figures 4.11 - 4.13 show images of the polymer after soaking in Bindzil 10 for 4 hours. The spongy nature of the sulphonated polymers has dramatically changed in that they have a hard surface with increased brittleness. While the water absorption capacity was reduced by approximately 42% compared to the sulphonated PHP, a significant increase of the surface area was achieved with both treatments, although SEM images (Figure 4.11a) show that the silica solution (Bindzil 10) clogged most of the interconnect windows located slightly below the surface. However, no sign of

[1] Amount of water against dry weight of polyHIPE

clogging was observed beyond 1000 μm from the surface of the polyHIPE (Figure 4.12).

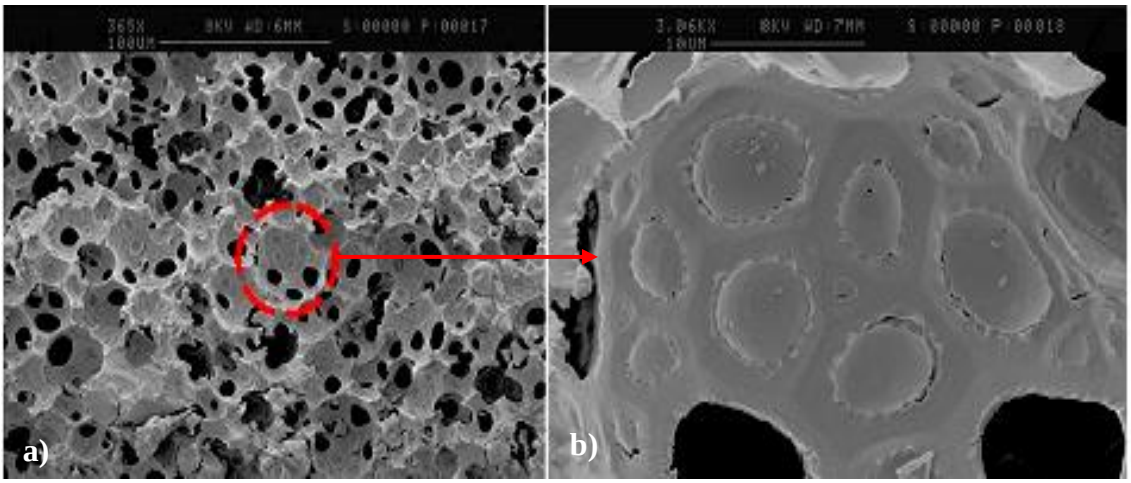

Figure 4.11: a) SEM images at 360x magnifications demonstrating the effect of soaking sulphonated PHP in Bindzil 10 solution which shows signs of clogging on the top surface to 1000 μm below the surface. b) Closed up image at 3000x magnification of the clogged areas.

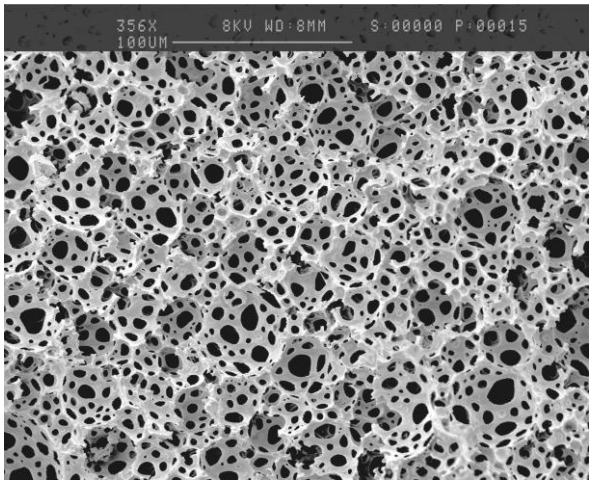

Figure 4.12: SEM images at 350x maginification shows the central region of the sulphonated PHP soaked with Bindzil 10.

The images for the polyHIPE after treatment with the HA solution are depicted in Figures 4.13 - 4.14. Super saturation was observed on the top and at locations closer to the surface, where large clusters of HA was detected as shown in Figure 4.13. The HA tends to agglomerate on the surface, where plenty of the pores are clogged with the substances. The pore sizes for the modified polymers were altered

significantly, with a 66.21% and a 12.26% increase being observed for coating with silica and HA, respectively. A 26.21% increase was attained for the interconnect size after treatment with silica compared to the sulphonated PHP, whereas the HA solution imparted a negligible improvement.

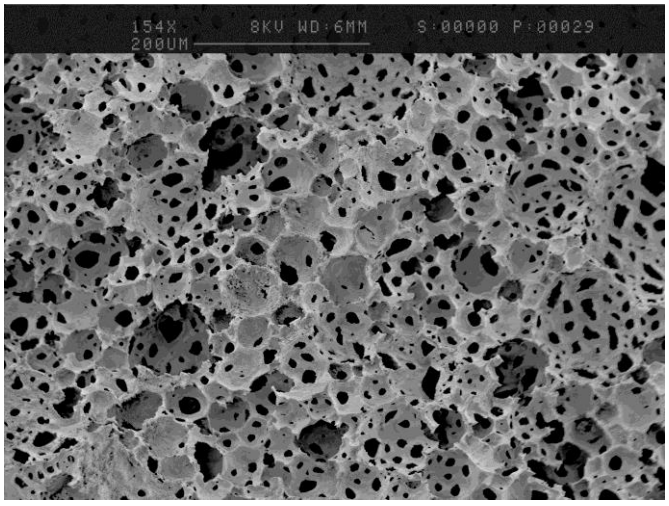

Figure 4.13: SEM images of the sulphonated PHP soaked in 0.5% w/v HA solution.

Unlike the previous HA PHP (Figure 4.5c), the surface of HA-S PHP were much more granular due to the deposition of HA (Figure 4.13 – 4.14). The deposition was heterogenous, was found all over the polyHIPE skeleton. Thicker deposition occurred on the surface of the polyHIPE as shown in Figure 4.14(a), while a considerably more even coating was observed in the interior cavity of the polyHIPE and these covered very large areas in the interior cavity (Figure 4.14b). The deposition process needs to be improved in order to obtain a better distribution of HA particles on the polymer wall, and to achieve homogeneity in every coating process, thus reducing variations in every polymer disc.

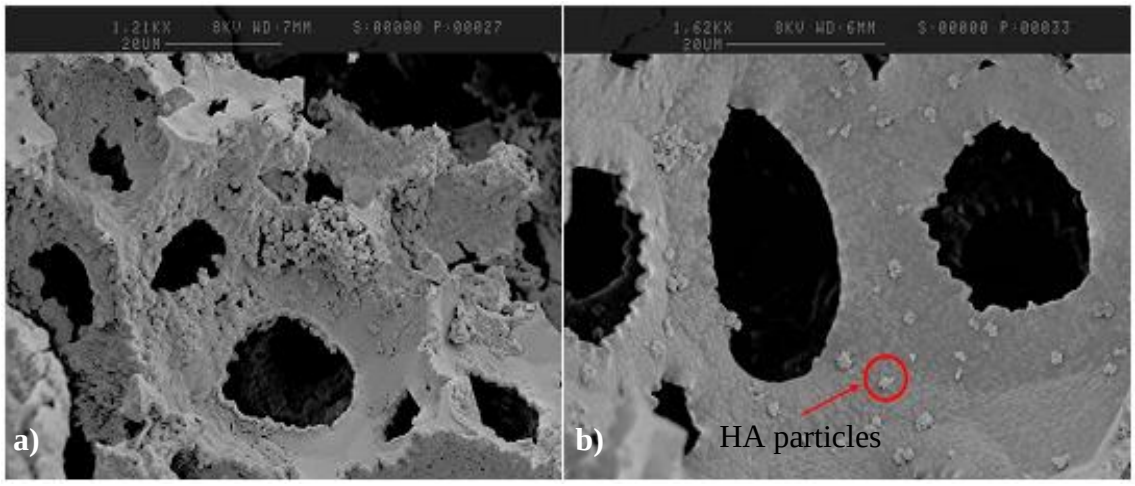

Figure 4.14: a) Deposition of HA observed at the central pores of the polymer disc. b) Close up view of amorphous HA particles on the sulphonated PHP.

4.4 Observation and Conclusions

The simplest way to control the architectural properties for the polyHIPE is through varying the mixing times and the dosing times. These parameters have been proven to have significant effects on the pore and interconnect sizes, but they have shown negligible effect on the polyHIPE's structures. Since measuring the pore and interconnect size was done manually using SEM images with the help of ImageJ software, the tendency to pick up the best pores that did not represent the actual condition of the polyHIPE was high. The technique used might have contributed to error during the calculations, but since the number of pores and interconnects were taken as an average from 70-100 data, we considered that this method can at least partially represent the actual structure/condition of the polymer, with the assumption that the other parts possess the same characteristics as the viewed parts. Besides this, measurement error was hard to avoid due to the inconsistency/irregularity in the shape of these properties. Further study was carried out to test the *S.cerevisiae* W303-PHP biocompatibility, its growth and ethanol production with all the polyHIPEs generated in Section 4.1. Since failure to produce a good post-modification of the sulphonated PHP (modification with silica-Bindzil 10 and HA), these two polyHIPEs were not tested for ethanol production.

CHAPTER 5: ETHANOL PRODUCTION IN BATCH FERMENTATION

5.1 Production of Ethanol in Batch Process by Suspended Cell

For a control study, *S.cerevisae* W303 was grown in both a shake flask and in a 5L bioreactor for ethanol production (Section 3.5). The shake flask fermentation was carried out in a 250 ml flask. 45 ml of medium was used and inoculated with 5 ml (10% of the total working volume) of inoculum. While for growth in the bioreactor, 3600 ml of medium was used and inoculated with 400 ml of inoculum (10 v/v inoculum), and sparged with air continuously throughout the fermentation. The inoculum was prepared from the active seed culture grown prior for 16 hours in a YPG medium at 30^{o}C with absorbance fixed at 0.8, which contained approximately ~$2x10^{7}$ CFU/ml of active yeast cells. The medium used consisted of 25 gL^{-1} of glucose, 5 gL^{-1} of yeast extract and 10 gL^{-1} of peptone, and the cultures were grown for 66 hours. The growth, ethanol production and carbon utilisation were recorded and compared for both systems.

The kinetics data for the growth of *S.cerevisiae* and ethanol production in shake flask fermentation and in the bioreactor is recorded in Table 5.1. The growth of yeast increased exponentially, after being in lag phase for 4 hours and reached its maximum value after 27 hours. The specific growth rate (μ) of *S.cerevisiae* W303 in shake flask fermentation was 0.152 hr^{-1}, with a doubling time (τ_d) of 4.56 h. The maximum biomass and ethanol concentration were 4.30 gL^{-1} and 11.15 gL^{-1}, respectively. These corresponded to a biomass ($Y_{X/S}$) and ethanol yield ($Y_{P/S}$) of 0.19 g/g glucose and 0.50 g/g glucose, respectively, which were achieved upon completion of sugar consumption. For the bioreactor, the following results were obtained: a maximum ethanol concentration of 10.05 gL^{-1}, a slight increase in the specific growth rate of 0.159 h^{-1}, 4.6 gL^{-1} of biomass and a significant increase of the productivity at 1.40 $gL^{-1}h^{-1}$.

Table 5.1: Summary of fermentation for batch processes (shake flask and 5L bioreactor)

Parameter	Shake Flask	Bioreactor
Specific growth rate, μ (h^{-1})	0.152	0.159
Maximum ethanol concentration (gL^{-1})	11.15 $\pm$ 0.81	10.05 $\pm$ 0.74
Ethanol yield, $Y_{P/S}$	0.50	0.45
Overall ethanol productivity, P ($gL^{-1}h^{-1}$)	0.41	0.59
Maximum viable cell (CFU/ml)	7.3×10^7	2.1×10^8
Maximum ethanol productivity P_{max} ($gL^{-1}h^{-1}$)	0.83	1.40
Glucose consumption (%)	100	100
Maximum biomass concentration, X (gL^{-1})	4.3 $\pm$ 0.3	4.6 $\pm$ 0.5
Biomass yield, $Y_{X/S}$	0.19	0.20
Time to enter stationary growth phase (h)	20 and 30[2]	24
Time glucose exhaustion (h)	27	17
Time for maximum ethanol concentration (h)	27	17

Referring to Table 5.1 and Figure 5.1, it was observed that the time for maximum ethanol production and glucose exhaustion for both modes occurred at a similar time, while the maximum biomass attainable lagged slightly afterward. A slightly different pattern for biomass production was observed for shake flask fermentation, where two stationary phases were obtained at 20 and 30 hours. Glucose exhaustion and maximum ethanol production was observed at 17 hours for the cells grown in the bioreactor, while the cells in the shake flask fermentation took 10 hours longer, probably due to the conditions where the availability of oxygen in the culture was limited. Direct sparging of air into the bioreactor induced a respiration process instead of fermentation, which was supported by a reduced ethanol production,

[2] diauxic growth created two stationary phases

increased specific growth rate and markedly higher biomass production compared to the shake flask fermentation. Oxygen availability also increases the sugar utilisation rate in the bioreactor, where complete exhaustion was achieved 10 hours earlier compared to shake flask fermentation. Maximum growth in both the shake flask and the bioreactor was achieved upon completion of the sugar utilisation. However, in shake flask fermentation, clear evidence of diauxic growth (discussed in detail in Section 5.2) was observed in shake flask fermentation, but such a pattern was not observed in the bioreactor growth.

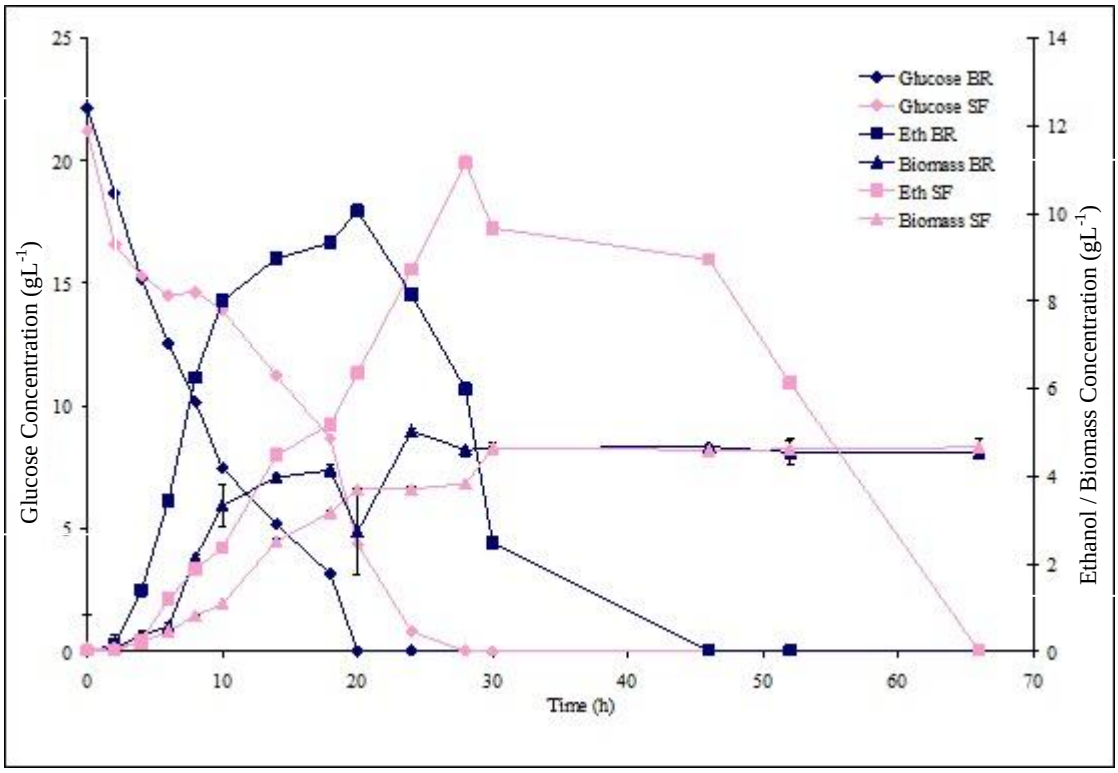

Figure 5.1: Profile of glucose concentration, biomass and ethanol production by free cell *S.cerevisiae* W303 grown in YPG media at 30^{o}C in 5 L bioreactor (BR) and shake flask (SF).

5.1.1 *Discussion*

Accumulation of ethanol started when cells entered the exponential phase, after being in the lag phase for four hours. The ethanol continued to accumulate until 27 hours of fermentation, giving the highest concentration of 11.15 gL^{-1} and overall

productivity of 0.41 $gL^{-1}h^{-1}$. The curve plotted in Figure 5.2 shows that the ethanol concentration dropped rapidly after achieving the maximum concentration, and gradually reduced until it was exhausted at ~65 hours of fermentation. The reduction was due to the assimilation of the ethanol as a consequence of the glucose depletion.

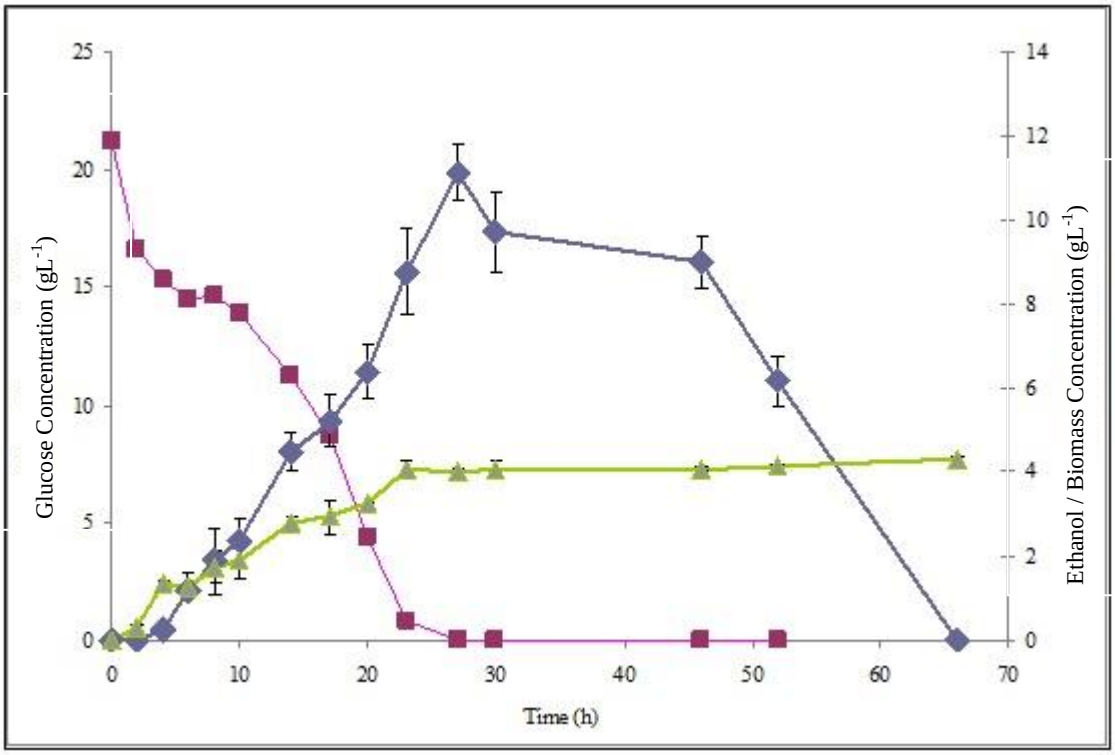

Figure 5.2: Profile of glucose consumption (■), biomass concentration (▲) and ethanol (♦) production by free cell *S.cerevisiae* W303 grown at 30°C in shake flask with shaking fixed at 200 rpm. The assimilation of ethanol started when the glucose as sole carbon and energy source was completely used by the yeast.

The production pattern of ethanol follows the growth associated product, in which the production speeds during the exponential growth. Prolonging the cultivation time resulted in decreased ethanol productivity (Figure 5.3), which was due to the exhaustion of glucose in the culture. The *S.cerevisiae* altered its metabolic pathway from glucose catabolism to ethanol assimilation and consumed ethanol to maintain its cellular activity. At this stage, the number of viable cells reduced from 10^8 to 10^7 CFU/ml as a result of the deprived condition with poor nutritional values. The productivity of ethanol started as early as 4 hours and increased gradually up to 27 hours, before dropping significantly to zero productivity within 6 hours.

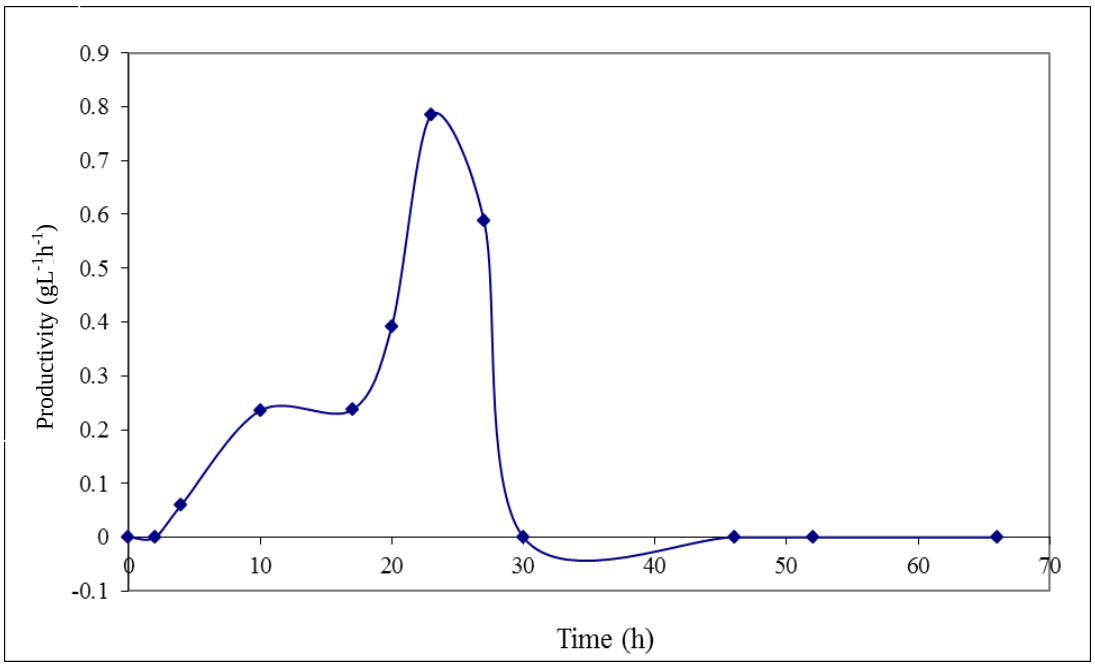

Figure 5.3: Ethanol productivity in shake flask fermentation at 30°C by free cell *S.cerevisiae* W303 grown in YPG media and shaking was fixed at 200 rpm.

The yeast initially consumed glucose for its metabolism, producing both ethanol and new cells in the aerobic condition. However, after depletion of glucose as the sole energy source, the yeast assimilated ethanol for its cellular maintenance which can only happen in the presence of oxygen. A small increment in the OD after 27 hours (Figure 5.4), which corresponded to a reduction of ethanol concentration, showed that the yeast switched its metabolic pathway to ethanol assimilation and continued producing new cells. A similar diauxic growth pattern was observed after 40 hours in the batch culture of Flesichmann yeast, supplemented with 20 gL^{-1} of glucose and 10 gL^{-1} of peptone (Da Cruz *et al*., 2002). They mentioned that this condition can be avoided by increasing the glucose supply from 20 gL^{-1} to 150 gL^{-1} to ensure availability of glucose throughout the fermentation process, hence preventing the assimilation of ethanol by the yeast. However, switching to ethanol assimilation through the respiratory pathway was also due to low sugar uptake flux into the yeast cell, and this condition can occur even though the remaining glucose or other sugars in the culture was high (Ramon-portugal *et al*., 2004).

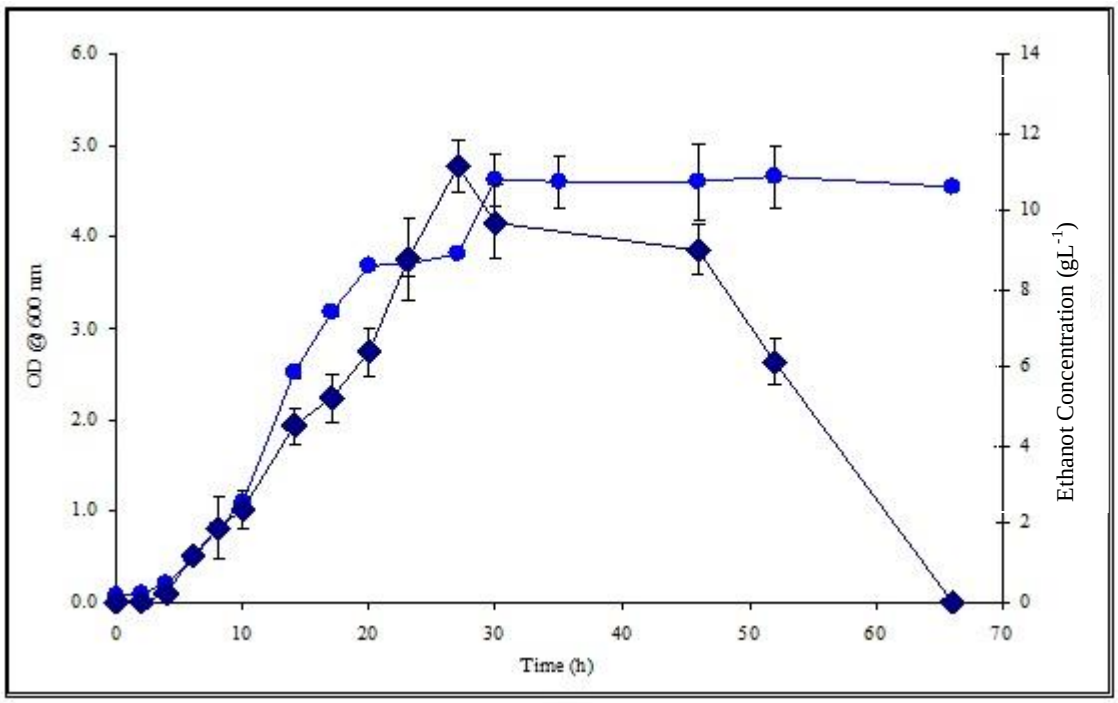

Figure 5.4: The profile of OD profile (•) and biomass content in the shake flask culture of free S.cerevisiae W303 grown in YPG media at 30°C showed a diauxic growth pattern after 27 hours of fermentation that occurred simultaneously with ethanol (♦) assimilation. Shaking was fixed at 200 rpm.

Yeast metabolism is rather complex, and varies significantly between strains. This study indicated that the assimilation of ethanol as an alternative carbon source only occurred after the exhaustion of glucose, but, occasionally, ethanol can be metabolised simultaneously with glucose in aerobic conditions when the sugar flux uptake in the cell is much lower than the respiratory capacity (Ramon-Portugal *et al.*, 2004). This happened when the energy requirements for cell maintenance exceeded the energy generation from the breakdown of glucose. As a result, ethanol was used as a substitute for glucose and was assimilated by the yeast (ethanol metabolism is completely aerobic) in order to gain more energy for cell regulation. However in this study, the termination of the ethanol production and the onset of its metabolism occur promptly in response to glucose depletion, while in some species, there was a time delay in-between glucose metabolism and ethanol assimilation. The delayed occurred because the yeast needs time for new gene regulation and expression. The rapid shift of glucose fermentation to oxidative metabolism (ethanol assimilation) was presumably enhanced by the presence of peptone in the media (Da cruz *et al*., 2002), and this also indicated that this yeast responds very quickly to its surroundings. In

order to prevent the assimilation of ethanol, the glucose must be kept available within the system. But this is not necessarily true, as some yeast can consume both glucose and ethanol simultaneously to produce ATPs for the cell's usage, although the glucose was still present (Souto-Maior *et al*., 2009).

SEM images of yeast cells were taken from the 16 and 72 hours shake flask cultures in order to study the size and the morphology of cells in the exponential and stationary phases, respectively. It is show in Figure 5.5a (exponential phase-active cell) and Figure 5.5b (stationary phase-non active/aged cell) that the shape of these cells differs significantly between the phases. The sizes of young and active budding cells were broadly distributed, ranging from 2.5-7.5 μm, with irregular or slightly oval shapes (Figure 5.5c) due to budding activities and formation of pseudohyphae (Hogan, 2006). On the other hand, the aged yeast exhibited a more spherical shape, and the size distribution was narrower compared to the cell in the exponential phase, ranging between 3.5 – 4.3 μm (Figure 5.5d). In general, cells were more rounded and had thicker walls than that in the exponential phase when observed with phase-contrast microscopy (Werner-Washburne *et al*., 1993). More budding cells were observed in the active growth phase and the numbers reduced significantly during the stationary phase. Besides this, more cell coagulation was observed in the exponential phase compared to the stationary phase, as shown in Figures 5.5 (e) and 5.5(f) respectively.

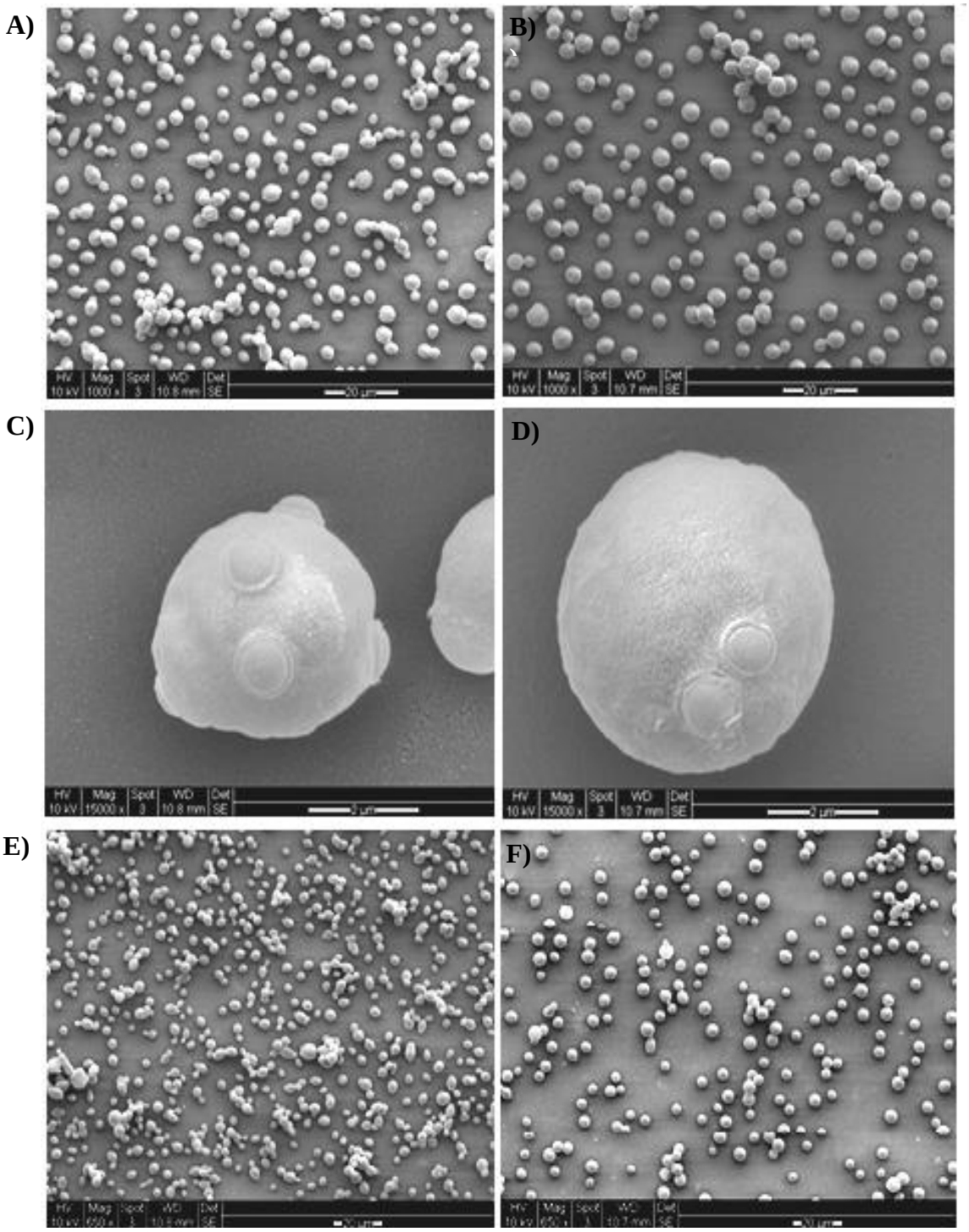

Figure 5.5: a) Cells in the exponential phase have two distinguished features: i) spherical for the mature and newly separated cells; and ii) ovalish due to elongation during budding. b) The shape of yeast is spherical and homogenous during the stationary phase. Closed up view of *S.cerevisiae* W303 in the exponential stage (c) and in the stationary stage (d). A higher degree of flocculation was observed in the exponential phase (e) compared to the cells in the stationary phase (f).

Size reduction of *S.cerevisiae* was also observed by Tibayrenc *et al*. (2010) as the diameter reduced from 6.5 μm to 5 μm when it entered the stationary phase growth. It was attributable to the depletion of glucose, but it recovered quickly after adding the glucose. Other stressors such as temperature and furfural (product from lignin degradation) played a significant effect on the reduction of cell sizes (Tibayrenc *et al*., 2010). Other studies also reported the reduction in cell size occurred whenever the yeast was subjected to stresses such as ethanol, glucose depletion, heat, osmosis, pressure and hazardous chemicals such as acetate and furfural.

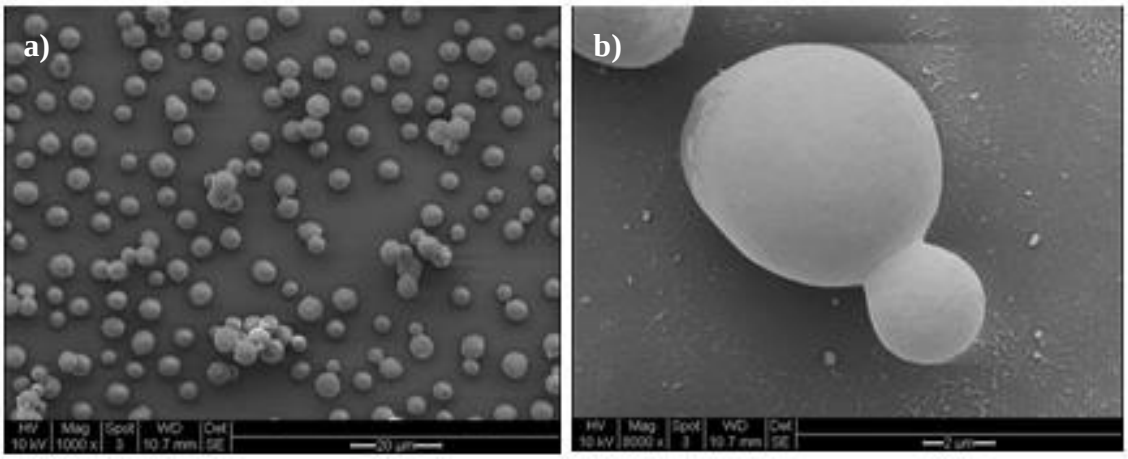

Figure 5.6: a) In the stationary phase, only small cell aggregates were observed with less than ten cells bound together during.. b) Yeasts were still budding but the numbers dropped significantly compared to the exponential phase.

5.2 Effect of Different Media on the Ethanol Production:Suspended Culture

The study of different media compositions was carried out in the shake flask culture to investigate its effect on the enhancement of growth and ethanol production. This study was carried out in a 250 ml volumetric shake flask using 45 ml of the medium and was inoculated with 5 ml fresh inocula. Previous study had shown that glucose was consumed within 27 hours, therefore in this part; the fermentation was carried out for 24 hours only. Four media were tested and the concentration of the individual components was listed in Table 5.2.

Table 5.2: Medium for the growth and ethanol production

Medium	Component	Composition (% w/v)	pH
1	Glucose	2	not adjusted
	Yeast extract	0.5	
	Peptone	1	
2	Glucose	2	adjusted to 5.5
	Yeast extract	0.5	
	Peptone	1	
3	Glucose	2	not adjusted
	Yeast extract	0.5	
	NH_4SO_4	1	
	KH_2PO_4	1	
	$MgSO_4.7H_2O$	0.5	
4	Glucose	2	not adjusted
	Yeast extract	1	
	Peptone	2	

* The pH values for the unadjusted pH medium varies between 6.1 – 7.1.

Samples were analysed at the end of the incubation period for the ethanol concentration, biomass and unused glucose. The results obtained are depicted in Figure 5.7 showing the effect of medium types on the biomass and ethanol production. Adjusting the pH to 5.5 while the other parameters were held constant, resulted in an increased ethanol concentration from 6.92 gL^{-1} (non-adjusted pH – Medium 1) to 7.49 gL^{-1}. A slight increase of <10% was also observed in the biomass production. On the other hand, replacing the peptone with ammonium sulphate and enriched with K^+ and Mg^{2+} (Medium 3) did not pose any impact on both biomass and ethanol production compared with the production of Medium 1. It was assumed that nitrogen requirement from both organic and non-organic supplies was sufficient for the fermentation, while the yeast extract alone was enough to supply all the essential nutrients (sourced from complex nitrogen) that are vital for both growth and ethanol synthesis. Although there was a possibility of replacing complex nitrogen with cheap ammonium salt, but the amino acid in the complex nitrogen sources (e.g. the yeast extract and the casamino acid) was needed to speed up the fermentation processes (Da cruz *et al*., 2002). On the other hand, the availability of carbon sources in Medium 1 were higher than

Medium 3 (because of additional C from the yeast extract and peptone) but there was no significant difference in the biomass production was observed compared to the production in Medium 3.

Significant differences with p >0.005 were observed in the ethanol production using all four types of medium as depicted in Figure 5.7. Changing the pH to 5.5 gave a slight increase in ethanol production in Medium 2, compared to the unadjusted pH (Medium 1). Doubling the peptone concentration in Medium 4 resulted in a significant improvement in biomass production compared to all three media. The highest ethanol concentration was also observed with Medium 4. Since no significant improvement in terms of ethanol production can be achieved after increasing the peptone concentration (Medium 4), or substituting NH_4SO_4 with enriched minerals as in Medium 3, Medium 2 was used for further work as it not only produced the highest ethanol concentration but also reduced the overall cost of medium preparation.

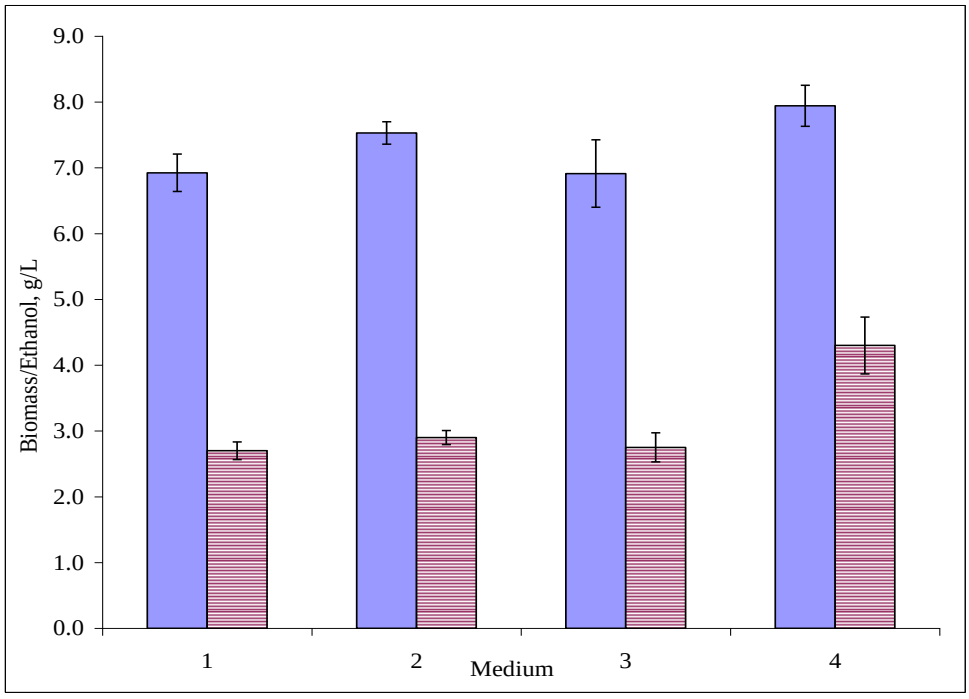

Figure 5.7: The influence of medium composition on the ethanol production (solid bar) and biomass concentration (lined) in a shake flask culture. (Medium 1 – (M1) - 5 gL^{-1}YE, 10 gL^{-1}P and 20 gL^{-1} G; Medium 2 (M2)- 5 gL^{-1} YE, 10 gL^{-1}P, 20 gL^{-1} G, pH 5.5; Medium 3 (M3)- 5 gL^{-1} YE, 10 gL^{-1} NH_4SO_4, 10 gL^{-1} KH_2PO_4, 5 gL^{-1} $MgSO_4.7H_2$, 20 gL^{-1} G; and Medium 4 (M4)- 5 gL^{-1} YE, 20 gL^{-1}P, 20 gL^{-1} G).

5.3 Partial Characterisation of *Saccharomyces cerevisiae* W303

The immobilisation process, or surface adhesion, of the microorganism is affected by three important components, which are: i) the physico-chemical properties of microorganisms, ii) the characteristics of the surface material and iii) the environment (e.g. types of medium, temperature, shear stress, period of exposure, surface tension of the medium, and bacterial concentration). The physico-chemistry of the microorganisms is the important driving force, though it interacts differently for given surface and process conditions (Kilonzo *et al*., 2011). Strain types, particle shape, surface wettability and surface charge are some of the important factor that initiate cell-surface adhesion. Therefore, knowledge of the surface chemistry (e.g. hydrophobicity) of the yeast is essential for understanding its interaction with the surface materials. These properties can be determined by using water contact angle analysis (Vazquez-Juarez *et al*., 1994), or the microbial-adhesion to-solvents (MATS) test (Rosenberg *et al*., 1980; Vazquez-Juarez *et al*., 1994). The MATS test provides a simpler and cheaper technique for speedier data collection but is less accurate compared to its counterpart (White and Walker, 2011). For the purpose of immobilization, the yeast sizes are also an important aspect to be considered for preparing a suitable PHP. Therefore, size analysis was carried out using two types of measurement: i) image analysis (SEM) and ii) particle size analyser. Since the size and surface hydrophobicity varied with the growth stages, the measurement was done for cells at the exponential (16 hours culture) and stationary stages (72 hours culture).

5.3.1 *Determination of Yeast Size*

The size distributions were measured with a particle size analyser (PSA) and compared with those obtained from the SEM images. The results were shown in Figures 5.8 and 5.9. According to Figure 5.8, the yeast sizes were distributed ranging from 2 μm – 18 μm at all concentrations tested (10^7-10^9 cells/ml), and peaked at approximately 5.2 μm. On the other hand, the size measured using the ImageJ peaked at ~4.4 μm - 5 μm. The largest single cell observed using the ImageJ was

approximately 7 μm in size, while PSA analysis showed a much wider and larger distribution that reached beyond 10 μm. This large size (> 7 μm) was contributed by the clustered and budding cells that were considered as one particle. These cell clusters were evident as shown in Figures 5.5. The size of *S.cerevisiae* is varied according to strain and environment factors. Maercier-Bonin *et al*. (2004) reported a size distribution of *S.cerevisiae* was in the range of 2.5 to 13.5 μm, which peaked at 3.65 μm. A narrower size distribution was reported for the 24-hours culture of *S.cerevisiae* KCTC 7919, ranging from 2 μm – 6 μm and peaked at 2.9 μm (Kim *et al*., 2009). Vergnault *et al*. (2004) observed a single yeast sized 5 μm, which formed cell aggregates with a diameter between 20 to 50 μm when measured with PSA. The size variability was not only affected by age and cell concentration, but also by temperature, and inhibitors such as acetate and ethanol (Tibayrenc *et al*., 2010). The PSA analysis was much more accurate for measuring strains that resist flocculation, where in some strains it was easily induced by high cell concentration. In this study, we did not observe any peak shift, even at high cell concentration (10^9).

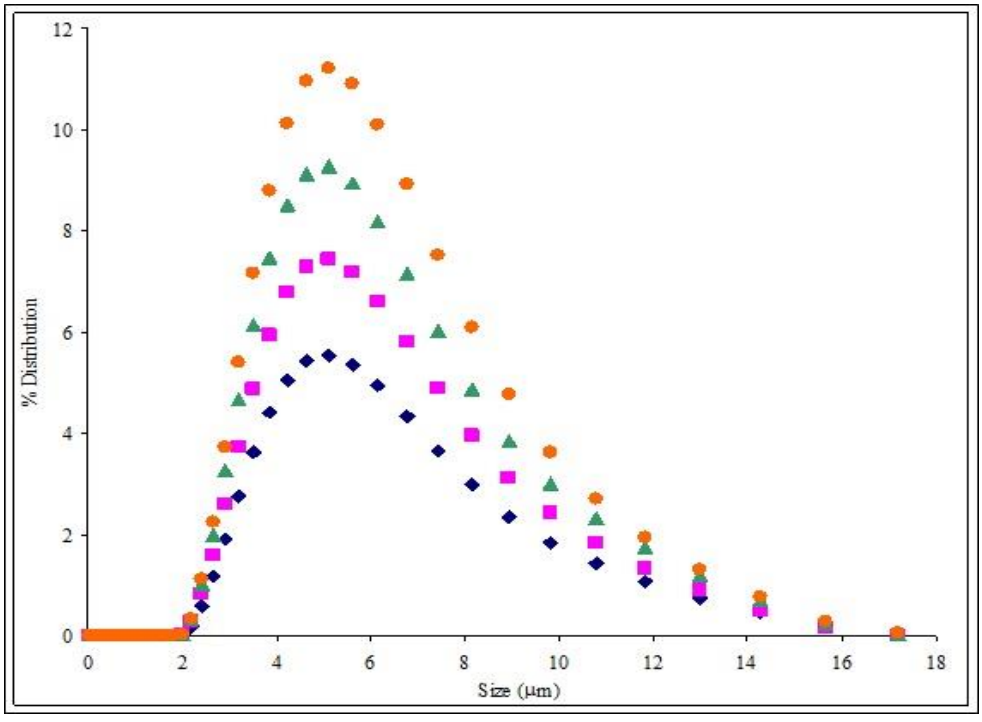

Figure 5.8: Size distribution of yeast cells at the exponential stage sampled at difference absorbance (♦ - 0.6 ; ■ – 0.8; ▲- 1.0; and ● – 1.2.).

The size variation observed for 100 cells in the exponential and the stationary stages measured with ImageJ is shown in Figure 5.9. Both profiles peaked at sizes ranging from 3 μm -3.9 μm. A sharper peak was observed for cells in the stationary phase, but a broader distribution was observed for the exponential cells. Significant numbers of cells with size larger than 6 μm were observed in the exponential stages (active cells), and completely extinct in the stationary stages. Cell shrinkage was also observed for other *S.cerevisiae* strain, where the diameter decreased progressively from 6.5 μm to 5 μm as it enters stationary stage (Tibayrenc *et al*., 2010) .

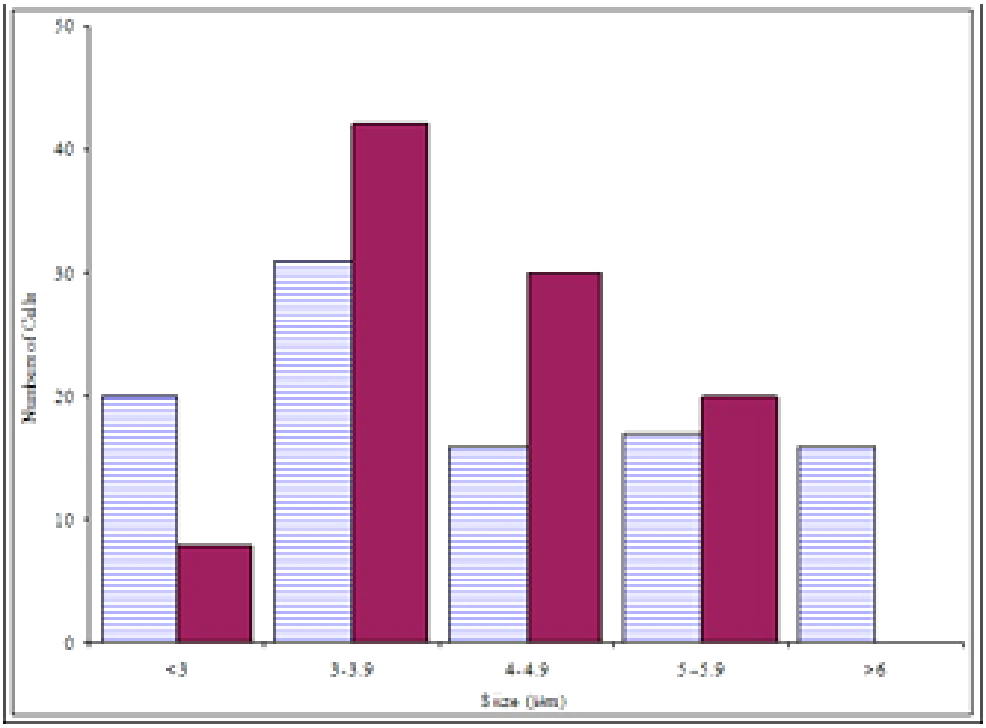

Size (μm)	Exponential Phase		Stationary Phase	
	No	STD	No	STD
2-2.9	20	0.20	8	0.08
3-3.9	31	0.19	42	0.26
4-4.9	16	0.24	30	0.27
5-5.9	17	0.22	20	0.21
>6	16	0.42	0	0
Total	100	-	100	-

Figure 5.9: Size distribution of yeast in the exponential (lined bar) and stationary stages (solid bar) measured with ImageJ.

Statistical analysis with Minitab software was carried out for 3 distinguishable categories: i) the exponential phase, ii) the stationary phase and iii) the immobilised cells in sulphonated PHP grown for 48 hours revealed an insignificant size difference (p = 0.052) for each of the cell categories (Table 5.4). The mean cell diameter of 3.9 $\pm$ 1.5 μm, 4.3 + 0.9 μm and 4.0 $\pm$ 1.0 μm were recorded for the exponential, the stationary and the immobilised cells, respectively. Although cells at the exponential stage exhibited the smallest diameter, they had the highest standard deviation (SD), due to the broader size range. The biggest cell size with the smallest SD was obtained with the stationary cells, showing a more uniform size compared to the others.

Table 5.3: Analysis of variance using Minitab software

One-way ANOVA: SIZE versus STAGE

Source	DF	SS	MS	F	P
stage	2	7.79	3.89	2.99	0.052
Error	317	412.70	1.30		
Total	319	420.49			

Individual 95% CIs For Mean Based on Pooled StDev

Level	N	Mean	StDev	---+---------+---------+---------+------
Exponential	110	3.893	1.453	(--------*-------)
Stationary	110	4.267	0.907	(--------*-------)
Immobilized	100	4.044	0.970	(--------*--------)

---+---------+---------+---------+------
3.75 4.00 4.25 4.50

5.3.2 *Properties of Yeast cells*

Adherence of *S.cerevisiae* W303 grown at 16 and 72 hours to various hydrocarbons is presented in Table 5.4. *S.cerevisiae* W303 in the stationary phase exhibits a low affinity towards solvents (less that 30%). These results suggest that the strain used in the study was probably hydrophilic, because of its lower affinity towards hexadecane and decane, of 11.18% and 0.87%, respectively. Its electron donating property was also poor, indicated by its low affinity towards chloroform (10.93%). However, there was a possibility that *S.cerevisiae* W303 may possesses an electron accepting capacity, since the affinity towards ethyl acetate was significantly ($p < 0.05$) higher than decane in both phases. An industrial type *S.cerevisiae* showed similar

characteristics towards the solvents as in the present study, but with slightly higher affinity, which varies approximately between 7 to 30% (Mercier-Bonin *et al*., 2004).

Table 5.4: Cell surface hydrophobicity of *S.cerevisiae* W303

Solvent/Cell stage	Exponential State	Stationary State
	Adhesion (%)	Adhesion (%)
Hexadecane	11.18 $\pm$ 1.09	8.45 $\pm$ 0.51
Chloroform	10.93 $\pm$ 1.60	11.3 $\pm$ 0.68
Ethyl acetate	10.98 $\pm$ 1.91	27.25 $\pm$ 2.69
Decane	0.87 $\pm$ 0.07	15.75 $\pm$ 0.92

*Percentage of population binds to solvents

In general, the hydrophobicity increases as the cells enter the stationary phase, which was represented by higher affinities towards tested solvents, except for hexadecane, which gave approximately a 25% reduction compared to the affinity in the exponential phase. Increased hydrophobicity for cells in the stationary phase was also reported by other researchers(Vazquez-Juarez *et al.*,1994; Smit et al., 1992). A 100% increase of hydrophobicity was observed for *S.cerevisiae* Y41 cultured for 72 hours, compared to cells cultured for 24 hours. Cells in thet stationary phase are generally more hydrophobic due to the alteration of the wall and cell composition (Werner-Washburne *et al*., 1993). Besides culture age, the hydrophobicity was highly influenced by the growth media, surface protein and cell structure (Merritt and An, 2000). Since many researchers query the accuracy of MATS, the best method to determine cell hydrophobicity is by using contact angle analysis. White and Walker (2011) reported a hydrophilic *S.cerevisiae* (determined using contact angle analysis), but at the same time it showed a high affinity towards solvents.

5.4 Immobilisation: Effect of the Immobilisation Technique on the Cell Adhesion and Ethanol Production in a Shake Flask Culture.

Two types of immobilisation (Section 3.3.4) were tested: i) shake flask seeding and ii) force seeding using the polyHIPEs prepared in Chapter 4. All the PolyHIPEs seeded with *S.cerevisiae* W303 were then transferred to an individual flask, containing 50 ml of the growth medium, incubated for 24 hours, and shaken at 200 rpm (Figure 5.10) (Section 3.5.2). The polyHIPEs used in this study were different with respect to the porosity, mixing and dosing time. The effects of surface hydrophobicity/hydrophilicity on cells' adherence were assessed in the shake flask fermentation and the data collected at the end of the fermentation is presented in Table 5.5 and Table 5.6. All results are an average of three replicates.

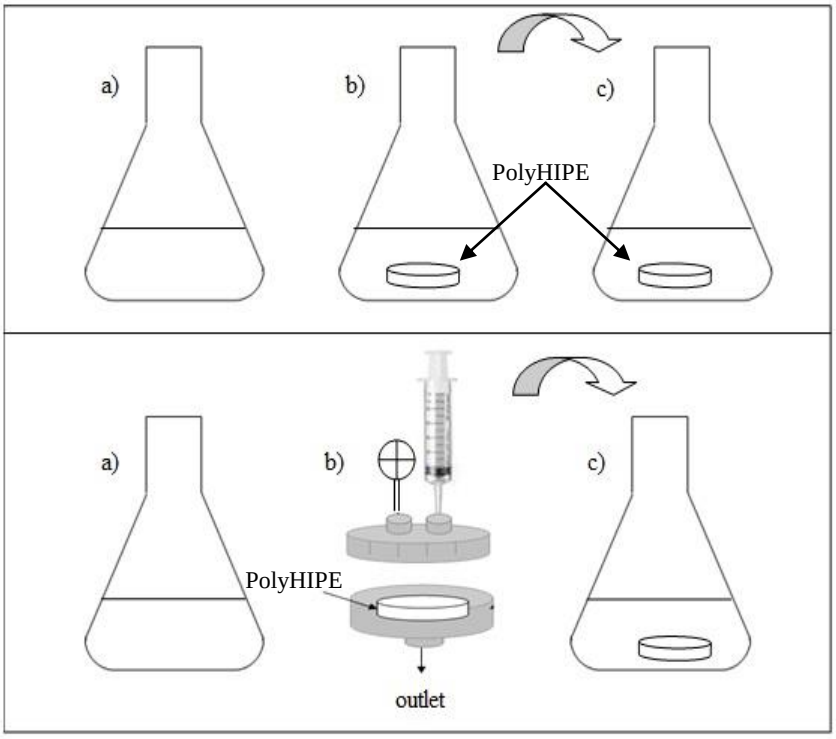

Figure 5.10: Schematic diagram of the fermentation process by immobilised *S.cerevisiae* W303 using two different seeding techniques. The upper diagram represented a shake flask seeding techinuqu while the lower diagram employed a force seeding technique. a) Inoculum prepared from a 16 hours culture, b) seeding step and c) fermentation for 24 hours shake at 100 rpm.

Table 5.5: Ethanol and biomass production using the shake flask seeding technique.

Polymer	Pore size	Ethanol (gL^{-1})	$^{3}Y_{P/S}$ (g/g)	Biomass released (gL^{-1})	Protein (μg/ml)
HA PHP	57 ± 8	6.63 ± 0.77	0.332	1.5 ± 0.27	456 ± 41
TVP PHP	38 ± 4	5.14 ± 1.98	0.257	1.2 ± 0.31	383 ± 37
Sulphonated PHP	60 ± 10	7.98 ± 1.18	0.399	1.3 ± 0.38	514 ± 24
PS-DVB PHP	55 ± 7	6.51 ± 1.33	0.326	1.4 ± 0.25	474 ± 60

- Refer to Section 3.3.4

Table 5.6: Ethanol and biomass production using force seeding technique.

Polymer	Pore size	Ethanol (gL^{-1})	$^{10}Y_{P/S}$ (g/g)	Biomass released (gL^{-1})	Protein (μg/ml)
HA PHP	57 ± 8	8.06 ± 1.23	0.403	2.3 ± 0.23	476 ± 37
TVP PHP	38 ± 4	7.93 ± 1.54	0.397	1.8 ± 0.15	488 ± 58
Sulphonated PHP	60 ± 10	8.26 ± 0.78	0.413	1.4 ± 0.20	493 ± 43
PS-DVB PHP	55 ± 7	8.93 ± 1.94	0.447	1.4 ± 0.37	520 ± 93

- Refer to Section 3.3.4

A dramatic increase of growth in the TVP-PHP was observed following the force seeding technique, supported by a 30% increase in protein content (488 ± 58 μg/ml) compared to the shake flask technique (383 ± 37 μg/ml). This might be attributable to there being more cells available in the polyHIPE that employed the force seeding technique, therefore growth was enhanced significantly, thus increasing ethanol production by 54.8% to 7.93 ± 1.54 gL^{-1}. The number of released cells also increased from 1.2 gL^{-1} to 1.8 gL^{-1}. The highest protein content (520 ± 93 μg/ml) and ethanol concentration (8.93 ± 1.94 gL^{-1}) were observed with the PS-DVB PHP. The fact that there are more cells entrapped in this PHP suggests that *S.cerevisiae* W303 favours hydrophobic surfaces rather than hydrophilic surfaces (TVP PHP and sulphonated PHP). On the other hand, the lowest growth (383 ± 37μg/ml) and ethanol concentration (5.14 ± 1.98 gL^{-1}) were observed with the TVP PHP using the shake flask technique. This condition was assumed to be partly attributable to its small pore

[3] Theoretical for ethanol production is 0.511 g/g glucose

sizes (compared to other PHPs), where the cell penetration into this PHP during the inoculation was hindered. On the other hand, the protein content for the PS-DVB PHP was increased from 474 μg/ml in the shake flask technique to 520 μg/ml in the force seeding technique.

Overall, more cells (protein content) were observed in the force seeding technique in all the polyHIPEs except for the sulphonated PHP. Protein content was reduced by 4.0% in force seeded sulphonated PHP compared to shake flask seeding. On the other hand, the number of cells released into the medium was increased slightly, by 7.7%. Despite the decrease in protein content compared to the shake flask technique, an increase in ethanol production was achieved using the HA-PHP and the sulphonated-PHP, enhanced by approximately 21.6% and 3.5%, respectively. Comparing both methods, ethanol production was considerably higher using the PS-DVB and the sulphonated PHPs compared to the TVP and the HA PHPs. However it was impossible to conclude the finding for the best polyHIPE that supports both growth and ethanol production, as the increases of ethanol were contributed by both immobilised and free cells.

In general, both techniques were able to seed *S.cerevisiae* W303 in all the polyHIPEs, but higher growth and ethanol production were observed for the force seeding technique. The yeasts were able to adhere and attach themselves to all the polyHIPEs regardless of the types of surface (hydrophobic/hydrophilic). The immobilised yeast was capable of growing/proliferating in the polyHIPE, thus producing ethanol, although the production was reduced by 20-55% compared to free cell fermentation (shake flask). Overall, a higher ethanol production and protein content were achieved using the force seeding technique. Active migration of cells occurred when the yeast cells were force-seeded using the pump syringe, resulting in more cells being immobilised in the polyHIPE. While in the shake flask seeding technique, the passive migration of cells was generally driven by gravity and large interconnects/openings, occurred at a very slow rate. Another drawback of the shake flask seeding technique is that it requires additional preparation time which can increase the overall cost of the production.

Some unwetted areas were observed in the tested polyHIPEs, suggesting that a channelled or truncated flow of nutrients was occurring, with very minimal or almost no growth detected in such areas (Figure 5.11). This condition is best avoided as it will reduce the reactor performance and efficiency. In this study, the nutrient enriched medium played two important roles; it can either: i) be a driving force that induced cell migration, or, ii) help transmit the detached cells to the neighbouring pores and spread them to the entire matrix. It was quite surprising that this problem also occurred in the sulphonated PHP as we know that this polyHIPE possesses a highly adsorbent property, therefore flow limitation was expected to be eliminated. Unlike with the hydrophobic polyHIPEs, the channelling process is common, because medium transfer by capillary action is due to its low permeability to water, therefore flows of the medium generally prefer an easy route/exit (large opening).

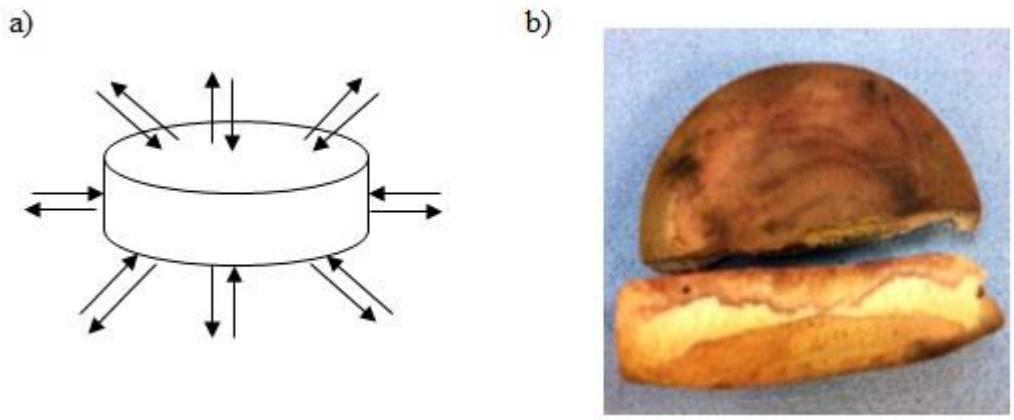

Figure 5.11: a) Arrows shows the medium entering and exiting the polyHIPE from various angles. b) Picture of the polyHIPE showing the unwetted area.

5.5 Conclusion

The effects of nutrient composition and the partial characterisation of *S.cerevisiae* W303 provide an understanding of the interaction of yeast-surface chemistry. Further study of the effect of inoculation techniques proved the advantages of forced inoculation over the shake flask technique; therefore this method will be used in the following work. Since all the polyHIPEs acted as a good support for the

yeast attachment, it will be further tested in the continuous mode. The introduction of a one way inlet and outlet will provide a constructive solution for the channelling problem. The results of the batch fermentation by free cells will be used as a comparison with the results produced by the immobilised cells in the continuous fermentation.

CHAPTER 6: ETHANOL PRODUCTION BY IMMOBILISED *Saccharomyces cerevisiae* W303 IN CONTINUOUS MODE

6.1 Continuous Operation

The main objectives for the continuous ethanol fermentation was increased the productivity by dealing with the product and substrate inhibition that occurred in the batch process. Inhibitory effect caused by ethanol accumulation was controlled to minimum by continuous removal of the product; on the other hand also prevented this metabolite from being consumed by the yeast. However, in order for the continuous operation to be applied commercially, it is necessary to obtain steady, complete glucose consumption with high ethanol outflow. Besides, it must also able to give higher ethanol productivity and *S.cerevisiae* concentration and viability must remain high throughout the process. In the case of immobilization techniques, proper selection of the supports that allow the passage of CO_2 is one of the crucial part. Retention of CO_2 caused by improper channelling of the gas bubbles creates dead zones, hence reducing the productive capacity of the microreactor itself.

The monolith microreactor was operated at a relatively high dilution rate (D_r = 22 h^{-1}) in comparison to the specific growth rate obtained in batch culture (0.15 h^{-1}). Operating at high dilution rate is often beneficial for providing external force to facilitate cell migration and switching the respiratory process to fermentative metabolism to enhance ethanol production. With respect to this issue, experiments were conducted at D_r = 22 h^{-1} which surpassed the critical dilution rate of the growth of *S.cerevisiae* W303.

6.2 Effect of Surface Chemistry on Cell Growth and Ethanol Production in a Monolithic Microreactor

The first part of the continuous study was to investigate the best surfaces for good cell attachment while providing space for cell growth and proliferation. To avoid variability of the results, polyHIPEs with relatively similar pore size were used. However, this was almost impossible, and much work was required to achieve the same pore and interconnect sizes for all the polyHIPEs tested, therefore the range used in Table 6.1 was considered appropriate for this study. A range of polyHIPEs with varying surface wettability, were tested, with the pores sizes between 55 – 57 μm. Introduction of a continuous medium supply to the microreactor (one way inlet and outlet) induced the wetting capacity of the polyHIPE as the medium was forced to flow through the microreactor, which subsequently achieved a more even cell distribution. Experiments were run for maximum of 72 hours, and samples were taken at regular time intervals to test for the cells released and the ethanol concentration. The condition of the cells growing in the microreactor was viewed with a SEM at the end of the fermentation time to study the effect of surface chemistry on the behaviour and the cell adhesion.

Table 6.1 Properties of polyHIPEs used to investigate the effect of the yeast attachment and the ethanol production.

PolyHIPE Type	Pore (μm)	Interconnect (μm)	Retention Time (min)	Water uptake (g H_2O/ g PHP)
PS-DVB	55 ± 7	12 ± 3	2.7	0.4
HA	57 ± 10	18 ± 4	2.3	3.4
Sulphonated-NH_4OH (S- NH_4OH)	55 ± 5	16 ± 5	3.8	11.5
Sulphonated-KOH (S-KOH)	56 ± 5	15 ± 3	3.9	13.0

The medium was fed into the microreactor, in which glucose was converted to ethanol and was removed continuously to the waste tank. The ethanol was produced within the microreactor, and the retention time of these microreactors was unique for the different types of polyHIPE (Table 6.1). Apart from ethanol, the outlet stream of the microreactor consisted of the unreacted medium, acetic acid, CO_2 and detached cells. The rig arrangement is depicted in Figure 6.1.

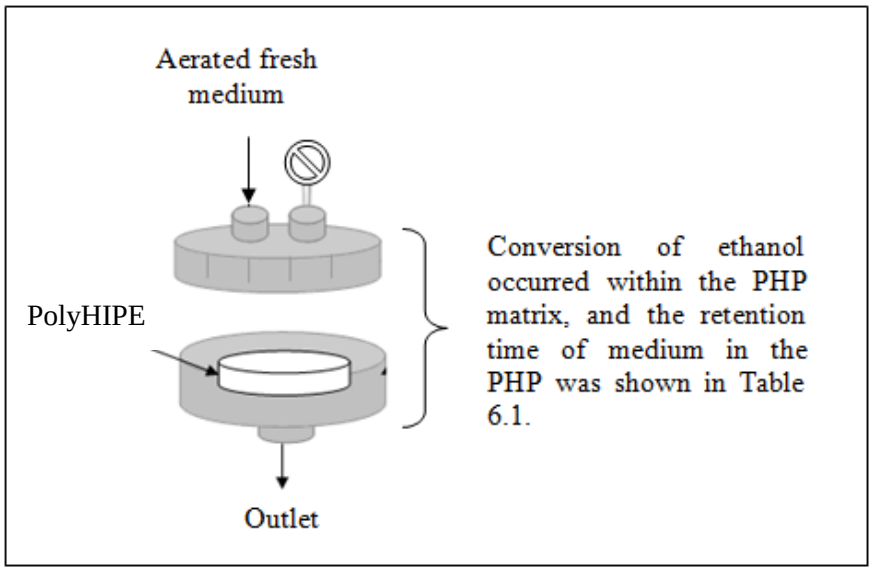

Figure 6.1: The conversion of glucose to ethanol occurred when the medium was passed through the polyHIPE, within the estimated time for conversion

The adhesion of cells to surfaces was regulated by several mechanisms, and theoretically was mediated by the surface protein (Guillemot *et al*., 2007) while Kang *et al*. (2005) reported that the hydrophobic nature of the cell/surface was the controlling factor for the microbial adhesion. Other researchers reported that the adhesion strength was highly influenced by the electrostatic force of the cell, and could be either reversible or irreversible. Hydrophobic surfaces with little or no charge exhibited the strongest adhesion, followed by hydrophilic materials with a positive or neutral charge, and the lowest adhesion forces occurred in the negatively charged hydrophilic materials such as mica or glass (Gotzinger *et al*., 2007). However, the electrostatic surface charge of the cell varies significantly with the growth stage of the cell and upon the constantly changing environment; for example, depletion of the nitrogen sources reduces the hydrophobicity of cell surfaces (Vasquez-Juarez, 1994).

The prevailing environment, for example the types of medium and the shear stress of the environment, also contribute significantly to cell-surface adhesion. In addition, the chemical properties of the support material, such as the surface charge (Van Haecht *et al*., 1984; Thonart *et al.*, 1982), the surface roughness (Dhadwar *et al*., 2003; Gotzinger *et al*., 2007), the degree of hydrophobicity and hydrophilicity (Nakari-Setala *et al*., 2002), have been thoroughly reported to influence growth and cell attachment. Besides this, the physico-chemical properties of the yeast such as zeta potentials, cell surface hydrophobicity, cell density and cell age also determine the types and degree of attachment.

6.2.1 *Discussion on Growth of S.cerevisiae W303 in the Microreactor*

Cell adhesion, in general, favours hydrophobic and rougher surfaces over hydrophilic and smooth surfaces. Sulphonated polyHIPE reveals a blistering effect on its surfaces giving a rougher structure due to microwaving. While the PS-DVB and the hydroxyapatite (HA) PHPs both had smooth surfaces, which were generally less attractive for cell adhesion. In the literature, the main driving force for cell adhesion was hydrophobicity, but in this study the lowest biomass content (0.10 g) was observed with the PS-DVB PHP (Table 6.2). The only explanation for this could be the hydrophobicity of this polyHIPE, which repels water (the medium) and might cause lots of channelling. Some parts of the polyHIPEs revealed dried areas showing poor accessibility (e.g.due to insufficient porosity and interconnect size). The medium distribution was poor, therefore reducing the growth. However, when experiments were carried out with other polyHIPEs (e.g. Sulphonated and HA PHPs) all areas in the polyHIPEs were completely wetted with the medium. Therefore, growth was boosted nearly ~4-6.5 fold higher compared to the PS-DVB PHP in both sulphonated polyHIPEs. 0.34 g and 0.63 g of immobilised biomass were achieved with the sulphonated polyHIPE neutralised with NH_4OH and KOH, respectively. The amount of released cells in these reactors was also 10 times higher than that obtained with the PS-DVB PHP (Table 6.2). The availability of the medium had been the main factor that induced the growth and cell proliferation, although according to the literature, hydrophilic surfaces generally provide weak bonding with the yeast cells compared to the hydrophobic surfaces.

Although hydrophilic surfaces increases the tendency for cell wash out, but the increased surface roughness of the sulphonated PHP was expected to attract more cells and strengthen the bonding (Merrit and An, 2000). It remains uncertain whether the increased biomass observed in the sulphonated polyHIPEs was due to the increased hydrophilicity or the cell-surface interaction. It has been widely reported that the anchorage of cells to solid surfaces often prefers rough rather than smooth surfaces. On the other hand, a 4.5 fold increase of biomass content over the PS-DVB PHP was also observed in the HA PHP (0.46 g) which has higher surface wettability. The HA PHP absorbed at least 7 times more water than the PS-DVB PHP (Table 6.2), therefore medium circulation was greatly enhanced, subsequently increasing the wetness and attracting more cells. With this result, it may be appropriate to suggest that the hydrophilicity proved to be a major factor for the increased growth and biomass content in these microreactors. However, Ca^{2+} might contribute slightly to the increasing biomass (other than hydrophilicity), therefore this factor cannot be neglected. This effect of hydrophilicity have also been reported by Kilonzo *et al*. (2011) to be a superior driving force for yeast adherence compared to hydrophobicity. A cotton cloth (hydrophilic surfaces) managed to adsorb 80-90% of the *S.cerevisiae*, while the polyester cloth (hydrophobic surfaces) only managed to retain 30-40% of the yeast cells on its surface. In addition, as the cotton cloth also exhibited a rougher surface with a greater surface area compared to the polyester cloth, thus provided more favourable spots for yeast adhesion.

Table 6.2: Effect of surface chemistry on fermentation performances

PolyHIPEs	**Shake Flask (free cell)**	**HA PHP**	**PS-DVB**	**S-NH_4OH**	**S-KOH**
Biomass (g)	4.30 ± 0.32	0.46 ± 0.08	0.10 ± 0.06	0.34 ± 0.03	0.63 ± 0.15
Biomass (g cell/g PHP)	-	1.93 ± 0.13	0.49 ± 0.05	0.98 ± 0.07	1.93 ± 0.23
Number of cell released (CFU/ml)	7.3×10^7	3.3×10^8	6.7×10^7	8.0×10^8	1.3×10^8
Maximum biomass released (gL^{-1})	-	1.13 ± 0.24	0.83 ± 0.01	0.98 ± 0.07	0.92 ± 0.07
Maximum Ethanol (gL^{-1})	11.15 ± 0.81	5.83 ± 1.34	5.13 ± 0.78	6.87 ± 1.34	5.49 ± 1.12
Ethanol Yield on initial sugar (g/g)	0.50	0.23	0.21	0.28	0.25
Yield on glucose consumed (g/g)	0.50	0.38	0.37	0.42	0.36
Glucose consumed (%)	100	67 – 71	51 – 63	68 – 70	36 – 52
Time to reach maximum ethanol	27	>40	>40	66	>66

* Maximum ethanol production was achieved at 27 hours before rapid consumption occurred.

Prior to this study, the hydrophobic PHP (i.e. the PS-DVB PHP) was expected to retain higher biomass content compared to the hydrophilic polyHIPE due tostronger bonding of the cells to the surface. But, restrictions of flow and the inability to retain water caused a dramatic reduction of growth in the hydrophobic polyHIPEs. In this case, the cells were expected to grow in limited wetted areas. Those cells that did not find a wetted location for attachment were subsequently removed from the system by hydrodynamic forces. These results reveal that in the non-aqueous environment, water or nutrient availability are important factors affecting the yeast localisation. On the other hand, the condition was different in the HA PHP. Due to the massive flocculation that occurred in the presence of Ca^{2+} (Figure 6.2), more cells were

retained in the microreactor. As the size of the cell flocs were larger than the interconnect windows, it prevented the cells from being washed out which finally gave the highest biomass content of all the polyHIPEs tested. Besides this, due to the hydrophilicity of *S.cerevisiae* W303 (as tested in Section 5.4.2) there might be a repulsive interaction occurring with the PS-DVB PHP. This also revealed that the attraction to water (flowing medium) was far greater that the attraction to hydrophobic surfaces, therefore yeast cells preferred to be in the aqueous environment, which was detected by the high number of cells released (~10^8 CFU/ml). This might be the reason why reduced growth was observed in the PS-DVB PHP compared to hydrophilic surfaces (S-NH_4OH and S-KOH PHP). A strain with hydrophilic properties was linked to a higher cell wall protein – glycosylated - and had been reported to possess a lower adhesion capability (Nakari-setala *et al*., 2002).

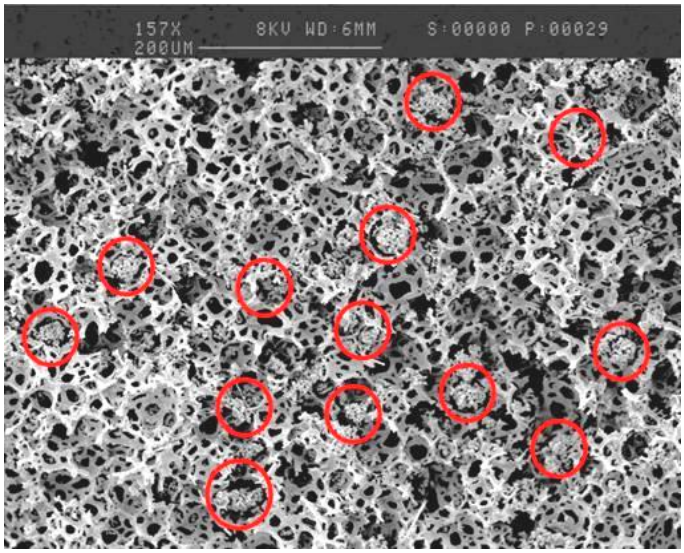

Figure 6.2: The growth of *S.cerevisiae* at the centre of a HA PHP. Cell clusters (in red circle) were found in all over the polyHIPE.

Although hydrophobic organisms prefer hydrophobic surfaces, while hydrophilic organisms prefer hydrophilic surfaces, this study indicated a slightly different result. A lower growth was observed within the sulphonated polyHIPEs (highly hydrophilic with a charged surface) compared to the HA PHP (which was less hydrophilic) by approximately 13%-16%. A strong repulsion due to the electrostatic effect might encourage cell sloughing as indicated by the higher biomass released of 0.98 gL^{-1} in the S-NH_4OH PHP compared to 0.83 gL^{-1} in the PS-DVB PHP (Table

6.2) (Mercier-Bonin *et al*., 2004). The yeast cells in this study might have the same surface charge as the polyHIPE's surface meaning repulsion was more pronounced, counterbalancing the hydrophilicity effect. Sulphonated PHPs were designed to possess hydrophilic properties and carry water at 10-50 times more than their weight. Similarly, less cell adherence was observed on a glass surface (highly hydrophilic) by a slightly hydrophilic *S.cerevisiae* compared to the adherence on a mildly hydrophobic surface due to the electrostatic effects and hydrophilic repulsion (Guillemot *et al*., 2006; Guillemot *et al*., 2007). The degree of sulphonation has been studied by Choi and Kang (2005), who regard it as the responsible factor that reduces the number of attached cells on the hydrophilic surface. In their studies, increasing the degree of sulphonation reduces the number of cells attached on the altered surface due to the increase in surface charge density.

6.2.2 *Observation of Growth using SEM*

The basis of the immobilisation process has two factors: i) the ability of cells to initiate attachment to surfaces, and ii) the ability of cells to remain attached when various external pressures were forced on them (Gallerdo-Moreno *et al*., 2004). In this study, the immobilisation mechanism of yeast was speculated to be caused by two methods: i) the direct interaction (adherence) of the cell and the polyHIPE's surface or ii) the containment of the cells - where the polyHIPE acted as a sink preventing cell wash out, but at the same time allowing the flow of nutrient/product. S-NH_4OH, S-KOH and PS-DVB PHPs exhibited almost similar cell adherence patterns when observed with the SEM. Moderate growth was observed on the surface of these polyHIPEs, although the tendency for heterogenous growth was evident in certain areas (Figure 6.3).

More cells were observed on the surface of the microreactor, which was considered to be the highly populated area of the microreactor due to easy access to glucose, nitrogen and oxygen causing cells to multiply rapidly. Increased force must be added to increase the migration rate of the cells into the microreactor to avoid blockage. The growth of yeast in the polyHIPE from below the surface to the bottom

of the reactor exhibited two distinct types. A monolayer growth (Figure 6.4) can be observed in the polyHIPE slightly beyond the surface, which shifted to flocculation as it moved away from the surface (Figure 6.5). More cell flocs with a larger size were observed in the central cavity, at approximately 2.5 mm below the surface. No exact reason was known for the shift from monolayer growth to flocculations. Two factors that might be contributing to this phenomenon were: i) it was an adaptive response towards the increased level of stresses in the microreactor particularly the level of oxygen, and ii) the coagulated aged cells had lost their surface charge and become detached from the support wall. Oxygen deficiency due to rapid consumption by the heterogenous growth on the surface was detrimental to the cells located in the polyHIPE (Walsh *et al*., 1993). As the top surface was covered by cells, the depletion of the oxygen concentration in the feed medium was expected to reduce rapidly, subsequently triggering flocculation. Flocculation is one of the protective responses of *S.cerevisiae* when living in a less favourable environment, where it protects the cell by creating a shield of the outer cells with the presence of the FLO 1 gene. Other conditions that might trigger such actions were contamination, lack of sugar and nitrogen, and also exposure to a very high ethanol concentration (Hogan, 2006). The major drawbacks of flocculation were that it not only increased the resistance for efficient mass transfer for the cells, but also could cause severe clogging in the microreactor. Observations of the growth for the PS-DVB PHP are shown in Figure 6.6 - 6.7.

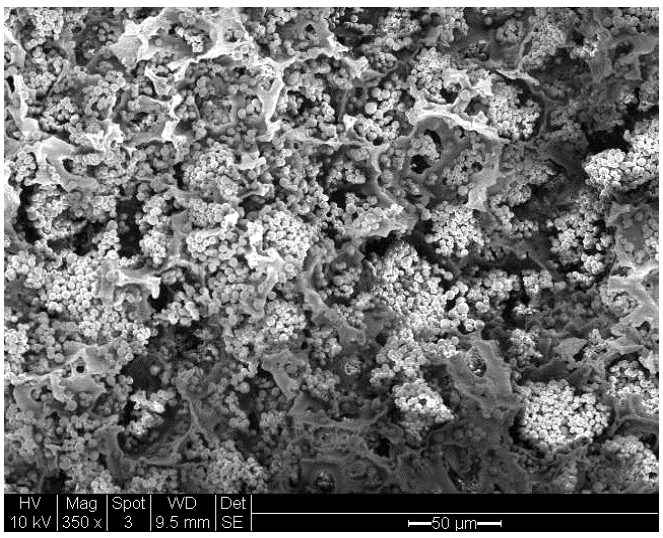

Figure 6.3: Top surface of the S-NH_4OH PHP showing dense cell populations.

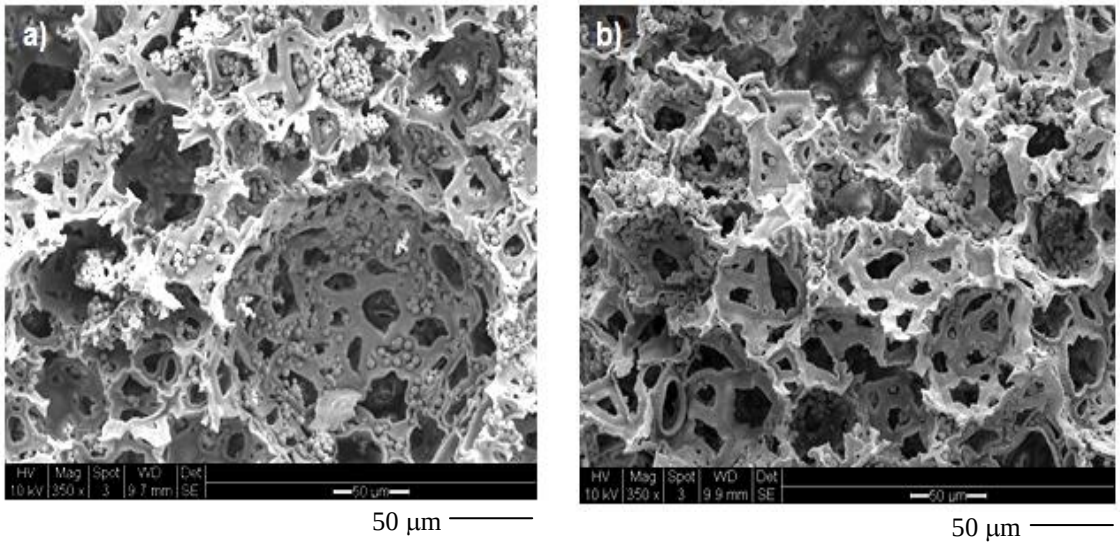

Figure 6.4: Growth of *S.cerevisiae* W303 in S-NH_4OH PHP. Figure (a) and (b) were taken at two different locations approximately 1 mm from the surface. The scale bars below the images represent 50 μm in length.

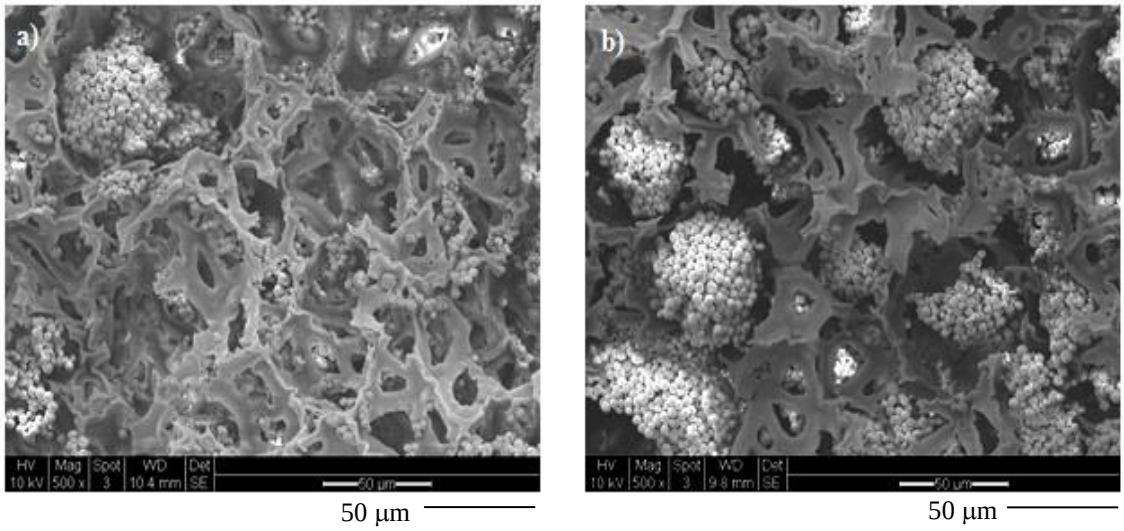

Figure 6.5: Observation of cells behaviour growing in the sulphonated PHP. Cells coagulation was more significant at location away from the surface, a) taken at location 2.5 mm below the surface and b) location closed to bottom of reactor. The scale bars below the images represent 50 μm in length.

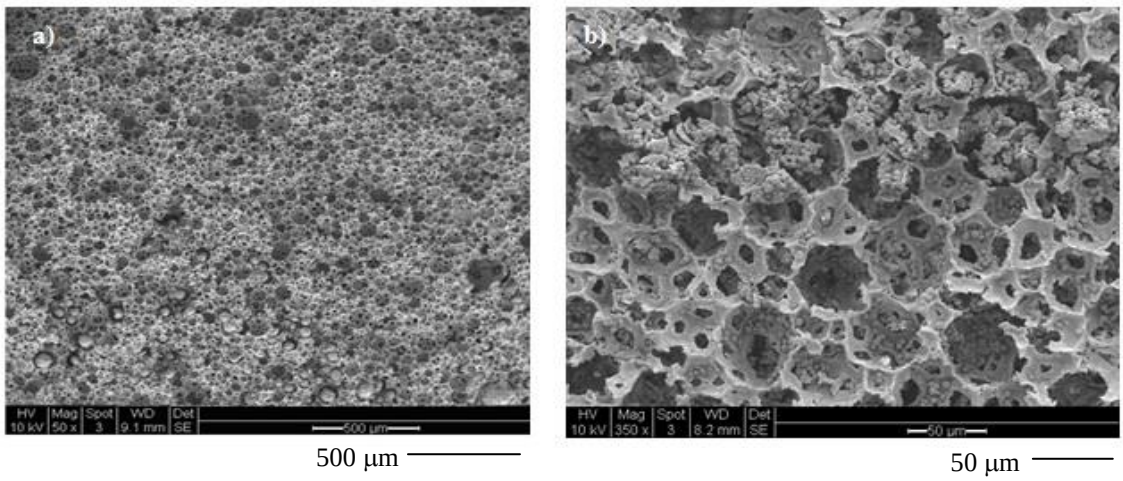

Figure 6.6: Growth of *S.cerevisiae* W303 in the cross section PS-DVB PHP viewed after 72 hours of fermentation. Figure (a) general view of the cross section and (b) closed up vieew of cells growing in the centre of microreactor.

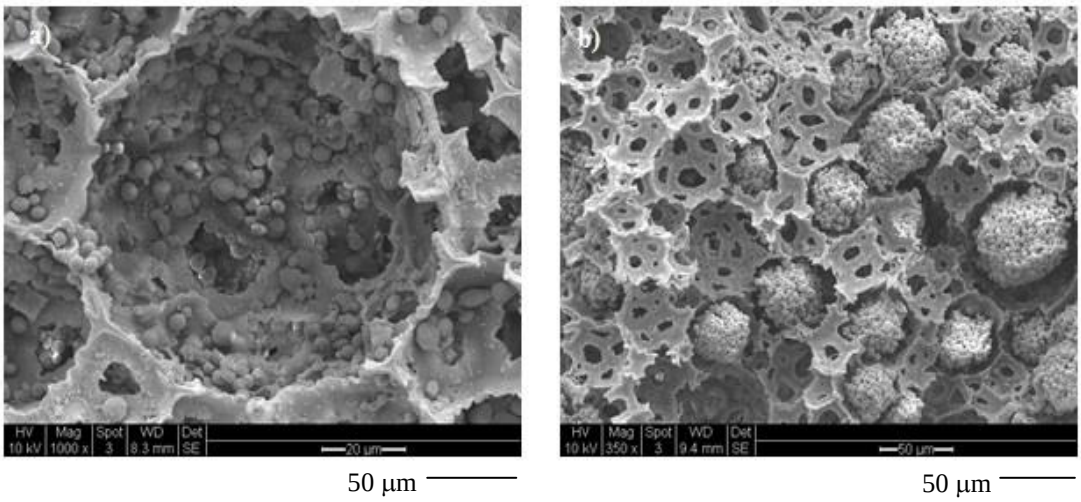

Figure 6.7**:** Growth of *S.cerevisiae* W303 in PS-DVB PHP viewed after 72 hours of fermentation. Figure (a) and (b) were taken at two different locations approximately 1 mm from the surface.

The ability to form flocs is unique depending on the strain of *S.cerevisiae* and was influenced by many factors. Ionic strength, types of medium, pH, temperature, Ca^{2+} concentration and agitation are some of the reported factors that contribute to cell flocculation (Verbelen *et al*., 2006). In this study, *S.cerevisiae* W303 in the HA PHP exhibited a completely different growth pattern to that in other polyHIPEs. The signs of either a monolayer of cells or individual cells on the polyHIPE wall were completely absent. Cells bind themselves together and form small or large aggregates

(microcolonies), and attach strongly to the wall. Cell flocculation appeared to be all over the HA PHP. Hydroxyapatite ($Ca_{10}(PO_4)_6(OH)_2$) is a mineral bone which has been widely used in tissue cultures for enhancing the bone ingrowth and osteointegration. Upon fermentation, this mineral was leached out from the polyHIPEs due to the acidity of the medium (pH 5.5), therefore releasing Ca^{2+} ions into the medium. These ions subsequently induce flocculation by enhancing the expression of the genes (Queller, 2008). Figures 6.8 – 6.9 show images of cells growth in the HA polymer.

Although cell flocculation might ease the separation process later on, sluggish ethanol production was generally associated with cell flocculation, especially when it occurred at the early stage of fermentation (Verbelen *et al*., 2006). Cell flocs can consist of up to one thousand individual cells, and a strongly flocculating strain can accumulate on the carrier at a very fast rate, thus increase the resistance for mass transfer. The operation of the HA reactor was unsteady towards the end of fermentation (> 48 hours), which shows a reduction of glucose utilisation and ethanol production that might be associated with the mass transfer issue. This will be discussed in section 6.2.3.

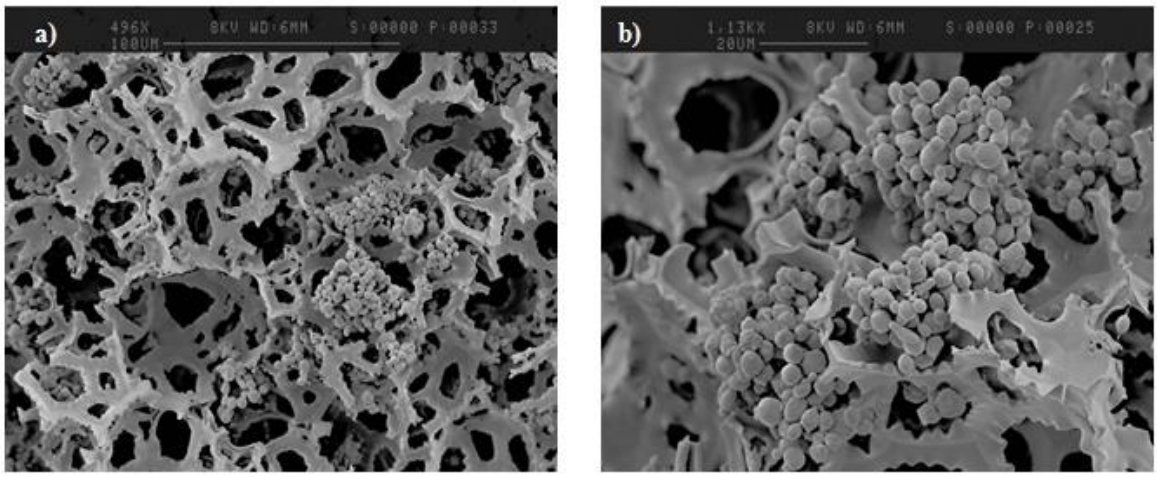

Figure 6.8: Cells growing in the HA PHP exhibited a different pattern from the PS-DVB and both of the hydrophilic polyHIPEs. The cells preferred forming microcolonies due to Ca^{2+} rather than attaching themselves to the support walls. a) Cells growing 1mm below the surface, and b) Images of cells located at the center of polyHIPEs (1100x magnification).

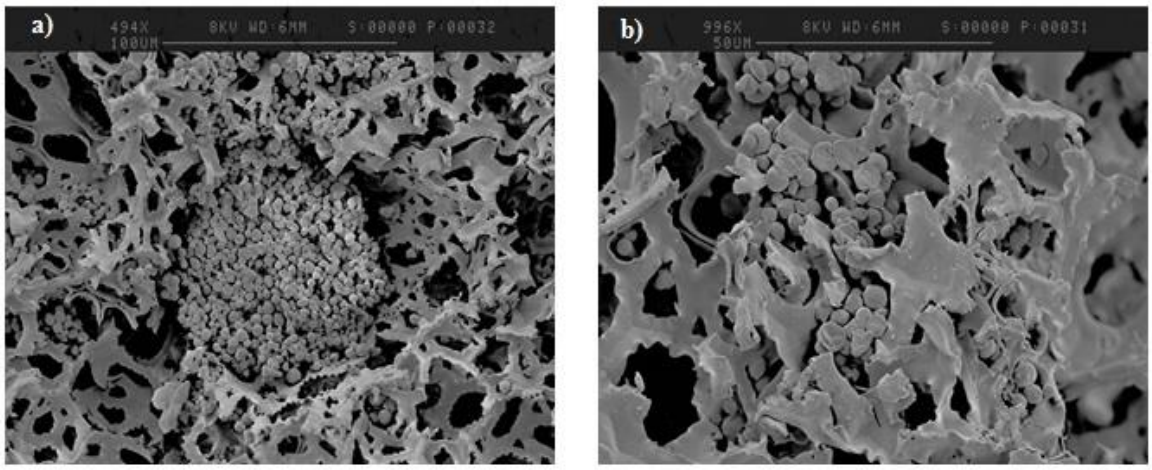

Figure 6.9: SEM images showing the bottom part of the HA PHP after 72 hours fermentation. a) Cells were not attached to the polyHIPE's wall but formed clusters at various parts of the polyHIPEs. b) Lysed cells was was observed in the polyHIPE.

6.2.3 *Discussion of Glucose Utilisation and Ethanol Production by immobilised S.cerevisiae W303 in the Microreactor*

The final ethanol production, collected at 72 hours, is summarised in Table 6.2. The value for the ethanol concentration and the biomass released in the effluent line varies significantly between microreactors, ranging between 5.13 – 6.87 gL^{-1} and 0.83 – 1.13 gL^{-1}, respectively.

For the highly hydrophilic polyHIPEs (S-NH_4OH and S-KOH), the ability to absorb water (up to 20 times their own weight) encouraged cell-surface interactions, subsequently resulting in a more even cell distribution within the cavities. As a result, a 20% increase in ethanol production was achieved with the hydrophilic polyHIPE (S-NH_4OH PHP) compared to the hydrophobic polymers (PS-DVB PHP). There was also a parallel increase of biomass and growth observed with S-NH_4OH, therefore increasing the catalytic efficiency of the reactor, giving the highest ethanol concentration of 6.87 gL^{-1}. On the other hand, a reduction of ethanol concentration by 20% was observed when the S-NH_4OH PHP was replaced with the S-KOH PHP (Table 6.2). Moreover, the slowest glucose consumption (Figure 6.10) and ethanol production pattern (Figure 6.11) were observed with this polyHIPE, although at 66

hours it managed to surpass the ethanol production by the PS-DVB PHP. The effect of K^+ was expected to play a significant role in reducing the rate of ethanol production, which showed a more sluggish production compared to the other polyHIPEs. It is reasonable to suggest that glucose consumption had been greatly impaired due to the high K^+ concentration, which might be leached out into the media, resulting in less glucose being converted to ethanol compared to the production in the S-NH_4OH and HA PHPs. Reduced glucose uptake was also observed by da Silva *et al*. (1992) when the concentration of the added potassium ions exceeded 60 mM. Below this threshold value, an increased concentration of K^+ ions can facilitate glucose assimilation therefore increasing the growth. It is also important to note that although the available biomass in this microreactor (S-KOH PHP) was the highest (0.63 g), but the ethanol produced did not represent a good improvement in parallel to the increased cell growth. It is possible to assume that the leached out K^+ ions were maybe high and detrimental to the yeast. This ion reduced the glucose uptake and also the catalytic efficiency of the *S.cerevisiae* W303 to convert glucose to ethanol. Therefore, high biomass content was achievable with S-KOH, but unfortunately it did not contribute to a significant improvement in the ethanol production. On the other hand, although a higher biomass content was observed with the HA PHP compared to the S-NH_4OH PHP, the nature of growth (flocculation) might reduce the efficiency of the biocatalyst, resulting in a lower ethanol concentration (5.83 gL^{-1}), which was reduced by 17% compared to the S-NH_4OH PHP. A high concentration of Ca^{2+} ions reduced the fermentation efficiency in a sugar based medium (e.g. glucose) and the effect was more pronounced in the sucrose-based medium (Chotineeranat *et al.*, 2010; Soyuduru *et al*., 2009). Addition of Ca^{2+} might be toxic to certain strains of yeast, and can influence both the pH and the ionic strength of the medium. While the fact that the hydrophobicity of the PS-DVB PHP impaired the growth of the immobilised *S.cerevisiae* W303, it had subsequently reduced the catalytic activity of the microreactor resulting in the lowest ethanol production of 5.13 gL^{-1}.

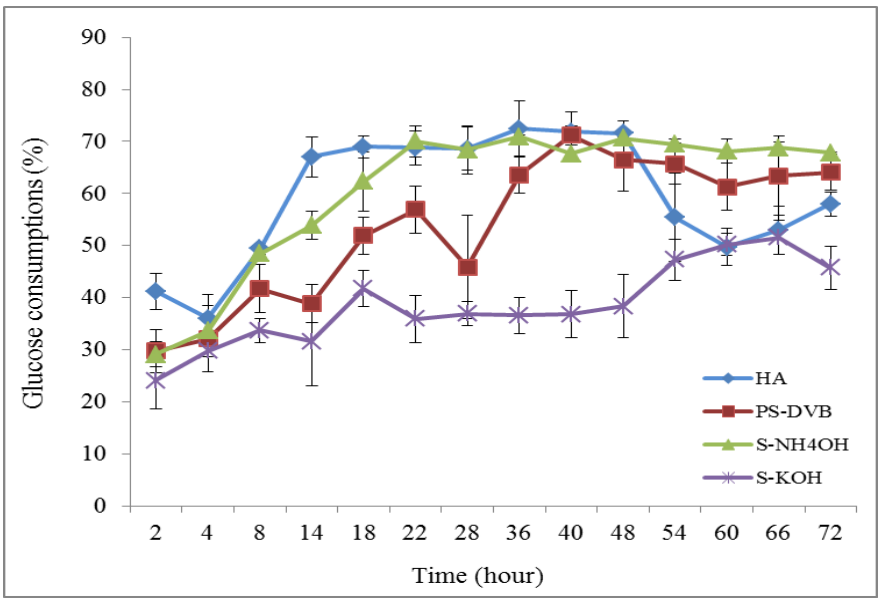

Figure 6.10: Profile of glucose consumption by *S.cerevisiae* W303 immobilised in various polyHIPE. YPG medium was run continuously to the reactor for 72 hours and temperature fixed at 30°C.

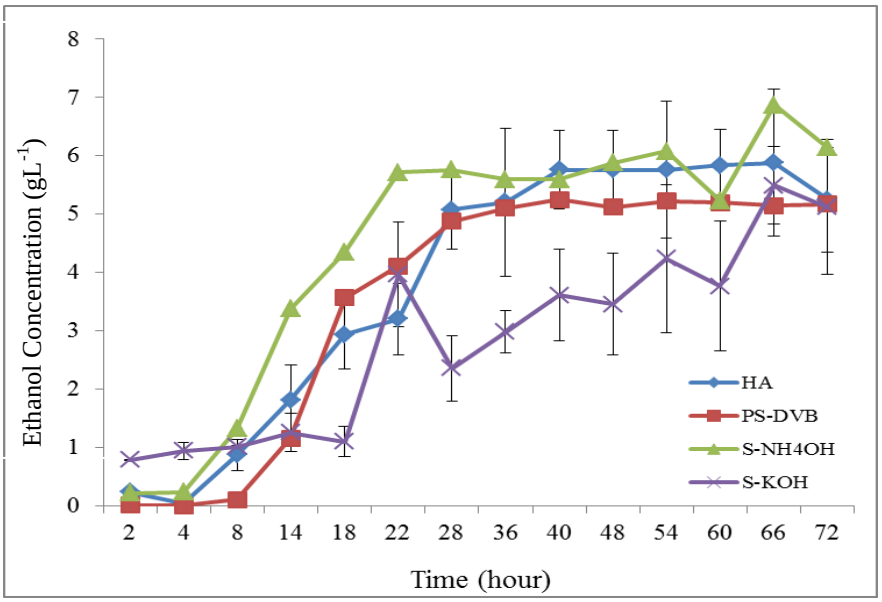

Figure 6.11: Profile of ethanol production for *S.cerevisiae* W303 immobilised in various polyHIPEs. YPG medium was run continuously to the reactor for 72 hours and temperature fixed at 30°C.

Figures 6.10 and Figure 6.11 depict the glucose utilisation and ethanol production profile for the polyHIPEs tested in this study, respectively. In general, the HA, PS-DVB and S-NH_4OH PHPs exhibited almost similar patterns for both cases, but the rate for the PS-DVB PHP was much slower compared to the other three

microreactors. Meanwhile the maximum glucose utilisation was almost similar for the HA, S-NH_4OH and PS-DVB PHPs, where at least 60-70 % of the initial glucose concentration was utilised per pass. The lowest glucose consumption was observed with the S-KOH PHP, where the maximum glucose consumption occurred at a value less than 50%. The slow glucose consumption contributed to the low ethanol accumulation observed in Figure 6.11. However, at t = 48 hours, glucose uptake was gradually increased from 32% to 52 % which later contributed to an increase in ethanol concentration of 5.49 gL^{-1} produced at t = 66 hours. In contrast, glucose utilisation for the HA PHP showed a gradual decrease at 48 hours, probably due to increased flocculation, subsequently reducing the glucose uptake rate. Ethanol profiles for the hydrophilic polyHIPEs appeared more sluggish compared to the hydrophobic surfaces. Ethanol production in S-NH_4OH PHP reached steady state at 22 hours, but ended with slightly sluggish production occurred at 54-72 hours. The HA and the PS-DVB PHPs exhibited a more stable pattern although steady state production was reached 18 hours later than S-NH_4OH PHP.

6.2.4 *Comparison with Shake Flask Culture(Free Cells)*

Although the yield of ethanol based on the initial glucose was exceptionally low in all polyHIPEs (0.21 – 0.28 g Eth/g glucose) compared to the yield obtained in the shake flask free cell culture of *S.cerevisiae* W303 (0.50 g Eth/g glucose), the yields based on the glucose consumed were much higher, varying between 0.36 – 0.38 g Eth/g glucose consumed for the PS-DVB, HA and S-KOH PHPs (Table 6.2). This result indicated that these microreactors supported low fermentation activity, in which the yield reported - based on the glucose consumed - was lower than the theoretical yield (0.51 g Eth/g glucose). A tremendous increase in ethanol yield over glucose consumed was observed for the cells immobilised on the S-NH_4OH PHP giving a final value of 0.42 g Eth/g glucose. The enhanced fermentative capacity of the *S.cerevisiae* W303 was probably attributable to the additional nitrogen source, coming from the ammonium ion-NH_4^+ in the polyHIPE or simply because the period of medium retention was longer in this microreactor compared to the others (Table 6.1).

Increasing trends for ethanol productivity were observed for all types of polyHIPEs as shown in Figure 6.12. Ethanol was produced at different rates and continued to increase towards the end of the fermentation (72 hours). S-NH_4OH PHPexhibited the highest (4.81 gL^{-1}.h) and fastest rate for ethanol productivity, which was improved by 11.7 times over the productivity observed in the shake flask with free *S.cerevisiae* W303. Comparable productivity was observed with the HA and PS-DVB PHPs, with overall productivity observed at 4.22 $gL^{-1}h^{-1}$ and 3.92 $gL^{-1}h^{-1}$, equivalent to a 10.3 and a 9.6 fold improvement over shake flask fermentation, respectively. Although the productivity of the S-KOH PHP was the highest during the initial phase of fermentation (t < 14 hours), its speed reduced gradually and remained the lowest throughout the fermentation. Overall productivity of the S-KOH PHP was observed at 3.15 $gL^{-1}h^{-1}$, giving a 7.7 fold improvement over the productivity in the shake flask culture (0.41 $gL^{-1}h^{-1}$).

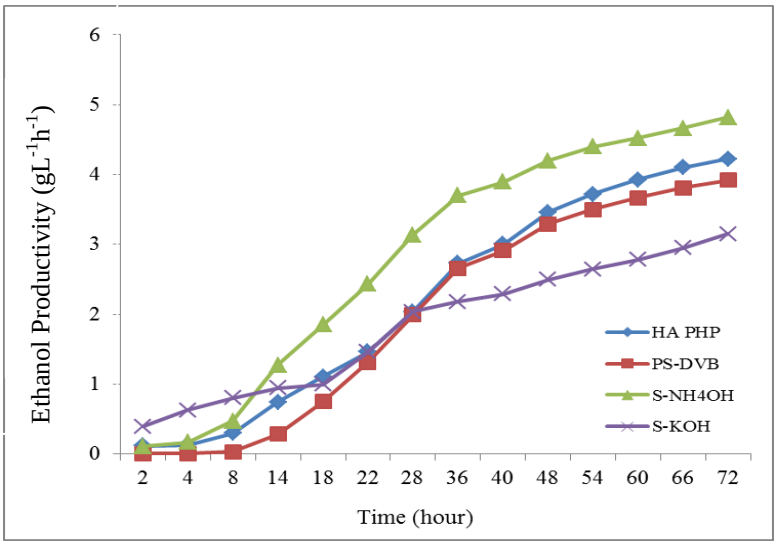

Figure 6.12: Profile of ethanol productivity in continuous fermentation employing various types of polyHIPEs. Fermentation was supplied with YPG media at 30°C and run for 72 hours.

6.2.5 *Conclusions*

All experiments carried out with immobilised cells using the HA, PS-DVB, S-NH_4OH and S-KOH PHPs proved that both growth and ethanol production were occurring simultaneously. The effect of hydrophilicity on the cell adhesion and cell

growth cannot be defined based on this study, as cell-surface interactions were mediated by many other factors as discussed previously. However, an increased hydrophilicity contributed to an enhanced wetness of the polyHIPEs, thus providing a better supply of medium to the immobilised cells compared to the hydrophobic polyHIPEs. Enhanced growth was observed with the HA, S-NH_4OH and S-KOH PHPs due to the increased water uptake capacity of these microreactors. Moreover, a truncated medium supply was observed occasionally in the PS-DVB PHP depicted by dry areas, which was difficult to control and might cause variations in every run. The production of ethanol in batch culture stopped at 27 hours of fermentation due to depletion of glucose, while ethanol was produced continuously in the microreactor at up to 72 hours of fermentation. The productivity of ethanol increased with increased fermentation for all four types of polyHIPEs. However, due to the flocculative growth imposed by *S.cerevisiae* W303 in the HA PHP, it was reasonable to suggest that during prolonged operations the catalytic conversion might be reduced significantly. Larger cell aggregates accumulate that will either reduce the fermentative capacity of the cells or might cause severe blockage in the microreactor.

6.3 The Effect of Pore Sizes on the Shear Stress of Cells Growing in the Microreactor

Surface growth has been a major problem in the preliminary studies of continuous production in a monolithic microreactor (Akay, 2006a). As the yeast is prone to invade and grow on the top surface rather than migrating into the monolith, a proper selection of pores and interconnect size was carried out to investigate the best properties that will increase the rate of cell migration into the microreactor, and promote the monolayer growth within its cavities. Besides this, the selection of pore and interconnect sizes must be thoroughly studied, as the hydrodynamic properties of the medium in the microreactor was dependent on these two properties. High hydroforce (shear rate) was needed to break down the microcolonies, and force them deeper into the monolith. In an attempt to increase the cell migration rate into the polyHIPEs, a study was carried out to test the effect of pore sizes on the behaviour of cell penetration, growth and ethanol production. Three types of sulphonated PHP were produced with different average pore diameters (D) measured at D = 55, 45 and 35 μm, with the corresponding interconnect (d) sizes being d = 18, 16 and 10 μm, respectively. All these PHPs were prepared with the same composition, but the dosing and mixing time was varied accordingly. However, as sulphonated polyHIPEs require post treatment (e.g. soaking in sulphuric acid) to increase their hydrophilicity, the degree of sulphonation of each of the individual polyHIPEs may vary significantly with interconnect sizes. Homogeneous diffusion of sulphuric acid into the polyHIPE with a small pore size was difficult to achieve especially for the polyHIPEs with the smallest pores. It may result in slowing down the diffusion rate of sulphuric acid. As the soaking time was fixed at two hours in every process, it probably failed to provide enough time for the sulphuric acid to diffuse into the entire matrix, which later on affected the degree of sulphonation and the water uptake properties of the monolith. In some cases, certain parts of the polyHIPEs, especially the central region, were not efficiently sulphonated.

All the microreactors were inoculated with 2.6 ml of fresh seed culture containing approximately 2 x 10^8 CFU/ml of active *S.cerevisiae* W303 using a syringe pump. Fermentations were run for 72 hours and samples were taken to analyse the

ethanol concentration, the sugar consumption, the biomass content and the number of cells released. The microreactors were sampled at the end of fermentation, and treated with glutaraldehyde and ethanol prior to viewing with the SEM. The polyHIPEs were then weighed to determine the amount of immobilised biomass. The ethanol concentration, yield and growth were estimated and are as shown in Table 6.3.

Table 6.3: Kinetic data of the effect of pore size on the ethanol production.

Pore	**Shake Flask (Free Cell)**	**Small (35 µm)**	**Medium (45 µm)**	**Large (55 µm)**
Pore diameter (µm)	-	35 ± 3	45 ± 5	55 ± 5
Retention time (min)	-	2.5	3.1	3.8
*Maximum Ethanol Production	11.15 ± 0.81	1.82 ± 0.60	6.61 ± 0.48	6.87 ± 1.34
Stable Ethanol Level (gL^{-1})	-	1.29 ± 0.50	6.19 ± 0.18	5.59 ± 0.40
Cumulative Ethanol (gL^{-1})	11.15 ± 0.81	56.7 ± 4.5	354.6 ± 4.7	346.7 ± 7.8
Overall Ethanol Productivity (gL^{-1}/h)	0.41	0.86	4.92	4.81
*Maximum Glucose consumed (gL^{-1})	25	9.05	14.27	17.19
Range of Stable Glucose consumptions (%)	100	30.5-37.2.	57.0-60.1	68.0-70.0
*Ethanol Yield on initial glucose	0.50	0.07	0.26	0.28
*Ethanol Yield on used glucose(g/g)	0.50	0.20	0.46	0.42
Biomass in PHP (g)	4.30	0.20 ± 0.02	0.24 ± 0.01	0.34 ± 0.03
g Biomass/g PHP (g/g)	-	0.71 ± 0.16	0.93 ± 0.04	0. 98± 0.07
Max number of cells released (CFU/ml)	7.3×10^7	1.8×10^7	5.2×10^7	8×10^8
*Time to reach steady state Ethanol	27	na	28	22

- The retention time of medium in the microreactor varies significantly
- Data for batch process/free cell run were taken at 27 hours (at maximum ethanol concentration).
-* Data were taken or derived based on the maximum ethanol concentration*.
- Cumulative production – total ethanol being produced throughout fermentation.

6.3.1 *The effect of Pore Sizes on the Rate of Cell Migration, Growth and Number of Cells Released*

Referring to Table 6.3 and Figure 6.13, the highest immobilised biomass was observed with the large pore sized polyHIPE (0.34 g), followed by the medium sized polyHIPE (0.24 g) and the lowest was observed with the small sized polyHIPEs (0.20 g). A similar pattern was observed for the packing density (g Biomass/g PHP), where the maximum value was observed with the large pore sized polyHIPE at 0.98 g/g PHP, while the lowest was obtained with the smallest pore sized PHP (0.71 g/ g PHP). Moderate packing density at 0.93 g/g PHP was achieved with the medium sized PHP (45 μm), which was 5.3% lower than that obtained with the large pore sized PHP and a 23.7% increase compared to the smallest pore sized polyHIPE. The ability of cells to penetrate and adhere themselves onto the microreactors was influenced by not only the pore and interconnect sizes of the reactor, but also by the surface heterogeneity of the polyHIPE due to varying degrees of sulphonation. Vasconcelos *et al*. (2004) reported a much lower packing density for Fleischmann yeast growing on the untreated sugar cane stalks, of the 0.346 g/g support, which increased slightly when immobilised on the treated surface of the 0.445 g/g support.

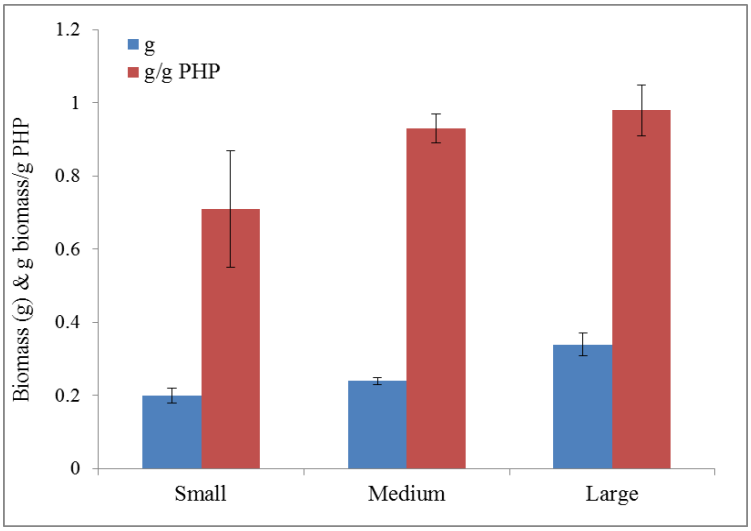

Figure 6.13: Immobilized biomass and packing density obtained with small (D = 35 μm), medium (D = 45 μm) and large (D = 55 μm) pore sized polyHIPEs. The blue bar represent amount of biomass in (g) and red bar represent the density of biomass per g polyHIPE (gg^{-1} PHP).

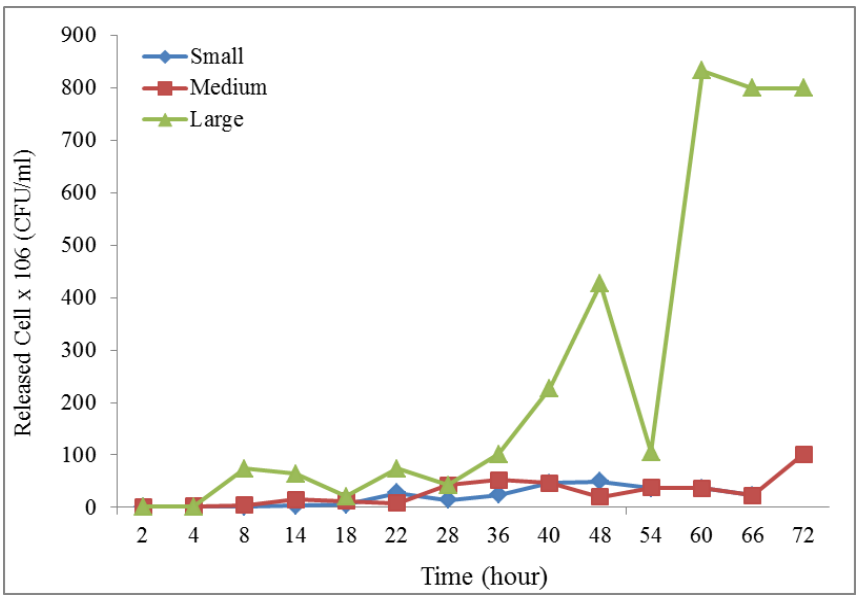

Figure 6.14: Profile of cell released from polyHIPEs during fermentations. *S.cerevisiae* W303 were inoculated on three different pore sized polyHIPEs [Small (D = 35 μm); Medium (D = 35 μm) and Large (D = 35 μm)] while YPG media was fed continously to the reactor for 72 hours and temperature maintained at 30^{o}C.

Referring to Figure 6.14, the number of cells released by large sized polyHIPEs increased by 10 fold (10^7 CFU/ml) at 8 hours of fermentation compared to the polyHIPEs with small (~10^6 CFU/ml) and medium sized (~10^6 CFU/ml) pores. A very slow increase in the number of cells released was observed with the smallest pore size. It took at least 22 hours for this polyHIPE to achieve the number of released cells at 10^7 CFU/ml, while the medium sized polyHIPE took approximately 14 hours. The maximum number of cells released was observed at 1.8 x 10^7, 5.2 x 10^7 and 8 x 10^8 CFU/ml for small, medium and large pore sized polyHIPEs, respectively. A slow increase in the cells released might depict that a slow cell growth was actually occurring in the polyHIPEs. The reduced growth was confirmed by there being less biomass obtained within the small pore sized polyHIPEs. An enhanced growth of 20% was obtained when the pore size of the polyHIPEs was increased from 35 μm to 55 μm.

6.3.2 *Observation of Growth using the SEM*

Accumulation of growth was evident with 35 μm pores due to the small openings that restricted the migration of cells into the polyHIPE. At D = 35 μm, the small interconnects reduce the migration rates of *S.cerevisiae* W303, while easy access to a highly nutritional medium (glucose, nitrogen and oxygen) induces cell proliferation on the top surface (Vasconcelos *et al*., 2004). It was evident since the whole surface of this polyHIPE was covered by a thick multi-layer of cells acting like a sieve, which subsequently prevented other individual cells from penetrating the polyHIPE (Figure 6.15a & b). Therefore less cell growth was observed within the microreactor (Figure 6.15c), which was also supported by there being the lowest number of cells released (~10^6 CFU/ml). This multilayer of cells increased the pressure build up within the system, which finally stopped the medium supply. Fermentation for this polyHIPE was terminated 8 hours earlier compared to the other polyHIPEs due to cell blockage. In some runs, the fermentation was ceased at 50 hours (data not shown).

PolyHIPEs having pore sizes between 45-55 μm, provided adequate opening to facilitate cell penetration, and on the other hand, enhanced the cell removal (Figure 6.14). The excessive surface growth obtained with the small sized polyHIPEs was controlled within this size range. Excessive accumulation of cells observed in the 35 μm polyHIPE was not observed with these polyHIPEs therefore increasing the stability of the reactors. SEM images (Figure 6.16) show the growth of cells observed on the top of the polyHIPEs with pore size 55 μm (Figure 6.16a) and 45 μm (Figure 6.16b & c). No significant difference in terms of cell behaviour or cell morphology was observed using these polyHIPEs. However, some dense parts were observed on the top surface of the 45 μm polyHIPEs as shown in Figure 6.16(c), and this appearance was absent in the 55 μm polyHIPE. Fermentation was prolonged up to 72 hours in both microreactors with no signs of restricted flow.

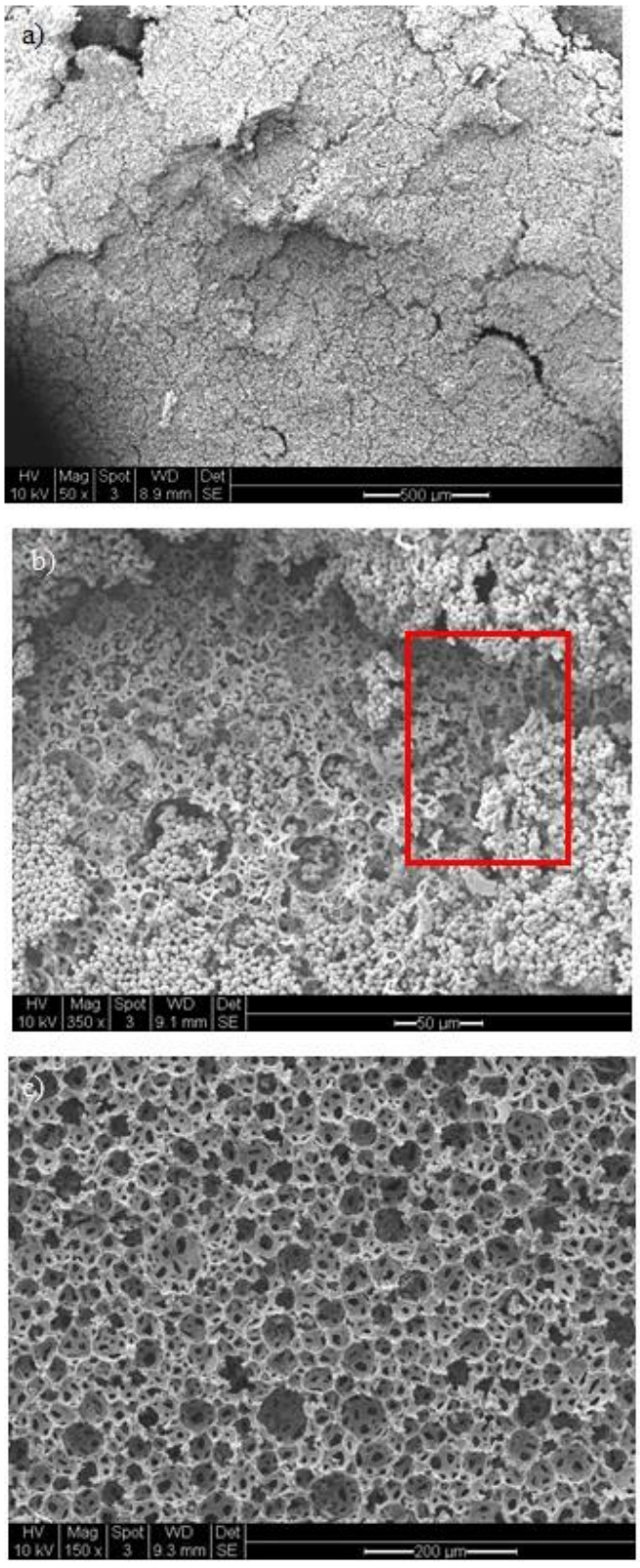

Figure 6.15: Analysis of growth in small size polyHIPE (D = 35 µm). a) Multilayer growth covered the surface of the microreactor after 62 hours of fermentation resulting from increased resistance to cell penetration due to small interconnect sizes. b) Analysis of microreactor surface. c) General view of the analysis of cell growth at the centre of polyHIPEs.

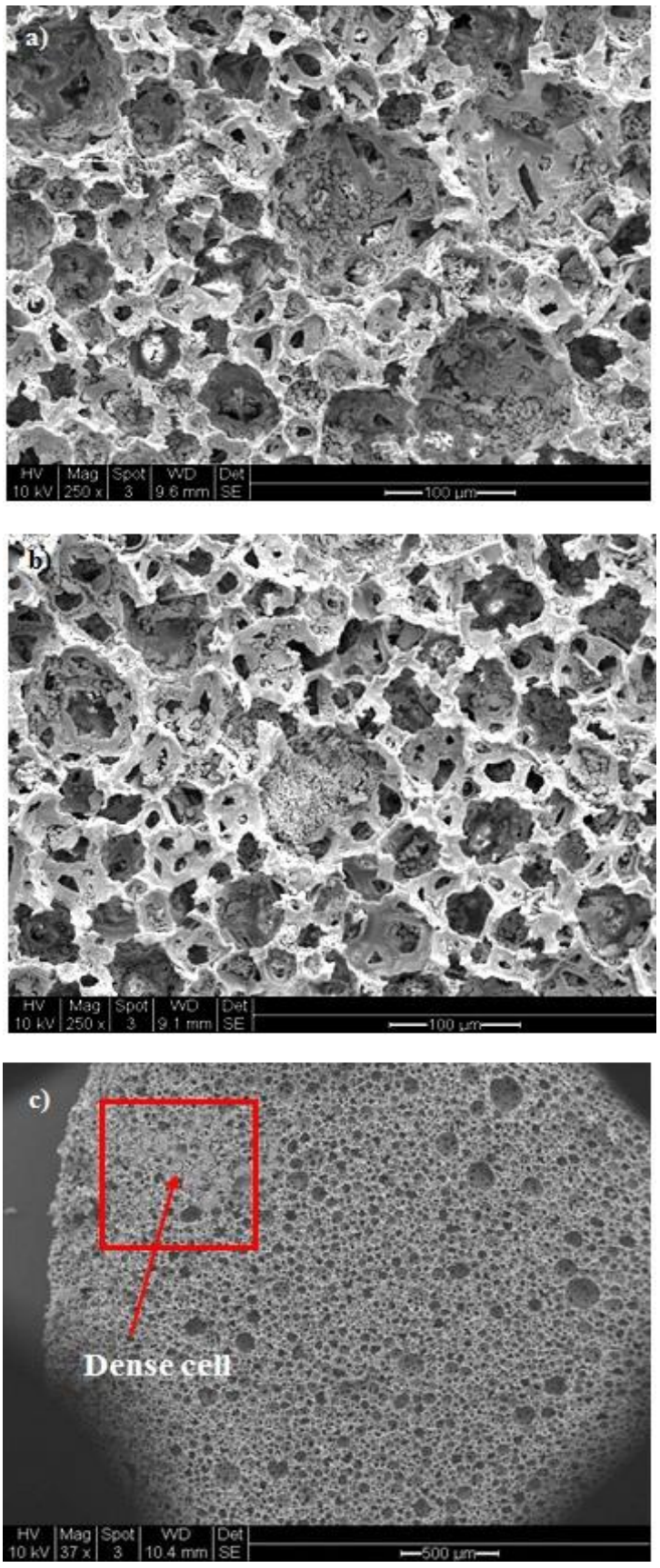

Figure 6.16: View of the surface growth of the sulphonated polyHIPEs. a) D = 55 µm, b) Growth on the surface of polyHIPE with pore size (D = 45 µm) and c) General view shows some parts on the surface of polyHIPE (D = 45 µm) were densed with cells.

When the cross-sections of these polyHIPEs were analysed closely with the SEM, heterogeneous cell distribution was observed all over the polyHIPEs, irrespective of pore size. Large and medium pore sized polyHIPEs (Figure 6.17-6.18) facilitated much better growth and cell migration within the matrix compared to the small pore sized polyHIPE (Figure 6.15), although the distribution was heterogeneous throughout these microreactors (Figure 6.17-6.18). For example, in 45 μm polyHIPEs, in areas containing a high cell density, the regions that were close to these areas generally contained less or no cells as shown in Figure 6.18 (a&b). On the other hand, cell migration was very poor in the 35 μm polyHIPE, with signs of cell growth/accumulation only observed at less than 1 mm deep. It was not possible to conclude that the overall cell numbers reduced with increasing matrix depth, because the cells formed distinct behaviour (initiation of flocculation) as they moved further down to the bottom of the reactor.

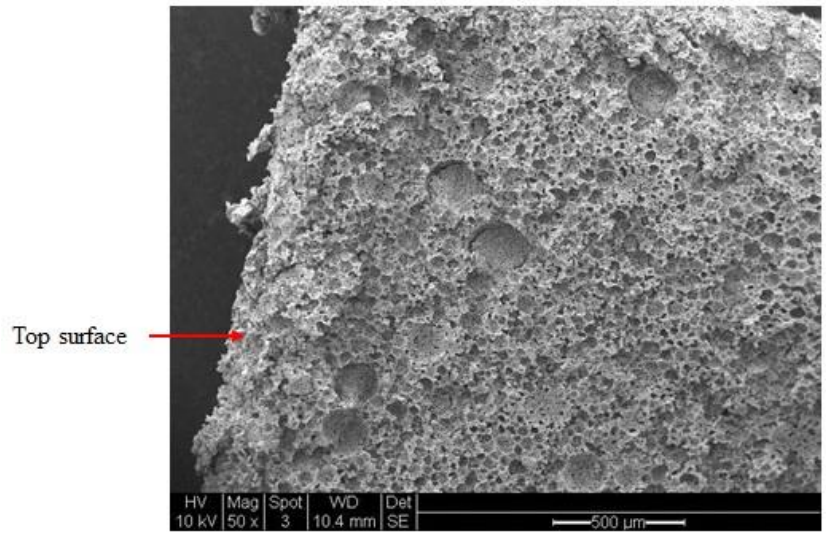

Figure 6.17: General view showing the cross-sections of the 55 μm polyHIPE.

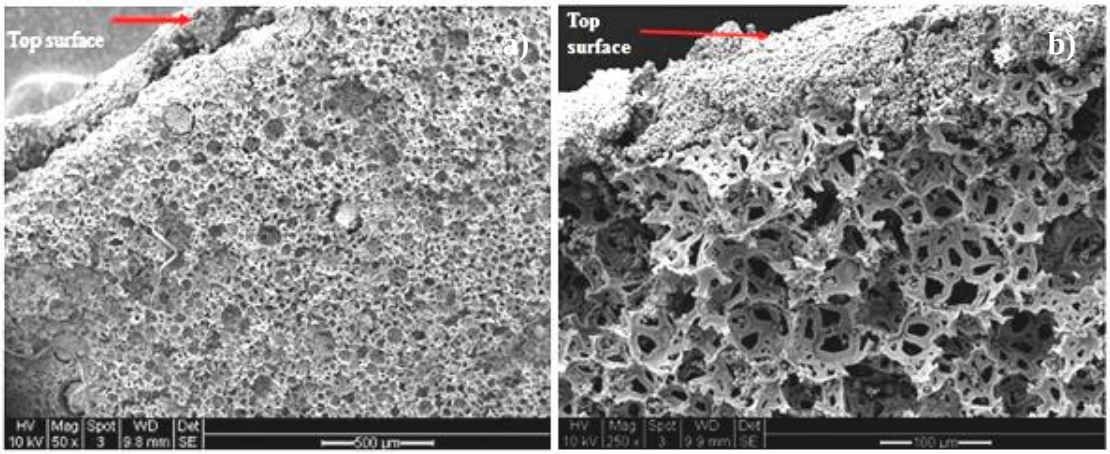

Figure 6.18: a) General view showing the cross-sections of a 45 μm polyHIPE. b) Some dense locations observed on the top surface of 45 μm polyHIPEs. Red arrows show dense cells on the polyHIPEs surface.

This study has demonstrated that the size of the pores and interconnects must be able to accommodate the migration of cells into the monolith, in order to increase the rate of cell migration, thus preventing them from colonising the surface of the microreactor. However, we did not observe any pore sizes that were dependent on the behaviour of the yeast cell, although a small pore size (35 μm) did reduce the penetration depth of the yeast cells compared to the microreactor with larger pore sizes (45 - 55 μm). Fewer cells were observed in the small pore sized polyHIPEs, which might be attributable to a disruption of flow occurring as cells tend to coagulate and block the pathway of flow to different areas of the monolith. Invasion of cells on the top surfaces must be avoided to stop the uncontrolled growth causing additional resistance to mass transfer, which at the end would totally hinder the external mass transfer into the microreactor. Large pore sized polyHIPEs (55 μm) had suitable openings that facilitated a good migration rate, therefore reducing the density of cells located either on the top or in the independent cavity located in the middle of the polyHIPE (Figure 6.19a). The close-up view of cells in the polyHIPEs shows that this material permits budding and growth, and the image of the budding cells taken at the centre of the microreactor is shown in Figure 6.19(b). More packed pores were observed with 45 μm polyHIPEs in certain areas/pores located in the middle of the matrix (Figure 6.19c &d). While larger pores exhibited monolayer growth within their cavities, massive cell flocs were observed in the polyHIPE with smaller pores.

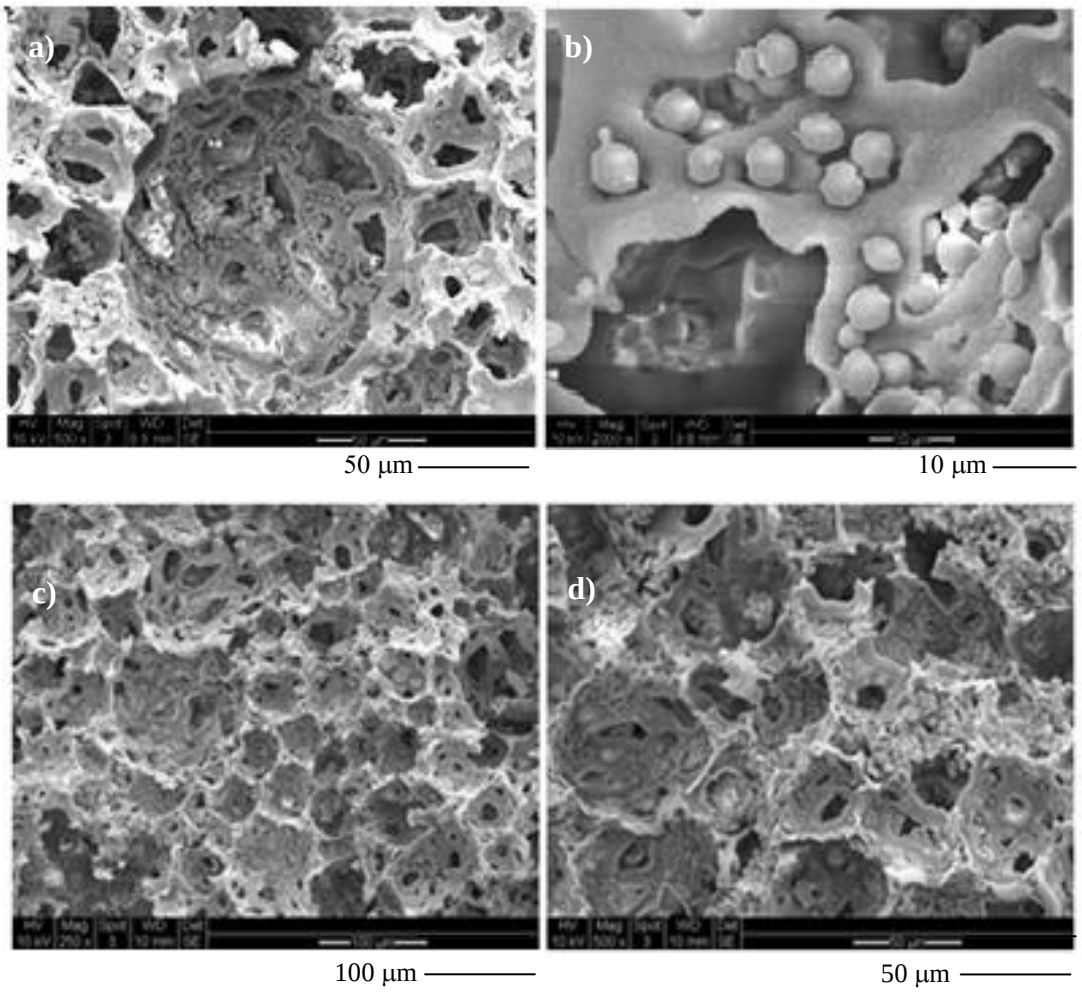

Figure 6.19: a) Growth in the coalescent pores located closer to the surface in the polyHIPE (D = 55 μm) viewed at 500x magnification. b) Cell proliferation located in the centre of the 45 μm polyHIPE. c) and d) Appearance of growth at the centre of 45 μm PHP.

The SEM shows that, in general, there was no difference in terms of cell behaviour or any distinguished pattern of cell attachment with the wall of the microreactor. The pore sizes have been reported to greatly affect the behaviour of the osteoblast tissue (Stangl *et al.*, 2001; Bokhari *et al.*, 2005), but none of these findings were related to this study. Accommodation of the monolayer growth was found to be independent of pore size, although the number of flocculating cells was reduced in the 45 μm polyHIPEs. Large (55 μm) or small (D = 35 μm) pore sizes do not induce either the monolayer of flocculation directly, but were highly influential in determining the release of cells. Akay (2006a) reported that a monolayer growth was obtained with *Pseudomonas syringae* immobilised on the PS-DVB polyHIPE having a nominal pore size of D = 25 μm, while the growth was substantially reduced when

cultured using the polyHIPE with a nominal pore size of 100 μm, and traces of biofilm formation were detected. Immobilised cells on the 25 μm polyHIPE showed activity stability up to 30 days before the flow of the medium was completely hindered due to excessive growth occurring on the top of the reactor. No further explanation was provided concerning whether the monolayer growth was induced by pore size or was a strain dependent property.

6.3.3 *The effect of pore sizes: Discussion of Glucose Utilisation and Ethanol Production by immobilised S.cerevisiae W303 in the Microreactor*

According to Figure 6.20, the glucose utilisation of *S.cerevisiae* W303 was increased when the pore sizes of the polyHIPEs increased accordingly. The utilisation profile for the 55 μm and the 45 μm polyHIPEs were quite similar, but the rate for the 55 μm polyHIPE was much greater than the later. Optimal consumption was observed approximately at ~68% for the 55 μm polyHIPEs, which started at 22 hours of fermentation, and remained stable afterwards. Glucose consumption for the 45 μm polyHIPEs was achieved 6 hours later, with optimum values occuring at ~ 60%. On the other hand, the profile for the smallest pore sized polyHIPE fluctuated, due to the unstable conditions or the growth that occurred in the polyHIPE. The glucose utilisation mainly occurred within the cells growing on the top surfaces, therefore not more than 40% of the initial sugar could be consumed due to the short retention time. The utilisation of glucose occurring within the 35 μm polyHIPE was expected to be very minimal due to very little growth in the polyHIPE.

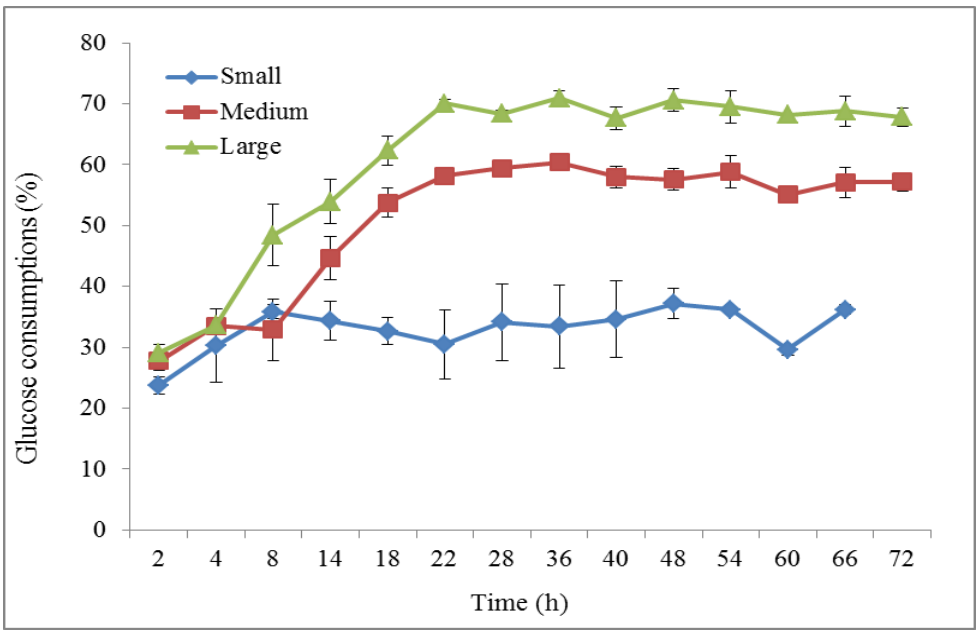

Figure 6.20: Profile of glucose utilisation by *S.cerevisiae* W303 immobilised on small (D = 35 μm), medium (D = 45 μm) and large (D = 55 μm) pore sized sulphonated polyHIPEs supplied with YPG media at 30°C.

Results depicted in Figure 6.21 show that the ethanol concentration reduced gradually with pore size in the first 16 hours of fermentation. However at 18 hours, the ethanol production by the 45 μm polyHIPEs surpassed the production in the 55 μm polyHIPEs, while the production in the 35 μm remains the lowest throughout the fermentation. The highest ethanol concentration and biomass concentration for the 25 μm polyHIPES was obtained at 1.12 gL^{-1} and 0.20 g, respectively, and the profile fluctuated slightly although it showed an increasing trend as the fermentation proceeded (Figure 6.24). SEM analysis revealed that the cells growing on the top surface of the 35 μm polyHIPEs had affected the cells growth in the polyHIPE severely. Therefore a very low maximum ethanol concentration (1.82 gL^{-1}) was observed in this microreactor, which was reduced by 72.5% and 73.0% compared to the ethanol produced in the 45 μm and 55 μm microreactors, respectively (Table 6.3). It was assumed that the ethanol production in the 35 μm polyHIPE was generated by the cells growing on the top rather than the cells growing inside the reactor.

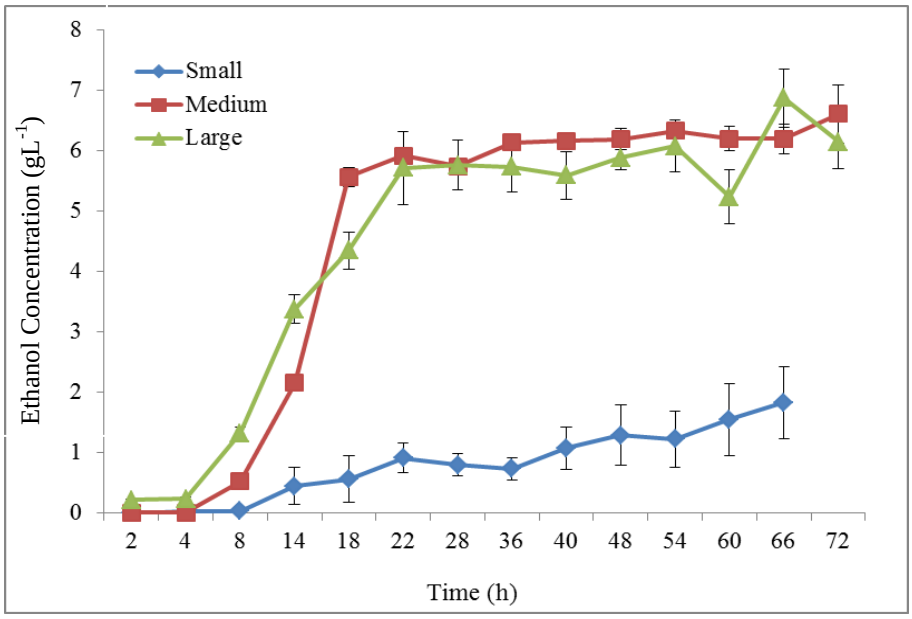

Figure 6.21: Profile of ethanol production by *S.cerevisiae* W303 immobilised on small (D = 35 μm), medium (D = 45 μm) and large (D = 55 μm) pore sized sulphonated polyHIPEs supplied with YPG media at 30°C.

Cells retained in the polyHIPE (D = 45 μm) were only 70.5% of that in the polyHIPE (D = 55 μm), but produced a comparable steady state ethanol production. Although a higher maximum ethanol concentration was achieved with bigger pores, reading fluctuations were more pronounced throughout the 72 hours of operation compared to the production in the 45 μm polyHIPE. The results obtained with the 45 μm polyHIPE were more stable, and a shorter time was needed to achieve a steady state ethanol production compared to the 55 μm polyHIPE. Jimat *et al* reported that stable productivity of α-amylase in the suphonated polyHIPEs was achieved when the matrix had reached the limits of its capacity to sustain further increases of biomass. However, that derivation of the steady state condition was quite misleading because many empty spaces were observed in the matrix that probably could accommodate more cells if the fermentation was prolonged for more than 24 hours. In the present study, however, we believe that steady state operation was achieved when there was a substantial amount of cells available in the polyHIPEs, to convert the glucose to ethanol within the respective retention times. Any further increases of biomass entrapped were actually increasing the utilisation of glucose, but instead of producing ethanol, glucose was utilised for cell maintenance, through the aerobic pathway. Therefore, in this study, although a higher sugar utilisation was observed with large

pore sized polyHIPEs (Figure 6.20), the amount of ethanol being produced was more or less the same as the ethanol produced by the cells immobilised in 45 μm polyHIPEs (Figure 6.21). Besides this, the stage where steady state was achieved was when the rate of cells released was the same as the rate of newly produced cells.

Investigation into the effect of pore size was reported earlier for the α-amylase production by Jimat (2011) using *Bacillus subtilis* sp. immobilised on the sulphonated PHPs at 30, 36 and 42 μm. The optimum pore sizes for both maximum α-amylase and biomass production was observed with 36 μm pore sizes, followed by 42 μm polyHIPEs, while 30 μm polyHIPEs gave the lowest production. Therefore the increased enzyme production was concluded to be highly associated with the increased biomass content in those polyHIPEs, subsequently increasing the productivity. Such a trend was not observed in this study, because the availability of high biomass content did not simply contribute to the increase in ethanol productivity. In this study, the highest biomass content was observed with the 55 μm polyHIPEs (0.34 g), while the highest stable ethanol productivity (of 6.19 gL^{-1}) was reported with the 45 μm polyHIPE, but with slightly less biomass (0.24 g). This trend was consistent with the trend observed earlier, where the highest biomass content (0.63 g) was observed with the S-KOH polyHIPEs, but did not contribute to the highest ethanol concentration/productivity (Table 6.2). Furthermore, the ethanol concentration in the S-KOH polyHIPE fluctuated much more where stable ethanol production was almost not occurring.

Therefore, the following speculations were made about this finding:

i) The surface chemistry or pore size could contribute to the migration rate of the viable cells and increase the biomass content in the polyHIPEs.
ii) There are some compounds or conditions in the polyHIPEs that were favourable for biomass production, while suppressing the fermentation route, thus producing less ethanol.

iii) A reduced pore size from 55 to 45 μm probably increased the density of cells in each of the pores (monolayer growth), therefore increasing the catalytic capacity of the reactor.

iv) Medium sized polyHIPEs (45 μm) might provide an adequate mass transfer length from the medium to the cells, thus enhancing the catalytic properties of the active viable cells to convert more glucose to ethanol.

Ethanol yield based on the glucose consumed was optimum at 0.46 g Eth/g glucose obtained with the 45 μm polyHIPEs, while 0.42 and 0.2 g Eth/g glucose consumed were observed with the 55 μm and 35 μm polyHIPEs, respectively. This finding might suggest that the confined conditions in the 45 μm polyHIPE affected the *S.cerevisiae* W303 performance, increasing its fermentative capability and hence producing a higher ethanol concentration. But how this condition altered the metabolic pathway of *Saccharomyces cerevisiae* W303 in the molecular level has yet to be determined.

6.3.4 *Comparison with Shake Flask Culture (Free Cell S.cerevisiae* W303*)*

Ethanol productivity for the 45 μm polyHIPEs was slower than in the 55 μm polyHIPEs in the first 40 hours of fermentation. However, at 48 hours, it was assumed that the biomass content of the 45 μm polyHIPE had achieved a sufficient amount to efficiently utilise the supplied glucose at the optimum rate. Therefore at this point, ethanol productivity in this polyHIPE had surpassed the productivity obtained in the large pore sized polyHIPE, and a slow but continuous increase was observed until the end of fermentation. The final maximum productivity was achieved at 4.92 $gL^{-1}h^{-1}$, while a slightly lower productivity was observed with the large pore sized polyHIPE, of 4.81 $gL^{-1}h^{-1}$. On the other hand, the productivity of the smallest pore sized polyHIPE remained the lowest of all, with only 0.86 $gL^{-1}h^{-1}$. These productivities corresponded to approximately 12.0, 11.7 and 2.1 fold increases respectively compared to the overall productivity observed in the shake flask culture (0.41 $gL^{-1}h^{-1}$),. Besides this, the number of viable cells was eventually lower in the polyHIPEs

compared to that in the shake flask, except for the 55 μm microreactor. The viable cells in this microreactor increased to 10^8 CFU/ml compared to 10^7 obtained with the shake flask culture. The number of cell losses in the effluent was considered to be low, and could be easily compensated by the growing immobilised cells (Vasconcelos *et al*., 2004).

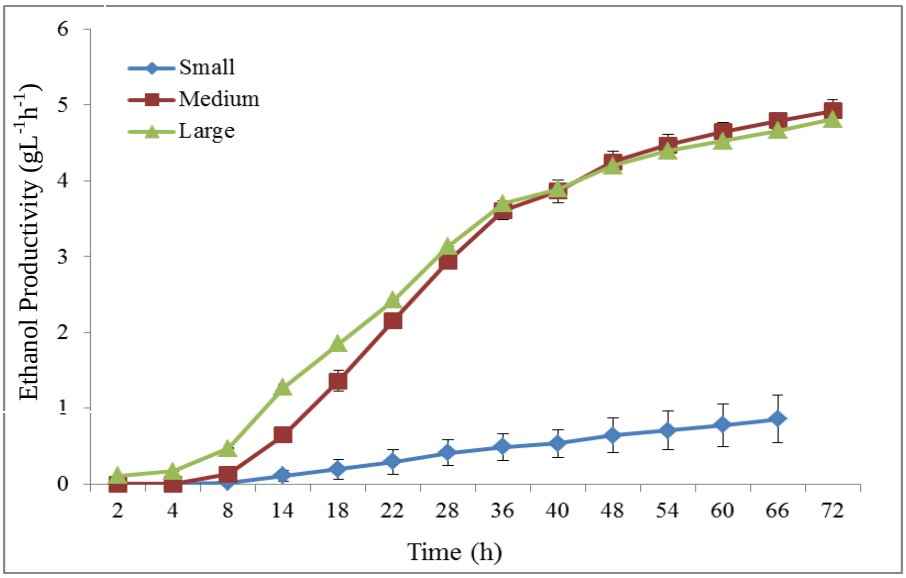

Figure 6.22**:** Ethanol productivity profile by *S.cerevisiae* W303 immobilised on small (D = 35 μm), medium (D = 45 μm) and large (D = 55 μm) pore sized sulphonated polyHIPEs supplied with YPG media at 30°C.

6.4 Microbioreactor and Intensification Study (Comparison of Steady State Continuous Production in Microreactor vs Batch Shake Flask Production)

A nearly similar microreactor configuration in the continuous operation had been reported for the production of α-amylase (Jimat, 2011) and phenol degradation experiments (Akay *et al*., 2005c). In α-amylase production, the microreactors were run for maximum 24 hours only, therefore no ultimate reactor blockage had been reported.While in phenol degradation experiments, the microreactor had shown stability up to 30 days of continuous operation although parts of the bioreactor (2/5) had been disregarded and not contributing to the reactor performances (Akay *et al*., 2005c). In the present study, most of the microreactor (regardless the type) was operated successfully for at least 72 hours (for microreactors having pores (D) and interconnect size (d) beyond 40 μm and 15 μm, respectively). Although the conversion of glucose did not achieve 100% towards the end of fermentation, intensification had been achieved with the HA and the S-NH_4OH PHP in terms of reducing the time for producing ethanol at the same level of glucose utilisation. In shake flask fermentation by free cell *S.cerevisiae* W303, it took at least 20 hours for the yeast to use up 60% of the initial glucose. While in this study a 60% glucose consumption was achieved within approximately 14 and 18 hours (for the HA and the S-NH_4OH PHP, respectively) before the microreactor started using 60% of glucose per feed (25 gL^{-1}) per pass (3-5 minutes), efficiently. Relatively, at 60% glucose consumption, the number of released cells in the effluent stream achieved 10^7 CFU/ml showing that there might be enough cells in the polyHIPEs to use and convert the glucose. However, insufficient retention time of the media in the microreactor (polyHIPEs) could be the reason why 100% glucose conversion was not achievable at the moment.

The approximate intensification productivity was calculated differently from the general calculation methods for the continuous process. The difference in terms of calculation is shown in Equation 6.1 (Akay *et al*., 2005c) and Equation 6.2. Calculation for steady state productivity in common continuous operation includes the

volume of the reactor (Equation 6.1), while microreactor productivity (P_M) did not consider this terms in the calculation.

Productivity (P_C) = C^* x D where D = F/V ……Equation 6.1

Where Pc is in $gL^{-1}h^{-1}$, C* is the ethanol concentration (gL^{-1}) achieved during steady state operation, D is the dilution rate in h^{-1}, F is the flowrate of medium (Lh^{-1}) and V is the volume of the reactor (L). Whereas, the productivity in the microreactor (P_M) is based on the concentration of the ethanol measured in the outlet stream over the retention time of medium in the reactor (t_R), as follows:

$$\text{Productivity}\,(P_M) = \frac{C^*}{t_R} \qquad \text{……..……Equation 6.2}$$

e.g :Approximate calculation for the ethanol productivity in 45 μm Sulphonated PHP at 22 hours of fermentation (Figure 6.21)

$$(P_M) = \frac{6.00\ gL^{-1}}{3\ min} = 2\ gL^{-1}min^{-1} = 120\ gL^{-1}h^{-1}$$

Referring to Figure 6.23, the ethanol concentration in the microreactor (red dotted line) increased gradually with time and reached maximum at t = t_{Mmax}. The concentration remained stable up to time (t_∞). However if the reactor was unstable (due to excessive cell growth or minor blockage), which might occurred after a prolong run, will cause a reduction in ethanol concentration. In some extreme condition, there was a possibility that the concentration will finally dropped to zero as shown by the reducing trend (red line) that occurred after t_∞. On the other hand, the microreactor productivity (solid red line) shows a contant production (P_{M*}) between time t_{Mmax} to t_∞. However, if the reactor malfunctioned, both concentration and productivity will gradually reduce with time and might dropped to zero at t_i. On the other hand, although the ethanol concentration (C_B) for the batch flask fermentation was higher (black solid line) compared to the microreactor (C_M), but the concentration declines to zero due to ethanol assimilation. The drawback of batch fermentation in comparison to batch is that it requires additional time (t_0) and cost for preparation and cleaning. According to the previous run, steady state operation in fully aerated microreactor was achievable after approximately 30 hours, where maximum ethanol

production per pass was in the range 4-6 gL^{-1}. This, if translated into microreactor productivity ($P_M(t)$) was equivalent to approximately ~120 $gL^{-1}h^{-1}$ boosted nearly 120 time compared to the productivity in the batch process ($P_B(t)$ ~ 1 $gL^{-1}h^{-1}$) . General productivity of the batch process was limited to 1.8 – 2.3 $gL^{-1}h^{-1}$ which is uneconomical for commercialization (Baptista *et al*., 2006) (Figure 6.23).

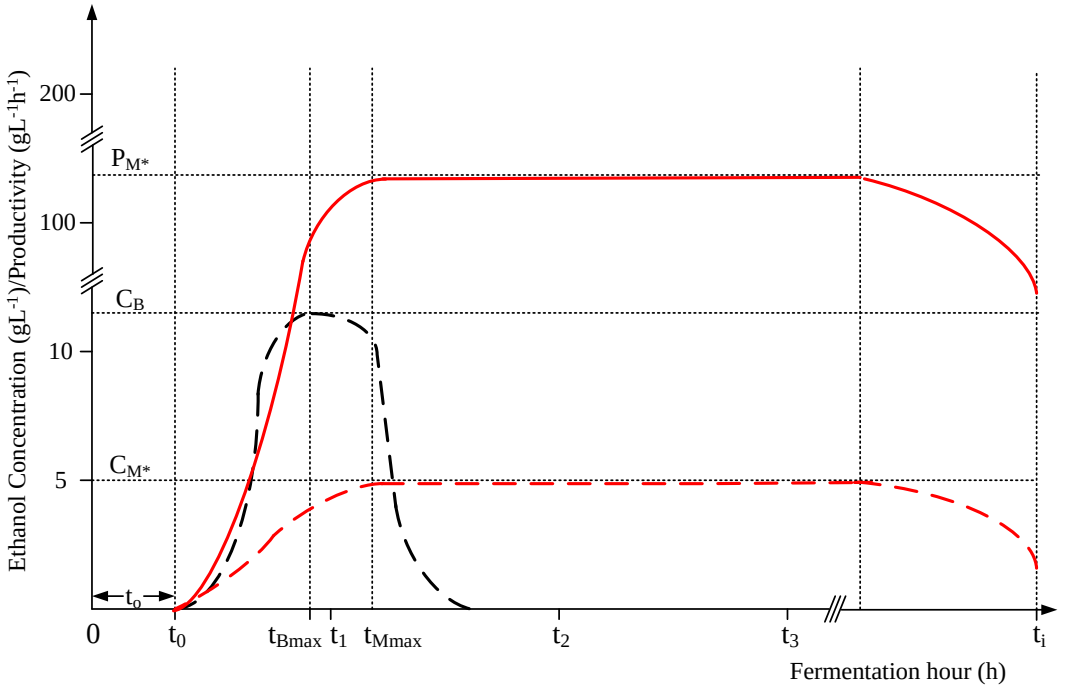

Figure 6.23: Theoretical plot for the ethanol production in shake flask (batch production by free *S.cerevisiae* W303) and microreactor (continuous production) grown in YPG media at 30°C. Black dotted line (ethanol concentration in shake flask fermentation) red dotted line (ethanol concentration in microreactor) and solid red line (productivity of microreactor).

This process had demonstrated that using one of the general strategies (cell retention in the microreactor) managed to boost up the productivity (Figure 6.23). Assuming that the average single yeast weigh around 1.3 x 10^{-11} g (Allain, 2007), the microreactors were approximately filled with at least 10^{10} cells and can reach up to 10^{11} per reactor volume. In the miniaturized systems, transportation processes occur across a length scale of 100-0.1 μm (or less), not only the diffusion/conduction path length is reduced, but high process selectivity can be achieved after being repeated several hundres/thousands time in the microscopic volumes (pores) (Burke, 2007;

Akay *et al*., 2005c). The reduction of path and repetitive process that occur in each pore produces enhancement to the product of interest.

Figure 6.24 represent the extension of data collected from this study, where microreactors were feed with 25 gL^{-1} glucose at 1 ml/min, and the volume of the polymeric microreactor of 2.6 ml (cm^3). The productivity curve plotted against the fermentation time represented this specific microreactor study (red line). The productivity was expressed as the amount of ethanol detected in the outlet stream per residence time of the reactor. The approximate residence time in this study was set at 3 minutes (average time) although it may vary as the operation proceeds owing to the increase cell density which affected the initial void volume of the microreactors. There was also a probability that the retention time is reduced due to increase cell growth (packing porosity) but the catalytic conversion of the reactor was also increased significantly due to increasing number of active cell which eventually might compensate the losses in the retention time. Theoretically, the ethanol will be secreted to the medium at constant rate and concentration, proceed efficiently until it reaches t_d, at which the reactor performances is degrading due to excessive blockage by the cells. However, if efficient removal of unneccesary cells (death/old cell) and the reactor keep it dynamic condition, the constant productivities can be maintain up to t_∞, whilst eliminates the non-productive time (t_o) that is needed for the start up of every new batches, thus optimize the production cost. The black line represents a batch shake flask productivity where a minimum time of (t_0) is required for preparation and cleaning everytime a new batch is set up. Few batches of batch fermentation (repeated batch) as represented by black line in Figure 6.24 is required to match a productivity for microreactor, which mean more time is allocated for the non-productive preparation.

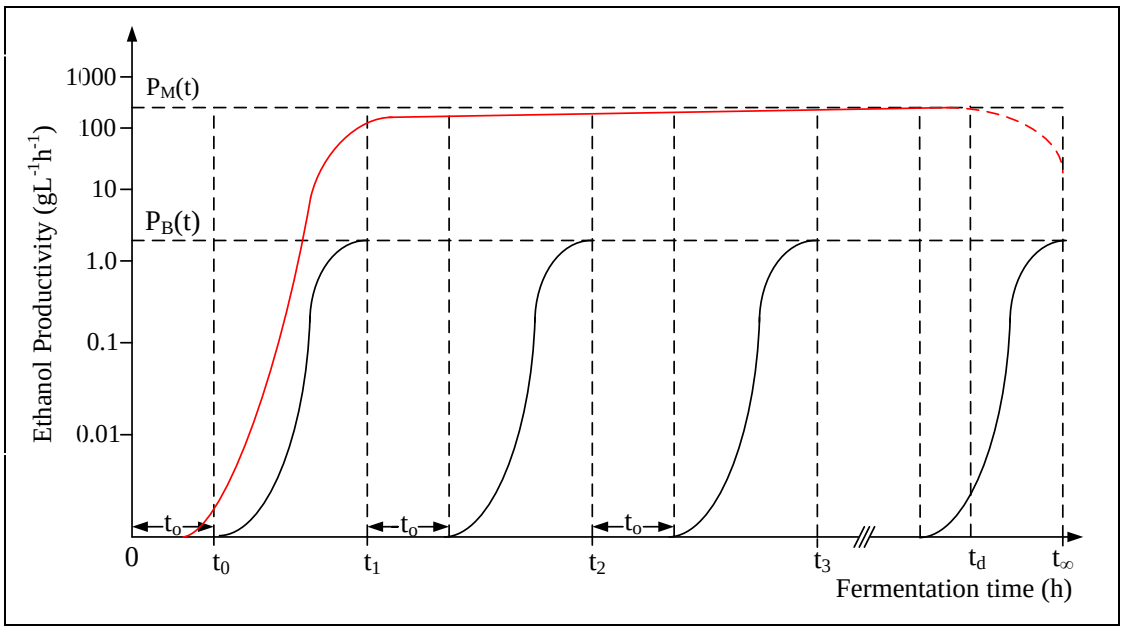

Figure 6.24: Approximate production of microreactor studies over shake flask batch fermentation for *S.cerevisiae* W303 grownin YPG media at 30°C. Red line (productivity in microreactor), black line (productivity in batch shake flask culture by free *S.cerevisiae* W303)

In this study, steady state excretion of the ethanol (flow rate set at 1 ml/min) was reached within 16-30 hours of operation occurring at approximately 120-200 $gL^{-1}h^{-1}$. During this state, the increase of cell biomass was still very active (represent by the number of cell released) while ethanol production was almost constant. In the α-amylase production, steady state operation was achieved after 13 hours of operation while the phenol degradation system achieved steady state within 5 minutes only. These three operations was designed with same reactor configuration (height and dimension of polyHIPE disc) and supplied continuously with medium at the same flowrate (1 ml/min).

It is worth noting that the typical average ethanol production establish in this study was approximately in the range of 1.5 - 10 $mmolL^{-1}min^{-1}$. Allain (2007) reported in his findings that the typical industrial ethanol fermentation was maximum at 1.7 $mmolL^{-1}min^{-1}$. This value was challenged by a new route of ethanol synthesis, called cell-free ethanol production where 'zymase' enzyme was used to replace the living yeast as a medium to produce ethanol (Allain, 2007). This new system was capable of

producing ethanol at much higher rate of approximately 9 mmol$L^{-1}min^{-1}$, but at the expense of incredibly high cost of enzymes.

On the other hand, an intensification factor is used to measure the magnitude of improvement made by the microreactor over the productivity in the shake flask batch culture. The intensification factor was calculated with consideration to the reactor volume for a reduced time taken to produce ethanol in the HA and S-NH_4OH PHPs was calculated at 70% glucose consumption over shake flask batch production. The factor was then compared with the production occurring at the same level of glucose consumption in the shake flask culture. The calculation was done as follows:

$$\frac{\text{Ethanol concentration}}{\text{Volume reactor x time}} = \frac{\text{g}}{\text{L x t}} = \frac{\text{g}}{\text{L.min}} \quad \text{……Equation 6.3}$$

$$\text{S - NH}_4\text{OH PHP} = \frac{\dfrac{3.5\ \text{gL}^{-1}\ \text{x}\ 3.5\ \text{ml}}{3.8\ \text{min}}}{\dfrac{5.5\ \text{gL}^{-1}\ \text{x}\ 50\ \text{ml}}{22\ \text{h x}\ 60\ \text{min}}} \quad \text{…..…….....Equation 6.4}$$

$$= \frac{3.5\ \text{gL}^{-1}\ \text{x}\ \ 22\ \text{h x}\ 60\ \text{min x}\ 3.5\ \text{ml}}{5.5\ \text{gL}^{-1}\ \text{x}\ 3.8\ \text{min x}\ 50\ \text{ml}} = 15.5$$

$$\text{HA– PHP} = \frac{\dfrac{1.4\ \text{gL}^{-1}\ \text{x}\ 2.6\ \text{ml}}{2.3\ \text{min}}}{\dfrac{5.5\ \text{gL}^{-1}\ \text{x}\ 50\ \text{ml}}{22\ \text{h x}\ 60\ \text{min}}} = \frac{1.4\ \text{gL}^{-1}\ \text{x}\ 22\ \text{h x}\ 60\ \text{min x}\ 2.6\ \text{ml}}{5.5\ \text{gL}^{-1}\ \text{x}\ 2.3\ \text{min x}\ 50\ \text{ml}} = 8.1 \quad \text{……Equation 6.5}$$

Comparable ethanol production times in the shake flask culture with free *S.cerevisiae* W303 (with respect to the reactor volume) were reduced by 15.5 and 8.1 times when operating in the continuous fermentation using *S.cerevisiae* W303 immobilised on the S-NH_4OH and HA microreactor, respectively. The intensification was calculated at 70% glucose consumption because that was the maximum glucose conversion achievable using these microreactors. The reduced production time was assumed to be partly contributed by the reduced diffusion length for medium transfer, where catalytic conversion was repeated thousands of times within its vicinity (pores) thus enhancing the yield and speeding up the process (Akay, 2006a).

6.5 Conclusions

This chapter addressed attempts to develop a new reactor system that promoted adhesion and proliferation of *S.cerevisiae* W303 within its cavity, subsequently producing stable ethanol concentration in the effluent. The highest productivity was achieved with the S-NH_4OH PHP compared to the other polyHIPEs, and the efficiency of this microreactor increased when the pore size was reduced from 55 μm to 45 μm. With respect to the stable growth and ethanol production, the sulphonated PHP with a nominal pore size of 45 μm has greater advantages over its two counterparts, which would contribute to the further improvement of ethanol production in prolonged operation. This PHP was used in the medium optimisation to further enhance the sugar utilisation that corresponded to increased growth and ethanol production. In a further study, the flowrate was manipulated in order to analyse the effect of the retention time and the rate of cell migration.

CHAPTER 7: OPTIMISATION OF PROCESS CONDITIONS AND MEDIUM REQUIREMENTS

7.1 Introduction

This chapter discusses the effect of the medium flow-rates, the medium requirements (the effect of the initial glucose concentration, the effect of the C/N ratio and the effect of increasing the individual N components) and oxygen on the growth and direction of fermentation. The growth factors such as oxygen and nitrogen were manipulated in order to control the growth of *S.cerevisiae* W303, in which glucose concentration is often channelled into ethanol synthesis instead of producing new cells. In this part, the traditional approach of optimisation, the one factor at a time (OFAT) technique, was used to optimise the sugar utilisation, growth and ethanol production. This technique was chosen for its simplicity and straightforward analysis. Sulphonated PHP with pore size of D = 45 μm was used for the rest of the work, and medium was supplied continuously at 1 ml/min and temperature of the reactor was maintained at 30^{o}C throughout the fermentation.

7.2 The effect of Medium Flowrate (Dilution Rates) on the Fermentation Performance

Ethanol fermentation in *S.cerevisiae* varies significantly depending not only on the strain, but also on the environment. This study was carried out to investigate the maximum fermentation capacity of the immobilised yeast at varying dilution rates with regard to retention time, the growth of yeast and the wash out condition. The higher the dilution rate, the shorter the retention time, and vice versa. Besides this, increasing the dilution rate is associated with an excess supply of carbon sources. When glucose and oxygen are in excess, respiration is shifted to respiro-fermentative metabolism, which means that ethanol will be produced instead of biomass. In addition, for the chemostat culture, the conversion of glucose to ethanol only

happened when the dilution rate surpassed a particular dilution rate (independent for each process condition) (Rieger *et al*., 1983).

Experiments for the effects of the dilution rates were carried out by supplying the culture with a highly aerated medium consisting of 25 gL^{-1} of glucose, 10 gL^{-1} of peptone and 5 gL^{-1} of yeast extract at flow rates varying from 0.5 to 1.52 ml/min which is equivalent to the dilution rate (D_R) of 7 – 22 h^{-1}. The experiments were carried out for 72 hours, or terminated earlier if they malfunctioned due to cell blockage. The results are shown in Table 7.1.

7.2.1 *The effect of Dilution Rates on the Growth Characteristics and Cell Wash Out*

In general, the profile for the number of cells released and the biomass content increased when the dilution was increased from 7 h^{-1} to 20 h^{-1}. The values for both properties, however, reduced slightly when the flowrate was increased further to 22h^{-1}. The highest cell wash out occurred at dilution rate D_R = 20 h^{-1}, yielding 7.5 x 10^7 CFU/ml. The cells released were reduced slightly by 7.1% when the dilution rate was further increased to 22 h^{-1}, obtained at 6.0 x 10^7 CFU/ml (Table 7.1). At high dilution rates, more cells were washed out due to the high shear rate, but as the fermentation continued, the yeast started to adapt and produce more cells at much higher rate. Therefore, the final biomass concentration was increased from 0.24 g (D_R = 14 h^{-1}) to 0.39 g and 0.41 g at 22 h^{-1} and 20 h^{-1}, respectively.

Operating at low dilution rates (D_R = 7-10 h^{-1}) resulted in a significant reduction of cells released into the effluent stream. Cell wash out at D_R = 7h^{-1} and 10 h^{-1} remain the lowest, obtained at 1.3 x 10^7 CFU/ml and 1.2 x 10^7 CFU/ml, respectively. These numbers were slightly lower than the number of cells released with the smaller pore sized sulphonated PHP (D=35 μm; 1.8 x 10^7 CFU/ml, 0.20 g, D_R = 14 h^{-1}), suggesting that cell migration was amplified by the hydroforce rather than by the large interconnect size. However, these three reactors exhibited a similar

characteristic, whereby the growth/migration of *S.cerevisiae* W303 in the polyHIPEs was prevented by the fast accumulation of cells on its surfaces. However, the biomass content was increased from 0.19 g to 0.21 g, when the dilution rate was increased from 7 h^{-1} to 10 h^{-1}, and the values obtained were presumably contributed mainly by the cells on the top surfaces. Although increasing the biomass content was observed after raising the dilution rates to 10 h^{-1}, these reactors failed after 54-60 hours, when the flow of the medium was completely hindered by excess surface growth. The range of dilution rates tested in this study did not represent the lethal effect of cell wash out, although the number of cells released into the medium increased proportionally with increased dilution rates. The point where the dilution rate becomes limiting is when the amount of biomass entrapped is declining, therefore Dr = 7-22 h^{-1} supported good yeast growth.

Table 7.1: Fermentation kinetics for continuous operation at various dilution rates.

Dilution Rate (h^{-1})	**Shake Flask (Free Cell)**	**7**	**10**	**14**	**20**	**22**
Flowrate (ml/min)	-	0.5	0.7	1	1.44	1.52
Estimation of Retention time (min)	-	6.0	4.3	3.0	2.1	1.9
Max. ethanol concentration (gL^{-1})	11.15 $\pm$ 0.81	2.53 $\pm$ 1.22	6.13 $\pm$ 0.87	6.61 $\pm$ 0.48	4.23 $\pm$ 0.53	4.34 $\pm$ 0.34
Stable ethanol concentration (gL^{-1})	-	na	Na	6.19 $\pm$ 0.18	3.30 $\pm$ 0.65	3.14 $\pm$ 0.58
Biomass in PHP (g)	-	0.19 $\pm$ 0.02	0.21 $\pm$ 0.04	0.24 $\pm$ 0.01	0.41 $\pm$ 0.04	0.39 $\pm$ 0.02
Cell packing density (g Biomass/ g PHP)	-	0.82 $\pm$ 0.05	0.87 $\pm$ 0.04	0.93 $\pm$ 0.04	1.44 $\pm$ 0.07	1.51 $\pm$ 0.03
*Ethanol based on initial sugar (g/g)	0.50	0.18	0.25	0.26	0.17	0.17
*Ethanol yield based on glucose consume (gg^{-1})	0.50	0.26	0.37	0.46	0.32	0.35
Maximum cell released (CFU/ml)	7.3×10^7	~ 1.3×10^7	~1.2×10^7	~5.2×10^7	~7.5×10^7	~6.0×10^7
Stable glucose consumed per pass (%)	-	68.5	66.9	60.1	53.5	50.1
*Maximum substrate used (g)	25	17.3	16.73	14.3	13.38	12.53
Cumulative ethanol production (gL^{-1})	11.15 $\pm$ 0.81	76.7 $\pm$ 4.11	84.6 $\pm$ 5.62	354.6 $\pm$ 4.8	143.8 $\pm$ 10.1	174.9 $\pm$ 10.6
Overall Productivity	0.41	1.42	1.57	4.92	2.00	2.43
Increment of Productivity over Batch	-	3.5	3.8	12.0	4.88	5.93
Maximum operation time	27	56-60 hours	54-60 hours	>72 hours	>72 hours	>72 hours

- *Volume of reactor was fixed at 3 ml; Based on maximum ethanol concentration
- Cumulative production – total ethanol being produced throughout fermentation.

7.2.2 *SEM Analysis on the Microreactor*

The penetration and the cell adherence of the microreactor at D_R=7 h^{-1} were viewed with the SEM. At the low D_R =7 h-^{1}, more cells were growing on the top, with very few cells observed in the central cavity. Figure 7.1(a) shows that the top surface was invaded by the fast growing yeast. The cells were distributed evenly on the top surface but, the number of cells reduced dramatically in the pores of the middle cavity of the microreactor (Figure 7.1b). The rate of cell growth was higher than the rate of cell migration, which caused the excess growth on the polyHIPE surface. The slow flow rate (weak hydroforce) was unable to force the cells into the microreactor, thus causing uneven cell distribution on the top surface. Melzoch *et al*. (1994) reported that excess surface growth had circumvented the flow of the medium into the bead support**.** As a consequence, the cell stopped budding and ceased growing inside the beads and the conversion of glucose to ethanol only occurred at the surface of the beads. A reduced cell density inside the support cavity was also observed by Bokhari *et al*. (2006) in a static culture. Tissue cells multiplied rapidly on the surface and the density was reduced in the internal part of the polyHIPE due to the slow rate of migration.

The surface growth was successfully controlled by increasing the medium flowrate beyond 1 $mlmin^{-1}$ **(**D_R = 14 h^{-1}). The higher flowrate increased the shear forces which broke the cell clusters and forced them deeper into the polyHIPEs. Therefore, no extreme growth on the surface was observed for the reactor operating at 14 -22h^{-1}, and stable production successfully achieved for up to 72 hours of fermentation. At these flowrates, more cells were immobilised or retained which yielded an increasing biomass concentration at medium and high flowrates (14-22 h^{-1}) compared to low dilution rates (7-10 h^{-1}). Besides this, the homogeneity of cell distribution and cell density in the interior reactor was improved dramatically after increasing the dilution rate to 14 h^{-1}, (Figure 7.1c).

On the other hand, the depth of cell penetration into the microreactor did not rely on the dilution rate. For the tested dilution range, the maximum depth of penetration was similar, which meant that cells were observed throughout the polyHIPEs, but the density of the attached cells with respect to distance in the microreactor varied significantly. While low flowrates resulted in low cell density in the polyHIPEs, highly flocculated, dense cells were observed throughout the polyHIPEs at $D_R = 20\ h^{-1}$ as shown in Figure 7.1(d).

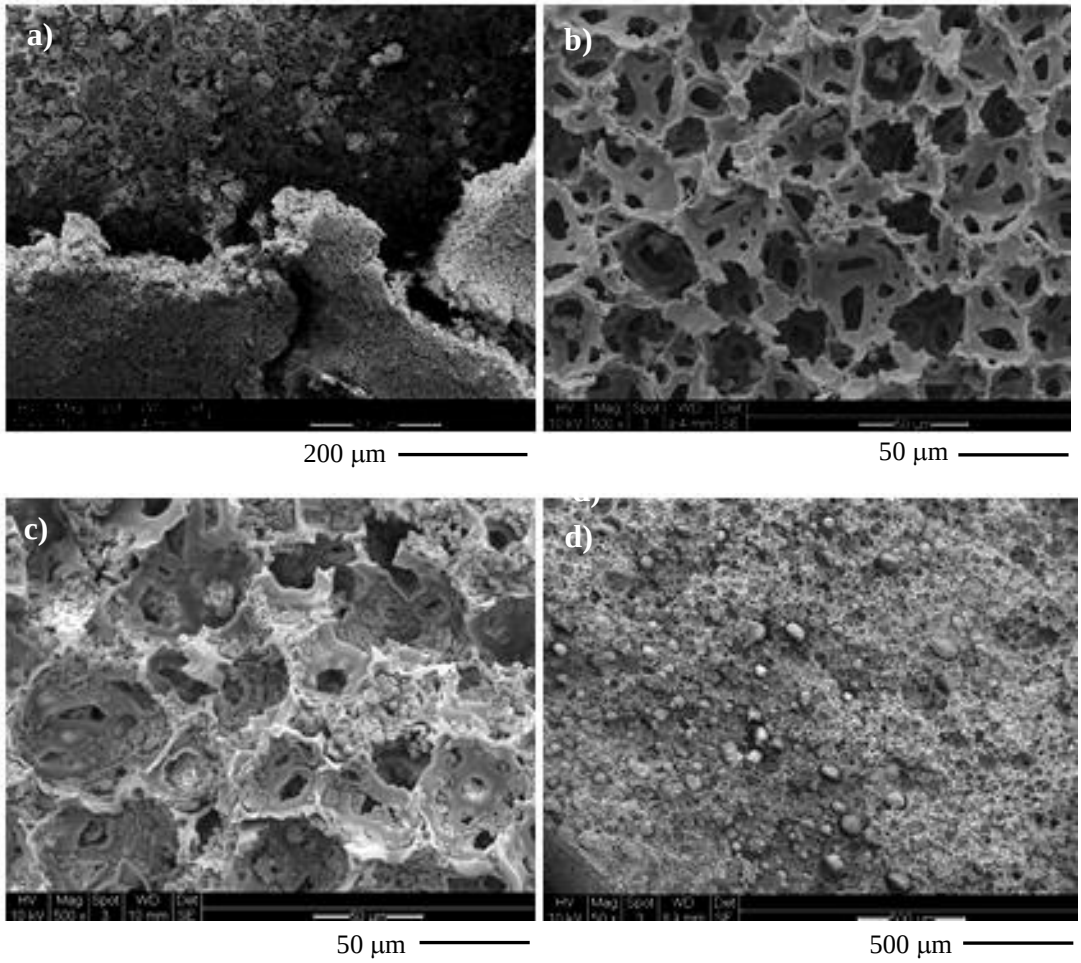

Figure 7.1: a) Cells invasion resulting in poorly distributed cells which caused the reactor to malfunction after operating for 56 hours at dilution rate 7 h^{-1}. b) Poor cell density in the reactor (operating at D = 7 h^{-1}), approximately 2 mm from the surface. c) Homogeneous cell distribution at the cross section of the microreactor (D = 14 h^{-1}). d) Heavily flocculated cells were observed in the microreactor operated at D = 20 h^{-1}.

7.2.3 *Effect of Dilution Rate on Glucose Utilisation and Ethanol Production*

Referring to Figure 7.2, the glucose consumption showed a reducing trend when the dilution rate was increased from 7 h^{-1} to 22 h^{-1}. For dilution rates 7-14 h-1, the amount of glucose consumed remained almost stable between 66.9-68.5%). However, the values dropped sharply after increasing the dilution rate to 20-22 h^{-1}, where the glucose consumption was reduced to 53.1% at 20 h^{-1} and 50.1% at 22 h^{-1}. With respect to the retention time, only a slight increase of glucose utilisation (13.9%) was observed when the retention time was increased from 3 minutes (D = 14 h^{-1}) to 6 minutes (D = 7 h^{-1}). Comparing this with the previous results (Chapter 6), the value was found to be even lower compared to the utilisation observed in experiments using 55 μm polyHIPEs. The might be due to the reduced growth observed within the polyHIPE at low dilution rates (Figure 7.1b). It was presumably that the glucose consumption was mainly carried out by cells growing on the top surfaces, and the retention time of the medium in the cell layer was low, therefore it did not show an increased glucose utilisation (Figure 7.2). Although the medium had to go through the polyHIPE, there were not enough cells to consume the remaining glucose.

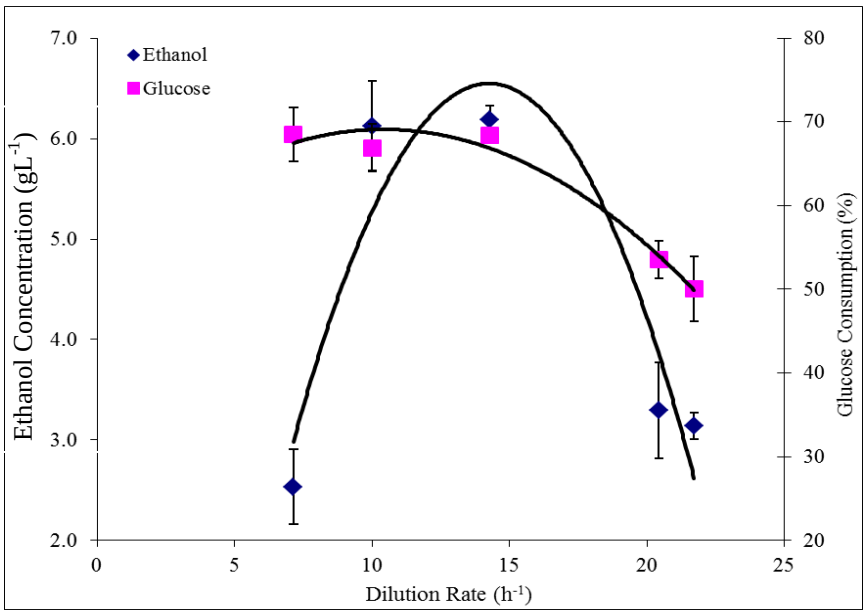

Figure 7.2: The effect of dilution rate on the ethanol production and glucose consumption by *S.cerevisiae* W303 immobilised on sulphonated PHP (D=45 μm). YPG media was supplied continuously to the reactor at 30°C.

Although the highest glucose utilisation (68.5%) was observed at D_R = 7 h^{-1}, the optimum ethanol production (6.61 gL^{-1}) for the tested flowrate was obtained at a slightly higher dilution rate (14 h^{-1}). Although more glucose was consumed at the lower dilution rate, there was a probability that glucose was channelled for cell maintenance and biomass generation, subsequently reducing the ethanol production. Although only 0.19 g and 0.21 g of biomass was observed at D_R = 7 and D_R = 10 h^{-1}, which was 20.8% and 12.5% lower than the biomass obtained at 14 h^{-1} (0.24 g), respectively,but, if the fermentation can be prolonged to 72 hours, the biomass content might be higher than 0.24 g. At D_R = 7 – 10 h^{-1}, the fermentation time was reduced by nearly 28% compared to the normal operating time (72 hours) due to blockage. Gradual reduction of glucose consumption was observed with increasing dilution rates. At D_R= 10 h^{-1}, maximum glucose consumptions was 66.9%, reducing to 60.1%, 53.5% and 50.1% at D_R = 14, 20 and 22 h^{-1}, respectively. At D_R = 20 and 22 h^{-1} reduction of holding up time in the reactor caused a significant decrease in glucose consumption. Besides this, the fermentative capacity of the yeast cells was possibly reduced, but on the other hand, it induced the respiration capacity, which shows increasing biomass concentration retained in the polyHIPE. The ethanol production was reduced to half (3.30 g/L at D_R = 20 h^{-1}), while the biomass production was boosted to 0.411 g (20 h^{-1}) which was approximately 70% higher compared to cells at 14 h^{-1} (0.24 g). The lowest ethanol concentration (3.14 gL^{-1}) was obtained when the medium was supplied at 1.52 ml/min (D = 22h^{-1}). The highest ethanol concentration was observed at 2.53 gL^{-1} and 6.13 gL^{-1} at D_R =7 and 10 h^{-1}, respectively.

When the D_R was increased beyond 14 h^{-1}, the sugar consumption and ethanol yield reduced dramatically and a less marked increased of biomass accumulation in the polyHIPE was observed (Table 7.1). The ethanol yield, based on g ethanol per g glucose consumed, was increased from 0.26 g/g to 0.46 g/g when the dilution rate was raised from 7 to 14 h^{-1}. A sharp reduction was observed when the D_R was increased further to 22 h^{-1}, giving the maximum yield based on a glucose consumption of 0.35 g/g. No noticeable effect on the biomass yield and ethanol production was observed after increasing the dilution rate from 20 to 22 h^{-1}. It was assumed that the maximum capacity for cell respiration had been achieved within the short/single pass of the

medium, indicating that cell or medium recirculation may be very beneficial to improve the overall yield and increase substrate utilisation (Brandberg *et al*., 2007). Vasconcelos *et al*. (2004) also reported a loss of sugar utilisation capacity, when glucose was supplied at increasing dilution rates. The loss was as a result of the rate/speed of sugar utilisation failing to accommodate the excess glucose supply, causing a large reduction in the fermentation efficiency.

At low D_R (7-10 h^{-1}), the effects of the carbon-limited condition predominates, while at high dilution rates (20-22 h^{-1}), the low retention time may affect the fermentative capacity of the reactor. Both conditions resulted in a lower ethanol concentration compared to the ethanol production observed at 14 h^{-1}. The effect of the carbon-limiting condition was also observed by Souto-Maior *et al*. (2009) at low dilution rates, D = 0.06 h^{-1}, where a complete respiratory metabolism was achieved, resulting in low ethanol concentration. Van Hoek *et al*. (2000) reported a more extreme condition where ethanol production was completely absent when the continuous culture was supplied with 25 gL^{-1} of glucose at dilution rates below 0.3 h^{-1}. In the fully aerobic conditions, the yield of biomass reached up to 0.57 g/g glucose, and can be reduced substantially by reducing either the nitrogen sources, oxygen, or both. Another study reported a much lower yield at 0.50 g/g glucose in a fully respiratory environment (Sonnleitnert and Kappeli, 1985). The bottleneck of glucose and ethanol oxidation was discussed in detail by these authors.

The effect of the fermentation efficiency was difficult to compare with other studies due to the different theoretical framework. The current system was operated in the microscale environment, operating at dilution rates (7-22 h^{-1}) higher than the growth rate of the *S.cerevisiae* W303 obtained in the batch culture (0.152 h^{-1}). In contrast, most reported systems studied the effect of dilution rate in a range lower or slightly higher than the maximum specific growth rate of the organism (< 0.5 h^{-1}) (Larsson *et al*., 1993; Jansen *et al*., 2005). This might explain why a completely oxidative process (absence of ethanol) was not observed in this study. Although a substantial increase of biomass content was obtained with high dilution rate cultures, the increment did not contribute to

the enhancement of ethanol production. In fact, the ethanol concentration was reduced dramatically, which was associated to the reduction of glucose consumption, or possibly due to the incapability of cells to metabolically convert the glucose within the shorter period of time (loss of fermentative capacity). The decreasing ethanol concentration suggests that the impaired retention time outweighs the possibility of switching the process to fermentation.

7.2.4 *Conclusions*

This study emphasised the important role of the hydrodynamic forces in the continuity of the reactor systems. As a conclusion, the similarity of the pore sizes or dilution rates were both parameters which influenced the rate of cell migration/wash out throughout the fermentation. A higher rate of cell migration/wash out, corresponding to larger pore sizes and higher dilution rates has been shown in this study. The increased rate of migration reduced the surface growth, thus increasing the reactor stability and productivity. There was a clear correlation between dilution rates and the amount of the residual glucose in this tested range, where glucose consumptions gradually decreased with increasing dilution rates. The reduction of ethanol yield and glucose consumption, at high dilution rates, was attributable to the short retention time of the substrate in the system which reduced the efficiency of the cells to use and convert the substrate to the product of interest (ethanol). With respect to cell penetration and surface growth, this result suggested that apart from operating the continuous culture at dilution rates higher than the specific growth rate to trigger ethanol production, most importantly, it must be able to provide a sufficient shear rate to prevent surface growth. Besides, it must also provide sufficient time for the glucose conversion to take place. In this study, the dilution rate of 14 h^{-1} was found suitable for providing the extra shear stress, while facilitating both growth and ethanol production. Further increase of the dilution rate reduced the efficiency of the glucose conversion. At low dilution rates, there was a possibility that ethanol was consumed simultaneously with glucose but more work must be carried out for verification (Rieger *et al*., 1983).

7.3 Effect of Glucose Concentration on the Ethanol Productivity

The ethanol yield is highly dependent not only on the initial glucose concentration, but also on the availability of oxygen. At low glucose levels, the metabolisms were completely respiratory, producing biomass and CO_2. In fermentation, increasing the level of glucose in the presence of oxygen shifts the metabolic respiration to partly fermentation, where ethanol is produced as the by-product. Care must be taken when increasing the amount of glucose in the feed medium because the solubility of oxygen in the medium reduced with increased medium viscosity. The oxygen supply in this continuous process came solely from dissolved oxygen (by continuous sparging of air into the medium tank), so the viscosity of the medium played an important role. Medium viscosity increased with the addition of glucose, hence reducing the solubility of oxygen in the medium. The path of reaction for *S.cerevisiae* W303, was determined by the availability of oxygen, where fermentation process is favourable in low oxygen concentrations. It should be noted that oxygen must be available within the reactor to ensure the synthesis of new cells to maintain a high density culture, and to ensure that the glycolytic and TCA cycles of yeast were not disturbed, thus increasing the reactor stability. Continuous distortion of the glycolytic and TCA cycles due to insufficient oxygen caused instability in the yeast mechanism and could reduce both growth and ethanol productivity. At a high glucose content (e.g. 150 gL^{-1}), the respiratory enzyme was inhibited, therefore inducing the fermentation routes (Jamai *et al*., 2001).

The effect of glucose concentration has been mentioned briefly in Chapter 2 (Section 2.5.2). Increasing the glucose concentration is beneficial for inducing the fermentative capacity of *S.cerevisiae*. In this study, the concentration of the glucose was varied from 10 to 50 gL^{-1} of glucose, while the yeast extract and peptone was maintained at 5 gL^{-1} and 10 gL^{-1}, respectively.

Table 7.2: Steady state results with varying glucose concentration.

Initial Glucose concentration (gL^{-1})	**10**	**25**	**50**
Max Ethanol concentration (gL^{-1})	1.885 ± 0.60	6.61 ± 0.48	6.58 ± 0.18
Stable Ethanol Production (gL^{-1})	na	6.19 ± 0.18	6.31 ± 0.45
Ethanol yield based on initial glucose (g/g)*	0.19	0.26	0.13
Percentage of theoretical yield (%)	37.3	50.9	25.4
Ethanol yield based on glucose used (gg^{-1})*	0.20	0.46	0.36
Biomass in PHP (g)	0.14 ± 0.01	0.24 ± 0.01	0.37 ± 0.03
Biomass density (g/g PHP)	0.66 ± 0.02	0.93 ± 0.04	1.37 ± 0.05
Biomass yield based on glucose consumed (g/g)	0.014	0.017	0.018
Maximum Number of Cell released (CFU/ml)	~1.95 x 10^7	~5.2 x 10^7	~8 x 10^8
Maximum glucose consumption (%)	~ 95.0	~ 60.1	~37.0
[a]Substrate used (g)	9.5	14.3	18.5
Cumulative Ethanol Production (g)	79.5 ± 15.5	354.6 ± 4.8	413.6 ± 8.5
Productivity ($gL^{-1}h^{-1}$)	1.10	4.92	5.74
Increments (folds) over P_{batch}	2.7	12.0	14.0
Operation period (time)	> 72 hours	>72 hours	>72 hours

- Data were derived based on maximum ethanol concentration. *
- Data were taken by average from 3 replicates.
- Data were taken or derived based on the maximum ethanol concentration[a].
- Cumulative production – total ethanol being produced throughout fermentation.

7.3.1 *The effect of the Initial Glucose Concentration on the Growth and Number of Cells Released*

An increase in biomass concentration was observed in the polyHIPEs when the initial glucose concentration was increased from 10 to 50 gL^{-1}. The lowest biomass content of 0.14 g was observed with 10 gL^{-1} (Table 7.2). Biomass concentration was increased by 71.4% when the glucose concentration was increased to 25 gL^{-1}. The highest increase of biomass was obtained in 50 gL^{-1} of glucose which was 164.3% higher than biomass in 10 gL^{-1}. Increased glucose concentration (with substantial nitrogen sources) increased the sugar uptake rate and enhanced the rate of new cell synthesis, therefore boosting the biomass production in 50 gL^{-1} of culture. It was assumed that at this stage (50 gL^{-1}), oxygen was not a limiting factor, therefore glucose was consumed aerobically, thus more cells were produced instead of ethanol.

In line with the biomass content, the number of cells released was also increased proportionally to increase the glucose concentration (Figure 7.3). In the beginning of the fermentation process (after 4 hours fermentation), the number of cells released into the effluent line at 25 gL^{-1} and 50 gL^{-1} was two fold higher than the value obtained at the lower glucose concentration (10 gL^{-1}), indicating that the growth rate of yeast in the microreactor was significantly enhanced due to the increase in glucose concentration (Figure 7.4). At this point, the amount of nitrogen in the medium was not a limiting factor for the continuous growth of yeast, which showed an increase in the weight of the biomass entrapped in the microreactor as well as in the effluent. Both of the profiles for 25 gL^{-1} and 50 gL^{-1} of glucose (Figure 7.3) show a continuous increase of released cells, so it can be assumed that the growth continued to increase in the microreactor as there were plenty of empty walls for cell attachment. In contrast, the number of cells released in the 10 gL^{-1} of glucose increased slowly, and achieved a maximum (1.95×10^7 CFU/ml) at 54 hours of fermentation. However, the number of cells decreased slowly afterwards, with final cell release being observed at 1.4×10^7 CFU/ml. Glucose could be the limiting factor preventing further growth, and the supply of glucose was only sufficient for the maintenance of living cells, but not for the generation of new cells.

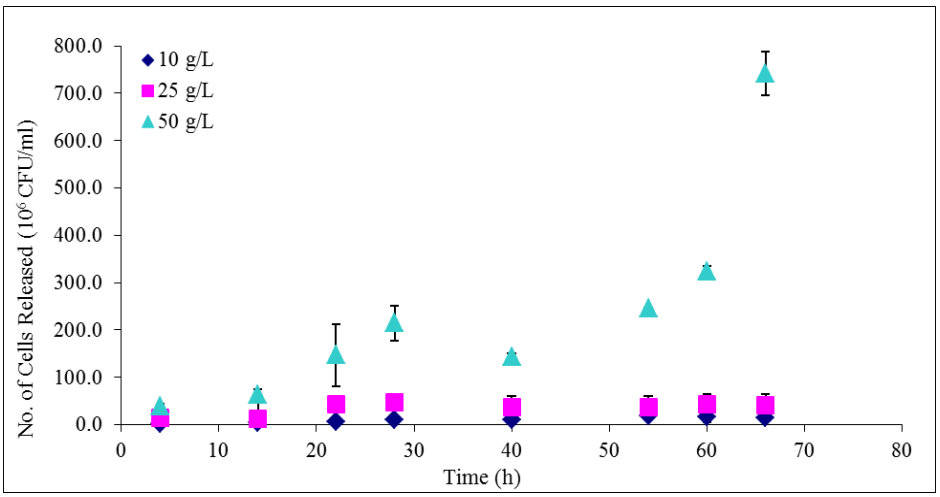

Figure 7.3: Profile of cell released in the effluent stream during fermentation of *S.cerevisiae* W303 immobilised on sulphonated PHP (D=45 μm). YPG media was supplied continuously to the reactor at 30°C.

These results demonstrated an increase in biomass concentration in the excess glucose chemostat, and on the other hand an increase of substrate consumption but with low biomass production. The increased glucose consumption was reflected in the enhancement of the ethanol, glycerol and acetic acid production in comparison to the productivity in the carbon limited culture.

7.3.2 *The effect of the Initial Glucose Concentration on the Substrate Utilisation and Ethanol Production*

Under aerobic conditions with glucose as the source of carbon and energy, *S.cerevisiae* generally prefers respiration over fermentation. However, this condition may be shifted to fermentation by introducing a high glucose concentration; this restricts the synthesis of respiration enzymes; and fermentation is used to generate energy for cells maintenance. According to Di Serio *et al*., (2003), respiration predominates when the sugar concentration is less than 100 gL^{-1} although there was no specific claim about how much glucose must be present in the culture before metabolism is shifted to fermentation and ethanol synthesis can occurred. The minimal

value of the glucose required for the metabolic shift to ethanol production, is dependent on both the uptake rate of glucose into the cell, which is strain dependent (Rieger *et al*., 1983). The present study revealed that, although the concentration of glucose was as low (10 gL^{-1}) and conversion time (3 minutes), the system produced a variable but very low yield of alcohol.

Figure 7.4 presents the sugar utilisation profile using 10, 25 and 50 gL^{-1} of glucose over the time course of the fermentation. Very low glucose outflow was detected when the culture was supplied with 10 gL^{-1} of glucose. Initial glucose outflow was detected at 2. 0 gL^{-1}, and dropped to 0.58 gL^{-1} after 18 hours of fermentation and remained below 0.6 gL^{-1} afterwards. The glucose consumption was maximal at approximately 9.5 gL^{-1} per pass at the given biomass value of 0.14 g. At this concentration, the amount of glucose might only be sufficient for cell maintenance, thus restricting the production of new cells, depicted by the consistent number of cells removed in the effluent stream (Figure 7.4). Sugar consumption was very high, reaching nearly 95.0% of the initial glucose. In this study, glucose was expected to be the rate limiting substrate that reduced the growth inside the microreactor.

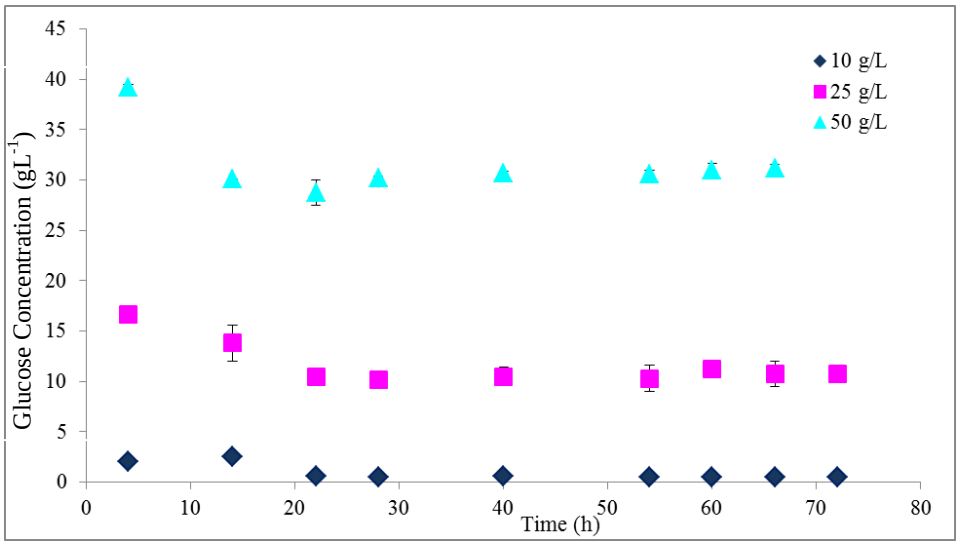

Figure 7.4: Amount of glucose in the effluent during fermentation of *S.cerevisiae* W303 immobilised on sulphonated PHP (D=45 μm). YPG media (with varying glucose concentration 10, 25 and 50 gL^{-1}) was supplied continuously to the reactor at 1 ml/min.

Increasing the supply of glucose to 25 gL^{-1} not only increased the amount of biomass by 71.4%, but also increased the amount of sugar uptake. Although the percentage of glucose consumption decreased from 95.0% to 60.1%, the final amount of fermentable sugar increased to approximately 9.5 gL^{-1} in the glucose limited culture (10 gL^{-1}), compared to ~14.3 gL^{-1} achieved in the 25 gL^{-1}. The same condition was observed in the 50 gL^{-1} culture. The amount of sugar uptake at the end of fermentation was increased to ~18.5 gL^{-1}, which was nearly double the amount taken by the cells in the 10 gL^{-1} culture, and 29.3% higher than in the 25 gL^{-1} culture. However, the percentage of glucose consumption was greatly impaired, with only 37.0% of the initial glucose supply being used by the immobilised cells. In general, the amount of glucose uptake increased with increasing glucose supply, but it reduced the amount of sugar consumption based on the initial supply. At the end of fermentation, a total of 9.5 gL^{-1}, 14.3 gL^{-1} and 18.5 gL^{-1} was consumed by *S.cerevisiae* W303 per pass when supplied with 10, 25 and 50 gL^{-1} of glucose, which is also equivalent to 95.0%, 60.1% and 37.0% of the amount of glucose being converted/utilised, respectively.

The production of ethanol supplemented with 10 gL^{-1} glucose increased linearly with time up to 28 hours of fermentation. However, the production of ethanol was sluggish after 30 hours and fluctuated at the end of fermentation. It is speculated that there was competition between respiration and respiro-fermentation (with the assumption that oxygen was in excess) as plenty of active cells were growing in the microreactor, while the amount of glucose available was limited. This is supported by a stably increasing number of cells being released into the effluent stream up to 58 hours, indicating that a consistent growth of cells occurred in the system. Larsson *et al*. (1993) reported that respiratory metabolism occurred when yeasts were cultured under low dilution rates, where glucose was limited. However, in this study, it is shown that although the glucose was quite low, the fermentation and growth occurred simultaneously. There was also a possibility that the ethanol produced was consumed simultaneously due to glucose exhaustion. If there was a substantial amount of oxygen present, ethanol might be used for energy generation to accommodate the limited amount of glucose as sole carbon and energy supply. This might explain the fluctuation observed in the ethanol profile. Ethanol oxidation was reported when the remaining

glucose fell below 0.5 gL^{-1}. Simultaneous glucose and ethanol oxidation was also reported in the continuous culture when the glucose consumption limits had been reached.

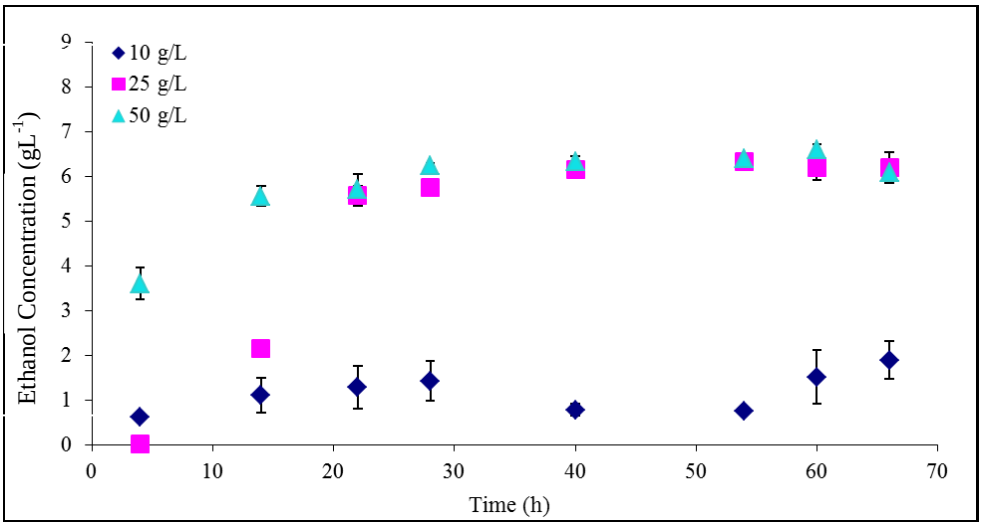

Figure 7.5: Profile of ethanol production by *S.cerevisiae* W303 immobilised on sulphonated PHP (D=45 μm). YPG media (with varying glucose concentration 10, 25 and 50 gL^{-1}) was supplied continuously to the reactor at 1 ml/min.

Ethanol synthesis supplemented with 50 gL^{-1} of glucose was the fastest in the first 20 hours of fermentation. The rate of ethanol production then gradually decreased and levelled with the production achieved in 25 gL^{-1} of culture at 40 hour of fermentation, giving an ethanol production of approximately between 6.18-6.22 gL^{-1}. Increasing the glucose concentration from 25 gL^{-1} to 50 gL^{-1} resulted in an insignificant increase of stable ethanol production by less than 2.0%, but boosted the biomass production significantly. It also caused a dramatic impairment to the ethanol theoretical yield (ethanol yield based on initial sugar - Table 7.2). The ethanol yield based on glucose consumed was also reduced from 0.46 (25 gL^{-1}) to 0.36 (50 gL^{-1}). This shows that although the glucose uptake increased in the 50 gL^{-1} chemostat, the amount of glucose converted to ethanol was greatly reduced. The increased glucose uptake was due to the increased metabolic consumption (high glycolytic capacity), which normally occurs in excess glucose. Although more glucose was consumed, it was converted to other metabolites such as acetaldehyde and pyruvate instead of ethanol. The tendency of

higher unutilised glucose appearing in the effluent was evident as shown in Figure 7.5. This was expected to be caused by a few factors, such as the availability of oxygen, or the maximum glycolytic capacity having reached saturation. Besides this, the short retention time of the reactor was expected to be the major reason. Because of this, the study on the effect of the initial glucose concentration was limited to 50 gL^{-1}, because any further increase was expected to give insignificant enhancement of the ethanol yield.

7.3.3 *Comparing Ethanol Productivity with Shake Culture (Free cell S.cerevisiae* W303*)*

The total ethanol produced within 72 hours of fermentation increased with increasing glucose concentration. The cumulative ethanol concentration obtained with 10 gL^{-1} culture was 79.5 gL^{-1}, and increased to 354.6 gL^{-1} in 25 gL^{-1} culture. The highest ethanol accumulation was obtained with 50 gL^{-1}, giving a total of 413.6 gL^{-1} of ethanol observed at the end of fermentation. The profile of ethanol productivity shows the increasing trends regardless of varying rates (Figure 7.6). The overall ethanol productivity increased proportionally with the glucose concentration. The lowest ethanol production was obtained at 10 gL^{-1}, of 1.10 $gL^{-1}h^{-1}$. The productivity increased almost 4.5 fold when the glucose supplement was increased from 10 gL^{-1} to 25 gL^{-1}, reaching 4.92 $gL^{-1}h^{-1}$ at the end of fermentation. The highest productivity (5.74 $gL^{-1}h^{-1}$) was observed at 50 gL^{-1}, which gave an increase of over 14 fold compared to the productivity observed in the batch process by free cell *S.cerevisiae* W303 (0.41 gL^{-1}).

It was estimated that the productivity will remain at the optimum value of 1.1 $gL^{-1}h^{-1}$ if the culture is continuously supplied with 10 gL^{-1} for an extended period. On the other hand, the productivity of the culture supplemented with 25 and 50 gL^{-1} will continue to increase, but the rate may be reduced as fermentation proceeds. Continuous increase is possible if the integrity of the microreactor remains stable and does not degrade (e.g. break, swell). Furthermore, if cell blockage or the super saturation of the

cell capacity in the microreactor can be avoided, it is expected that the ethanol production will stabilise and can be prolonged as long as dead cells and metabolites are removed efficiently from the system.

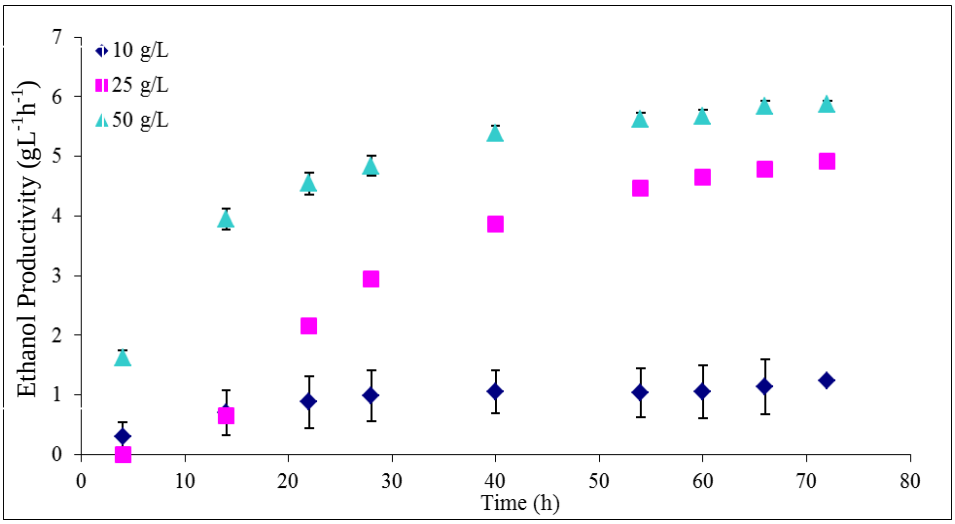

Figure 7.6: Profile of ethanol productivity of *S.cerevisiae* W303 immobilised on sulphonated PHP (D=45 μm). YPG media (with varying glucose concentration 10, 25 and 50 gL^{-1}) was supplied continuously to the reactor at 1 ml/min.

7.3.4 *Conclusions*

At low glucose supply (10 gL^{-1}), at least 98.7% of glucose coversion was achived after 20 hours of fermentation in a single pass of the microreactor. This showed that at this flowrate (1 ml/min), the yeast was able to convert approximately ~10 gL^{-1} of glucose within 3 minutes retention time and the wash out of cells in the microreactor achieved constant value (steady state growth) due to limited glucose supply. Increasing the sugar concentration in the feed medium to 25 gL^{-1}, influenced the glycolytic capacity of the immobilised cells, thus increasing the amount of fermentable sugar uptake. On the other hand, a further increase of sugar supplementation (50 gL^{-1}) caused a reduction in ethanol productivity although more glucose was consumed per pass.

7.4 Effect of Nitrogen Concentration (C/N ratio)

A nitrogen source is needed for the synthesis of new biomass, influencing the tolerance level of the yeast towards ethanol and the rate of ethanol synthesis (Dragone *et al*., 2007). In the presence of nitrogen, the yeast catabolised glucose and used the ethanol as an energy source and building materials for synthesising new cells. As the cultivation carried out in the previous section did not show any increased in ethanol yield, therefore it was speculated that the nitrogen concentration were in excess and drove the cells to undergo respiration instead of respiro-fermentation. As the mechanism is unexplainable at the molecular level, an effort was made to study the fermentation characteristic at much lower nitrogen concentrations. In this study, glucose was set at 25 gL^{-1}, while the yeast extract and peptone content were reduced to 2.5 gL^{-1} and 5 gL^{-1} respectively. Additional N-sources might be provided by the yeast cells that undergo lysis, where lots of amino acids and vitamins were released to the medium. So in this consensus, the nitrogen source in the medium can be kept low, as this will reduce the price for the medium preparation. The cost of the nitrogen sourced so far is very expensive and contributed to 40% of the fermentation medium cost.

The production of ethanol in the microreactor involved two stages. The first stage was the propagation of the yeast in the cavity, referred to as the growth stage. The second stage involved the conversion of glucose to ethanol, known as the respiro-fermentative process, which normally occurred stably when the cells in the effluent were more than ~ 10^7 - 10^8 cells/ml. In most reported case studies, the C/N ratio of the fermentation medium plays a vital role in the growth of yeast. While ethanol production is correlated proportionally to the production of biomass, sufficient nitrogen supply is crucial in order to maintain stable growth and ethanol productivity. Determining the right amount of nitrogen is important in order to avoid excess growth, which will truncate the route for ethanol production especially in an oxygen enriched condition. This not only demolished the objective, but also increased the production cost. The medium composition and the kinetic data on the effect of nitrogen requirements are listed in Table 7.3.

Table 7.3: Effect of C/N ratio on the biomass and ethanol production in the microreactor by *S.cerevisiae* W303 at 30^{o}C.

Medium	Glucose (G) (gL^{-1})	Yeast Extract (YE) (gL^{-1})	Peptone (P) (gL^{-1})	Glucose consume (%)	Biomass (gL^{-1})	Max. Ethanol (gL^{-1})
M 1	25	5	10	60.1	0.24	6.61
M 2	25	2.5	5	57.6	0.16	2.16
M 3	25	0.5	1	48.2	0.09	0.86
M 4	25	10	10	55.3	0.19	3.17
M 5	50	5	5	36.0	0.34	5.49
M 6	50	5	10	37.0	0.37	6.58

7.4.1 *The effect of Nitrogen Concentration (C/N) on the Glucose Utilisation (M1-M3)*

This study has proved that the nitrogen concentration in the medium is highly influential to the amount of sugar uptake by the immobilised cells. Referring to Table 7.3, at an approximately similar oxygen supply, the biomass content and the maximum ethanol achieved with the culture show a proportional decrease with decreasing supply of nitrogen sources. This condition had been related to the reducing glucose uptake by the cells in the nitrogen deprived environment. Final glucose consumptions were reduced with a reducing amount of nitrogen source. Maximum glucose consumption at 60.1% was observed in M1, which then reduced to 57.6 % and 48.2% in M2 and M3 respectively. This was equivalent to 9.9 (M1), 10.6 (M2) and 13.0 gL^{-1} (M3) of glucose remaining unreacted. A reduced glucose uptake by cells might result in reduced growth, subsequently reducing the ethanol production. A slow growth, due to low substrate uptake, results in very slow productivity, thus reducing the efficiency and the reactor stability.

The profile of the glucose consumption in the culture supplemented with M1, M2 and M3 is shown in Figure 7.7. The rate of consumption was reduced significantly

in M3, while only a slight reduction was observed in M2 in the first 28 hours. The profile for M3 was the least stable among the three media tested.

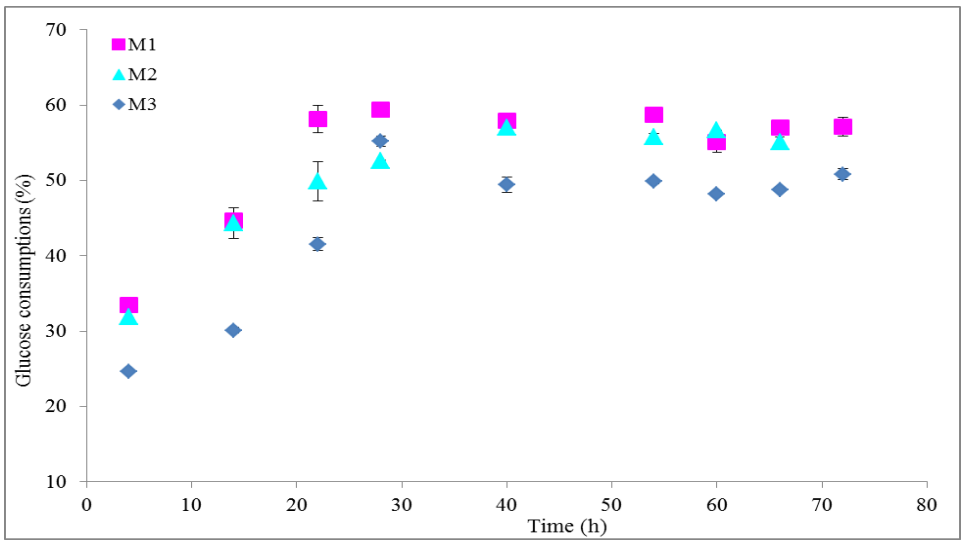

Figure 7.7: Profile of glucose consumption by *S.cerevisiae* W303 immobilised on sulphonated PHP (D=45 μm) supplied with M1, M2 and M3 continuously. (M1 consisted of 5 gL^{-1} YE, 10 gL^{-1} P, 25 gL^{-1} G; M2 consisted of - 2.5 gL^{-1} YE, 5 gL^{-1} P, 25 gL^{-1} G and M3 consisted of – 0.5 gL^{-1} YE, 1 gL^{-1} P, 25 gL^{-1} G).

7.4.2 *The effect of Nitrogen Concentration (C/N) on the Growth and Ethanol Production (M1-M3)*

Switching from a highly nutritional medium (M1) to a nitrogen deficient medium (M3) caused a sharp reduction not only to glucose consumption but also to biomass content, the number of cells released and the ethanol concentration. The biomass content dropped from 0.24 g in M1, to 0.16 g in M2, and finally to 0.09 g in M3 (Table 7.4). The number of cells released also decreased proportionally with the reduced nitrogen concentration. The maximum cell release was reduced from 5.2 x 10^7 CFU/ml to 5.0 x 10^6 CFU/ml when switching M1 with M3. It is worth noting that the biomass content in the N-limited culture (M1) was much lower than the biomass obtained in the C-limited culture (Section 7.3), suggesting that the low N triggers cessation of new cell production, while the limitation of C in the carbon limiting

medium was compensated by the additional carbon that may be present in the YE and peptone (apart from their role as N sources), therefore they are able to produce more biomass.

Table 7.4: Data comparison of varying nitrogen concentrations in continuous fermentation with 25 gL^{-1} glucose by *S.cerevisiae* W303 at 30°C.

Medium	M1	M2	M3
Maximum Ethanol concentration (gL^{-1})	6.61 ± 1.11	2.16 ± 0.47	0.86 ± 0.13
Steady Ethanol Production (gL^{-1})	6.19 ± 0.87	1.25 ± 0.37	0.67 ± 0.24
*Ethanol yield based on initial substrate (gg^{-1})	0.26	0.08	0.03
*Ethanol yield based on substrate consume (gg^{-1})	0.46	0.15	0.07
Biomass in PHP (g)	0.24 ± 0.01	0.16 ± 0.02	0.09 ± 0.01
Biomass density (g/g PHP)	0.93	0.627	0.421
Maximum Cell released (CFU/ml)	~5.2 x 10^7	~8.2 x 10^6	~5.0 x 10^6
% Glucose consumed	60.1	57.6	48.2
[a]Maximum Substrate used (g)	14.3	14.2	12.1
Total Ethanol (gL^{-1})	354.6 ± 4.8	78.1 ± 3.6	42.1 ± 2.7
Steady state Productivity ($gL^{-1}h^{-1}$)	4.92	1.08	0.58
Improvement over batch process (fold)	12.0	2.6	1.4

- Based on max ethanol production*
- Data was taken or derived based on the maximum ethanol concentration[a].

To study the effect of nitrogen content on growth and ethanol production, the glucose concentration was kept constant at 25 gL^{-1}, while the nitrogen supplement was reduced (by factor of 5 (M2) or 10 (M3) –Table 7.3). The reduction of the nutrient

supply not only had a negative influence on the growth rate and glucose utilisation, but also caused severe reduction in ethanol production. An adequate supply of nitrogen concentration (M1) with a maximum input of oxygen, results in the maximum glucose consumption, and produced the highest ethanol concentration at 6.61 gL^{-1} with a final biomass content being achieved of 0.24 g. When the culture was supplied with half of the nitrogen content in M1, a sharp decrease of ethanol production was observed. The ethanol in the M2 medium was reduced to 2.16 gL^{-1}, which was approximately 67.3% lower than the ethanol produced in M1. On the other hand, the biomass content was reduced to a lesser extent, being approximately 33.3% lower than in M1.

Further reduction of nitrogen, (considered as a nitrogen deficient medium - M3), while maintaining the same oxygen supply, dramatically impaired the ethanol production, with the optimum production occurring at only 0.86 gL^{-1}. The low production was an attribute of the minimal growth (0.09 g) that occurred in the microreactor due to nitrogen starvation. The profiles for ethanol productivity using 3 levels of nitrogen supply are shown in Figure 7.8. In contrast to M1, the ethanol productivity in M2 and M3 levelled off at approximately 22 hours of fermentation. The final ethanol productivity for M2 and M3 were obtained at 1.08 $gL^{-1}h^{-1}$ and 0.58 $gL^{-1}h^{-1}$, which was 4.6 and 8.5 times lower than that obtained in M1 (4.92 gL^{-1}.h).

The suppression of growth and ethanol production was explained on the basis of the reduced glucose uptake by the cells. A contrasting effect of the nitrogen deficiency was studied by Schulze *et al*. (1995) employing batch fermentation with a limited supply of $(NH_4)_2SO_4$ as the sole nitrogen source. Upon depletion of the nitrogen, the glucose utilisation proceeded until all the glucose was used up (50 gL^{-1}), which subsequently increased the level of extracellular ethanol and exhausted the CO_2 evolution. The effect of nitrogen deficiency was prominent when more carbon was channelled to the accumulation of more intracellular trehalose and glycogen instead of ethanol. It was expected that if the retention time in the microreactor could be prolonged, the fermentative capacity of the reactor might be able to provide a similar effect as observed by Schulze (higher ethanol production).

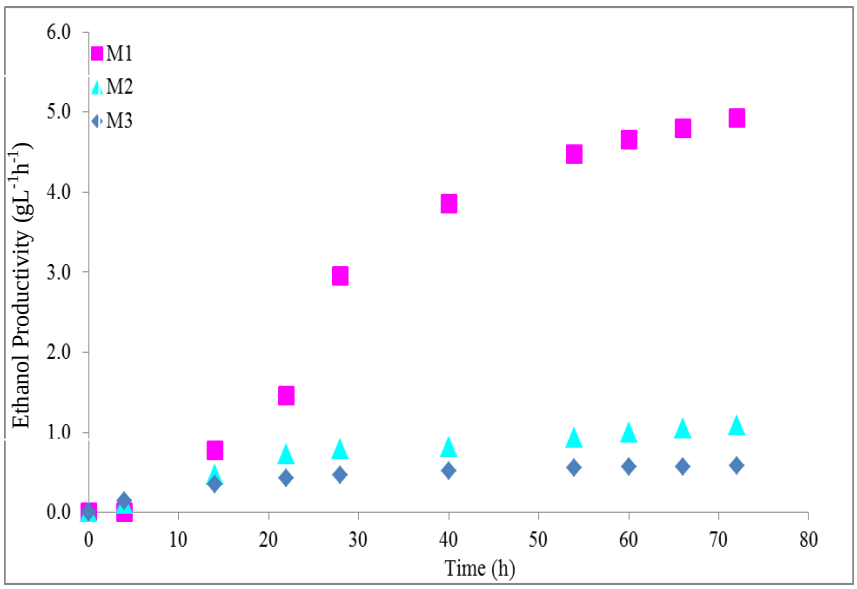

Figure 7.8: Profile of ethanol productivity by *S.cerevisiae* W303 immobilised on sulphonated PHP (D=45 µm) supplied with M1, M2 and M3 media continuously. (M1 consisted of 5 gL^{-1} YE, 10 gL^{-1} P, 25 gL^{-1} G; M2 consisted of - 2.5 gL^{-1} YE, 5 gL^{-1} P, 25 gL^{-1} G and M3 consisted of – 0.5 gL^{-1} YE, 1 gL^{-1} P, 25 gL^{-1} G).

The shift from a glucose limited to a nitrogen limited culture fermented by *S.cerevisiae* TMB3400, showed a reduction of biomass yield from $Y_{X/S}$ = 0.48 to $Y_{X/S}$ = 0.22, whilst increasing the synthesis of ethanol, acetic acid and glycerol in the culture medium (Souto-Maior *et al*., 2009). The substrate uptake rate was also increased in the limited nitrogen culture, which was typically followed by an overflow of metabolism as indicated by the glycerol accumulation. However, the glycerol production was not monitored in this study, therefore it was impossible to confirm that the reduction of growth and ethanol was attributable to the channelling of the glucose metabolism towards other products. This study only shows an agreement with Souto-Maior *et al*. (2009) on the reduced growth, but not on the enhancement of the ethanol production. The reason for this deviation is not clear so far. In contrast to previous authors, Larsson *et al*. (1993) and Brandberg *et al*. (2007) reported that no change was observed in terms of glycerol formation following the nitrogen starvation.

It is worth noting that the effect of either reducing the glucose (50 to 10 gL^{-1}- while the nitrogen content was held constant) or the overall nitrogen content (M1 to M3

while glucose maintained at 25 gL^{-1}) by 5 fold, provides a similar level of biomass reduction of approximately ~62.0% for both conditions. Nevertheless, biomass synthesis in the nitrogen limited culture (0.09 g) was significantly lower than that in the glucose limited culture (10 gL^{-1} – 0.14 g). The supply of nitrogen was known to be an important factor for biosynthesis. Continuous supply of limiting nitrogen sources was known to limit the cell growth/synthesis of new cells, changes in RNA content, or possibly increase the amount of glycerol production even though the mechanism for this reaction remains unclear (Brandberg *et al*., 2007). Complete starvation of nitrogen for a long period was lethal for cell growth, such that synthesis of new cells completely ceased, therefore reducing the fermentative capacity of the reactor. This finding suggests that a sufficient nitrogen supply was crucial to maintain a high cell density in the reactor.

7.4.3 *The effect of increasing Yeast and Peptone Concentration on the Biomass and Ethanol Production (M4-M6)*

Data for increasing the individual concentration of either the yeast extract or peptone was presented in Table 7.5. Increasing the amount of peptone from 5 gL^{-1} (M5) to 10 gL^{-1} (M6) while other components were held constant yielded an enhancement of both ethanol production and biomass content. On the other hand, increasing the individual yeast extract from 5 gL^{-1} (M1) to 10 gL^{-1} (M4) yielded contrasting results, where it reduced both the ethanol concentration and the biomass sharply. Although this was not expected, the decrease of these properties was approximately 52.0% and 20.8% lower than in M1, respectively. These subsequently reduced the overall ethanol productivity to 2.63 $gL^{-1}h^{-1}$, with only a 6.41 fold enhancement against the productivity obtained in the batch culture (SF), compared to a factor of 12 achieved in M1. Besides this, the glucose consumptions in M4 were also lower than the utilisation of M1, although the total overall amount of nitrogen was higher (Figure 7.9).

Table 7.5: Effect of increasing yeast and peptone concentration in the ethanol fermentation with initial glucose concentration of 25 gL^{-1} and 50 gL^{-1}.

Medium	M1	M4	M5	M6
Glucose (gL^{-1})	25	25	50	50
Initial yeast extract concentration (gL^{-1})	5	10	5	5
Initial peptone concentration (gL^{-1})	10	10	5	10
Maximum Ethanol concentration (gL^{-1})	6.61 ± 1.11	3.17 ± 0.36	5.49 ±	6.58 ± 0.18
Steady Ethanol Production (gL^{-1})	6.19 ± 0.87	3.05 ± 0.33	Na	6.31 ± 0.45
*Ethanol yield based on initial substrate concentration (g/g)	0.26	0.12	0.11	0.13
*Ethanol yield based on substrate consume (g/g)	0.46	0.23	0.30	0.36
Biomass in PHP (g)	0.24 ± 0.01	0.19 ± 0.01	0.34 ± 0.02	0.37 ± 0.03
Biomass density (g/g PHP)	0.93 ± 0.04	0.86 ± 0.04	1.21 ± 0.03	1.37 ± 0.05
Maximum Cell released (CFU/ml)	~5.2 x 10^7	~5.7 x 10^7	~7.3 x 10^8	~8.0 x 10^8
% Glucose consumed	60.1	~55.3	~36.2	~37.0
[a]Total Ethanol Produced (gL^{-1})	354.6 ± 4.8	189.9 ± 4.9	211.3 ± 5.6	413.6 ± 8.5
Overall Productivity ($gL^{-1}h^{-1}$)	4.92	2.63	2.93	5.74
Improvement over batch process (fold)	12.0	6.41	7.14	14.0
Maximum operation (h)	>72 hours	>72 hours	>72 hours	>72 hours

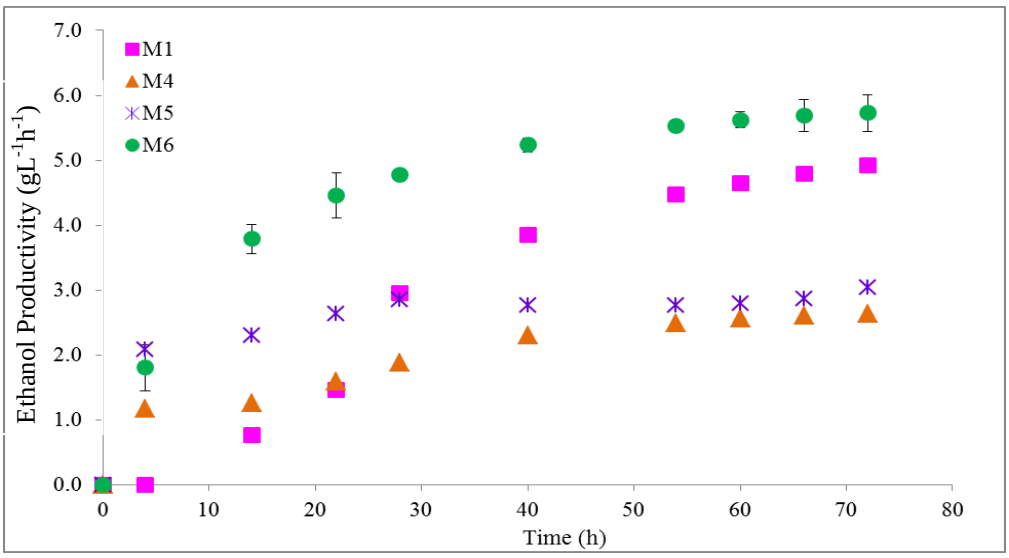

Figure 7.9: Profile of ethanol productivity by *S.cerevisiae* W303 immobilised on sulphonated PHP (D=45 μm) supplied with M1, M4, M5 and M6 media continuously. (M1 consisted of 5 gL^{-1} YE, 10 gL^{-1} P, 25 gL^{-1} G; M4 consisted of - 10 gL^{-1} YE, 10 gL^{-1} P, 25 gL^{-1} G; M5 consisted of – 5 gL^{-1} YE, 5 gL^{-1} P, 50 gL^{-1} G and M6 consisted of – 5 gL^{-1} YE, 10 gL^{-1} P, 50 gL^{-1} G)

On the other hand, increasing the peptone concentration in M6 (while the amount of yeast extract remained constant), yielded a sharp increase of ethanol concentration, and glucose and ethanol productivity compared to the production in the medium supplemented with reduced peptone (M5). An enhancement of approximately 16.6%, 8.8% and 51.0% over the production in M5 was achieved for these kinetics, respectively. Wang *et al*. (2007) reported that supplementing a combination of 15 gL^{-1} of peptone and 50 mM Mg^{2+} yielded more cells, contributing to a 20% enhancement of ethanol concentration. In high gravity fermentation, these components were considered to be the most significant factors contributing to the enhancement of the ethanol yield above other factors such as yeast extract, glycine, acetaldehyde and biotin (Wang *et al*., 2007).

Figure 7.10 depicts the profile of ethanol production in various media (M1-M6). Overall, the production in M1, M4 and M6 managed to obtain the steady state condition where the production rate levelled or was nearly constant towards the end of fermentation. On the other hand, ethanol production in M2 and M3 showed a

fluctuating profile. Sluggish production of ethanol was associated with reduced cell growth in the reactor due to an insufficient amount of nitrogen (Breisha, 2010). Meanwhile, production in M5 failed to reach steady state despite the higher nitrogen supplement than in M2 and M3. It was observed that the quantity of peptone in these media was less than 10 gL^{-1} therefore it might have affected the stability of ethanol secretion. Cultures supplemented with 10 gL^{-1} peptone (M1, M4 and M6), regardless of the amount of carbon source, showed stability, with considerably steady production achieved at the end of fermentation.

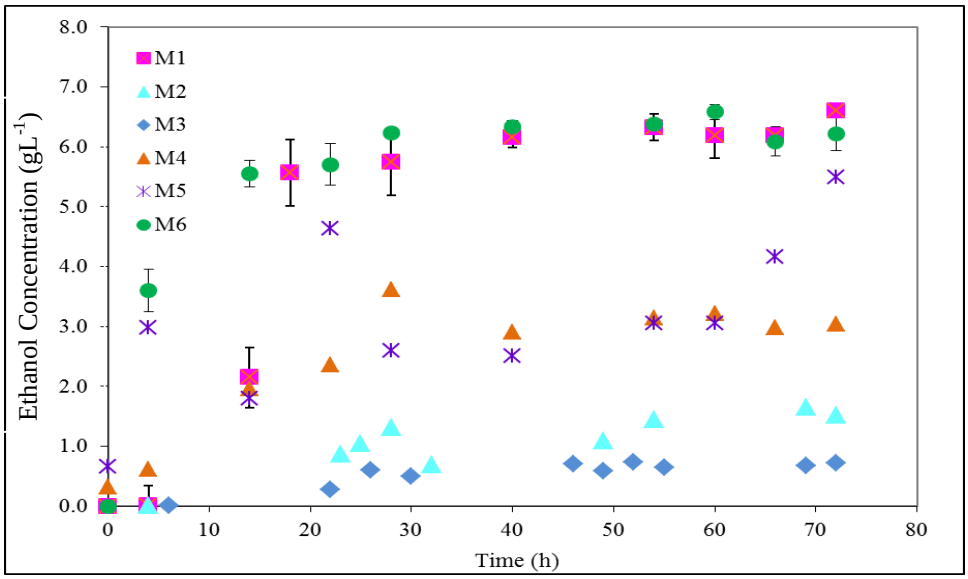

Figure 7.10: Profile of ethanol concentration by *S.cerevisiae* W303 immobilised on sulphonated PHP (D=45 μm) supplied with six different mediums in continuous operation. M1 (Normal medium) M2 (Medium supplied with moderate nitrogen content), M3 (Nitrogen deprived medium) M4 (Medium with excess peptone) M5 (Medium with excess glucose) and M6 (Medium with excess glucose and peptone).

Nitrogen deficiency has also been reported to influence the growth and cell morphology of *S.cerevisiae* grown on solid media (agar plates). Kuriyama and Slaughter (1995) reported that a nitrogen deficient environment decreased the sugar consumption and the growth rate, while the separation of daughter cells from the parent cells was markedly poor. This condition caused formation of branched psuedohyphal growth instead of the normal ovalish shape, which can be observed when grown on the

highly nutritional medium agar or in submerged fermentation. It was further suggested that the morphological changes (generally associated with the metabolic stress due to the nutrient imbalance) of the cells may be used to identify the types of stressors that may contribute to reduced growth/ethanol production.

7.4.4 *Conclusion*

In conclusion, glucose consumption, ethanol production and biomass content in the microreactor declined proportionally with the reduction of total nitrogen supplied to the reactor. This study also revealed that the peptone concentration had more influence than the yeast extract in determining the ethanol production stability. The optimum nutrient feeding, with respect to the ethanol concentration and productivity, for glucose in the range of 25-50 gL^{-1} was found to be 10 gL^{-1} of peptone and 5 gL^{-1} of yeast extract although the reason is unclear. Reduction of any of these nitrogen sources clearly limited the cell growth, which subsequently reduced the reactor capability for utilising glucose, thus reducing the ethanol production.

7.5 The effect of Aerobic and Microaerobic Conditions on the Growth and Ethanol Production

S.cerevisiae is classified into 3 groups based on the dependency on oxygen requirements: a) obligate aerobes (displaying exclusive respiratory metabolism); b) facultative fermentative (displaying both respiratory and fermentative metabolism) and c) obligate fermentative (strictly fermentation) (Merico *et al*., 2007). Ethanol is a product that was released to the liquid medium from sole glucose utilisation by *S.cerevisiae* in the presence of oxygen. However this phenomenon is different when *S.cerevisiae* is cultured in the continuous system/chemostat, in which the direction of metabolism is also controlled by the dilution rates and the availability of carbon sources (glucose). In some critical chemostat operations (e.g. operating at dilution rates far below μ_{max}), a strictly oxidative metabolism dominates, which means no ethanol is produced as a by-product (Rieger *et al*., 1983). Oxygen, however, may be controlled in order to shift the respiration process towards fermentation in both batch or continuous process. Kinetic data of the continuous fermentation in aerobic and anaerobic condition is presented in Table 7.6. The results revealed that *S.cerevisiae* W303 can grow aerobically as well as microaerobically.

7.5.1 *Effect on Glucose Utilisation*

Attempts at reducing the oxygen supply to the culture, with the aim of controlling the growth of the yeast and inducing fermentation, have been successful and have produced contrasting results (compared to the nitrogen limitation medium) in terms of ethanol production/productivity. Glucose utilisation was boosted by 16.0% in the microaerobic condition, cosuming nearly 66.4% of the supplied glucose. Despite the increase, the glucose utilisation profile in microaerobic conditions, shown in Figure 7.11, was less stable compared to the utilisation in aerobic conditions, probably triggered by the imbalance of redox potential in the immobilised yeast metabolism due to low oxygen concentration.

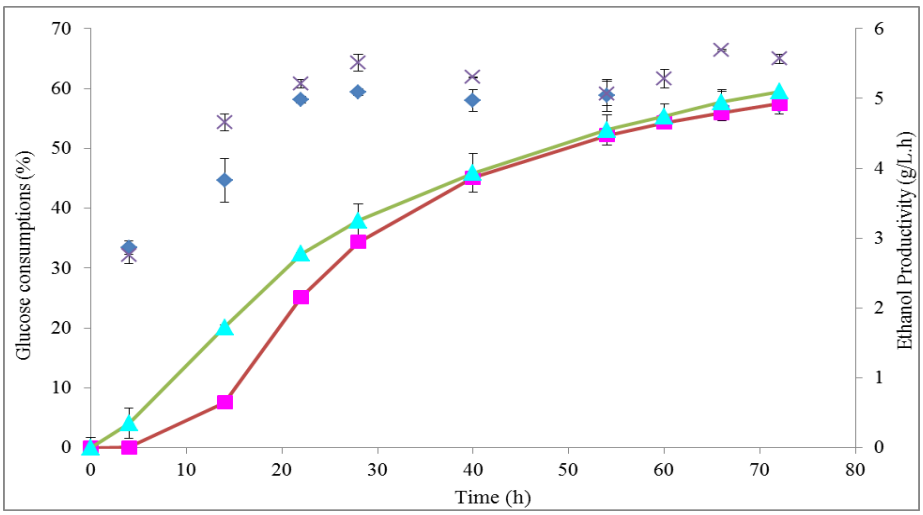

Figure 7.11: Profile of glucose consumption and ethanol productivity by *S.cerevisiae* W303 immobilised on sulphonated PHP (D=45 μm) in continuous fermentation (aerobic and microaerobic conditions). ♦ Glucose (aerobic) x Glucose (microaerobic) ■ Ethanol productivity (aerobic) ▲ Ethanol productivity (microaerobic).

Table 7.6: Data comparison of aerobic and microaerobic fermentation

Condition	Aerobic	Microaerobic
Maximum Ethanol concentration (gL^{-1})	6.61 ± 0.48	7.36 ± 0.27
Stable Ethanol Production (gL^{-1})	6.19 ± 0.18	6.25 ± 0.10
Ethanol yield based on initial glucose (gg^{-1})*	0.26	0.30
Percentage of theoretical yield (%)	50.9	57.7
Ethanol yield per glucose consumed (gg^{-1})*	0.46	0.44
Biomass in PHP (g)	0.24 ± 0.01	0.30 ± 0.01
Biomass density (gg^{-1} PHP)	0.93 ± 0.04	0.80 ± 0.05
Biomass yield based on glucose consumed (gg^{-1})	0.017	0.018
Maximum Number of Cell released (CFU/ml)	~5.2 x 10^7	~3.7 x 10^7
Maximum glucose consumption (%)	~ 60.1	~66.4
[a]Substrate used (g)	14.3	16.6
Overall Ethanol	354.6 ± 4.8	367.2 ± 12.7
Productivity ($gL^{-1}h^{-1}$)	4.92	5.10
Increments (folds) over P_{batch}	12.0	12.4
Operation period (time)	>72 hours	>72 hours

7.5.2 *Effect on Biomass and Ethanol Production*

The ethanol concentration increased from 6.61 gL^{-1} to 7.36 gL^{-1} when fermentation was switched to microaerobic condition, showing that the respiration process had been limited (Figure 7.11). Increases of 11.3 % and 3.7% were observed with respect to the ethanol production and the productivity, respectively. Furthermore, in line with the oxygen limited condition, the biomass production was reduced from 0.93 g/g support to 0.80 g/g support, which was lowered by 7.0% compared to the aerobic condition. Although the biomass content (0.30 g) was higher in the microaerobic process, the number of cells released was also reduced from 5.2 x 10^7 in aerobiosis to 3.7 x 10^7 CFU/ml in the microaerobic conditions. This may suggest that slower growth was occurring in the oxygen-deprived environment in comparison to the aerobic culture, but the increase in biomass weigh might be attributable to the increase in carbohydrate storage. The possibility of lowered growth in the microaerobic condition might be contributed by the inability of the fermentative route to provide enough energy for the synthesis of new cells, when respiration was hindered in the absence of oxygen (Merico *et al*., 2007).

Referring to Figure 7.11, the ethanol production in the microaerobic culture surpasses the production in the aerobic culture at 40 hours of fermentation, entering the pseudo state condition, although the production slightly fluctuated at the end of fermentation. In a study by Wiebe *et al*. (2008), *S.cerevisiae* CEN.PK113-1A required 36 hours to enter steady state after switching to anaerobic (0%) from aerobic (20.8%) conditions, although the cell's response towards oxygen truncation was rapid. A longer time (28-35 hours) was needed to regulate cellular metabolism before it could fully adapt to anaerobiosis.

The yield of biomass based on the sugar consumed was higher in the microerobic culture than in the aerobic condition, although the number of cells released showed the opposite (refer to Table 7.6 and Figure 7.12). When *S.cerevisiae* W303 was

grown in a stressed condition (e.g. an oxygen deprived media), the increased glucose consumption might be channelled for the production of carbohydrate storage (e.g. glycerol, trehalose etc.) to maintain its redox balance. Without oxygen, not only the growth or synthesis of new cells was repressed, but the separation of the daughter from the parental cell was also affected. The accumulation of stored carbohydrate increased the weight of the individual cells, which might explain why the results showed an increasing biomass content (0.30 g), but reduced the number of viable cells in microaerobic fermentation in comparison to the aerobic condition. It is worth noting that, although a nitrogen deprived environment (in the presence of oxygen) was reported to trigger glycerol formation as in the oxygen-deprived condition, the condition where the biomass content was higher while the number of cells released was decreased, was not observed in the nitrogen-limiting condition. Contrastingly, both properties (the biomass content and the number of cells released) were reduced proportionally with a reduction in nitrogen content, therefore it was difficult to estimate whether glycerol was produced in line with the reduced nitrogen content. Brandberg *et al*. (2007) mentioned that when there was a sufficient amount of oxygen available, it eliminated the glycerol formation even in the nitrogen starvation condition.

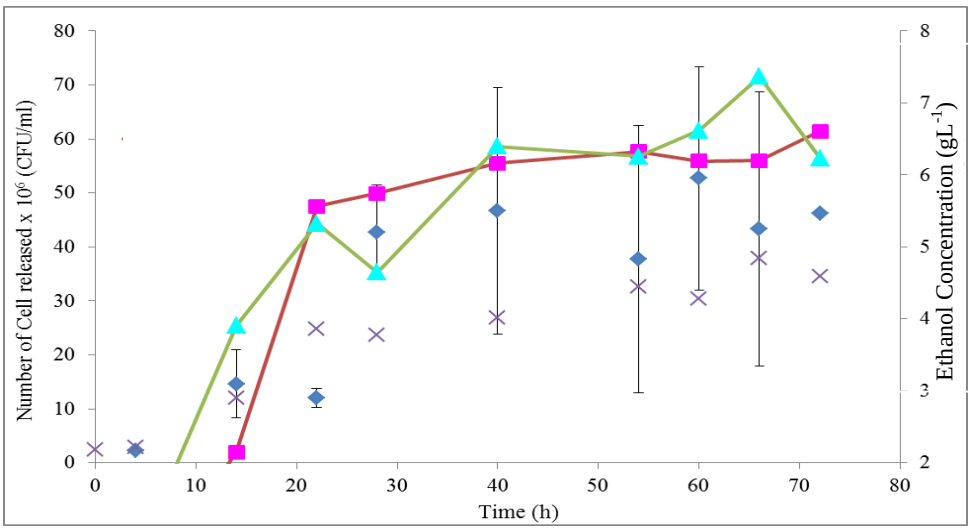

Figure 7.12: Profile of cell released and ethanol production of *S.cerevisiae* W303 immobilised on sulphonated PHP (D=45 μm) and grown in aerobic and microaerobic conditions. ■ Ethanol production (aerobic) ▲ Ethanol production (microaerobic) ♦ number of cell released (aerobic) **x** number of cell released (microaerobic).

This study was in agreement with Schulze *et al*. (1995) who reported an increase in both ethanol secretion and carbohydrate content (trehalose and glycogen) when *S.cerevisiae* CBS 8066 was grown in anaerobic batch cultivation. In contrast, Alfenore *et al*., (2004) stated that *S.cerevisiae* showed a higher preference for the glycerol production instead of ethanol synthesis when the condition was shifted from the fully aerobic to the microaerobic condition (limited oxygen) in the fed batch reactor. They obtained an increase of 4 fold in glycerol-biomass yield over the yield in the aerobic culture, which was attributed to the excess NADH to be oxidised. Wiebe *et al*. (2008), on the other hand, detected the glycerol production in fully anaerobic conditions, and a minimal supply of oxygen at 0.5% was enough to eliminate its synthesis. Glycerol was formed for the purpose of re-oxidising surplus NADH, a product from the anabolism process, and can use up to 10% (w/w) of the carbon supplied (Brandberg *et al*., 2007). Besides glycerol, other metabolites products from the tricarboxylic acid cycle (TCA), such as citrate, succinate, fumarate and malate, were marginally higher in the anaerobic culture than in the aerobic culture, but there was no clear explanation to describe the finding (Wiebe *et al*., 2008).

7.5.3 Conclusions

Attempt to control growth by eliminating the supply of oxygen shows considerable success, where the growth (indicated by the number of cells released) was relatively lower in the microaerobic process than in the aerobic process. Both glucose utilisation and ethanol production were increased in the microaerobic process. There was also a small possibility that a substantial amount of the supplied glucose was channelled into glycerol production when oxygen was minimum, thus limiting the enhancement of ethanol production. Therefore a minimal amount of oxygen without initiating the respiration pathway might be compulsory to maintain the redox balance in the viable cells thus eliminating the need to produce glycerol. This in turn, might enhance the amount of glucose being degraded to ethanol through the glycolysis cycle.

7.6 Overall Discussions and Conclusions

The effect of oxygen limitation showed a profound effect on the improvement of glucose utilisation over the microerobic process, while nitrogen limitation gave the opposite effect. Nitrogen limitation was more profound in reducing the growth in the reactor, where production of biomass was greatly impaired. Excess oxygen, on the other hand supported the enhancement of biomass production (g cell/g support) through respiration, and was also a better controller to prevent the production of unnecessary by-products. Although reducing the supply of oxygen increased the ethanol production, the stability of the reactor was reduced significantly. Overall, study from this chapter might provide the early conclusion that the occurrence of ethanol production observed in the microreactor may either result from the oxygen limitation in the reactor, or may be because the system was operated at dilution rates higher than the specific growth rate (μ_{max}) of *S.cerevisiae* W303. Even at $D_R = 7\ h^{-1}$, it surpassed the specific growth rate ($\mu = 0.152\ h^{-1}$) of the free cell by 46 times, therefore a considerable amount of ethanol and biomass accumulation was observed although the ethanol production failed to achieve steady state conditions. Failure to reach steady state was possibly attributable to the ethanol utilisation due to low glucose supplied that was insufficient for the maintenance of the reactor. However, this can only be confirmed by supplying the reactor with a mixture of glucose and ethanol.

Results from reducing the nitrogen supply caused severe reduction in the ethanol production which was associated to lower growth (low biomass and number of cells released). This finding supported earlier research which suggested that the fermentative capacity of the yeast is dependent on the specific growth rate of the organism (Brandberg *et al*., 2007). Yeast extract and peptone were reported to be responsible for promoting the enhancement of the ethanol production, increasing the stability of fermentation, thus providing a protective effect over growth, cell viability and fermentative capacity especially in the high gravity fermentation (Laopaiboon *et al*., 2009; Breisha, 2010).

Although it been mentioned in the literature that in general, ethanol was produced when oxygen was depleted, this study has shown that *S.cerevisiae* W303 have the ability to produce ethanol in the presence of oxygen (Merico *et al*., 2007; Rieger *et al*., 1983). Operating at various dilution rates above the specific growth rate of the organism induced the ethanol production. Meanwhile, this organism also able to grow in microaerobic condition and generated new cells at a much slower speed than in the aerobic process, where substantial increased in the ethanol production was also observed in the oxygen deficient environment. Stability in this microaerobic process was achieved presumably through the production of glycerol for the continuation of metabolic activities, and had been discussed in detail by Merico *et al*. (2007). The ability to grow in anaerobic or microaerobic conditions was strictly dependent on the nutritional condition of the medium, while many strains of *Saccharomyces* spp. are capable of generating respiratory-deficient mitochondrial mutants, called petites.

Despite numerous studies having been carried out to determine the effect of these variables (e.g. glucose and nitrogen) on the reactor's feasibility, the results are variable. No clear cut evidence can be derived on the effect of oxygen and nitrogen on the effectiveness of the glucose consumption that leads to higher growth and ethanol secretion, or vice versa.

CHAPTER 8: ETHANOL PRODUCTION USING A TWO STAGE MICROREACTOR IN SERIES AND PROCESS INTENSIFICATION

8.1 Two Stage Microreactor

The best feature of the monolithic microreactor is the possibility of working at dilution rates higher than the u_{max} without a reduction of cell concentration or instability in the ethanol production. This monolithic microreactor is best operated at the highest dilution rate possible, (provided sufficient retention time for carbon utilisation is given) since it provides extra shear for the cells growing on the surfaces, thus enhances the cell migration rate. On the other hand, although operating at low dilution rates increased the consumption efficiency of the initial sugar concentration, it did not provide enough strength to break the cell and the stability of the reactor dropped rapidly between 54-60 hours.

The effect of the polyHIPE's properties and the three limiting nutrients - carbon, nitrogen and oxygen concentration - were predetermined and discussed in detail in the previous chapter. The use of oxygen was crucial in maintaining the viability of the living cells and maintaining a stable ethanol production. The maximum conversion at various operating conditions with different concentrations of essential nutrients in the single reactor (sulphonated polyHIPE) managed to convert and use between 30-60% of the glucose supplied per pass and produced ethanol with varying yields. Therefore, a two-stages microreactor in series was introduced in order to increase the reaction time, so that more glucose can be converted, and subsequently increase the ethanol production. The fermentation kinetic data is presented in Table 8.1.

Table 8.1: Comparison of Fermentation kinetic data in single and two-stages microreactor in aerobic and microaerobic conditions

Fermentation	**Single Stage**		**Two-Stages microreactor**	
Condition	Aerobic	Microaerobic	Aerobic	Microaerobic
Maximum ethanol concentration (gL^{-1})	6.61 $\pm$ 0.48	7.36 $\pm$ 0.27	5.97 $\pm$ 0.34	6.81 $\pm$ 0.10
Ethanol yield, $Y_{P/S}$	0.26	0.30	0.24	0.27
Ethanol yield based on glucose consumed	0.46	0.44	0.33	0.35
Overall ethanol productivity, ($gL^{-1}h^{-1}$)	4.92	5.10	4.88	4.90
Maximum Glucose consumption per pass (%)	60.1	66.4	72.2	78.4
Biomass (g)	0.24	0.30	i) 0.24 ii) 0.15	i) 0.22 ii) 0.12
Biomass yield per glucose consumed, $Y_{X/S}$	0.017	0.018	0.021	0.017
Biomass density (gg^{-1})	0.93 $\pm$ 0.04	0.80 $\pm$ 0.05	-	-
Maximum no of cell released (CFU/ml)	~5.2 x 10^7	~3.7 x 10^7	~54.7 x 10^7	~49.5 x 10^7
Fold increase over P_{batch}	12.0	12.4	11.9	12.0

While the single reactor (in both aerobic and microaerobic conditions) could not consumed more than 70.0% of the glucose in the complex media, the glucose utilisation was enhanced by 20.1% in the two-stage-aerobic reactor (72.2%) compared to the single stage-aerobic reactor. On the other hand, the glucose utilisation in the microaerobic-two-stage reactor (78.4%) was the highest among the four (Table 8.1). The increased glucose uptake was due to additional requirement for carbon sources needed for the yeast in the second reactor (Figure 8.1).

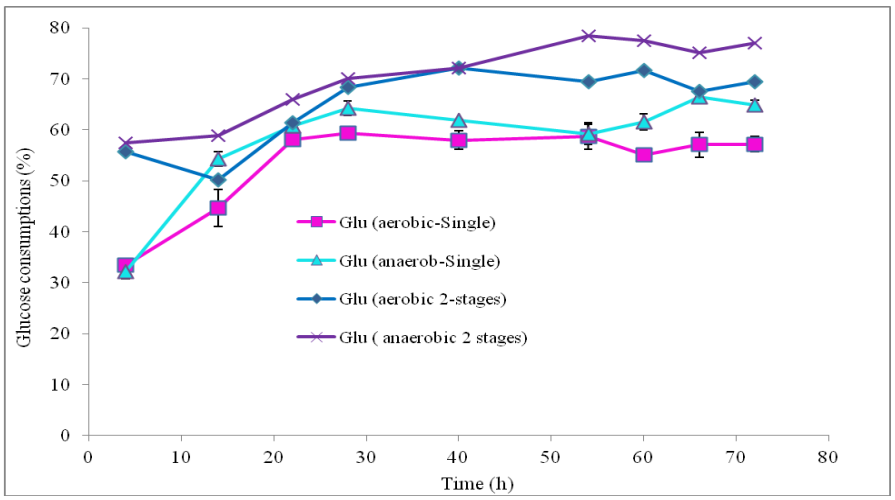

Figure 8.1:: Glucose consumption by *S.cerevisiae* W303 immobilised on sulphonated PHP (D=45 μm) and grown in aerobic and microaerobic conditions (in single stage and two-stages microreactor). The temperature of the reactor were maintained at 30^{o}C and supplied continuously with YPG media. (Error bar not shown for data clarity).

Overall, the ethanol concentration in the two-stage reactor was relatively lower in comparison to a similar single stage reactor in both the aerobic and microaerobic conditions (Figure 8.2). Although the number of cells released was higher in the two-stage system, the ethanol production was reduced by 9.7 % and 7.5% in aerobic and microaerobic conditions, respectively. This was not expected, however the evolution of CO_2 from the second reactor might have affected the immobilised yeast in reactor 1, thus reducing the fermentation capacity of these cells. The effect of CO_2 on the yeast and its fermentation performance has been described in detail in Section 2.6.4.

The severe oxygen limitation inhibits some of the key metabolism in the yeast and altered the stability. On the other hand, the ethanol productivity in both reactor systems, either in the presence or reduced oxygen concentration, also varied considerably. The productivities in both aerobic and microaerobic conditions remained in the range of 4.88 - 5.10 $gL^{-1}h^{-1}$. But it is worth noting that the ethanol productivity in the 2-stage reactor was lower than in the single stage reactor, although the glucose consumption was higher, probably due to the enhancement of carbon utilisation for cell respiration or carbohydrate storage.

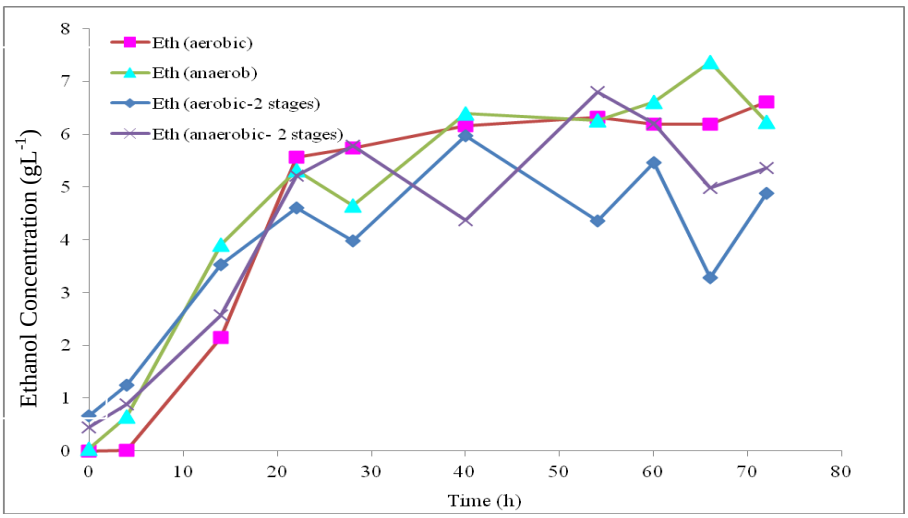

Figure 8.2: : Ethanol concentration profile of *S.cerevisiae* W303 immobilised on sulphonated PHP (D=45 μm) and grown in aerobic and microaerobic conditions (in single stage and two-stages microreactor). The temperature of the reactor were maintained at 30^{o}C and supplied continuously with YPG media. (Error bar not shown for data clarity).

8.2 Growth in the Microreactor

This section is designed to discuss the overall findings of the microreactor condition throughout the study. Figure 8.3 shows the environment in which the *S.cerevisiae* was grown in the S-NH_4OH PHP for 72 hours. The operation of the microreactor was susceptible to the contaminations that might occur during sampling or leakage at the connection of the reactors parts. Contamination by bacteria generally resulted in a reduced ethanol production due to the production of lactic acid by the *Lactobacillus* sp. that affected the optimum condition for ethanol synthesis, or simply due to the nutrient competition between yeast and these contaminants (Bayrock and Ingledew, 2004). In the present study, contamination was observed with rod and coccus shape microorganism and no thorough identification had been done (Figure 8.4 b-d). However, it is expected that the contamination lowers the yield and triggers tribulations to the reactor efficiency and ethanol production (data not shown). The lysis of aged cells also occurred in the microreactor as shown in Figure 8.4(a). The content of the cells was washed out by hydro forces but some remained attached to the polyHIPE walls.

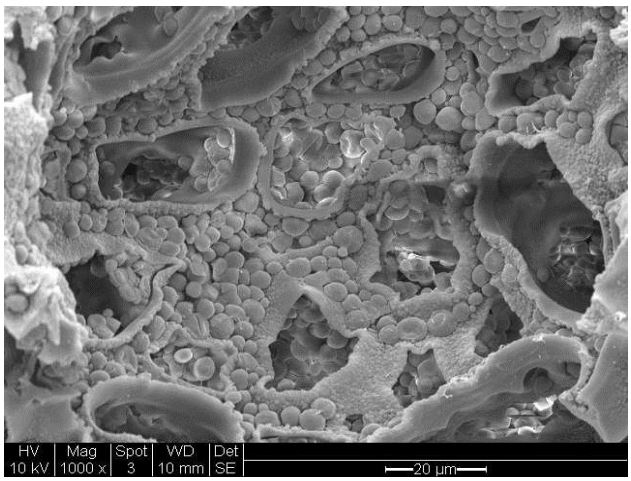

Figure 8.3 SEM image at 1000x magnification show a healthy condition with no sign of contamination

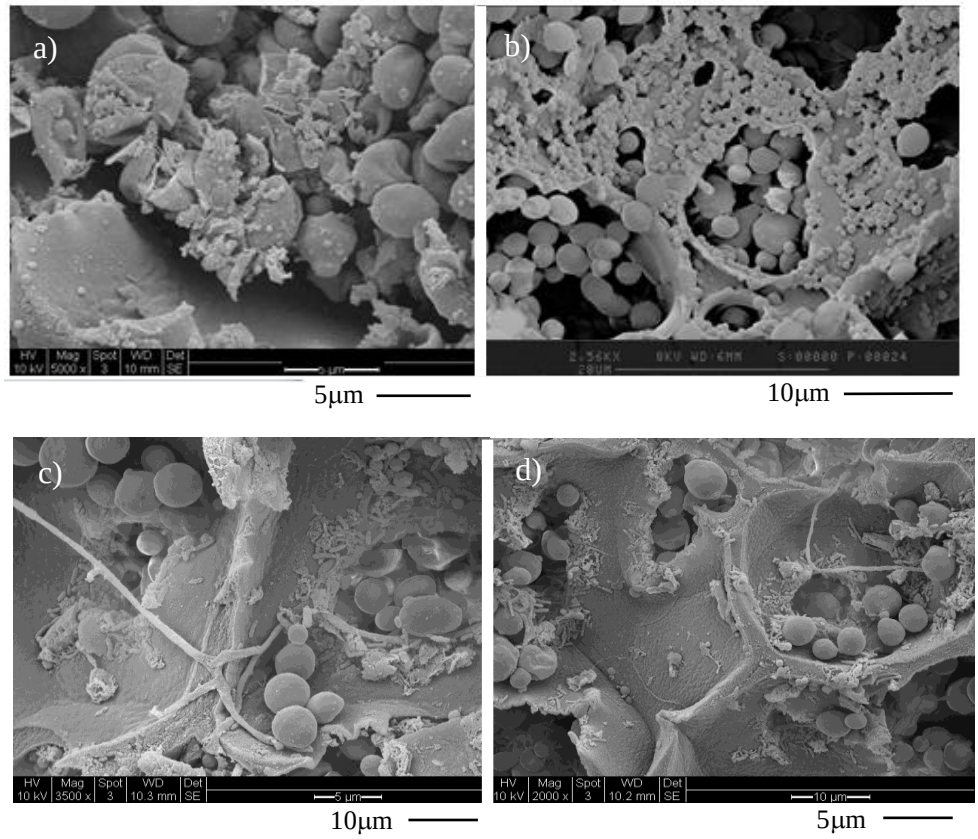

Figure 8.4: a) Cell lysis in the microreactor. b) Contamination caused by coccus shape bacteria. c) and d) SEM images showing contamination by unknown species (rod shape bacteria) detected in the microreactor.

Contamination of the medium is one of the common problems in the continuous operation. It often caused by either leakage at the connections/opening, or migration of live cultures (chemotaxis) into the medium especially when low medium flowrate is applied. In this study, contamination by chemotaxis was kept to minimum since the medium flowrate was high enough to hinder the cell migration. In some reported microreactor system, the flowrate of medium was very low (μL/min) and the contamination was prevented by reducing the diameter of the microchannel inlet and increasing the temperature of the feed line (Zhang *et al*., 2006). In this study, chemotaxis was effectively prevented due to the setting of the flowrate at 1 ml/ml, which were far greater than the average migration rate of *S.cerevisiae* in linear condition.

8.3 System Stability

Both reactor configurations were operated up to 72 hours of fermentation although oscillations in both aerobic and anaerobic ethanol production were not expected. Efficient cell removal was expected to be an important factor in promoting reactor stability. However, the two stage reactor was less stable than the single stage reactor due to:

i) An unsmooth and truncated flow of medium from the first reactor to the second reactor might contribute to a reduced ethanol productivity rate.
ii) A reduced flowrate of the medium from the reactor 1 outlet promoted excessive surface growth on the second reactor and caused occasional breakdown of the reactor system.
iii) The evolution of CO_2 in the second reactor might have affected the fermentation performances of reactor 1.

The operation of anaerobic reactor for both single and two stages systems showed instability over aerobic reactors. Eliminating the supply of oxygen in the

systems causes sluggish operation especially in the ethanol productivity curve (Figure 8.2). However, this process can be further improved by introducing the periodic operation at which a supply of growth nutrient (e.g: oxygen) is changed after recurring time interval (Silveston *et al*., 2008). The changes refer to periodic supply between medium and oxygen to the reactor or; medium supply occurs continuously but intermittent supply of oxygen. This state of operation is called the stimulation stage.

The steady state condition in the single stage reactor was maintained for at least up to 40 hours, while in the two-stage system this was not achievable. The ultimate sinusoidal graph of the ethanol concentration provided with an insight that this system was less stable compared to single stage microreactor.

CHAPTER 9 CONCLUSIONS AND RECOMMENDATIONS

9.1 Conclusion

Although the preparation of high internal phase emulsions (HIPEs) requires the use of toxic chemicals (e.g. divinylbenzene and concentrated sulphuric acid), the polymerisation of the emulsion produces a material that is non-toxic and highly stable to temperature and chemicals. In the microreactor applications, polyHIPEs, provide a large surface area for cell adherence, while the interconnects of suitable diameter provide passage not only for the medium and oxygen, but also the removal of dead cells from the microreactor disc to prevent blockage/overpopulation that would increase the resistance to mass transfer. Since old cells and unbound cells are constantly removed and replaced with newly-produced cells, this helps to create a fresh environment for optimum cell activity.

In the present study, *S.cerevisiae* W303 was immobilised in the polyHIPE disc (D = 28 mm; h = 5 mm), and placed in a PTFE block, while a medium containing carbon and nitrogen sources was supplied continuously at varying flowrates. PolyHIPEs with different surface chemistry were tested. Both hydrophilic and hydrophobic surfaces had managed to retain the yeast within its scaffold, subsequently producing ethanol at varying rates. Although the actual direct interactions that influence the attachment of *S.cerevisiae* were still largely unknown, the effect of hydrophilicity was profound in facilitating migration and cell growth. Other factors dominating the adherence and physiological state of the yeast were influenced by the chemical composition of the surface, the dynamic environment and the age of the yeast cells.

Parameters such as flowrate and interconnect sizes played a very important role in facilitating cell migration into the polyHIPE scaffold. Yeast cells on the surface multiplied rapidly due to the availability of a highly nutritional medium and oxygen,

tending to create micro-colonies with high binding strength which often act like a huge single cell. To a certain extent, these colonies blocked the interconnects, while the pores acted as a sink preventing the newly-produced cells from moving further deeper into/out of the system. This, if prolonged for certain periods, will block the whole system, and cause a reactor malfunction. Both high dilution rates and large interconnects increased the rate of cell migration, on the other hand, reduced the productivity of ethanol. Excessive surface growth, however, was the most important factor to consider because failure to control this altered the reactor's stability. This study has proven that small interconnect sizes and low dilution rates of the medium result in excessive growth on the top surface of the microreactor where the operation had to be terminated earlier due to cell blockage.

The efficiency of the reactor might vary depending on the location of cells within the polyHIPEs. Cells exhibiting monolayer growth might be the most efficient point at which the internal mass transfer can be kept to a minimum. At the bottom of the reactor, where cell flocculation was dominating, the efficiency of the reactor might be impaired slightly due to the increased mass transfer resistance. Nevertheless, flocculation does not necessarily mean that the productivity was reduced, because flocculation helps to increase cell density and stability thus subsequently increasing the fermentation rate. Although the mass transfer was reduced in the flocculation area, the availability of highly dense cells might increase the catalytic conversion and result in more ethanol production, thus outweighing the mass transfer problems. Although cell flocculation was found to be useful for the separation process later on, a sluggish ethanol production was generally associated with cell flocculation especially when it occurred at the early stage of fermentation (Verbelen *et al*., 2006). On the other hand, heterogeneous growth in the microreactor was expected to be beneficial for the production of ethanol. In locations where extra high cell density was present, the regions may result in a very low oxygen availability, which may initiate the glucose conversion through the fermentation pathway, subsequently producing ethanol.

Another attempt to increase the ethanol production was carried out by means of controlling the unnecessary growth of *S.cerevisiae* W303, with the intention of channelling the supplied glucose for the fermentation route instead of respiration. This was done by reducing the amount of supplied nitrogen (yeast extract and peptone) while the glucose concentration was held constant. This strategy was unsuccessful due to a significant reduction of growth that lowered the ethanol production. Therefore, another control strategy was employed, this time by supplying the culture with an oxygen limited medium, but was of limited success because of a process stability issue in long term operation. Although the anaerobic condition produced a higher ethanol production than the aerobic culture, the profile for the ethanol production, the number of cells released and the glucose profile were sluggish. This may suggested that the stability of the anaerobic culture was relatively impaired in comparison to the aerobic culture.

Since the single microreactor could not take up more than 70.0% of the supplied glucose, an attempt was made to increase the glucose conversion by introducing the multistage reactors in series. Although the conversion of glucose was enhanced by 20.0% in the second reactors (in both the aerobic and the anaerobic condition), this two-series system was less stable than the single-reactor system. This was associated with the reduced flowrates of medium outflow from reactor one, which impaired the rate of migration in the second reactor, and caused excessive growth on the surface.

Overall, the main aim of immobilising *S.cerevisae* W303 on polyHIPEs and utilising the microreactor for continuous ethanol production was successful. Although the microreactor operation showed a reduction in terms of glucose utilisation and ethanol concentration, the ethanol productivity was enhanced significantly in comparison to batch shake flask culture by free *S.cerevisiae* W303, which resulted in more ethanol accumulation along the fermentation period. The time taken for ethanol production was also reduced by 10-20 fold over the batch culture, which could be accounted for by the availability of a highly dense cell population that speeded up the catalytic conversion of glucose to ethanol. Characterisation of microreactor performances based on the ethanol productivity and reduction of production time was

successful with a considerable improvement over the batch culture of free *S.cerevisiae* W303. The following conclusions may be drawn from the present study:

- *S.cerevisiae* W303 was able to adhere to (or be retained by) all types of polyHIPE at varying degrees of attachment/density.
- With respect to ethanol productivity, all microreactors showed significant improvements against the productivity achieved in the shake flask culture.
- Pore size affects the smoothness of medium circulation/cell migration and subsequently induces cell growth within the reactor, as well as facilitating the released of loosely bound cells out of the system.
- In the presence of oxygen, the fermentation activity for immobilised cells in the sulphonated microreactor was stable for up to 72 hours, whilst maintaining a high number of viable cells in the effluent throughout the fermentation process.
- Short retention times reduced the glucose utilisation, and subsequently reduced both growth and ethanol production.
- Low dilution rates (equivalent to a longer retention time) increased glucose consumptions but was outweighed by the limited glucose and low hydroforce, whicht induced biomass formation instead of ethanol, and a slow rate of cell migration (excess surface growth), respectively.
- Operating in the nutrient deprived environment (carbon-nitrogen-oxygen limitation) affected the glucose conversion and impaired both growth and ethanol production.
- Introduction of two-stage reactors in series increased the glucose consumptions in both aerobic and anaerobic conditions compared to single reactor systems, respectively.

This study aimed to fulfil the existing gap and provides some preliminary data for the comparison of the different operational modes currently reported in journals and publications. As no similar studies on the same reactor configuration have been carried out previously for ethanol production, the results obtained with this microreactor study cannot be verified or discussed in detail for a fair comparison. Therefore, it is hoped that this study, which provides preliminary insight into a new operational modes of

bioreactor as an alternatives to the existing technology will lead to more comprehensive studies.

9.2 Recommendations and Future Work

Although the sulphonated PHP showed good biocompatibility with *S.cerevisiae* W303 and other previously mentioned applications, the use of concentrated sulphuric acid during its preparation is the most potential drawback that might strongly limit its development. Since the polymer products are non-toxic and highly stable in extreme environments such as high temperature, pH, chemicals and shear properties, therefore they are very suitable for bio-applications. This study/systems can be improved further, as follows:

- ❖ It is crucial to introduce an efficient trapping system, in order to collect the vaporised ethanol that escapes in the gas stream. Quantifying the ethanol in the liquid and gas stream will provide an accurate measurement of yield thus producing a more accurate kinetics calculation.
- ❖ Quantification of other metabolites (e.g. CO_2, acid acetic, aldehydes) and the cell component of the immobilised *S.cerevisiae* W303 will provide more information on the fermentation/respiration pathway that takes place in the microreactor.
- ❖ Quantification of the dissolved oxygen content might provide useful information on how much oxygen is needed for cell regulation in order to tune the bioreactor for the fermentative activity, instead of only acting as a scaffold for cell growth.
- ❖ Design of a new system equipped with a controller and probes for easy monitoring. It is best to produce a housing made from clear glass for easy monitoring of the surface growth.
- ❖ Employing non flocculative yeast with highly robust properties might increase the efficiency of this system. It is possible to adjust/alter the reactor to carry out the simultaneous saccharification and fermentation (SSF) by immobilising both

the enzyme and the yeast in the same scaffold, thus cheaper substrates can be used.

- Intoducing air sparging to break the cell colonies and flush the flocculated cell might enhance the reactor integrity for a longer period.
- The newly proposed microreactor could potentially be employed in syngas fermentation.

REFERENCES

Ademe, E. P. (1999). The potential of liquid biofuels in France. Renewable Energy. 16: 1084-1089.

Akay, G, Birch, M.A. and Bokhari M.A. (2004). Microcellular PolyHIPE Polymer Supports Osteoblast Growth and Bone Formation in Vitro. Biomaterials (25) 3991-4000.

Akay, G., Bhumgara, Z. and Wakeman, R. J. (1995) 'Self-Supported Porous Channel Filtration Modules - Preparation, Properties and Performance'. Chemical Engineering Research & Design, 73 (A7): 782-797.

Akay, G. (2006a). Bioprocess and Chemical Process Intensification. Encyclopedia of Chemical Processing. 181-194.

Akay, G. (2006). Renewable Resources. Tce. 27-30.

Akay, G., Bokhari, M.A., Byron, V.J. and Dogru, M. (2005a). Development of Nano-Structured Micro-Porous Materials and Their Application in Bioprocess-Chemical Process Intensification and Tissue Engineering. Chemical engineering: Trends and Developments. John Wiley & Sons.

Akay, G., Birch, M.A., Bokhari, M.A., Byron, V.J., Erhan, E. and Keskinler, B. (2005b). Sustainable (Bio) Chemical Process Technology – Incorporating the 6th International Conference on Process Intensification. Delft.

Akay, G., Erhan, E. and Keskinler, B. (2005c). Bioprocess Intensification in Flow through Monolithic Microbioreactors with Immobilized Bacteria. Biotechnology and Bioengineering. 90(2)180-190.

Alexander, M.A. and Jeffries, T.W. (1990). Respiratory Efficiency and Metabolite Partitioning as Regulatory Phenomena in Yeasts. Enzyme and Microbial Technology. 12 (1) 2-19.

Alfenore, S., Cameleyre, X., Benbadis, L., Bideaux, C. Uribelarrea, J-L, Goma, G., Molina-Jouve, C. and Guillouet, S.E. (2004). Aeration strategy: A need for very high ethanol performance in *Saccharomyces cerevisiae* fed-batch process. Applied Microbiology and Biotechnology. 63(5): 537-542.

Allain, E.J. (2007). Perspective Cell-Free Ethanol Production: The Future of Fuel Ethanol?. Journal of Chemical Technol Biotechnol. 82:117-120.

Alonso, D.M., Bond, J.Q. and Dumesic, J.A. (2010). Catalytic Conversion of Biomass to Biofuels. Green Chem. 12:1493-1513.

Amin, G. and Verachtert, H. (1982). Comparative Study of Ethanol Production by Immobilized Cell Systems using *Zymomonas mobilis* or *Saccharomyces bayanus*. Applied Microbiology and Biotechnology. 14:59-63.

Aon, J.C. and Cortassa, S. (2001). Involvement of Nitrogen Metabolism in the Triggering of Ethanol Fermentation in Aerobic Chemostat Cultures of *Saccharomyces cerevisiae*. Metabolic Engineering. 3:250-264.

Bai, F.W., Anderson, W.A., and Moo-Young, M. (2008). Ethanol Fermentation Technologies from Sugar and Starch Feedstocks. Biotechnology Advances (26) 89–105: 91.

Bai, F.W., Chen, L.J., Zhang, Z., Anderson, W.A., and Moo-Young, M. (2004). Continuous Ethanol Production and Evaluation of Yeast Cell Lysis and Viability Loss under High Gravity Medium Conditions. Journal of Biotechnology. 110: 287-293.

Balat, M., Balat, H. and Oz, C. (2008). Progress in Bioethanol Processing. Progress in Energy and Combustion Science. 34:551-573.

Balat, M. (2007). Status of Fossil Energy Resources: A Global Perspective. Energy Sources. Part B. 2:31–47.

Balat, M. and Ayar. Gunhan (2005). Biomass Energy in the World, Use of Biomass and Potential Trends. Energy Sources. 27:931–940.

Baptista, C.M.S.G., Coias, J.M.A., Oliviera, A.C.M., Rocha, J.M.S, Dempsey, M.J., Lannigan, K.C. and Benson, P.S. (2005). Natural Immobilisation of Microorganism for Continuous Ethanol Production.

Barbetta, A, Camroon, N.R. and Cooper, S.J. (2000). High Internal Phase Emulsions (HIPEs) Containing Divinylbenzene and 4-vinylbenzyl chloride and the Morphology of the Resulting PolyHIPE Materials. Chemical Communications. 3:221-222.

Barbetta, A. and Cameron, N.R. (2004). Morphology and Surface Area of Emulsion Derived (PolyHIPE) Solid Foams Prepared with Oil Phase Soluble Porogenic Solvents: Three-Component Surfactant System. Macromolecules. 37:3202-3213.

Barbetta, A., Dentini, M., De Veechus, M.S., Filippini, P., Formisano, G. and Caiazza, S. (2005). Scaffolds Based on Biopolymeric Foam. Advanced Functional Materials. 15(1) 118-124.

Bayrock, D.P. and Ingledew, W.M. (2004). Inhibition of Yeast by Lactic Acid Bacteria in Continuous Culture: Nutrient Depletion and/or Acid Toxicity. J. Ind. Microbiol Biotechnol. 31:362-368.

Bhumgara, Z. (1995). Polyhipe Foam Materials as Filtration media. Filtration & Separation. 245-251.

Birol, G., Onsan, Z.I., Kirdar, B., and Oliver, G. (1998). Ethanol Production and Fermentation Characteristics of Recombinant *Saccharomyces cerevisiae* Strains Grown on Starch. Enzyme and Microbial Technology. 22:672-677.

Birol, G., Doruker, P., Kirdar, B., Onsan, Z.I. and Ulgen, K. (1998a). Mathematical Description of Ethanol Fermentation by Immobilized *Saccharomyces cerevisiae*. Process Biochemistry. 33 (7) 763-771.

Bokhari, M. A. (2003) Bone Tissue Engineering using Novel Microcellular Polymers. PHD Thesis. University of Newcastle, Newcastle Upon Tyne, UK.

Bokhari, M. A., Birch, M. and Akay, G. (2003). Polyhipe Polymer: A Novel Scaffold for In-vitro Bone Tissue Engineering. Advances in Experimental Medicine and Biology. 534: 247-254.

Bokhari, M. A., Akay, G., Zhang, S. and Birch, M.A. (2005). The Enhancement of Osteoblast Growth and Differentiation in Vitro on a Peptide Hydrogel-polyHIPE Polymer Hybrid Material. Journal of Biomaterials. 26.

Brandberg, T., Gustafsson, L. And Franzen, C. J. (2007). The impact of Severe Nitrogen Limitation and Microaerobic Conditions on Extended Continuous Cultivations of *Saccharomyces cerevisiae* with Cell Recirculation. Enzyme and Microbial Technology. 40: 583-593.

Breisha, G.Z. (2010) Production of 16% Ethanol from 35% Sucrose. Biomass and Bioenergy. 34(8):1243-1249.

Brethauer, S. and Wyman, C.E. (2009). Review: Continuous Hydrolysis and Fermentation for Cellulosic Ethanol Production. Bioresource Technology. 110 (43) 4862–4874.

Burke, D.R.., Akay, G. and Bilsborrow, P.E. (2010). Development of Novel Polymeric Materials for Agroprocess Intensification. Journal of Applied Polymer Science. 118 (6):3292-3299.

Burke, D.R. (2007). Bioprocess Intensification: Development of Novel Materials for Soil Enhancement to Maximise Crop Yield. PhD Thesis. Newcastle University.

Burke, D.R.., Akay, G. and Bilsborrow, P.E. (2006). Bioprocess Intensification in Agriculture. CHISA 2006 - 17th International Congress of Chemical and Process Engineering.

Byron, V.J. (2000). The Development of Microcellular Polymers as Support for Tissue Engineering. Thesis. University of Newcastle, UK.

Calkan, B. (2006). Preparation of Novel Nano-Structured Macro and Meso-Porous Metal Foams for Process Intensification and Miniaturization. Thesis PHD, Newcastle University.

Calkan, O.F. (2007). Intensified, Integrated Gasification System Development. PhD Thesis. Newcastle University.

Cameron. N.R. (2005). High Internal Phase Emulsion Templating as a Route to Well-Defined Porous Polymer. Polymer. 46:1439-1449.

Cameron, N.R. and Barbetta, A. (2000). The Influence of Porogen Type on the Porosity, Surface Area and Morphology of Poly(divinylbenzene) PolyHIPE Foams. Journal of Materials Chemistry. 10:2466-2471.

Cameron, N.R., and Sherrington, D.C. (1996). Non-aqueous High Internal Phase Emulsion: Preparation and Stability. Journal of Chemical Society, Faraday Trans. 92 (9): 1543-1547.

Cameron, N.R., Sherrington D.C, Ando, I and Kurosu, H. (1997). Chemical Modification of Monolithic Poly (styrene-divinylbenzene) PollyHIPE® Materials. Journal of Material Chemistry. 6 (5): 719-726.

Cameron, N.R. and Sherrington D.C. (1997). Preparation and Glass Transition Temperature of Elastomeric PolyHIPE Materials. Journal of Material Chem. 7(11)2209-2212.

Cameron, N.R (2005). High Internal Phase Emulsion Templating as a Route to Well-defined Porous Polymers. Polymer. 46:1439-1449.

Cameron, N.R. and Sherrington, D.C. (1997). Synthesis and Characterization of Poly(aryl ether sulfone) PolyHIPE Materials. Macromolecules. 30:5860-5869.

Chandel, A.K., Narasu, M.L., Chandrasekhar, G., Manikyam, A. and Rao, L.V. (2009). Use of *Saccharum spontaneum* (wild sugarcane) as Biomaterial for Cell Immobilization and Modulated Ethanol Production by Thermotolerant *Saccharomyces cerevisiae* VS_3. Bioresource Technology 100(8):2404-2410.

Chotineeranat, S., Wansuksri, R., Piyachomkwan, K., Chatakanonda, P., Weerathaworn, P. and Sriroth, K. (2010). Effect of Calcium Ions on Ethanol Production from Molasses by *Saccharomyces cerevisiae*. Sugar Technology. 12(2):120-124.

Christenson, E.M., Soofi, W., Holm, J.L., Cameron, N.R. and Mikos, A.G. (2007). Biodegradable Fumarate-Based PolyHIPEs as Tissue Engineering Scaffolds. Biomacromolecules 8 (12) 3806-3814.

Cohen, N. and Silverstein, M.S.(2012). One-Pot Emulsion-Templated Synthesis of an Elastomer-filled Hydrogel Framework. Macromolecules. 45, 1612−1621.

Dake, M.S., Jadhav, J.P. and Patil, N.B. (2009). Role of Ca^{2+} and Ethanol in the Process of Flocculation. Asian Journal of Chemistry. 21(5): 3419-3426.

Da cruz, S.H, Cilli, E.M., and Ernandes, J.R. (2002). Structural Complexity of the Nitrogen Source and Influence on Yeast Growth and Fermentation. Journal of the Institute of Brewing. 108(1):54-61.

De Deken, R.H. (1966). The Crabtree effect: A Regulatory System in Yeast. J.Gen. Microbiol. 44:149-156.

Delgenes, J.P., Moletta, R. and Navarro, J.M. (1996). Effects of Lignocellulosic Degradation Products on Ethanol Fermentation of Glucose and Xylose by *Saccharomyces cerevisiae*, *Zymomonas mobilis*, *Pichia stipitis* and *Candida shehatae*. Enzyme and Microbial Technology. 19:220-225.

Dien, B.S., Cotta, M.A. and Jeffries, T.W. (2003). Bacteria Engineered for Fuel Ethanol Production: Current Status. Applied Microbiol Biotechnol. 63: 258-266.

Dizge, N., Keskinler, B. and Tanriseven, A. (2009). Biodisel Production from Canola Oil by Using Lipase Immobilized onto Hydrophobic Microporous Styrene-Divinylbenzene Copolymer. Biochemical Engineering Journal. 44:220-225.

Dizge, N., Aydiner, C., Imer, D.Y., Bayramoglu, M., Tanriseven, A and Keskinler, B. (2009a). Biodisel Production from Sunflower, Soybean and Waste Cooking Oils by Transesterification Using Lipase Immobilized onto a Novel Microporous Polymer. Bioresource Technology. 100: 1983-1991.

Dragone, G., Silva, D.P. and e Silva, J.B.D.A. (2004). Factors Influencing Ethanol Product at High Gravity Brewing. Swiss Society of Food Science and Technology. 37:797-802.

Edgardo, A., Carolina, P., Manuel, R., Juanita, F. and Jaime, B. (2008). Selection of Thermotolerant Yeast Strain *Saccharomyces cerevisiae* for Bioethanol Production. Enzyme and Microbial Technology. 43:120-123.

Erhan, E., Keskinler, B. and Akay G. (2002). Removal of phenol from water by membrane-immobilized enzymes: Part I. Dead-end filtration. Journal of Membrane Science. 206:1-2.

Erhan, E., Yer, E., Akay, G., Keskinler, B. and Keskinler, D. (2004). Phenol Degradation in a Fixed-Bed Bioreactor Using Micro Cellular Polymer Immobilized *Pseudomonas* s*yringae*. Journal of Chemical Technology and Biotechnology. 79:195-206.

Field, C. B., Campbell, J. E. and Lobell, D. B. (2007). Biomass Energy: The Scale of the Potential Resource.Trends in Ecology and Evolution. 23 (2).

Fleming, S. (2012). Agro-Process Intensification Using Nano-Structured Microporous Polymers as Soil Additives to Enhance Crop Yield. PhD Thesis, Newcastle University, UK.

Fortman, J.L, Chhabra, S., Mukhophadhyay, A., Chou, H., Lee, T.S., Steen, E. and Keasling, J.D. (2008). Biofuel Alternatives to Ethanol: Pumping the Microbial Well. Trends in Biotechnology. 26 (7) 375-381.

Fratesi, S.E., Lynch, F.L., Kirkland, B.L. and Brown, L.R. (2004). Effects of SEM Preparation Techniques on the Apperance of Bacteria and Bioflims in the Carter Sandstone. Journal of Sedimentary Research. 74(6)858-867.

Fronk, B. M., Neal, R. and Garimella, S. (2010). Evolution of the Transition to a World Driven by Renewable Energy. Journal of Energy Resources Technology. 132.

Fujii, N. Sakurai., A., Onjoh, K. and Sakakibara, M. (1999). Influence of Surface Characteristics of Cellulose Carriers on Ethanol Production by Immobilized Yeast Cells. Process Biochemistry. 34:147-152.

Fukui, S. and Tanaka, A. (1982). Immobilized Microbial Cells. Annual Reviews Microbiology. 36:145-172.

Gallardo-Moreno, A.M., Gonz´alez-Mart´ın, M.L., Bruque, J.M. and P´erez-Giraldo, C. (2004). The adhesion strength of *Candida parapsilosis* to glassand silicone as a

function of hydrophobicity, roughness and cell morphology Colloids and Surfaces A: Physicochem. Eng. Aspects. 249 :99–103.

Ghose, T.K. (1987). Measurement of Cellulase Activities. International Union of Pure and Applied Chemistry. 59(2)257-268.

Ghose, T.K. and Tyagi, R.D. (1982). Production of Ethyl Alcohol from Cellulose Hydrolysate by Whole Cell Immobilization. Journal of Molecular Catalysis. 16: 11-18.

Gotzinger, M., Weighl, B., Peukert, W. and Sommer, K. (2007). Effect of Surface Roughness on Particle Adhesion in Aqueous Solutions: A Study of S*accharomyces cerevisiae* and a Silica Particle. Colloids and Surfaces B: BIointerfaces. 55: 44-50.

Gnansounou, E. (2010). Production and Use of Lignocellulosic Bioethanol in Europe: Current Situation and Perspectives. Bioresource Technology. 101: 4842-4850.

Griffiths, M.S. and Bosley, J.A. (1993). Assessment of Macroporous Polystyrene-Based Polymers for the Immobilization of *Citrobacter freundii*. Enzyme and Microbial Technology. 15:109-113.

Guillemot, G., Vaca-Medina, G., Martin-Yken, H., Vernhert, A., Schmitz, P. and Mercier-Bonin, M. (2006). Shear-Flow Induced Detachment of *Saccharomyces cerevisiae* from Stainless Steel: Influence of Yeast and Solid Properties. Colloids and Surfaces B: Biointerfaces. 49: 126-135.

Guillemot, G., Lorthois, S., Schmitz, P. and Mercier-Bonin, M. (2007). Evaluating the Adhesion Force Between *Saccharomyces cerevisiae* Yeast Cells and Polystyrene From Shear-Flow Induced Detachment Experiments. Trans IChemE. 85(A6): 800-807.

Hogan, D. A. (2006). Quorum Sensing: Alcohols in a Social Situation. Current Biology. 16(12)457-458.

Hentze, H-P. and Antonietti, M. (2002). Porous Polymers and Resins for Biotechnology and Biomedical Applications. Reviews in Molecular Biotechnology. 90:27-53.

Hilge-Rotmann, B. and Rehm, H. (1991). Relationship between Fermentation Capability and Fatty Acid Compositions of Free and Immobilized *Saccharomyces cerevisiae*. Applied Microbiol Biotechnol. 34:502-508.

Hough, D.B., Hammond, K., Morris, C. and Hammond, R.C. (1991). Porous Polymeric Support Containing Biological Cells in Interconnected Voids. US Patent. Patent No. 5,071,747.

Jamai, L., Sendide, K., Ettayebi, K., Errachidi, F., Hamdouni-Alami, O., Tahri-Jouti, M.A., McDermott, T. and Ettayebi, M. (2001). Physiological Difference During Ethanol Fermentation Between Calcium Alginate-immobilized *Candida tropicalis* and *Saccharomyces cerevisiae*. FEMS Microbiology Letters. 204:375-379.

Jansen, M.L.A., Diderich, J.A., Mashego, M., Hassane, A., de Winde, J.H., Daran-Lapujade, P. and Pronk, J.T. (2005). Prolonged Selection in Aerobic, Glucose-Limited Chemostat Cultures of *Saccharomyces cerevisiae* Causes a Partial Loss of Glycolytic Capacity. Microbiology. 151:1657-1669.

Jimat, D.N. (2012). Bioprocess Intensification in the production of alpha-Amylase by Immobilized *Bacillus Subtilis* on Polymeric Polyhipe Matrix. PhD Thesis, Newcastle University, UK.

Jirku, V. (1995). Covalent Immobilization as a Stimulus of Cell Wall Composition Changes. Research Article Experientia. 51:569-571.

Jones, R.P. and Greenfield P.F. (1982). Effect of Carbon Dioxide on Yeast Growth and Fermentation. Enzyme and Microbial Technology. 4:210-223.

Kang, S and Choi H (2005). Effect of Surface Hydrophobicity on the Adhesion of *S.cerevisiae* onto Modified Surface by Poly (styrene – ran – sulfonic acid) random copolymers. Colloids and Surfaces B: Biointerface 46:70-77.

Karagoz, P., Erhan, E., Keskinler, B. and Ozkan, M. (2008). The Use of Microporous Divinyl Benzene Copolymer for Yeast Cell Immobilization and Ethanol Production in Packed-Bed Reactor. Applied Biochem Biotechnol. 152 (1) 66-73.

Karel, S. F., Libicki, S.B. and Robertson, C.R. (1985). The immobilization of whole cells: Engineering Principles. Chemical Engineering Science. 40(8): 1321-1354

Kesava, N.S., Panda, T. and Rakshit, S.K. (1995). Production of Ethanol by Immobilized Whole Cells of *Zymomonas mobilis* in an Expanded Bed Bioreactor. Process Biochemistry. 31(5)449-456.

Khan, E., Yang, P.Y. and Kinoshita, C.M. (1994). Bioethanol Production from Dilute Feedstock. Bioresource Technology. 47:29-36.

Kilonzo, P, Margaritis, A. and Bergougnou, M. (2009). Airlift Driven Fibrous-Bed Bioreactor for continuous Production of Glucoamylase Using Immobilized Recombinant Yeast Cells. Journal of Biotechnology. 143:60-68.

Kilonzo, P, Margaritis, A. and Bergougnou, M. (2011). Effects of Surface Treatments and Process Parameter on Immobilization of Recombinant Yeast by Adsorption to Fibrous Matrices. Bioresource Technology. 102:3662-3672.

Kim, H. Park, K. Oh, S. and Chang, I.S. (2009). Rapid Detection of Lactobacillus and Yeast Concentrations Using a Particle Size Distribution Anaalyser.

Kondili, E.M. and Kaldellis, J.K. (2007). Biofuel Implementation in East Europe: Current Status and Future Prospect. Renewable & Sustainable Energy Reviews. 11:2137-2151.

Koyama, K and Seki, M. (2004). Cultivation of Yeast and Plant Cells Entrapped in the Low Viscous Liquid-Core of an Alginate Membrane Capsule Prepared Using Polyethylene Glycol. Journal of Bioscience and Bioengineering. 97 (2). 111-118.

Kunz, M. (2008). Bioethanol: Experiences from Running Plants, Optimization and Prospects. Biocatalysis and Biotransformation. 26(1-2)128-132.

Kuriyama, H. and Slaughter, J.C. (1995). Control of Cell Morphology of the Yeast *Saccharomyces cerevisiae* by Nutrient Limitation in Continuous Culture. Letters in Applied Microbiology. 20:37-40.

Laopaiboon, L., Nuanpeng, S., Srinophakun, P, Klanrit, P. and Laopaiboon, P. (2009). Ethanol Production from Sweet Sorghum Juice Using Very High Gravity Technology: Effects of Carbon and Nitrogen Supplementations. Bioresource Technology. 100: 4176-4182.

Larsson, C., von Stockar, U., Marison, I. and Gustafsson, L. (1993). Growth and Metabolism of Saccharomyces cerevisiae in Chemostat Cultures Under Carbon-, Nitrogen-, or Carbon- and Nitrogen- Limiting Conditions. Journals of Bacteriology. 175 (15): 4809-4816.

Lebeau, T., Jouenne, T. and Junter, G.A. (1998). Diffusion of Sugars and Alcohols through Composite Membrane Structures Immobilizing Viable Yeast Cells. Enzyme and Microbial Technology. 22:434-438.

Lee, C.W. and Chang, H.N. (1985). Examination of Immobilized Cells in a Rotating Packed Drum Reactor for the Production of Ethanol from D-glucose. Enzyme and Microbial Technology. 7:561-563.

Lepine, O., Birot, M. and Delueze, H. (2008). Influence of Emulsification Process on Structure-Properties Relationship of Highly Concentrated Reverse Emulsion-Derived Materials. Colloid Polymer Science. 286:1273-1280.

Licinio Da Silva, N.L.C., Salgueiro, A.A., Ledingham, W.M., Melo, E.H.M. and Lima Filho, J.L. (1992). Effects of Potassium on the Ethanol Production Rate of *Saccharomyces cerevisiae* Carrying the Plasmid pCYG4 Related with Ammonia Assimilation. Applied Biochemistry and Biotechnology. 37:1-10.

Margaritis, A. and Kilonzo, P.M. (2005). Production of Ethanol Using Immobilized Cell Bioreactor Systems. Application of Cell Immobilisation Biotechnology. 375-405.

McKeown N.B., Budd, P.M., and Book, D. (2007). Microporous Polymers as Potential Hydrogen Storage Materials. Macromolecular Rapid Communications.28:995-1002.

Mercier-Bonin, M., Ouazzani, K., Schmitz, P. and Lorthois, S. (2004). Study of the Bioadhesion on a Flat Plate with a Yeast/Glass Model System. Journal of Colloid and Interface Science. 271:342-350.

Melin, E. and Shieh, W.K. (1992). Continuous Ethanol Production from Glucose using *Saccharomyces cereivisiae* Immobilized on Fluidized Microcarriers. The Chemical Engineering Journal. 50: 17-22.

Melzoch, K., Rychtera, M. and Habova, V. (1994). Effect of Immobilization upon the Properties and Behaviour of *Saccharomyces cerevisiae* Cells. Journal of Biotechnology. 32:59-65.

Menner, A. Salgueiro, M., Shaffer, M.S.P. and Bismarck,A. (2008). Nanocomposite Foams Obtained by Polymerization of High Internal Phase Emulsions. Journal of Polymer Science Part A: Polymer Chemistry. 46: 5708-5714.

Menner, A. and Bismarck, A. (2006). New Evidence for the Mechanism of the Pore Formation in Polymerising High Internal Phase Emulsions or Why PolyHIPEs Have an Interconnected Network Structure. Macromol. Symp 2006. 242. 19-24.

Merico, A., Sulo, P., Piskur, J. and Compagno, C. (2007). Fermentative Lifestyle in Yeasts Belonging to the *Saccharomyces* Complex. FEBS Journal. 976-989.

Merritt, K. and An, Y.H.(2000). Handbook of Bacterial Adhesion: Principles, Methods and Applications. 53-73.

Messing, R.A. and R.A.O (1979a). Pore Dimensions for Accumulating Biomass. I. Microbes that Reproduce by Fussion or Budding. 21:49-58.

Messing, R.A, and R.A.O.F.B.K. (1979b). Pore Dimensions for Accumulating Biomass. II. Microbes that Form Spores and Exhibit Mycelial Growth. 21:59-67.

Miller, G.L. (1959). Use of Dinitrosalicylic Acid Reagent for Determination of Reducing Sugar. Analytical Chemistry. 426-428.

Mitchell, D. (2008). A Note on Rising Food Prices. The World Bank Development Prospects Group. Policy research Working Paper 4682.

Mohamed, R. (2011). Preparation of Nano-Structured Porous Materials. PhD Thesis. Newcastle University.

Montee Alegre, R. Rigo, M. and Joekes, I. (2003). Ethanol fermentation of a Diluted Molasses Medium by *Saccharomyces cerevisiae* Immobilized on Chrysotile. Brazillian Archives of Biology and T echnology. 46(4):751-757.

Murata, K. (1993). Use of Microbial Spores as a Biocatalyst. Critical Reviews in Biotechnology. 13(3): 173-193.

Muller-Steinhagen, H. and Nitsch, J. (2005). The contribution of Renewable Energy to a Sustainable Energy Economy. Process Saf Environ Protect. 83(B4):285-297.

Musatto, S.I., Dragone, G., Guimarães, P.M.R., Silva, J.P.A., Carneiro, L.M., Roberto, I.C., Vicente, A., Domingues, L. and Teixeira, J.A. (2010). Technological trends, global market, and challenges of bio-ethanol production. Biotechnology Advances 28:817–830.

Nakari-Setälä, T., Azeredo, J., Henriques, M., Oliveira, R., Teixeira, J., Linder, M. and Penttilä, M. (2002). Expression of a Fungal Hydrophobin in the *Saccharomyces cerevisiae* Cell Wall Effect on Cell Surface Properties and Immobilization. Appl. Environ. Microbiol. 2002. 68(7):3385.

Nigam, J.N. (2000). Continuous Ethanol Production From Pineapple Cannery Waste Using Immobilized Yeast Cells. Journal of Biotechnology. 80:189-193.

Ndlovu, T.M. (2009). Bioprocess Intensification of Antibiotic Production Using Functionalised PolyHIPE Polymers. PhD Thesis, Newcastle University, UK.

Noor, Z. Z. (2006) Intensification of Separation Processes using Fuctionalised PolyHIPE Polymers. PhD Thesis. University of Newcastle upon Tyne.

Norton, J.S. and Krauss, W. (1972). The Inhibition of Cell Division in *Saccharomyces cerevisiae* (Meyen) by Carbon Dioxide. Plant & Cell Physiology. 13: 139-149.

Norton, S. and D'Amore, T. (1994). Physiological Effects of Yeast Cells Immobilization: Application for Brewing. Enzyme and Microbial Technology. 16:365-375.

Oliviera, S.M., Song, W., Alves, N.M. and Mano, J.F. (2011). Chemical Modification of Bioinspired Superhydrophobic Polystyrene Surfaces to Control Cell Attachment/Proliferation. The Royal Society of Chemistry, Soft Matter. 7: 8932-8941.

Painting, K. and Kirsop, B (8888). Technical Information Sheet No.2. A Quick Method for Estimating the Percentage of Viable Cells in a Yeast Population, Using Methylene Blue Staining. World Journal of Microbiology and Biotechnology. 6:346-347.

Parascandola, P., Alteriis, E., Sentandreu, R. and Zueco, J. (1997). Immobilization and Ethanol Stress Induce the Same Molecular Response at the Level of the Cell Wall in Growing Yeast. FEMS Microbiology Letters . 150:121-126.

Pakeyangkoon, P., Magaraphan, R., Malakul, P. and Nithitanakul, M. (2008). Effect of soxhlet extraction and surfactant system on morphology and properties of Poly(DVB)PolyHIPE. Macromolecular Symposia. 264 (1) 149-156.

Peinado, R.A., Moreno, J.J., Villalba, J.M, Gonzalez-Reyes, J.A., Ortega, J.M and Mauricio, J.C. (2006). Yeast Biocapsules: A New Immobilization Method and Their Applications. Enzyme and Microbial Technology. 40: 79-84.

Pierce Chemical Company (1996). "Modified Lowry Protein Assay." Rockford (U.S.A.) : Instructions.

Porro, D., Brambilla, L. and Alberghina, L. (2003). Glucose Metabolism and Cell Size in Continuous Cultures of *Saccharomyces cerevisiae*. FEMS Microbiology Letters. 229:165-171.

Pump Industry Analyst, (July, *2007*). 2007(7):3-4.

Qi, W., Ma, J., Yu, W., Xie, Y., Wang, W. and Ma, X. (2006). Behaviour of Microbial Growth and Metabolism in Alginate-Chitosan-Alginate (ACA) Microcapsules. Enzyme and Microbial Technology. 38:697-704.

Ramon-Portugal, F., Pingaud, H. And Strehaino, P. (2004) Metabolic Transition Step from Ethanol Consumption to Sugar/Ethanol consumption by *Saccharomyces cerevisiae*. Biotechnology Letters (26) 1671-1674.

Riddle, K. and Mooney, D.J. Biomaterials for Cell Immobilization~ A Look at Carrier Design (Fundamentals of Cell Immobilization Technology). 8: 15-32. ISBN 1-4020-1887-8.

Rieger, M., Kappeli, O. and Fiechter, A. (1983). The Role of Respiration in the Incomplete Oxidation of Glucose by *Saccharomyces cerevisiae*. Journal of General Microbiology. 129:653-661.

Rosillo-Calle, F. (2006). Global Market for Bioethanol: Historical, Trends and Future Prospects. Energy for Sustainable Development. 1(X).

Sanchez, O.J. and Cardona, C.A. (2008). Trends in Biotechnological Production of Fuel Ethanol from Different Feedstocks. Bioresource Technology. 99:5270-5295.

Senac, S. and B. Hahn-Hagerdal (1991). Concentrations of intermediary metabolites in free and calcium alginate-immobilized cells of D-glucose fermenting *Saccharomyces cerevisiae* . Biotechnology Techniques. 5(1): 68.

Shuler, M.L and Kargi, F. (2002) Bioprocess Engineering Basic Concepts-Second Edition. Prentice Hall. 515-532.

Silveston, P.L., Budman, H. and Jervis, E. (2008). Forced Modulation of Biological Processes: A review. Chemical Engineering Science. 63:5089-5105.

Smit, G., Straver, M.H., Lugtenberg, B.J.J. and Kijne, J.W. (1992). Flocculence of *Saccharomyces cerevisiae* Cells is Induced by Nutrient Limitation, with CellSurface Hydrophobicity as a Major Determinant. Applied and Environmental Microbiology. 3709-3714.

Solomon, B.D., Barnes, J.R. and Halvorsen, K.E. (2007). Grain and Cellulosic Ethanol: History, Economics, and Energy Policy. Biomass and Bioenergy. 31:416-425.

Souto-Maior, A.M., Runquist, D. And Hahn-Hagerdal, B. (2009). Crabtree-negative characteristics of Recombinant Xylose-Utilizing *Saccharomyces cerevisiae*. Journal Biotechnology (143) 119-123.

Soyuduru, D., Ergun, M. and Tosun, A. (2009). Application of a Statistical Technique to Investigate Calcium, Sodium, and Magnesium Ion Effect in Yeast Fermentation. Appl Biochem Biotechnol. 152:326–333

Talebnia, F. and Taherzadeh, M.J. (2007). Physiological and Morphological Study of Encapsulated *Saccharomyces cerevsiae*. Enzyme and Microbial Technology. 41: 683-688.

Takeshige, K. and Ouchi, K. (1995). Effects of Yeast Invertase on Ethanol Production in Molasses. Journal of Fermentation and Bioengineering. 79 (5)513-515.

Thonart, P., Custinner, M. and Paquot, M. (1982). Zeta Potential of Yeast Cells: Application in Cell Immobilization. Enzyme Microb. Technol. 4: 191-194.

Tibayrenc, P., Preziosi-Belloy, L. and Roger, J. and Ghommidh, C. (2010). Assessing yeast viability from cell size measurements? Journal of Biotechnology. 149: 74–80.

Trovati, J., Giordano, R.C and Giordano, R.L.C. (2009). Improving the Performances of a Continuous Process for the Production of Ethanol from Starch. Appl. Biochem. Biotechnol. 156:506-520.

Tyagi, R.D., Gupta, S.K. and Chand, S. (1992). Process Engineering Studies on Continuous Ethanol Production by Immobilized *S.cerevisiae*. Process Biochemistry. 27: 23-32.

Van Haecht, J.L., De Bremaeker, M., and Rouxhet, P.G. (1984). Immobilization of Yeast by Adhesion to a Support without the Use of Chemical Agent. Enzyme Microbial Technology. (6).

Van Hoek, P., van Dijken, J.P. and Pronk, J.T. (2000). Regulation of Fermentative Capacity and Levels of Glycolytic Enzymes in Chemostat Cultures of *Saccharomyces cerevisiae*. Enzyme and Microbial Technology. 26: 724-736.

Van Maris, A.J.A., Abbott, D.A., Bellissimi, E., van den Brink, J., Kuyper, M., Luttik, M.A.H., Wisselink, H.W., Scheffers, W.A., van Dijken, J.P. and Pronk, J.T. (2006). Alcoholic Fermentation of Carbon Sources in Biomass Hydrolysates by *Saccharomyces cerevisiae*: Current Status. Antonie van Leeuwenhoek. 90:391-18.

Vazquez-Juarez, R., Andlid, T. and Gustafsson, L. (1994). Cells Surface Hydrophobicity and its Relation to Adhesion of Yeasts Isolated from Fish Gut. Colloids and Surfaces B: Bionterfaces. 2:199-208.

Vega, J.L, Clausen, E.C and Gaddy, J.L. (1988). Biofilm Reactors for Ethanol Production. Journal of Enzyme and Microbial Technology. 10:390-402.

Verbelen, J.P., De Schutter, D.P., Delvaux, F., Verstrepen, K.J. and Delvaux, F.R. (2006). Immobilized Yeast Cell Systems for Continuous Fermentation Applications. Biotechnology Letters. 28:1515-1525.

Vergnault, H., Mercier-Bonin, M. and Willemot, R.M. (2004). Physicochemical Parameters Involved in the Interactions of *Saccharomyces cerevisiae* Cells with

Ion-Exchange Adsorbents in Expanded Bed Chromatography. Biotechnol. Prog. 20: 1534-1542.

Verstrepen, K.J. and Klis, F.M. (2006). Microreview: Flocculation, Adhesion and Biofilm Formation in Yeasts. Molecular Microbiology. 60(1)5-15.

Wada, M., Kato, J. and Chibata, I. (1980). Continuous Production of Ethanol Using Immobilized Groving Yeast Cells. European Journal of Applied Microbiology and Biotechnology. 10:275-287.

Walter, A., Rosillo-Calle, F., Dolzan, P., Piacente, E. and da Cunha, K.B. (2008). Perspectives on Fuel Ethanol Consumption and Trade. Biomass and Bioenergy 32(8):730-748.

Wang, N. S. (2007). Glucose Assay By Dinitrosalicylic Colorimetric Method.

Wang, F., Gao, C., Yang, C. and Xu, P. (2007a). Optimization of an Ethanol Production Medium in Very High Gravity Fermentation. Biotechnol Lett. 29:233-236.

Werne-Washburne, M., Braun, E., Johnston, G.C. and Singer, R.A. (1993). Stationary Phase in the Yeast *Saccharomyces cerevisiae*. Microbiological Reviews. 57(2):383-401.

White, J.S. and Walker, G.M. (2011). Influence of Cell Characteristics on Adhesion of *Saccharomyces cerevisiae* to the Biomaterial Hydroxylapatite. Antonie van Leeuwnhoek. 99:201-209.

Wiebe , M. G., Rintala, E., Tamminen, A., Simoling, H., Salusjarvi, L., Toivari, M., Kokkonen, J.T., Kiuru, J., Ketola, R.A., Jouhten, P., Huuskonen, A., Maaheimo, H., Ruohonen, L. and Penttila, M. (2008). Central Carbon Metabolism of *Saccharomyces cerevisiae* in Anaerobic, Oxygen–Limited and Fully Aerobic Steady-State Conditions and Following a Shift to Anaerobic Conditions. FEMS Yeast Res. 8:140-154.

Williams, J.M., Gray, A.J., and Wilkerson, M.H. (1990). Emulsion Stability and Rigid Foams from Styrene or Divinylbenzene Water in Oil Emulsions. American Chemical Society, Langmuir. 6: 437-444.

Wyman, C.E. (1994). Ethanol from Lignocellulosic Biomass: Technology, Economic and Opportunities. Bioresource Technology. 50:2-16.

Yin, H. and Q. Cai (2008). High gravity and high productivity ethanol fermentation with self-flocculating yeast cells. Journal of Biotechnology. 136(1): 492-493.

Ylitervo, P., Franzen, C.J. and Taherzadeh, M.J. (2011). Ethanol Production at Elevated Temperatures using Encapsulation Yeast. Journal of Biotechnology. 156 (1) 22-29.

Yu, J., Yue, G., Zhong, J., Zhang X and Tan, T. (2010). Immobilization of *Saccharomyces cerevisiae* to Modified Bagasse for Ethanol Production. Renewable Energy. 35(6): 1130–1134.

Zhang, Z., Bocazzi, P., Choi, H., Peroziollo, G., Sinskey, A.J. and Jensen, K.F. (2006). Microchemostat-Microbial Continuous Culture in a Polymer-Based, Instrumented Microbioreactoe. The Royal Society of Chemistry. 6:906-913.

Zhao, Y. and Lin, Y.H. (2003). Growth of *Saccharomyces cerevisiae* in a Chemostat under High Glucose Conditions. Biotechnology Letters. 25: 1151-1154.